

ABSTRACT

BROWN, ROBERT ANDREW. Evaluation of Bioretention Hydrology and Pollutant Removal in the Upper Coastal Plain of North Carolina with Development of a Bioretention Modeling Application in DRAINMOD. (Under the direction of Dr. William F. Hunt III).

Bioretention cells are widely used as an infiltration-based stormwater control measure to reduce the negative impacts of urban stormwater runoff. Two sets of cells were monitored at Rocky Mount and at Nashville to measure the effects that underdrain configuration, media depth, surface storage volume, and underlying soil type had on hydrologic and water quality performance. Both sites are located in the Upper Coastal Plain of North Carolina, where in-situ soils tend to have a high sand content.

The two bioretention cells at Rocky Mount were designed with an internal water storage (IWS) zone and had varying degrees of sandy underlying soils. The underlying soils for these two cells were sand (Sand cell) and sandy clay loam (SCL cell). After the first year, the IWS zone depth was reduced by lowering the outlet. While the Sand cell, with its sandy underlying soils and deep IWS zone provided greater outflow reduction, it had minimal nitrogen treatment because of a short hydraulic residence time (less than three hours). On the other hand, the SCL cell had a longer hydraulic residence time (up to seven days), and it had significant concentration reductions for all forms of nitrogen, including nitrate.

Fill media is a major expense, so a study objective from the Nashville site was to evaluate the impact of varying media depth (0.6 m versus 0.9 m). A post-construction objective was to analyze the impact of under-sizing the surface storage zone. Construction and design errors resulted in the surface storage volumes of the bioretention cells to be approximately one-third of the design volume; moreover, the surface was clogged, which limited infiltration. After one year of monitoring, the clogging layer was removed, which doubled the surface storage volume. Deeper media depth promoted more exfiltration and met a low impact development goal of outflow reduction twice as often. Also, despite being relatively undersized, the repaired cells were able to treat nearly 90 percent of runoff, suggesting that current design guidance may be over-sizing the surface storage zone. Also in Nashville, another bioretention cell was installed in series with a pervious concrete system

that included a subsurface storage zone. These two practices in series had excellent peak flow and outflow reduction. For low impact development (LID) practices in series, serious consideration should be taken to balance the returns of flow rate and outflow reduction vis-a-vis cost. The bioretention cell was installed at a site with a high water table, so this impact was quantified. Because of the intercepted groundwater, the site exported 63 percent more total nitrogen than what was present in the runoff load.

Overall, bioretention cells can be designed and constructed with a variety of specifications, among them are media depth, underdrain configuration, media composition, drainage area to bioretention area ratio, and surface storage volume. One way to quantify various designs is using a long-term model. The hydrology data from the field sites were used to calibrate and validate DRAINMOD, a widely-accepted, long-term drainage model. The measured and predicted (modeled) results were in good agreement during both the calibration and validation periods; Nash-Sutcliffe coefficients for runoff, drainage, overflow, and exfiltration/evapotranspiration commonly exceeded 0.8. These results proved that DRAINMOD can be reliably used to simulate the hydrologic response of runoff entering a bioretention cell. With a reliable long-term bioretention model, designers and regulators will be able to shift from the current “one size fits all” design approaches and establish a "flexible" bioretention design methodology that is based on underlying soil type, design specifications, and climate.

Finally, in an attempt to improve construction practices, the effects of construction activity on underlying soils were explored. The effects of soil type, soil moisture, and excavation technique were tested. The results showed that excavating using the teeth of the bucket to scarify the surface (rake method) would maintain a more permeable surface than using the back of the bucket (scoop method).

Evaluation of Bioretention Hydrology and Pollutant Removal in the Upper Coastal Plain of
North Carolina with Development of a Bioretention Modeling
Application in DRAINMOD

by
Robert Andrew Brown

A dissertation submitted to the Graduate Faculty of
North Carolina State University
in partial fulfillment of the
requirements for the degree of
Doctor of Philosophy

Biological and Agricultural Engineering

Raleigh, North Carolina

2011

APPROVED BY:

William F. Hunt III
Chair of Advisory Committee

Aziz Amoozegar

Gregory D. Jennings

R. Wayne Skaggs

DEDICATION

To my family.
Thank you for your support.

BIOGRAPHY

Robert Andrew Brown was born on March 16, 1985, in Phoenixville, Pennsylvania, to Donald and Susanne Brown. He lived in West Chester, Pennsylvania, a suburb of Philadelphia, until he graduated from high school in June 2003. In the fall of 2003, Robert enrolled at the Pennsylvania State University, University Park Campus, where he majored in Agricultural and Biological Engineering, with a focus in Environmental Engineering. Robert's interests in the environment and surface water quality originated from his passion for fishing and various other outdoor activities. While at Penn State, Robert interned with the U.S. Fish and Wildlife Service for two summers. During this internship, he surveyed streams and was in charge of construction oversight for stream restoration projects. His interest for research was sparked during the last year of his internship, where as a part of his honors thesis, he studied the effects of rock cross vanes on bedload scour and deposition in restored streams. This project was under the direction of Dr. James Hamlett and Dr. Larry Brannaka.

Upon graduation in May 2007, Robert chose to move south to pursue a graduate degree focusing on low impact development stormwater practices at North Carolina State University, under the direction of Dr. Bill Hunt. While choosing to leave Happy Valley was a difficult decision because of the mentors and friends he had in the Agricultural and Biological Engineering Department, Robert quickly found a home in Raleigh and a welcoming and friendly department in the Biological and Agricultural Engineering Department at North Carolina State University. It was there that he met his wife-to-be, Jessica.

ACKNOWLEDGMENTS

There are many people and agencies that have made it possible for me to be where I am today, and I am extremely grateful for all of their support and assistance. Thank you to the agencies that have funded my research: Cooperative Institute for Coastal and Estuarine Environmental Technology, Water Resources Research Institute of the University of North Carolina, and North Carolina Department of Environment and Natural Resources.

First, I would like to thank my mentor, advisor, and friend, Dr. Bill Hunt. Your guidance has helped me grow as a person, researcher, writer, and presenter. You helped make my experiences at N.C. State unforgettable with your friendship, your support to travel to various conferences, and the stormwater team trips. There never seemed to be a dull moment when you were around. As I think back on my past (almost) four years, I would not have traded them for anything. Even though you promised better days for the basketball team when I first arrived, I will not hold it against you, and I will continue to “look toward next season.” Without your level of excitement, passion for stormwater research, or the graduate recruitment weekend, I may have never come to N.C. State, so my deepest thanks for everything you have done for me.

I would like to thank my committee members, Dr. Aziz Amoozegar, Dr. Greg Jennings, and Dr. Wayne Skaggs, for your advice and suggestions with my research and for your review of my manuscripts. Your experiences and input have helped me develop in the broader fields of watershed and stream restoration, drainage, soil science, and soil-water dynamics. I would also like to thank Dr. Francois Birgand for your suggestions with Chapter 5. I appreciate the input you provided on your views of the methods of water sampling and analysis of water quality results. Also, thanks to Mr. Dan Line for your input and help with Chapter 6. Working with you on the LID Wal-Mart project was a great experience, and I appreciate all of your help with reviewing my monitoring set-up plans. I would also like to thank Dr. Jason Osborne for your assistance with writing SAS code and interpreting some of

the statistical analyses. Thanks also to Mr. Brian Phillips for your help with formatting the long-term DRAINMOD weather files.

Next I would like to thank all of the Stormwater Team members (past and present) for their help at my field sites and their friendship. First and foremost, thank you to Shawn Kennedy for ALL of your help at my field sites. I would have never been able to collect as much reliable data as I did without your assistance. I would like to thank the following people who have either been at my field sites assisting me with my research or who have assisted me with running soil sample tests: Shawn Kennedy, Bill Hunt, Bill Lord, Dan Line, Mitch Woodward, Wilson Huntley, Brian Phillips, Chris Niewoehner, Jessica Roberts, Jon Hathaway, Ryan Smith, Jason Wright, Gabrielle Skipper, Jackie McNett, Ryan Winston, Matthew Jones, Trisha Moore, Stacy Luell, Erica Tillinghast, Brad Wardynski, Natalie Gurkin, Amelia Clark, and Cole Ammons. I would like to thank Jenny James and Linda Mackenzie for all of your help with analyzing the numerous water samples that I collected. Finally, thanks to Joe Wright for your precise excavation work in the construction impacts study and to Fred Ammons for your help in repairing the Nashville bioretention cells.

I would like to thank my officemate Randall for putting up with me having the executive-style desk setup for two and a half years. Even though the basketball team never really had a good season, I enjoyed going to the games with you and discussing sports during our breaks from work. Good luck with the rest of your research! I would also like to thank the following people who helped make graduate school memorable and joined me in some type of road trip or camping excursion: Jess, Arthur, Rick Jones, Evan, Hayes, Billy, Potter, Jodi, Gabrielle, Holly, Jackie, and Mike Merrick.

Thank you to my parents and my brother for all of your support and encouragement to get me through graduate school. Dad, thank you for your work ethic, always believing in me, and for putting the time commitment of graduate school in perspective relative to the number of years I would be working in my career. As you said, the additional few years went by really fast, and I was still able to have a good time while being a student and earning a graduate student stipend. Mom, thanks for always thinking about me and for listening to me when I called. To my brother, Mike, thank you for introducing me to the Agricultural

and Biological Engineering department at Penn State. I would have never found out about this field of study if it wasn't for you. I likely would have ended up crunching numbers somewhere in an office, instead of being able to work outdoors. Thanks for everything you taught me and for everything we did together. I just wanted to let you to know that I beat you to graduate from grad school, so I do expect you to address me as doctor. I also want to thank my grandparents and extended family for all of your support. Finally, I would like to thank my N.C. parents, Malcolm and Cindy, for providing me with a short escape from Raleigh to go fishing, eat some delicious southern cuisine, or watch some ACC basketball.

In saving the best for last, thank you Jess! You have probably helped me the most. I appreciate all of your love, support, encouragement, cooking, and for showing me all the cool things about the south and North Carolina. Our adventures all over the east coast have been A LOT of fun, and I cannot wait to live in the same town as you again. Even though I am a little crazy, thanks for saying 'yes' and for agreeing to go down Sliding Rock back in April. Now that this chapter of my life is ending, I am excited for our future together and to not be over 500 miles apart anymore.

TABLE OF CONTENTS

LIST OF TABLES	xii
LIST OF FIGURES	xvi
1 BIORETENTION LITERATURE REVIEW AND PROJECT OVERVIEW	1
1.1 SOURCES AND IMPACTS OF URBAN STORMWATER RUNOFF	1
1.2 STORMWATER TREATMENT – PAST AND PRESENT	2
1.3 RESULTS FROM PREVIOUS BIORETENTION STUDIES	4
1.4 PROJECT OVERVIEW	6
1.5 REFERENCES	9
2 UNDERDRAIN CONFIGURATION TO ENHANCE BIORETENTION EXFILTRATION TO REDUCE POLLUTANT LOADS	12
2.1 ABSTRACT	12
2.2 INTRODUCTION	13
2.3 METHODOLOGY	16
2.3.1 Site Description	16
2.3.2 Sampling Methods	19
2.3.3 Statistical Methods	21
2.3.4 Mass Balance Calculations	21
2.4 RESULTS	24
2.4.1 Hydrology	24
2.4.2 Water Quality	29
2.5 DISCUSSION	35
2.6 SUMMARY AND CONCLUSIONS	36
2.7 ACKNOWLEDGEMENTS	37
2.8 REFERENCES	38
3 IMPACTS OF MEDIA DEPTH ON EFFLUENT WATER QUALITY AND HYDROLOGIC PERFORMANCE OF UNDER-SIZED BIORETENTION CELLS	42
3.1 ABSTRACT	42
3.2 INTRODUCTION	43
3.3 SITE DESCRIPTION AND METHODS	45
3.4 FIELD DATA COLLECTION AND ANALYSIS	51
3.5 CALCULATING RUNOFF, OUTFLOW, OVERFLOW, AND EVAPOTRANSPIRATION	53
3.5.1 Runoff	53
3.5.2 Outflow and Overflow	54

3.5.3	Evapotranspiration	56
3.6	RESULTS AND DISCUSSION	57
3.6.1	Hydrology	57
3.6.2	Water Quality.....	62
3.6.2.1	Nitrogen Species.....	64
3.6.2.2	Phosphorus Species	66
3.6.2.3	Total Suspended Solids	67
3.6.3	Load Calculations	67
3.7	CONCLUSIONS.....	70
3.8	ACKNOWLEDGEMENTS	72
3.9	REFERENCES.....	72
4	IMPACT OF MAINTENACE AND IM(PROPERLY) SIZING BIORETENTION ON HYDROLOGIC PERFORMANCE.....	76
4.1	ABSTRACT	76
4.2	INTRODUCTION.....	77
4.3	METHODOLOGY.....	79
4.3.1	Site Description.....	79
4.3.2	Field Data Collection Methods.....	83
4.3.3	Statistical Methods.....	84
4.3.4	Mass Balance Calculations	85
4.4	RESULTS.....	87
4.4.1	Flow Characterization and Annual Water Balance.....	87
4.4.2	Volume and Flow Reduction	91
4.5	DISCUSSION	98
4.6	CONCLUSIONS.....	100
4.7	ACKNOWLEDGEMENTS	102
4.8	REFERENCES.....	102
5	ANALYSIS OF CLIMATIC FACTORS AND CONSECUTIVE EVENTS FOR FIELD MONITORED BIORETENTION CELLS.....	105
5.1	ABSTRACT	105
5.2	INTRODUCTION.....	106
5.3	METHODOLOGY.....	110
5.3.1	Site Description.....	110
5.3.2	Field Data Collection Methods	112
5.3.3	Statistical Methods.....	115
5.4	RESULTS.....	116
5.4.1	Consecutive Events.....	116

5.4.2	Precipitation Characterization of Water Quality Events.....	127
5.4.3	Correlation of Environmental Factors	128
5.4.4	Concentration Analysis.....	132
5.4.5	Load Analysis	136
5.5	CONCLUSIONS.....	139
5.6	ACKNOWLEDGEMENTS	141
5.7	REFERENCES.....	142
6.	LID TREATMENT TRAIN: PERVIOUS CONCRETE WITH SUBSURFACE STORAGE IN SERIES WITH BIORETENTION AND CARE WITH SEASONAL HIGH WATER TABLES	146
6.1	ABSTRACT.....	146
6.2	INTRODUCTION.....	147
6.3	METHODOLOGY.....	149
6.3.1	Site Description.....	149
6.3.2	Sampling Methods	152
6.3.3	Water Quality Methods.....	153
6.3.4	Runoff Calculation.....	154
6.3.5	Statistical Methods.....	155
6.4	RESULTS AND DISCUSSION	155
6.4.1	Precipitation Characterization and Hydrology.....	155
6.4.2	Water Quality.....	159
6.4.3	Comparison to Single Practices	163
6.5	CONCLUSIONS.....	164
6.6	ACKNOWLEDGEMENTS	165
6.7	REFERENCES.....	166
7.	MODELING BIORETENTION HYDROLOGY WITH DRAINMOD	170
7.1	ABSTRACT.....	170
7.2	INTRODUCTION.....	171
7.3	MODEL DESCRIPTION AND APPLICATION.....	178
7.3.1	DRAINMOD Description.....	178
7.3.2	Comparison of Bioretention Design Specifications to DRAINMOD Inputs..	181
7.4	DETERMINATION OF INPUT PARAMETERS	182
7.4.1	Site Description.....	182
7.4.2	Monitoring Methods	183
7.4.3	Drainage Coefficient.....	185
7.4.4	Soil	186
7.4.5	Climate.....	187

7.4.5.1	Temperature.....	187
7.4.5.2	Precipitation.....	187
7.4.5.3	Potential Evapotranspiration.....	188
7.5	MODEL RESULTS	189
7.5.1	Contributing Area Runoff.....	190
7.5.2	Nashville Site – Conventional Drainage Configuration	192
7.5.2.1	Post-Repair Monitoring Period (Year 2)	192
7.5.2.2	Pre-Repair Monitoring Period [Clogged and Undersized] (Year 1).....	196
7.5.3	Rocky Mount Site – IWS Drainage Configuration.....	200
7.5.3.1	Sandy Clay Loam (SCL) Cell.....	200
7.5.3.2	Sand Cell.....	207
7.6	ANALYSIS OF INPUT PARAMETERS.....	208
7.6.1	Drainage Configuration	209
7.6.2	Drainage Area to Bioretention Surface Area Ratio	214
7.6.3	Media Type	221
7.7	CONCLUSIONS.....	222
7.8	ACKNOWLEDGEMENTS	224
7.9	REFERENCES.....	225
8	IMPACTS OF CONSTRUCTION ACTIVITY ON BIORETENTION	
	PERFORMANCE.....	229
8.1	ABSTRACT.....	229
8.2	INTRODUCTION.....	230
8.3	CONSTRUCTION DESCRIPTION	234
8.4	MONITORING METHODS.....	238
8.5	RESULTS.....	241
8.5.1	Nashville (Sandy Soil Site).....	241
8.5.2	Raleigh (Clay Soil Site)	245
8.5.3	Combined Results	249
8.6	CONCLUSIONS.....	251
8.7	ACKNOWLEDGEMENTS	252
8.8	REFERENCES.....	253
9	RECOMMENDATIONS FOR FUTURE WORK	257
	APPENDICES	260
	A. APPENDIX: USER’S MANUAL FOR MODELING BIORETENTION WITH	
	DRAINMOD.....	261
	Background.....	261
	Step 1: Opening a File	262

Step 2: Creating a Contributing Area Runoff File	262
Step 3: Creating Weather Files.....	263
Step 4: Create Soil File for Asphalt (Parking Lot).....	268
Step 5: Change Drainage Design for Parking Lot.....	269
Step 6: Run DRAINMOD for Parking Lot Runoff	270
Step 7: Create Contributing Runoff File	271
Step 8: Setup DRAINMOD for Bioretention Cell Design.....	273
Step 9: Adding Contributing Runoff File.....	274
Step 10: Add/Create Soil File for Bioretention Media.....	274
Step 11: Verify/Enter Weather Information for Bioretention Site.....	279
Step 12: Enter Design Parameters.....	280
Step 13: Run simulation.	287
References:.....	287
B. APPENDIX: EXAMPLE SAS CODE	289

LIST OF TABLES

Table 2.1: Summary of Rocky Mount bioretention cell characteristics.	18
Table 2.2: Summary of analytical methods for water quality analysis.....	21
Table 2.3: Curve number and initial abstraction depths for pervious and impervious land uses and varying antecedent moisture conditions (USDA-NRCS 2004b).....	22
Table 2.4: Characterization of precipitation events for the first (deep IWS zone) and second (shallow IWS zone) monitoring periods.....	24
Table 2.5: Summary of frequency of events with drainage and overflow during both monitoring periods.....	28
Table 2.6: Average EMC and statistical analyses comparing grab samples from the SCL cell to runoff samples.....	30
Table 2.7: Summary of water quality results from the Sand cell and comparison of Sand cell paired samples to runoff and the SCL cell.....	31
Table 2.8: Summary of water quality results for events with drainage from SCL cell and statistical analyses of EMCs for runoff and SCL cell drainage samples.....	33
Table 2.9: Comparison of runoff and Rocky Mount bioretention cell treated runoff concentrations to benthic health water quality metrics (McNett et al. 2010).	34
Table 3.1: Summary of Nashville, NC bioretention cell characteristics.....	51
Table 3.2: Summary of analytical methods for water quality analysis.....	53
Table 3.3: Curve number and initial abstraction values for pervious and impervious land uses and varying antecedent moisture conditions.....	54
Table 3.4: Summary of water balance for various sized storm events.....	61
Table 3.5: Characterization of forms of outflow monitored.....	62
Table 3.6: Average EMCs (mg/L), efficiency ratios, and statistical analyses for parking lot runoff and outflow from the 0.6-m and 0.9-m media depth bioretention cells.....	64
Table 3.7: Pollutant load calculations for the 18 events with available flow and water quality data.....	68
Table 3.8: Seasonal summary of the precipitation depths of events used to calculate pollutant loads compared to normal seasonal precipitation depths.....	69
Table 3.9: Estimation of annual pollutant loads for the bioretention cells based on normal rainfall depths.....	69
Table 4.1: Summary of Nashville, NC bioretention cell characteristics.....	83
Table 4.2: Curve number and initial abstraction values for pervious and impervious land uses and varying antecedent moisture conditions (USDA-NRCS 2004a, 2004b).....	85
Table 4.3: Characterization of forms of outflow monitored.....	88

Table 4.4: Partitioning of hydrologic fates for various sized storm events	90
Table 4.5: Summary table of 24-hour effluent/influent volume ratios.	92
Table 4.6: Summary table of peak flow rate ratios.	94
Table 4.7: Flow duration and rainfall characteristics during both monitoring periods.....	96
Table 4.8: Durations of precipitation-normalized flow rates greater than specified values. .	98
Table 5.1: Summary of analytical methods for water quality analysis.	114
Table 5.2: Characteristics for events sampled consecutively.	126
Table 5.3: Rainfall characteristics for both monitoring periods where samples were collected from all three locations.....	127
Table 5.4: Spearman rank correlation coefficients (ρ) between runoff and environmental factors ($n = 23$, except for TSS, $n = 22$).	129
Table 5.5: Spearman rank correlation coefficients (ρ) between 0.6-m media depth outflow and environmental factors ($n = 25$).	129
Table 5.6: Spearman rank correlation coefficients (ρ) between 0.9-m media depth outflow and environmental factors ($n = 24$, except for TSS, $n = 23$).	130
Table 5.7: Average EMCs (mg/L), efficiency ratios, and statistical analyses for parking lot runoff and outflow from the 0.6-m and 0.9-m media depth bioretention cells (paired data from post-repair period only, $n=22$, unless otherwise noted).	133
Table 5.8: Comparing runoff concentrations from the pre-repair to post-repair periods. ..	136
Table 5.9: Summary of the cumulative pollutant loads calculated for 22 water quality events.	137
Table 5.10: Seasonal summary of the precipitation depths of events used to calculate pollutant loads compared to normal seasonal precipitation depths.	138
Table 5.11: Estimation of annual pollutant loads for the bioretention cells based on normal rainfall depths.	139
Table 6.1: Summary of analytical methods for water quality analysis.	154
Table 6.2: Rainfall characteristics of all events, events with outflow, and events sampled for water quality.	156
Table 6.3: Water quality concentrations for paired samples of asphalt parking lot runoff and outflow from the PC-B. (All concentrations are in units mg/L)	160
Table 6.4: Comparison of PC-B outflow and baseflow water quality concentrations.....	162
Table 6.5: Annual pollutant loads for parking lot runoff (computed) and monitored outflow.	163
Table 6.6: Comparison of performance for PC-B to a single LID practice – bioretention with 0.6-m and 0.9-m media depth (Chapter 4).....	164

Table 7.1: Comparison of calculating volume of water drained from media based on water table depth by using soil-water characteristic curve or by subtracting field capacity from saturated volumetric water content.	177
Table 7.2: DRAINMOD inputs are compared to typical bioretention design parameters...	181
Table 7.3: Relating DRAINMOD outputs applicable to bioretention cells.	182
Table 7.4: Soil-water characteristics for Rocky Mount and Nashville media.	186
Table 7.5: Comparison of measured/estimated and predicted (modeled) results for the Nashville bioretention cells, during the post-repair period.	193
Table 7.6: Comparison of measured/estimated and predicted (modeled) results for the Nashville bioretention cells, during the pre-repair period.	197
Table 7.7: Comparison of measured/estimated and predicted (modeled) results for the SCL cell at Rocky Mount.	201
Table 7.8: Comparison of measured/estimated and predicted (modeled) results for the Sand cell at Rocky Mount.	208
Table 7.9: Summary of Nashville site fate of runoff if an IWS zone was included that had an outlet 30 cm from the surface of the media.	210
Table 7.10: Analysis of the impact of an IWS zone with restrictive underlying soils.	212
Table 7.11: Analysis of reducing drainage coefficient for a conventionally drained bioretention cell with restrictive underlying soils (vertical conductivity of underlying soils = 0.1 cm/hr).	213
Table 7.12: Analysis of drainage area to bioretention area ratio for bioretention cells designed to capture the 25-mm event (media saturated hydraulic conductivity = 2.5 cm/hr).	215
Table 7.13: Analysis of drainage area to bioretention area ratio for bioretention cells designed to capture the 25-mm event (media saturated hydraulic conductivity = 5.0 cm/hr).	216
Table 7.14: Over-sizing and under-sizing bioretention cells based on surface storage depth.	217
Table 7.15: Over-sizing and under-sizing bioretention cells based on surface area.	219
Table 7.16: Varying design parameters for several bioretention cells that would treat 90 percent of annual runoff in Piedmont, NC (Raleigh-Durham weather [1950-2009]).	220
Table 7.17: Varying design parameters for several bioretention cells that would treat 90 percent of annual runoff in coastal counties of NC (Wilmington weather [1950-2009]).	221
Table 7.18: Comparison of SCL performance at Rocky Mount had a different media (from Nashville site) been used. (Infiltration parameters remained constant).	222
Table 8.1: Results from soil tests for hydraulic conductivity (K_{Sat}), surface infiltration, and dry bulk density for Nashville site.	242

Table 8.2: Changes in performance by using rake method over scoop method.	243
Table 8.3: Average soil cone index for individual infiltration test sites with corresponding infiltration rates.	245
Table 8.4: Results from soil tests for hydraulic conductivity (K_{Sat}), infiltration, and dry bulk density for Raleigh site.	247
Table 8.5: Changes in performance by varying excavation technique and soil moisture condition.	248
Table 8.6: Average soil cone index for individual infiltration test sites with corresponding infiltration rates.	249
Table 8.7: Effects of soil condition on infiltration and saturated hydraulic conductivity ...	250
Table 8.8: Effects of soil type on infiltration and saturated hydraulic conductivity.....	250
Table A.1: Thornthwaite correction factors for Tarboro and three eastern NC stations	267
Table A.2: Description of DRAINMOD hydrology outputs in terms of bioretention meaning.	271
Table A.3: Soil-water characteristic relationships for a variety of bioretention media.	275
Table A.4: Measured seepage rates from various bioretention cells in North Carolina.	286

LIST OF FIGURES

Figure 1.1: Diagram of features and hydrologic processes for a conventionally drained bioretention cell.	3
Figure 2.1: Diagram of a bioretention cell with internal water storage (IWS) zone.	14
Figure 2.2: Map of study location in reference to the coastal plain/Piedmont divisions (solid black line) in North Carolina	17
Figure 2.3: Bioretention cell images: Sand cell (left) and SCL cell (right).....	17
Figure 2.4: Cross sections describing the profiles of the Sand cell (top) and Sandy Clay Loam (SCL) cell (bottom); all units are in meters.....	17
Figure 2.5: Outflow volume versus runoff volume for the Sand cell.....	25
Figure 2.6: Outflow volume versus runoff volume for the SCL cell.....	26
Figure 2.7: Drainage volume versus treated runoff volume (runoff volume minus overflow volume) for the SCL cell.....	27
Figure 2.8: Summary of water balance (fate of runoff) for both monitoring periods.....	29
Figure 3.1: Location map of Nashville (solid star) with relation to Raleigh – NCSU campus (hollow star).....	46
Figure 3.2: Layout of bioretention cells at the study site.....	47
Figure 3.3: Bioretention cell shortly after planting and mulching were completed	48
Figure 3.4: Bioretention cell after a storm in November, 2008 (after 1 growing season)....	48
Figure 3.5: Woven geotextile fabric was placed on top of media (left) prior to the parking lot being paved with asphalt to prevent sediment from construction (right) from clogging the media.....	49
Figure 3.6: Fines layer present within top layer (25 to 75 mm) of the media.	50
Figure 3.7: Outflow rate in the 0.9-m media depth cells and total rainfall amount versus time for an event with overflow (left) and without overflow (right)	55
Figure 3.8: Exceedance probability of 24-hour effluent/influent volume ratio in Nashville bioretention cells.....	58
Figure 3.9: Water budget for 1 year monitoring period for Nashville bioretention cells.....	60
Figure 4.1: Bioretention cell layout diagram	80
Figure 4.2: Image of the bioretention cells after two years (July 2010).....	80
Figure 4.3: Image highlighting the granite fines (clogging) layer (dashed box) present in top 25 to 75 mm (1 to 3 in) of the media	81
Figure 4.4: Fate of runoff in bioretention cells for both pre- and post-repair monitoring periods.....	89
Figure 4.5: Exceedance probability plots for 24-hour effluent/influent volume ratios.	92

Figure 4.6: Exceedance probability plots for peak flow rate ratios.	94
Figure 4.7: Exceedance durations for specified precipitation-normalized flow rates for both monitoring periods.	97
Figure 5.1: Bioretention cell layout diagram.	111
Figure 5.2: Images of the bioretention cells	111
Figure 5.3: Example of evolution of cumulative pollutant load graph	117
Figure 5.4: Cumulative load versus cumulative volume graph for TSS.	119
Figure 5.5: Cumulative load versus cumulative volume graph for TP.	121
Figure 5.6: Cumulative load versus cumulative volume graph for Part-P.	121
Figure 5.7: Cumulative load versus cumulative volume graph for Ortho-P.	122
Figure 5.8: Cumulative load versus cumulative volume graph for nitrogen species in runoff.	124
Figure 5.9: Cumulative load versus cumulative volume graph for nutrient species in outflow from the 0.6-m media depth cells.	124
Figure 5.10: Cumulative load versus cumulative volume graph for nutrient species in outflow from the 0.9-m media depth cells.	125
Figure 6.1: Images of the pervious concrete (A) and bioretention cell that received drainage from pervious concrete site (B).	150
Figure 6.2: Site layout of the parking lot and SCMs.	151
Figure 6.3: Relationship of flow volume versus rainfall depth for runoff and outflow	157
Figure 6.4: Annual flow duration curve for outflow from the PC-B system and parking lot runoff from a 100 percent impervious asphalt surface.	159
Figure 7.1: Description of volumetric water content present in profile for Nashville media when the water table depth is 0.6 m, where the soil-water characteristic (solid line) and field capacity (long dashes) are presented.	177
Figure 7.2: Predicted (modeled) versus estimated runoff volume data for pre-repair (validation) period of the 0.6-m media depth bioretention cells at Nashville	191
Figure 7.3: Cumulative fate of runoff for 0.6-m media depth cells at Nashville, during the post-repair monitoring period.	195
Figure 7.4: Cumulative fate of runoff for 0.9-m media depth cells at Nashville, during the post-repair monitoring period.	195
Figure 7.5: Cumulative fate of runoff for 0.6-m media depth cells at Nashville, during the pre-repair monitoring period.	199
Figure 7.6: Cumulative fate of runoff for 0.9-m media depth cells at Nashville, during the pre-repair monitoring period.	199
Figure 7.7: Cumulative fate of runoff for SCL cell at Rocky Mount, during the calibration period (shallow IWS zone monitoring period).	202

Figure 7.8: Cumulative fate of runoff for SCL cell at Rocky Mount, during the validation period (deep IWS zone monitoring period).	203
Figure 7.9: Comparison of predicted versus measured water table depths for SCL cell at Rocky Mount, during the calibration period (shallow IWS zone monitoring period).	204
Figure 7.10: Comparison of predicted versus measured water table depths for SCL cell [February to May 2009].	205
Figure 7.11: Comparison of predicted versus measured water table depths for SCL cell [May to September 2009].	205
Figure 7.12: Comparison of predicted versus measured water table depths for SCL cell [September 2009 to January 2010].	206
Figure 8.1: Photos demonstrating rake method (left) versus scoop method (right) for excavation.	234
Figure 8.2: Overhead schematic of the soil testing layout.....	236
Figure 8.3: Layout of soil cores (circles) and double-ring infiltrometers (rectangles) in the field for the site that employed the scoop method	237
Figure 8.4: Typical graph of double-ring infiltrometer inner ring depths versus time.....	240
Figure 8.5: Saturated hydraulic conductivity versus dry bulk density for the Nashville site.....	244
Figure 8.6: Average compaction levels in the “wet” cell test plot for the scoop versus rake excavation methods at the Nashville site	244
Figure A.1: User interface for contributing area runoff file.	263
Figure A.2: Location of DRAINMOD utilities and input files.....	264
Figure A.3: Examples of format for <i>.wea</i> files for temperature (left), daily rainfall (middle), and hourly rainfall (right).....	265
Figure A.4: Interface of DRAINMOD weather utility.	266
Figure A.5: Input PET data for Nashville site for using the monthly Thornthwaite method with correction factors.	268
Figure A.6: Adjusted Green Ampt infiltration parameters for parking lot soil file.....	269
Figure A.7: Adjusted drainage system design for an impervious surface (parking lot).	270
Figure A.8: Example of an <i>.inp</i> file.	272
Figure A.9: User interface for contributing area runoff utility.	272
Figure A.10: User interface for bioretention design file.....	273
Figure A.11: User interface for adding contributing runoff file and drainage area to bioretention area ratio.	274
Figure A.12: Pressure plate apparatus (tension table) used to measure soil-water characteristic curves.....	276
Figure A.13: Interface for “ <i>Create Soil File</i> ” utility.	278

Figure A.14: Example of <i>.soi</i> file.	279
Figure A.15: System design interface in DRAINMOD.....	281
Figure A.16: Drainage design diagram for agricultural field with drainage pipes.....	282
Figure A.17: Drainage design diagram for bioretention cell with an IWS drainage configuration.....	282
Figure A.18: Interface for lateral saturated hydraulic conductivity for multiple layers.....	283
Figure A.19: Interface for crop root depths.....	284
Figure A.20: Interface and diagram for vertical seepage parameters.....	285
Figure A.21: Interface for controlled drainage weir settings (IWS zone configuration).....	287

1 BIORETENTION LITERATURE REVIEW AND PROJECT OVERVIEW

1.1 SOURCES AND IMPACTS OF URBAN STORMWATER RUNOFF

A direct result of urbanization is an increase in impervious surfaces, which leads to detrimental impacts caused by urban stormwater runoff. Impacts include: increased runoff volume, peak discharge, and pollutant export (Lee and Bang 2000; Line et al. 2002; Line and White 2007; Makepeace et al. 1995). As impervious surfaces increase, an according increase of pollutant sources occurs. For example, from highway runoff studies, automobiles were identified as a pollutant source (Barrett et al. 1998; Wu et al. 1998). A substantial amount of certain pollutant loads also originate from atmospheric deposition. In urban highway runoff, atmospheric deposition accounted for approximately 20 percent of total suspended solid loadings, 30 to 50 percent of heavy metals loadings (Cu, Cr, Pb), and 70 to 90 percent of nitrogen loadings (Wu et al. 1998). Stormwater pollutants of most concern include: nutrients, pesticides, volatile organic compounds, other organics, pathogens, heavy metals, and salts (Pitt et al. 2002). Dependent upon the source, some of these pollutants are of greater concern in specific land uses. Nutrients in urban runoff originate from fertilizers, animal waste, and atmospheric deposition (Bannerman et al. 1993; Wu et al. 1998). Volatile organic compounds and other organics are mainly found in runoff from industrial areas and near vehicle service establishments (Pitt et al. 2002). Fecal coliform, an indicator bacteria species, was found with higher levels in residential areas as compared to commercial or industrial areas because the primary source originates from animal waste (Bannerman et al. 1993). Zinc was found predominantly in areas with exposed galvanized metal, usually industrial roofs (Bannerman et al. 1993). Some heavy metals originate from automobiles and atmospheric deposition (Barrett et al. 1998; Wu et al. 1998). Finally, salts (chloride) are mostly found in areas that apply road salt during winter, and these concentrations are the highest in the early spring, following snowmelt runoff (Pitt et al. 2002). The sites presented

in this dissertation are located in a nutrient sensitive watershed, the Tar-Pamlico River Basin, so nutrients are the pollutants of concern examined herein.

In the most recent National Water Quality Inventory, 44 percent of river and stream miles, 64 percent of lake acres, and 30 percent of estuary square miles were identified as impaired (USEPA 2009). For all of these waterbodies, nutrients were identified as a top five cause for impairment, with urban stormwater runoff being a top ten source of impairment (USEPA 2009). Additionally, the Wadeable Streams Assessment discovered that 42 percent of U.S. stream miles were in poor biological condition, and the top two most widespread stressors were nitrogen and phosphorus (USEPA 2009). As a way to minimize the impacts of nutrients on sensitive watersheds, total maximum daily load (TMDL) standards can be implemented. A non-point source of pollution that is regulated with TMDLs is urban stormwater runoff. These loading standards can be met with a wide variety of stormwater control measures (SCMs); however, one of the more effective SCMs to treat stormwater runoff quality is bioretention.

1.2 STORMWATER TREATMENT – PAST AND PRESENT

Traditionally, the focus of stormwater management was to reduce peak flow rates. Whereas, the new focus has shifted to include reduction of pollutant export and restoration of the pre-developed hydrologic condition of the landscape. To achieve these goals, low impact development (LID) practices have been installed. These practices target stormwater runoff treatment at the source by promoting infiltration and evapotranspiration (ET) using natural approaches (Davis 2005). Examples of LID practices include: vegetated filter strips, vegetated swales, green roofs, cisterns, permeable pavement, and bioretention, with the latter being the focus of this dissertation. Bioretention is widely used because of its versatility and previously determined level of performance. It combines a natural and engineered system to manage stormwater from highly impervious surfaces. They are designed to improve the water quality of runoff by capturing and treating runoff from a regulation specified rainfall depth. Bioretention serves three major functions: restore the hydrologic condition of the landscape, improve water quality, and improve aesthetics.

Runoff temporarily ponds in the surface storage zone, commonly referred to as the bowl. Then, it infiltrates through the filter media, and either exfiltrates through the system to recharge shallow groundwater, evapotranspires through shrubs and grasses planted in the bioretention cell, or it collects in subsurface perforated pipes and is transported to traditional storm drains or drainage ditches. A diagram describing these processes and the features for a conventionally drained bioretention cell is displayed in Fig. 1.1. Infiltration is one of the primary mechanisms for bioretention cell functionality. Thus, to ensure long-term success, maintenance must be performed to sustain a permeable surface. Bioretention removes pollutants from runoff through the processes of adsorption, volatilization, ion exchange, biological decomposition, filtration, and sedimentation.

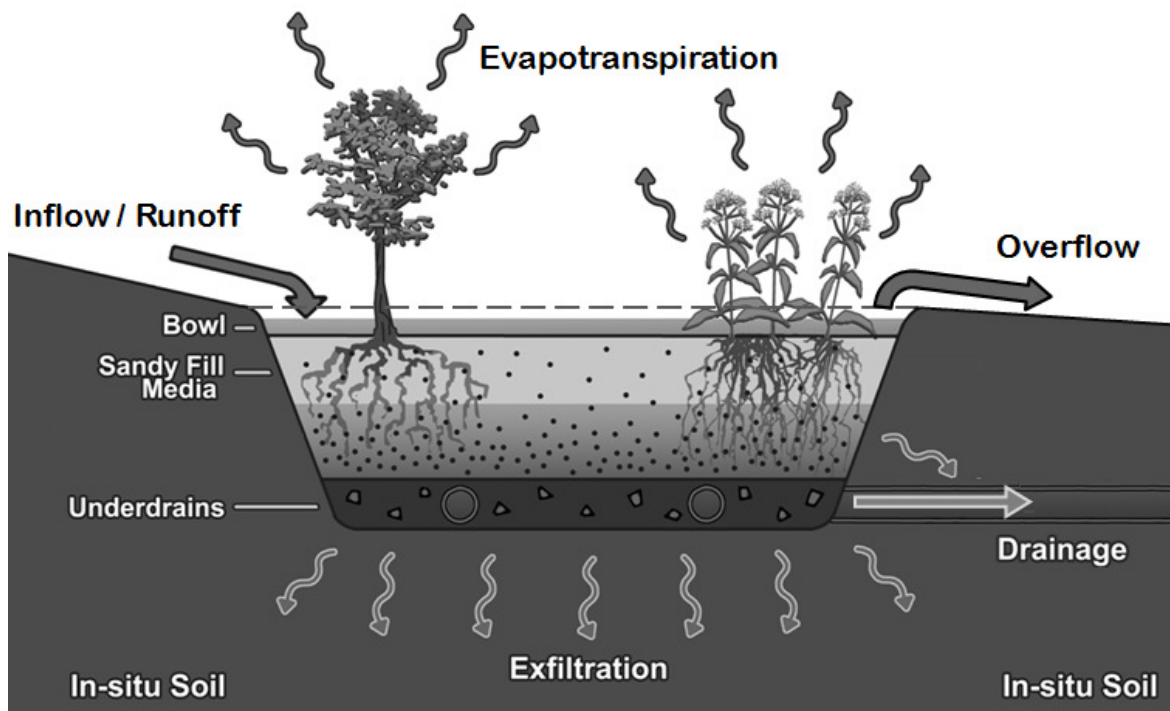


Figure 1.1: Diagram of features and hydrologic processes for a conventionally drained bioretention cell.

1.3 RESULTS FROM PREVIOUS BIORETENTION STUDIES

Since the original concept of bioretention was first introduced over 18 years ago in Prince George's County, Maryland, intensive bioretention research and installation experience have assisted in the evolution of bioretention design guidelines. However, further research is necessary to continue to refine design criteria. Research has shown bioretention cells are effective at removing many pollutants (i.e., sediment, heavy metals, oil/grease, nitrogen, phosphorus, pathogen indicator species, thermal pollution) from urban runoff, with the level of performance varying based on the design and soil media composition (Bratieres et al. 2008; Davis et al. 2001, 2003, 2006; Dietz and Clausen 2006; Hatt et al. 2009; Hsieh and Davis 2005a; Hunt et al. 2006, 2008; Jones and Hunt 2009; Kim et al. 2003; Li and Davis 2008; Roseen et al. 2006). However, in some of these studies, total nitrogen (TN) removal was absent due to poor bioretention media selection (Hunt et al. 2006), influx of groundwater into the underdrain (Line and Hunt 2009), or lack of an anaerobic zone to promote denitrification for the reduction of nitrate and nitrite ($\text{NO}_{2,3}\text{-N}$) (Kim et al. 2003). Total phosphorus (TP) removal efficiency was decreased when the bioretention media was enriched with phosphorus (Hunt et al. 2006; Hatt et al. 2009). Since prior research has shown some uncertainty with respect to nutrient performance and the study sites examined herein lie in a nutrient sensitive watershed, performance was measured for nitrogen and phosphorus species.

Nitrogen sequestration provided by bioretention has varied due to media composition, vegetation, and drainage configuration (Bratieres et al. 2008; Hunt et al. 2006; Kim et al. 2003; Lucas and Greenway 2008). Original bioretention designs included a conventional underdrain configuration, which consisted of lateral, perforated drain tubes present in a gravel layer beneath the filter media (Fig. 1.1). The media in conventionally drained bioretention cells is primarily aerobic, so microbial processes in the media convert total ammoniacal nitrogen (TAN) to $\text{NO}_{2,3}\text{-N}$ through nitrification. The absence of an anaerobic environment prevented $\text{NO}_{2,3}\text{-N}$ from converting to nitrogen gas through denitrification, so $\text{NO}_{2,3}\text{-N}$ is often released with the effluent. Consequently, "removal" of $\text{NO}_{2,3}\text{-N}$ has been

poor, and in most cases, effluent NO_{2,3}-N concentrations increased (Davis et al. 2001, 2006; Hatt et al. 2009; Hsieh and Davis 2005b; Hunt et al. 2006, 2008; Line and Hunt 2009; Roseen et al. 2006).

As a design modification to promote denitrifying conditions, Kim et al. (2003) proposed a raised underdrain outlet to create a continuously submerged anaerobic zone, also known as an internal water storage (IWS) zone. Pilot-scale bioretention studies using this configuration reported 70 to 80 percent mass removal rates of NO_{2,3}-N (Kim et al. 2003). Despite promising laboratory results, subsequent field studies by Hunt et al. (2006) and Dietz and Clausen (2006) were inconclusive about adding a saturated layer to reduce NO_{2,3}-N concentrations. However, with limited data, Davis (2007) reported high removal rates of NO_{2,3}-N, and Passeport et al. (2009) had a significant NO_{2,3}-N concentration reduction for one of the two cells studied. The cell with the significant NO_{2,3}-N reduction had a tighter underlying soil, so it maintained a longer saturation period (Passeport et al. 2009).

Besides the NO_{2,3}-N removal benefit, an IWS zone was shown to have a positive hydrologic impact on outflow reduction when underlying soils had higher hydraulic conductivities (Li et al. 2009; Passeport et al. 2009). However, more studies are needed to explore the impact of other in-situ soils and to optimize the IWS zone depth. At sites with slow exfiltration rates, successive events can cause a reduction in hydrologic performance and for more outflow volume to be generated for a cell with an IWS zone compared to one with conventional drainage (Li et al. 2009). Current research shows that from a hydrologic perspective, IWS zones should work best in regions with sandier underlying soils. These types of soils are found in coastal regions, which are where many protected waterbodies are located. In NC, the 20 coastal counties must comply with a specific set of more stringent stormwater regulations (NCDENR 2009).

In a comparison of six bioretention cells in NC and MD, Li et al. (2009) showed that deeper media depths promoted more exfiltration and ET and more closely mimicked predevelopment hydrology. They concluded that media depth may be a controlling design parameter to meet target hydrologic performance goals. Also, fewer instances of outflow

occurred for bioretention cells with larger bioretention surface area to drainage area ratios (Jones and Hunt 2009). Finally, bioretention has been extremely effective at reducing peak flow rates for all events other than those that overwhelm the surface storage zone (Hunt et al. 2008; Li et al. 2009).

1.4 PROJECT OVERVIEW

Prior to this project's start, the only bioretention field studies in North Carolina took place in the Piedmont, where underlying soils tend to have higher clay content (Hunt et al. 2006, 2008; Li et al. 2009; Line and Hunt 2009; Passeport et al. 2009). The results of these prior studies were used to improve design guidance and media selection recommendations and to establish state-wide pollutant removal credits for TN, TP, and total suspended solids. Pollutant removal credit was only awarded to cells that were constructed to capture a specific water quality volume based on the region [38 mm (1.5 in) in the coastal counties and 25 mm (1.0 in) everywhere else in NC]. Regardless of the underlying soil type, drainage configuration, surface storage capture volume, and media depth, the same design recommendations and credits were given. Therefore, the main objective of this research was to provide more detail on how these design configurations impact overall performance. This dissertation is divided into nine chapters. Chapters 2-6 describe the research results from field monitored bioretention cells in Rocky Mount and Nashville, NC. The results of modeling bioretention hydrology with DRAINMOD are presented in Chapter 7. Results from a field study exploring the impacts of construction activity on underlying soils are presented in Chapter 8, and recommendations for future work are summarized in Chapter 9.

More specifically, Chapter 2 discusses the impacts of designing bioretention cells with an IWS zone in the Upper Coastal Plain. The two bioretention cells constructed at the site in Rocky Mount were unique in that they had varying degrees of at least somewhat sandy underlying soils; one was sand and the other sandy clay loam. They were also studied for two different year-long monitoring periods, in which the IWS zone depth varied.

Chapters 3-5, discuss the hydrologic and water quality results in detail for the Nashville site. Multiple chapters were written from this site because additional opportunities emerged post-construction to monitor this site for two separate years. During a recent assessment of current bioretention knowledge, Davis et al. (2009) identified that fill media depth is a design specification in need of more research. For bioretention cells that require a specialized fill media that is mixed off-site, fill media represents one of the major costs. If performance of shallower systems were comparable to that of deeper systems, shallower systems would be preferred because of savings in soil material and excavation. Therefore, the primary objective of this research was to answer one of the critical questions associated with bioretention design and construction—the impact of fill media depth on bioretention performance. At this site, there were two sets of bioretention cells with varying media depths (0.6 m and 0.9 m). A secondary objective emerged post-construction, which was the impact of improperly sizing the surface storage zone. Due to construction and design errors, the surface storage volumes of the bioretention cells were severely undersized, and the surface was clogged with fine particles, which limited the infiltration rate. The water quality and hydrologic performance for bioretention cells that were clogged and sized to approximately one-third of the design volume are described in Chapter 3. After monitoring the cells for one year, the clogging layer was removed, which doubled the surface storage volume. Then the more appropriately sized cells were monitored for an additional year. The hydrologic and water quality results for the repaired cells are described in Chapters 4 and 5, respectively.

At the Nashville site, another bioretention cell was installed in series with a pervious concrete system that included a subsurface storage zone. Chapter 6 describes the results of having two infiltrating LID practices in series. The bioretention cell was installed at a location with a high water table, so an impermeable liner was installed to prevent groundwater from entering the bioretention media. However, the liner failed, so outflow occurred continuously. This study quantified the impact of installing bioretention cells at sites with high water tables. For this particular design and other LID practices in series, serious consideration should be taken to balance flow rate and outflow reduction versus cost.

Overall, bioretention cells can be designed and constructed with a variety of specifications: media depth, drainage configuration, media composition, drainage area to bioretention area ratio, and surface storage volume. However, a flexible performance metric needs to be established because systems with varying design features will perform differently. Since the beginning of the study, North Carolina has evolved its pollutant removal credit system to grant more credit for bioretention cells that include IWS zones and have underlying soils with higher hydraulic conductivities. The change in state standards was a direct result of the Rocky Mount field study. One option to create a flexible accounting standard would be to monitor numerous other combinations of design configurations. However, to achieve the same goal, but save the time and cost of monitoring countless field sites, the data collected from the field studies presented herein and those from other sites monitored in NC (Hunt et al. 2006; Li et al. 2009; Passeport et al. 2009) were used to calibrate and validate DRAINMOD to model long-term hydrology of bioretention cells, which is the focus of Chapter 7. The objective of this project was to field test DRAINMOD, a widely-accepted, long-term drainage model (Skaggs 1999), to determine if it could be used to model bioretention hydrology. There are many similarities in the soil-water dynamics in bioretention cells with underdrains as compared to agricultural fields with drainage pipes. An accurate and reliable model would allow for better predictions of how well bioretention cells will perform based on media depth, surface storage volume, underlying soil, and drainage configuration. Appendix A describes the necessary steps to model bioretention hydrology using DRAINMOD.

As another attempt to improve bioretention performance, the effect of construction activity on underlying soils was explored in Chapter 8. It specifically focused on how soil moisture and excavation technique impacted soil conditions in the bottom of the pit during excavation. The bottom of the pit was identified as an area of concern because this is where the interface for exfiltration is located. If construction techniques can minimize soil disturbance and allow for higher exfiltration rates, increased outflow and load reduction would be achieved.

1.5 REFERENCES

- Bannerman, R. T., Owens, D. W., Dodds, R. B., and Hornewer, N. J. (1993). "Sources of pollutants in Wisconsin stormwater." *Water Science and Technology*, 28 (3-5), 241-259.
- Barrett, M. E., Irish, L. B., Malina, J. F., and Charbeneau, R. J. (1998). "Characterization of highway runoff in Austin, Texas, area." *Journal of Environmental Engineering*, 124(2), 131-137.
- Bratieres, K., Fletcher, T. D., Deletic, A., and Zinger, Y. (2008). "Nutrient and sediment removal by stormwater biofilters: A large-scale design optimization study." *Water Research*, 42(14), 3930-3940.
- Davis, A. P., Shokouhian, M., Sharma, H., and Minami, C. (2001). "Laboratory study of biological retention for urban stormwater management." *Water Environment Research*, 73(1), 5-14.
- Davis, A. P., Shokouhian, M., Sharma, H., Minami, C., and Winogradoff, D. (2003). "Water quality improvement through bioretention: Lead, copper, and zinc removal." *Water Environment Research*, 75(1), 73-82.
- Davis, A. P. (2005). "Green engineering principles promote low-impact development." *Environmental Science and Technology*, 39(16), 338A-344A.
- Davis, A. P., Shokouhian, M., Sharma, H., and Minami, C. (2006). "Water quality improvement through bioretention media: Nitrogen and phosphorus removal." *Water Environment Research*, 78(3), 284-293.
- Davis, A. P. (2007). "Field performance of bioretention: Water quality." *Environmental Engineering Science*, 24(8), 1048-1064.
- Davis, A. P., Hunt, W. F., Traver, R. G., and Clar, M. (2009). "Bioretention technology: Overview of current practice and future needs." *Journal of Environmental Engineering*, 135(3), 109-117.
- Dietz, M. E., and Clausen, J. C. (2006). "Saturation to improve pollutant retention in a rain garden." *Environmental Science and Technology*, 40(4), 1335-1340.
- Hatt, B. R., Fletcher, T. D., and Deletic, A. (2009). "Pollutant removal performance of field-scale stormwater biofiltration systems." *Water Science and Technology*, 59(8), 1567-1576.

- Hsieh, C., and Davis, A. P. (2005a). "Evaluation and optimization of bioretention media for treatment of urban storm water runoff." *Journal of Environmental Engineering*, 131(11), 1521-1531.
- Hsieh, C., and Davis, A. P. (2005b). "Multiple-event study of bioretention for treatment of urban storm water runoff." *Water Science and Technology*, 51(3-4), 177-181.
- Hunt, W. F., Jarrett, A. R., Smith, J. T., and Sharkey, L. J. (2006). "Evaluating bioretention hydrology and nutrient removal at three field sites in North Carolina." *Journal of Irrigation and Drainage Engineering*, 132(6), 600-608.
- Hunt, W. F., Smith J. T., Jadlocki S. J., Hathaway, J. M., and Eubanks, P. R. (2008). "Pollutant removal and peak flow mitigation by a bioretention cell in urban Charlotte, NC." *Journal of Environmental Engineering*, 134(5), 403-408.
- Jones, M. P., and Hunt, W. F. (2009). "Bioretention impact on runoff temperature in trout sensitive waters." *Journal of Environmental Engineering*, 135(8), 577-585.
- Kim, H., Seagren, E. A., and Davis, A. P. (2003). "Engineered bioretention for removal of nitrate from stormwater runoff." *Water Environment Research*, 75(4), 355-367.
- Lee, J. H. and Bang, K. W. (2000). "Characterization of urban stormwater runoff." *Water Research*, 34(6), 1773-1780.
- Li, H., and Davis, A. P. (2008). "Heavy metal capture and accumulation in bioretention media." *Environmental Science and Technology*, 42(14), 5247-5253.
- Li, H., Sharkey, L. J., Hunt, W. F., and Davis, A. P. (2009). "Mitigation of impervious surface hydrology using bioretention in North Carolina and Maryland." *Journal of Hydrologic Engineering*, 14(4), 407-415.
- Line, D. E., White, N. M., Osmond, D. L., Jennings, G. D., and Mojonier, C. B. (2002). "Pollutant export from various land uses in the upper Neuse River basin." *Water Environment Research*, 74(1), 100-108.
- Line, D. E. and White, N. M. (2007). "Effects of development on runoff and pollutant export." *Water Environment Research*, 79(2), 185-190.
- Line, D. E., and Hunt, W. F. (2009). "Performance of a bioretention area and a level-spreader-grass filter strip at two highway sites in North Carolina." *Journal of Irrigation and Drainage Engineering*, 135(2), 217-224.

- Lucas, W. C., and Greenway, M. (2008). "Nutrient retention in vegetated and non-vegetated bioretention mesocosms." *Journal of Irrigation and Drainage Engineering*, 134(5), 613-623.
- Makepeace, D. K., Smith, D. W., and Stanley, S. J. (1995). "Urban stormwater quality: Summary of contaminant data." *Critical Reviews in Environmental Science and Technology*, 25(2), 93-139.
- N.C. Department of Environment and Natural Resources (NCDENR). (2009). "Chapter 2: North Carolina's stormwater requirements." *Stormwater best management practices manual*, North Carolina Department of Environment and Natural Resources, Division of Water Quality, Raleigh, N.C., 2.1–2.23.
- Passeport, E., Hunt, W. F., Line, D. E., Smith, R. A., and Brown, R. A. (2009). "Field study of the ability of two grassed bioretention cells to reduce storm-water runoff pollution." *Journal of Irrigation and Drainage Engineering*, 135(4), 505-510.
- Pitt, R., Chen, S., and Clark, S. (2002). "Compacted urban soils effects on infiltration and bioretention stormwater control designs." *Proceedings, 9th International Conference on Urban Drainage*, ASCE, Reston, Va.
- Roseen, R. M., Ballestero, T. P., Houle, J. J., Avelleneda, P, Widley, R., and Briggs, J. (2006). "Storm water low-impact development, conventional structural, and manufactured treatment strategies for parking lot runoff: Performance evaluations under varied mass loading calculations." *Transportation Research Record: Journal of the Transportation Research Board*, No. 1984, 135-147.
- Skaggs, R. W. (1999). "Drainage simulation models." *Agricultural drainage: Monograph No. 38*, R. W. Skaggs and J. van Schilfgaarde, eds., American Society of Agronomy, Madison, Wisc., 469-500.
- U.S. Environmental Protection Agency (USEPA). (2009). "National water quality inventory: Report to Congress—2004 reporting cycle." *Rep. No. EPA 841-R-08-001*, USEPA, Washington, D.C.
- Wu, J. S., Allan, C. J., Saunders, W. L., and Evett, J. B. (1998). "Characterization of pollutant loading estimation for highway runoff." *Journal of Environmental Engineering*, 124(7), 584-592.

2 UNDERDRAIN CONFIGURATION TO ENHANCE BIORETENTION EXFILTRATION TO REDUCE POLLUTANT LOADS

2.1 ABSTRACT

The bioretention drainage configuration of raising the outlet to create an internal water storage (IWS) layer in the media was originally intended to promote denitrifying conditions. The goal was to reduce nitrate and total nitrogen concentrations in nutrient sensitive watersheds. Two field studies in the Piedmont region of North Carolina, where the in-situ soils typically have high clay content, showed this design feature had potential to enhance exfiltration and reduce drainage from bioretention. Two bioretention cells in Rocky Mount, NC were monitored for two, year-long periods, to measure the impact of varying IWS zone depths over sandier underlying soils. Nearly 99 percent of runoff entering the bioretention cell with sand underlying soil (Sand cell) was never directly discharged to the stormwater network. However, the hydraulic residence time (contact time) of runoff in the media was less than three hours, and except for TSS, minimal pollutant removal was achieved. The other bioretention cell had a sandy clay loam underlying soil (SCL cell); the percentage of runoff leaving via exfiltration and evapotranspiration from this cell was 87 percent during the monitoring period with a 1.03-m IWS zone depth and 75 percent when the IWS zone depth was 0.73 m. The underlying soil of the SCL cell had a lower hydraulic conductivity, so water would remain in the IWS zone for up to seven days. The increased hydraulic residence time in the media resulted in lower outflow concentrations. For events monitored with drainage from the SCL cell, efficiency ratios of all the nitrogen species and TSS exceeded 0.5. As an additional metric of performance, the parking lot runoff and treated runoff from both the SCL and Sand cells were compared to concentrations consistent with “good” and “fair” benthic macroinvertebrate health in streams. Using this metric, the parking lot runoff only met the “fair” standard for total nitrogen (TN) and total phosphorus (TP), while treated runoff from the SCL cell achieved the “good” standard for both TN and

TP. However, due to the short hydraulic residence time of runoff in the media for the Sand cell, this cell only maintained the “fair” standard for TN and did not achieve the “fair” standard for TP.

2.2 INTRODUCTION

Low impact development (LID) practices are a new and evolving technology for stormwater managers to restore the altered hydrologic condition of the landscape created by urbanization. A primary goal and treatment mechanism of LID is to infiltrate runoff near the source. Increasing infiltration reduces runoff and recharges shallow groundwater, which helps maintain stream baseflow. Additionally, reduced runoff volume decreases pollutant loads discharged to the storm drain network. Since LID practices are still relatively new, researchers and designers continue to modify design features to increase pollutant removal, outflow reduction, and overall performance of the practices.

Bioretention is an example of a LID practice that has been researched intensively to determine the most efficient design with respect to media depth, media selection, vegetative cover, drainage configuration, ponding depth, and capture volume (Davis et al. 2009). Original bioretention designs included a conventional underdrain configuration, which consisted of lateral, perforated drains present in a gravel layer beneath the filter media. A drawback associated with this design configuration was that the filter media was predominantly aerobic, so organic nitrogen and ammonium that were captured during runoff events were transformed to nitrate and released as such in the effluent. Field monitored bioretention cells with conventional drainage reported poor “removal” of nitrate, and in most cases, effluent nitrate concentrations increased (Davis et al. 2001; Hatt et al. 2009; Hsieh and Davis 2005; Hunt et al. 2006, 2008; Roseen et al. 2006).

The lack of nitrate reduction was a concern in initial bioretention research because many of the study sites were located in nitrogen sensitive watersheds. If the design could be modified to promote denitrification, it would improve the efficiency of bioretention cells in removing nitrogen from stormwater runoff. Kim et al. (2003) first proposed a raised

underdrain outlet to create a continuously submerged anaerobic zone to promote denitrification and improve nitrate and total nitrogen reduction. The results from pilot-scale bioretention studies were 70 to 80 percent mass removal rates of nitrate plus nitrite ($\text{NO}_{2,3}\text{-N}$) (Kim et al. 2003). A diagram of a bioretention cell with an elevated underdrain, also known as internal water storage (IWS) zone, is shown in Fig. 2.1. Despite promising laboratory results, later field studies by Dietz and Clausen (2006) and Hunt et al. (2006) were inconclusive about adding a saturated layer to create anaerobic conditions. High removal rates of nitrate were reported in Davis (2007), but limited data were available. In Passeport et al. (2009), significant reductions of nitrate were reported for one of the two cells studied. The significant reduction occurred because of a longer saturation period, which was attributable to a less permeable underlying soil (Passeport et al. 2009).

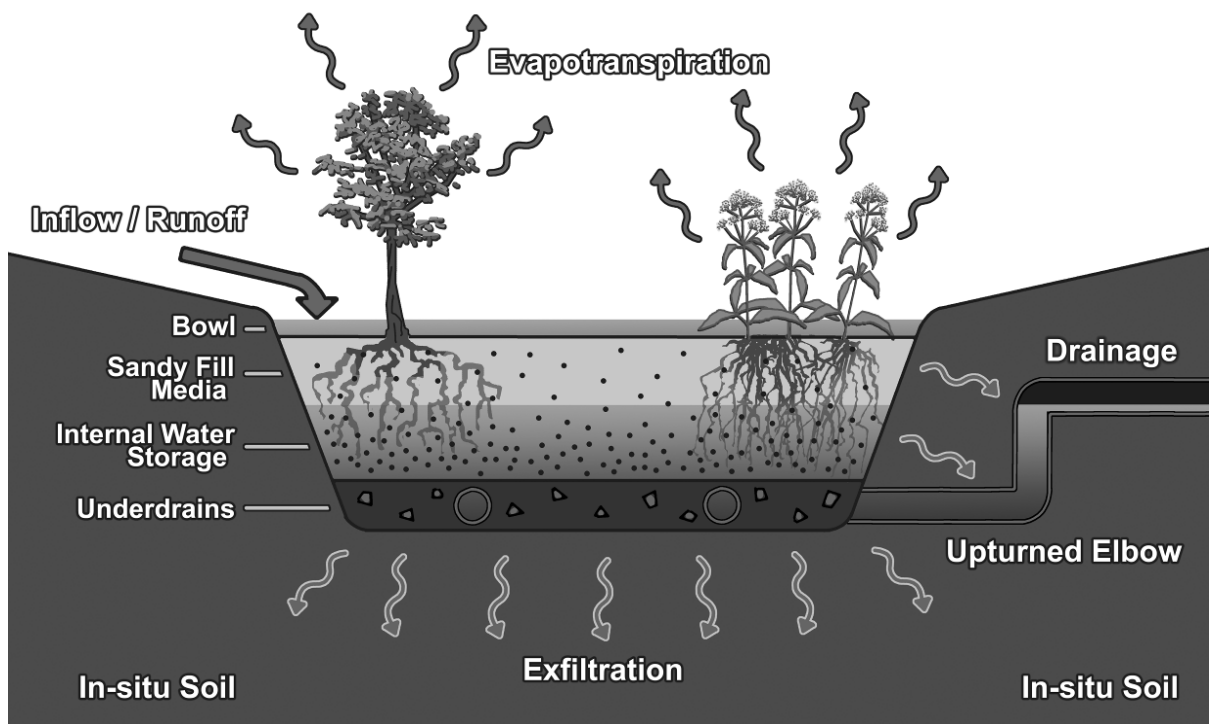


Figure 2.1: Diagram of a bioretention cell with internal water storage (IWS) zone.

Besides the nitrate removal benefit, an IWS zone has the potential to have a significant hydrologic impact on outflow reduction (Li et al. 2009; Passeport et al. 2009; Sharkey 2006). Two bioretention cells studied in Greensboro, NC had a media depth of 1.2 m (4 ft), and the in-situ soil was identified from a soil survey as a clay loam (Sharkey 2006). One cell had conventional drainage and the other had an IWS zone that included the bottom 0.6 m (2 ft) of the media. Drainage occurred twice as often for the cell with conventional drainage. However, there was an event where the outflow volume from the cell with the IWS zone was greater than the one with conventional drainage. This occurred because of the slow exfiltration rate and that two large events occurred with a short antecedent dry period, so the IWS zone was not able to fully drain between events (Li et al. 2009; Sharkey 2006). In Graham, NC two bioretention cells had varying IWS zone depths and underlying soils, and the results showed fewer events generated drainage in the bioretention cell with the deeper IWS zone and sandier underlying soil (Passeport et al. 2009). This occurred because more storage was available in the deeper IWS zone and the sandier underlying soil promoted a higher exfiltration rate which increased storage availability in the IWS zone.

If the IWS zone can drain completely between events, outflow volume will be greatly reduced, thus increasing groundwater recharge. As many states now have groundwater recharge requirements (e.g., PA, NJ, MD, VA), the IWS zone could be the solution to meet infiltration requirements and to meet other LID goals of replicating the natural hydrologic condition of the landscape. One target condition to match is the occurrence of events with outflow to the occurrence of events with surface runoff prior to development (Walsh et al. 2009). By not releasing outflow from the smallest and most frequent events, the number of events with outflow will more closely resemble the pre-developed or target condition, which will help to maintain and improve stream health in urban areas (Ladson et al. 2006; Walsh et al. 2009). The primary objective of this study was to measure the hydrologic performance of bioretention cells with IWS zones in a region with sandy underlying soils. Additional objectives were to further explore the roles that varying degrees of sandy underlying soils and different IWS zone depths had on water quality treatment and outflow reduction.

2.3 METHODOLOGY

2.3.1 Site Description

Two bioretention cells were constructed during the winter of 2005/2006 to treat parking lot runoff at the Imperial Centre in Rocky Mount, NC. Rocky Mount is located in the Upper Coastal Plain (Fig. 2.2). Based on the geologic formations in North Carolina, this region generally has sandier soils than those in the Piedmont. Both bioretention cells were designed with an IWS zone. The outlet in each cell was constructed to be 0.3 m (1 ft) beneath the bottom of the surface storage zone. The IWS zone was created by attaching a 90-degree PVC elbow and standpipe to the underdrain. The bioretention cells varied in vegetative cover and underlying soil. The cell planted with shrubs and perennials had an underlying soil texture of sand (Sand cell), and the other cell with centipede turf had an underlying soil texture of sandy clay loam (SCL cell) (Fig. 2.3). The average fill media depth was 1.1 m (3.6 ft) and 0.96 m (3.15 ft) for the SCL and Sand cells, respectively. A cross section of each cell describing the various soil layers and IWS zone depths is shown in Fig. 2.4. The site was monitored as constructed for 16 months from September 14, 2007, to January 13, 2009. The vegetation had matured during two growing seasons before monitoring began. After the first monitoring period ended, the IWS zone was reduced by 0.3 m (1 ft) to assess performance associated with a shallower IWS zone. The second monitoring period continued for an additional 12 months, concluding on January 11, 2010. A summary of the site characteristics is presented in Table 2.1.

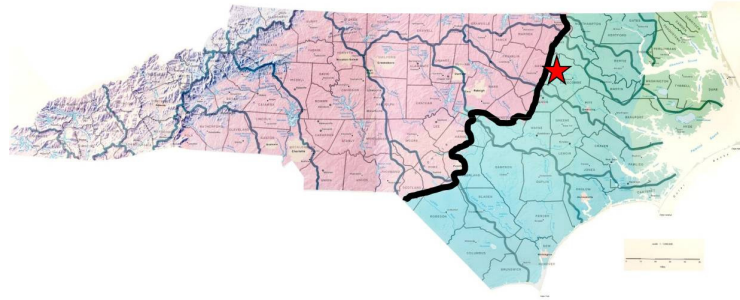


Figure 2.2: Map of study location in reference to the coastal plain/Piedmont divisions (solid black line) in North Carolina; Rocky Mount is located in the Upper Coastal Plain (solid star).



Figure 2.3: Bioretention cell images: Sand cell (left) and SCL cell (right).

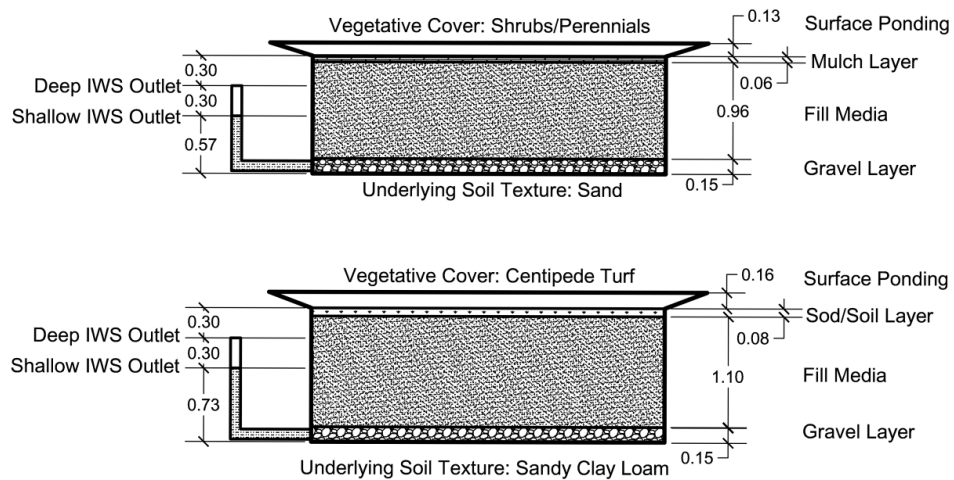


Figure 2.4: Cross sections describing the profiles of the Sand cell (top) and Sandy Clay Loam (SCL) cell (bottom); all units are in meters.

Table 2.1: Summary of Rocky Mount bioretention cell characteristics.

Characteristics	Sandy Clay Loam (SCL) Cell	Sand Cell
Vegetative Cover	Centipede turf	Shrubs/perennials
Bioretention Cell Area	146 m ² (1575 ft ²)	142 m ² (1530 ft ²)
Surface Storage Volume	23.6 m ³ (835 ft ³)	18.5 m ³ (655 ft ³)
Watershed Area	2200 m ² (0.54 ac)	2450 m ² (0.61 ac)
Watershed % Impervious	76%	72%
Surface Storage Design Event ^a	19 mm (0.75 in)	15 mm (0.60 in)
Surface Storage Drawdown Rate	2.5-12.5 cm/hr (1-5 in/hr)	Rapid ^b
IWS Drawdown Rate	7-11 mm/hr (0.28-0.43 in/hr)	200-300 mm/hr (8-12 in/hr)
IWS Exfiltration Rate ^c	2.1-3.3 mm/hr (0.08-0.13 in/hr)	60-90 mm/hr (2.4-3.6 in/hr)
Surface Layer Depth	Sod/Soil: 0.08 m (0.25 ft)	Mulch: 0.06 m (0.2 ft)
Fill Media Depth	1.1 m (3.6 ft)	0.96 m (3.15 ft)
Gravel Layer Depth	0.15 m (0.5 ft)	0.15 m (0.5 ft)
IWS Depth in Media (2007-2009)	0.88 m (2.9 ft)	0.72 m (2.35 ft)
Max. IWS Storage Volume Est. ^c	44.0 m ³ (1550 ft ³)	36.0 m ³ (1270 ft ³)
IWS Depth in Media (2009-2010)	0.58 m (1.9 ft)	0.42 m (1.35 ft)
Max. IWS Storage Volume Est. ^c	30.9 m ³ (1090 ft ³)	23.2 m ³ (820 ft ³)
Fill Media Characteristics ^d	96% sand, 2.9% silt, and 1.1% clay	
P-Index (Fill Media) ^e	6-15 (Low)	
CEC (Fill Media) ^e	1.1-1.3	

^a Calculated with discrete SCS-CN method

^b Not able to be measured because of lack of water ponding

^c Assumed effective porosity of sand and gravel were 0.30 and 0.25, respectively (McWhorter and Sunada 1977)

^d Determined by hydrometer method (Gee and Bauder 1986)

^e Measured by NC Department of Agriculture and Consumer Services

Water level loggers, manufactured by Infinities USA, were installed in the surface storage zone and in the IWS zone standpipe for both cells on February 12, 2009. These devices measured the water level drawdown in the surface storage and IWS zones. During the 11 months of monitoring, infiltration in the Sand cell was so rapid that water never ponded long enough on the surface for a level measurement to be recorded. This was due to

the high hydraulic conductivity of the fill media which was high because of high sand content (96 percent sand). Despite having similarly high sand content in the fill media of the SCL cell, the 0.08-m (3-in) soil layer associated with the sod reduced infiltration rate because of a higher percentage of fines (26 percent), in addition this could have contributed to increased capture and treatment of pollutants, later discussed. The infiltration rate in the SCL cell had considerable seasonal variation, 25-125 mm/hr, which was similar to results in Emerson and Traver (2008). They identified temperature dependency of hydraulic conductivity for the seasonal variation in infiltration rate. Initial water content has also been identified as another major contributing factor for infiltration rate variation (Skaggs and Khaleel 1982). The IWS zone drawdown rates were 7-11 mm/hr and 200-300 mm/hr for the SCL and Sand cells, respectively. To calculate the exfiltration rate, the IWS drawdown rate was multiplied by the effective drainable porosity, which was estimated to be 0.30 for sand (McWhorter and Sunada 1977). This equated to an exfiltration rate of 2.1-3.3 mm/hr in the SCL cell and 60-90 mm/hr in the Sand cell.

In characterizing the media, the phosphorus index (P-Index), which is a measure of phosphorus content in soil, was low (6-15) (Hardy et al. 2007). Particle size analysis was conducted using the hydrometer method, and it was determined that the fill media was 96 percent sand, 2.9 percent silt, and 1.1 percent clay. The fines content (silt and clay) in the fill media at this site was 4 percent, which is lower than the NC bioretention design recommendation of 8-12 percent (NCDENR 2009). Additionally, particle size analysis of the soil associated with the sod determined it had a sandy loam texture (74 percent sand, 22 percent silt, and 4 percent clay).

2.3.2 Sampling Methods

Automated samplers (ISCO 6712TM) with integrated bubbler modules (ISCO 730TM) were used to monitor drainage from the bioretention cells and collect flow-weighted samples. Two 30° v-notch weirboxes were installed on top of the standpipe outlet. The weirs were used in combination with the bubbler modules to measure drainage from the bioretention cells. Water levels were routinely field verified.

A tipping bucket rain gauge (ISCO 674 Rain GaugeTM) was installed to measure rainfall intensity, while a manual plastic rain gauge measured rainfall depth. A discrete rainfall event was defined as those greater than 2.5 mm (0.10 in) and having an antecedent dry period exceeding six hours. Runoff entered the cells as diffuse flow along the perimeter, so a 0.6-m (2-ft) wide collection trough was installed at the edge of pavement to collect a representative sample of runoff. Rainfall (0.5 mm in 15 minutes) triggered the sampler to enable, and once enough liquid ponded in the trough, a sample was pulled. The concentrations from this one location represented runoff to both bioretention cells.

Events with drainage were rare, so only 14 and 3 events had composite samples of drainage from the SCL and Sand cells, respectively. To quantify treatment by the media, grab samples were collected from the underdrains. For the SCL cell, a grab sample was pumped from the underdrains within 24 hours after an event concluded. Due to the rapid exfiltration in the Sand cell, a 51-mm diameter PVC pipe with a cap was lowered into the standpipe to collect a grab sample of the treated water. Only highly intense events would raise water in the IWS zone high enough to fill the Sand cell grab sampler; these were rare. The total numbers of events with grab samples from the SCL and Sand cells were 29 and 6, respectively.

Flow-weighted storm samples and grab samples were analyzed for nutrients and total suspended solids (TSS). The nutrient species analyzed were orthophosphate (Ortho-P), total phosphorus (TP), total ammoniacal nitrogen (TAN), nitrite+nitrite-nitrogen ($\text{NO}_{2,3}\text{-N}$), and total Kjeldahl nitrogen (TKN) (Table 2.2). Total nitrogen (TN) was calculated as the sum of $\text{NO}_{2,3}\text{-N}$ and TKN, particulate-phosphorus (Part-P) was the difference between TP and Ortho-P, and organic-nitrogen (ON) was the difference between TKN and TAN. Composite samples were transferred to laboratory containers, placed on ice, and delivered to the NCSU Center for Applied Aquatic Ecology laboratory (state-certified laboratory) within 24 hours. No preservation was used in the automated samplers; thus, samples that could not be recovered from the machine within 24 hours were discarded.

Table 2.2: Summary of analytical methods for water quality analysis.

Pollutant	Pollutant Name	Analytical Method	RL^a	Unit
NO _{2,3} -N	Nitrate + Nitrite nitrogen	SM 4500-NO ₃ -F ^b	0.0056	mg/L
TKN	Total Kjeldahl nitrogen	EPA 351.1 ^c	0.14	mg/L
TAN	Total ammoniacal nitrogen	SM 4500-NH ₃ -H ^b	0.007	mg/L
ON	Organic nitrogen	= TKN – TAN	N/A	mg/L
TN	Total nitrogen	= NO _{2,3} -N + TKN	N/A	mg/L
Ortho-P	Orthophosphate	SM 4500-P-F ^b	0.006	mg/L
Part-P	Particulate-phosphorus	= TP – Ortho-P	N/A	mg/L
TP	Total phosphorus	SM 4500-P-F ^b	0.01	mg/L
TSS	Total suspended solids	SM 2540 D ^b	1	mg/L

^a Reporting Limit^b Source (Eaton et al. 1995)^c Source (USEPA 1983)

2.3.3 Statistical Methods

Statistical analyses were conducted using SAS® version 8 (SAS Institute Inc., Cary, NC). The level of significance used in all analyses was $\alpha = 0.05$. Four statistical tests for normality (Shapiro-Wilk, Kolmogorov-Smirnov, Creamer-von Mises, and Anderson-Darling) were used to check the validity of the assumption that the data were normal. These tests showed better fits for normality when the data were log-transformed, so most of the water quality data were log-transformed as suggested by Strecker et al. (2001). To avoid issues with log-transforming data when samples for Ortho-P were below the reportable limit, half of the reportable limit was used (Newman et al. 1989). A paired t-test was used to determine significance if the data were normally distributed. If the data were not normally distributed but had symmetry, a Wilcoxon signed-rank test was performed to check for significance.

2.3.4 Mass Balance Calculations

Runoff was calculated for each event by subtracting an initial abstraction depth from the rainfall depth measured in the plastic rain gauge and multiplying this depth by the drainage area. Initial abstraction values were calculated based off of curve numbers for the

impervious asphalt parking lot and for the pervious surfaces (open space, poor conditions) (USDA-NRCS 2004a). The curve numbers varied based on antecedent moisture conditions at the site (USDA-NRCS 2004b). The range of the curve numbers and antecedent moisture conditions used in estimating runoff are presented in Table 2.3. For asphalt on a shallow slope, Pandit and Heck (2009) found that nearly all of the rainfall is transmitted to runoff. However, small depressions were observed in this parking lot, which created puddles, so the initial abstraction depths for the impervious surfaces were increased from those for the typical impervious surface curve number of 98.

Table 2.3: Curve number and initial abstraction depths for pervious and impervious land uses and varying antecedent moisture conditions (USDA-NRCS 2004b).

Antecedent Moisture Condition	Curve Number (Initial Abstraction) for:		Antecedent Dry Period
	<i>Pervious Land Use</i>	<i>Impervious Land Use</i>	
1 (dry)	72 (19.8 mm)	94 (3.3 mm)	> 120 hours
2 (average)	86 (8.4 mm)	95 (2.5 mm)	48 to 120 hours
3 (wet)	94 (3.3 mm)	96 (2.0 mm)	6 to 48 hours

Drainage volume was measured with a 30° v-notch weirbox that was mounted on the top of the outlet standpipe. Overflow occurred when the surface storage volume was at capacity, resulting in all incoming runoff to overflow the surface storage zone and directly enter into the stormwater network without receiving treatment through the media. Overflow was calculated based on rainfall intensity, bioretention cell surface storage characteristics, drainage area characteristics, and measured surface infiltration rates that varied by month. An Excel spreadsheet was created to model overflow volume on an hourly basis.

Evapotranspiration (ET) was estimated using the equation (Equation 2.1) developed by Zhang et al. (2001), where they correlated the ratio of mean actual evapotranspiration (AET) and annual precipitation (P) to potential evapotranspiration (PET), based on hydrologic data from over 250 watersheds across the world. The equation is:

$$\frac{AET}{P} = \frac{1 + w \frac{PET}{P}}{1 + w \frac{PET}{P} + \frac{P}{PET}} \quad (2.1)$$

where w is the plant-available water coefficient, which is representative of the way plants use soil-water for transpiration. A plant-available water coefficient of 0.5 was selected because this is the best fit for shortgrass and crops, which have similar root depths as the centipede sod, shrubs, and perennials found in the bioretention cells of this study.

The PET was calculated using the Thornthwaite method (Thornthwaite 1948). Thornthwaite is the simplest method to calculate PET because it only requires one temperature term – average monthly temperature. Data for this term were found on the State Climate Office of NC website for the Rocky Mount, NC (8 ESE) monitoring station – site ID: 317400 (SCO 2009). When the Thornthwaite method was compared to five other methods for estimating PET by Lu et al. (2005), it yielded the lowest annual values of PET. This can be attributed to the simplicity of the Thornthwaite equation, where the other methods have terms to account for radiation and other parameters. Since Thornthwaite underestimated PET, correction factors were included to provide a more reliable PET estimate (Amatya et al. 1995). Amatya et al. (1995) calculated correction factors for the Thornthwaite method at three sites in eastern North Carolina. The closest site to Rocky Mount was Tarboro – 25 km to the east.

All of the runoff volume that did not leave through drainage, overflow, or ET was assumed to be lost through exfiltration based on the water balance equation (Equation 2.2):

$$Vol_{Runoff} = Vol_{Overflow} + Vol_{Drainage} + Vol_{ET} + Vol_{EXF} \quad (2.2)$$

where Vol_{Runoff} = runoff volume, $Vol_{Overflow}$ = overflow volume, $Vol_{Drainage}$ = drainage volume, Vol_{ET} = evapotranspiration volume, and Vol_{EXF} = exfiltration volume. Exfiltration is water leaving the bioretention media through the bottom and sides of the cell and entering the in-situ soil. It can also be referred to as seepage.

2.4 RESULTS

2.4.1 Hydrology

The range and characteristics of the precipitation events varied during the two monitoring periods (Table 2.4). During the beginning of the first monitoring period, North Carolina was experiencing a severe drought. The first monitoring period lasted 16 months, and only 78 events were measured; whereas, the second monitoring period was 12 months and 73 events were measured. The mean event sizes were 16.4 mm and 14.1 mm, and the median event sizes were 12.3 mm and 11.2 mm for the first and second monitoring periods, respectively.

Table 2.4: Characterization of precipitation events for the first (deep IWS zone) and second (shallow IWS zone) monitoring periods.

IWS Depth	Events	Event Characteristics (mm)			Number of Events Greater than:			
		Mean	Median	Range	19 mm	25 mm	38 mm	51 mm
Deep	78	16.4	12.3	2.5-53.1	26	15	8	2
Shallow	73	14.1	11.2	2.5-121	15	8	3	1

The characteristics of precipitation events for events with drainage differed for the two cells. The exfiltration rate of the Sand cell was 60 to 90 mm/hr, so when the entire IWS zone was full, it could completely drain in less than three hours. Therefore, large events with low intensity and long duration were able to be fully assimilated (produce no drainage); this included the largest measured event (121 mm). The Sand cell also had fewer events with overflow compared to the SCL cell because of its rapid infiltration rate. High intensity rainfall events were required to pond water; rainfall intensity characteristics of the events generating overflow and drainage were an intensity of at least 31 mm/hr for a 30-minute duration. These intensities were never achieved during the second monitoring period, so overflow was never recorded during the second monitoring period. Despite a reduced IWS zone depth, there were fewer events with drainage during the second monitoring period from

the Sand cell because large, intense events were less common (Fig. 2.5). Lines representing direct runoff to outflow (1:1) and an effluent/influent volume ratio of 0.33 are depicted in Fig. 2.5. The effluent/influent volume ratio of 0.33 is described in Davis (2008) as a LID volume reduction goal. The Sand cell achieved the LID volume reduction goal for *all* events.

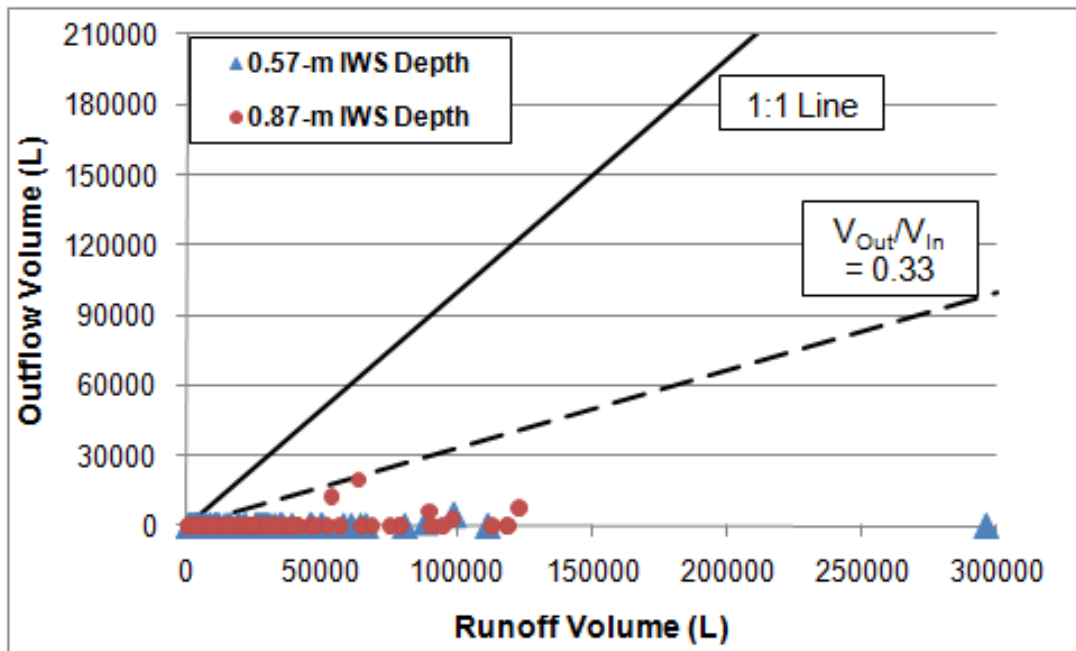


Figure 2.5: Outflow volume versus runoff volume for the Sand cell.

The exfiltration rate of the SCL cell ranged from 2.1 to 3.3 mm/hr, so when the entire IWS zone was saturated, it would take approximately seven and five days to fully drain during the first and second monitoring periods, respectively. With the longer duration to drain the IWS zone, events producing drainage would be governed by event size and antecedent dry period. Even though the media had a high sand content (96 percent), the infiltration rate was slower in the SCL cell because of the lower hydraulic conductivity of the 0.08-m sandy loam layer beneath the sod. The slower infiltration rate in the SCL cell made ponding more frequent, thus producing more events with overflow. During the first and second monitoring periods, three and seven events did not achieve the LID volume reduction

goal, respectively (Fig. 2.6). In Fig. 2.7, overflow volume was subtracted from the runoff volume to examine drainage volume versus treated runoff volume. Since the two monitoring periods differed in storm intensity and size, removing the overflow volume from consideration allowed the difference between (drainage) volume reductions for the two IWS zone depths (1.03 m and 0.73 m) to be analyzed. The deeper IWS zone achieved the LID volume reduction goal for all events, whereas the shallower IWS zone depth achieved it for 92 percent of the events. The deeper IWS zone had a greater hydrologic benefit for this site because it had more subsurface storage volume and the IWS zone was able to drain completely between most events.

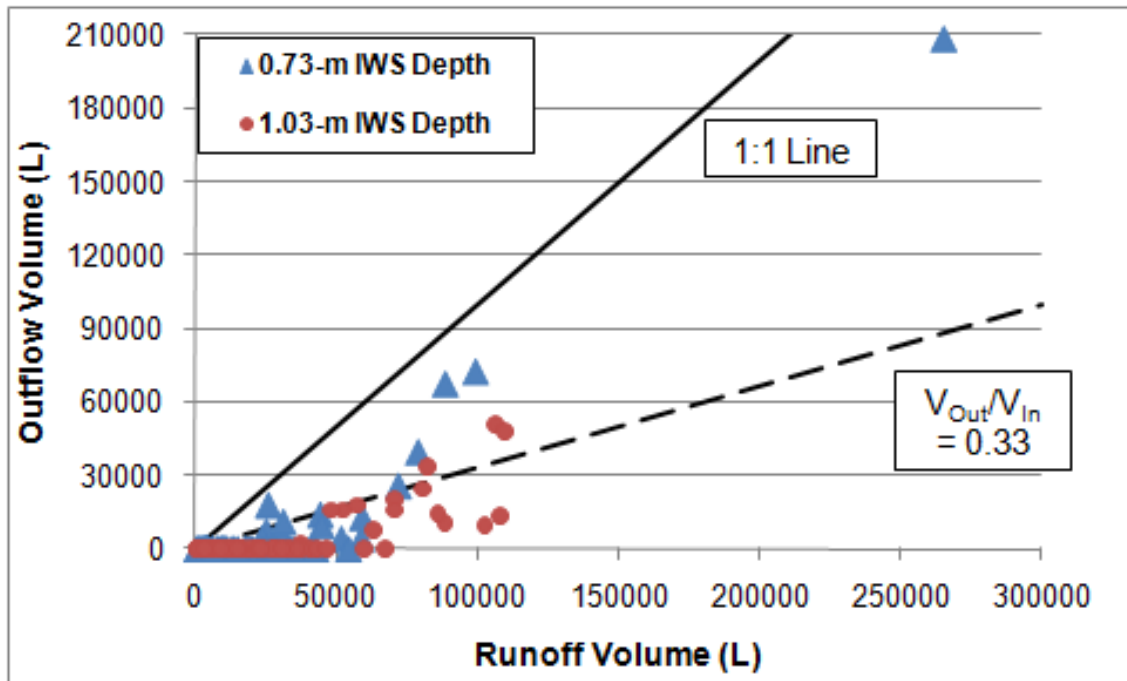


Figure 2.6: Outflow volume versus runoff volume for the SCL cell.

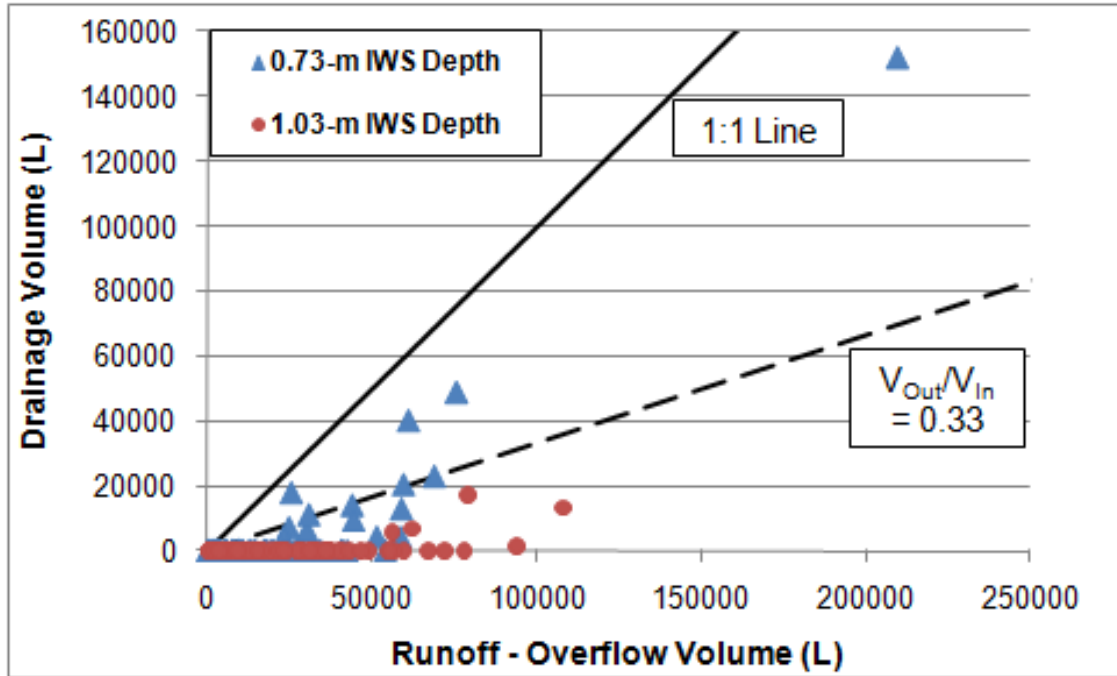


Figure 2.7: Drainage volume versus treated runoff volume (runoff volume minus overflow volume) for the SCL cell.

The surface storage volume design event for the SCL cell, as calculated by the discrete Soil Conservation Service-Curve Number (SCS-CN) method was 19 mm. More overflow was expected during the first monitoring period because the 19-mm event was exceeded in 26 and 15 events during the first and second monitoring periods, respectively. Only five events produced drainage during the first monitoring period. With an antecedent dry period greater than 48 hours, the smallest event to generate drainage was 49.3 mm. The largest event without drainage was 43.7 mm (16 percent of runoff was overflow), and the largest event with no drainage or overflow was 32.5 mm. The number of events during the second monitoring period that produced drainage was 16, and the smallest event to produce drainage with at least 48 hours since the previous event was 16.3 mm. The largest event not to produce drainage was 25.4 mm (no overflow produced either). These results are summarized in Table 2.5.

Table 2.5: Summary of frequency of events with drainage and overflow during both monitoring periods.

IWS Depth	Bioretention Cell	Number of Events with:		Smallest Event with Drainage ^a	Largest Event without Drainage
		<i>Drainage</i>	<i>Overflow</i>		
Deep	SCL	5	14 ^b	49.3 mm	43.7 mm
Shallow	SCL	16	5	16.3 mm	25.4 mm
Deep	Sand	4	5 ^b	22.9 mm	53.1 mm
Shallow	Sand	2	0	36.1 mm	121 mm

^a Antecedent dry period is at least 48 hours

^b Estimated based on rainfall data, drainage area characteristics, and estimated infiltration rates

The three primary factors that impacted the differences between the fate of runoff for the bioretention cells at Rocky Mount were (1) underlying soil, (2) surface infiltration rate, and (3) depth of IWS zone. Based on the fate of runoff (Fig. 2.8), the bioretention cell with sandier underlying soil (Sand cell) and deeper IWS zone depth (first monitoring period) generated the least amount of drainage and the bioretention cell with the faster infiltration rate (Sand cell) generated the least amount of overflow. Based on the outflow reduction metric, the Sand cell performed better than the SCL cell, but as will be discussed in the water quality section, the rapid infiltration and short hydraulic residence time (contact time) in the media limited the treatment of most nutrient species.

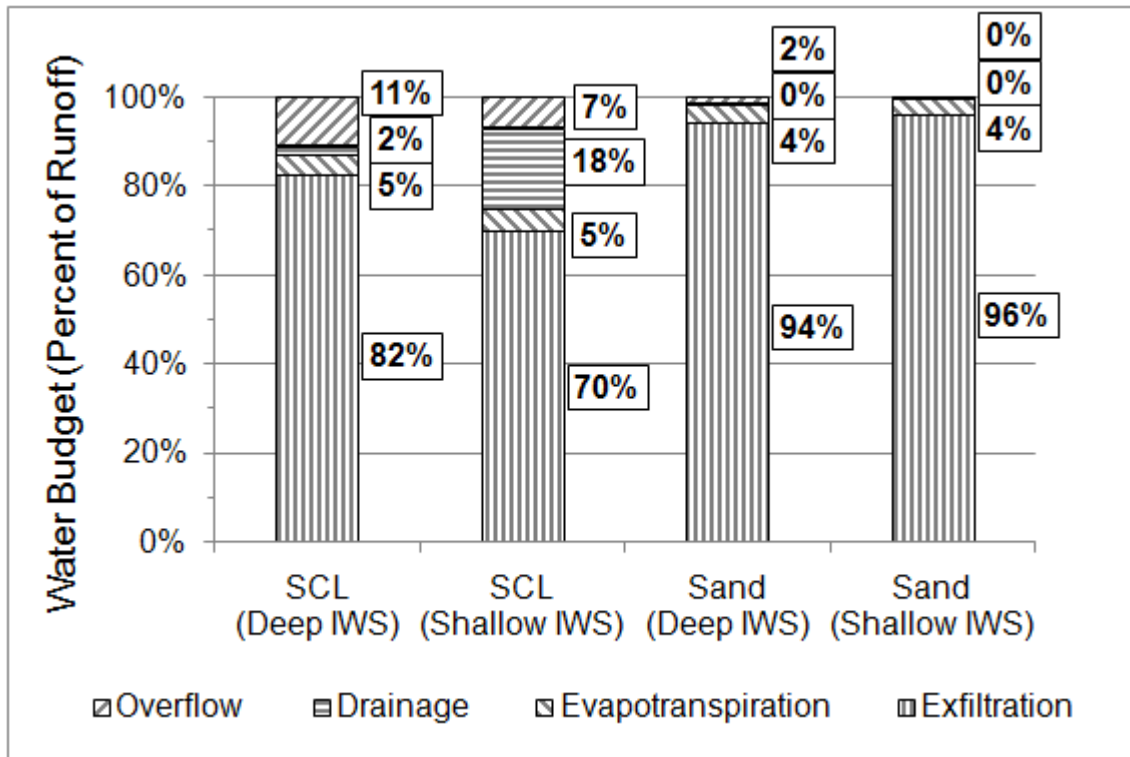


Figure 2.8: Summary of water balance (fate of runoff) for both monitoring periods. Percentages of runoff are listed in each bar, from top to bottom, as overflow, drainage, evapotranspiration, and exfiltration.

2.4.2 Water Quality

For the SCL cell, grab samples from both monitoring periods were combined to measure treatment of runoff. Average event mean concentrations (EMCs) for runoff samples and average grab sample concentrations for the SCL cell are presented in Table 2.6, along with concentration ranges. Significant reductions (p -value < 0.05) were reported for all pollutants except Ortho-P. The SCL cell grab samples were used to determine if seasonal (growing season) differences existed for pollutant treatment. Grab samples were used because they accounted for almost three times the number drainage samples from the SCL cell. A Wilcoxon signed-rank test was used to compare both concentrations of runoff and treated runoff from the SCL cell and percent removal efficiencies for each event between the growing ($n=15$) and non-growing seasons ($n=14$). Overall, there were no concentration

differences for any pollutant between seasons for treated runoff. For runoff concentrations, there was only a significant difference between season for NO_{2,3}-N and Ortho-P, with significantly higher concentrations during the growing season. When percent removal efficiencies were compared between the two seasons, the only pollutants with significant differences were NO_{2,3}-N and Ortho-P. Both pollutants had better removal efficiencies during the growing season; however, this was likely attributable to significantly higher runoff concentrations during this time period.

Table 2.6: Average EMC and statistical analyses comparing grab samples from the SCL cell to runoff samples.

Pollutant	Sample Location	N	Mean Conc. (EMC/grab)	Range	Significant Difference In/Grab^a
TKN	Runoff	29	1.59	0.27-5.87	p<0.0001 (-) SR ^b
	SCL	29	0.19	<RL-0.42	
TAN	Runoff	29	0.46	0.03-1.37	p<0.0001 (-) SR ^b
	SCL	29	0.04	<RL-0.13	
ON	Runoff	29	1.12	0.11-5.54	p<0.0001 (-) ^b
	SCL	29	0.15	<RL-0.41	
NO _{2,3} -N	Runoff	29	0.38	0.06-1.48	p=0.0019 (-) ^b
	SCL	29	0.21	0.04-0.76	
TN	Runoff	29	1.96	0.36-7.35	p<0.0001 (-) SR ^b
	SCL	29	0.40	0.11-1.18	
TP	Runoff	29	0.18	0.02-1.40	p=0.0002 (-) ^b
	SCL	29	0.06	0.02-0.23	
Ortho-P	Runoff	28	0.01	<RL-0.05	No SR ^b
	SCL	28	0.01	<RL-0.02	
Part-P	Runoff	28	0.15	0.02-1.39	p=0.0003 (-) ^b
	SCL	28	0.05	0.01-0.22	
TSS	Runoff	23	152	9-888	p<0.0001 (-) ^b
	SCL	23	8	1-49	

^a (+) = significantly increased; (-) = significantly reduced; SR = Wilcoxon signed rank test; paired t-test was used if not specified

^b Data were log-transformed for statistical analyses

To quantify treatment from the Sand cell, all of the samples (grab and composite) from both monitoring periods were used. Only eight and nine events were collected and paired with samples from the runoff and the SCL cell, respectively. Despite the small sample size, the statistical analyses showed that the treated runoff from the Sand cell was significantly more polluted than the treated runoff from the SCL cell for TKN, NO_{2,3}-N, TN, TAN, ON, TP, and Ortho-P, while there was no significant difference for Part-P and TSS (Table 2.7). These results indicate that the short hydraulic residence time is responsible for the poor treatment provided by the Sand cell for any pollutant not removed solely by filtration and sedimentation. Part-P and TSS both are treated by sedimentation and filtration and therefore were not significantly different. Only TAN and TSS were significantly lower from the Sand cell compared to the runoff concentrations. No significant differences were reported in TKN, ON, NO_{2,3}-N, TN, and Part-P, and significant increases were found for Ortho-P and TP. Therefore, as a result of the short hydraulic residence time in the media, the Sand cell had minimal treatment of pollutants before entering the in-situ soil, except for TSS and particulate-bound contaminants.

Table 2.7: Summary of water quality results from the Sand cell and comparison of Sand cell paired samples to runoff and the SCL cell.

Pollutant	Mean Conc. +/- Std. Dev. (n=9)	vs. Runoff (n=8)^a	vs. SCL (n=9)^a
TKN	0.82 +/- 0.45	No	p=0.0002 (+) ^b
TAN	0.07 +/- 0.04	p=0.0156 (-) SR ^b	p=0.0039 (+) SR ^b
ON	0.75 +/- 0.44	No	p=0.0002 (+) ^b
NO _{2,3} -N	0.49 +/- 0.65	No ^b	p=0.0106 (+) ^b
TN	1.31 +/- 0.91	No	p=0.0039 (+) SR ^b
TP	0.23 +/- 0.10	p=0.0213 (+) ^b	p=0.0039 (+) SR ^b
Ortho-P	0.10 +/- 0.03	p=0.0078 (+) SR	p=0.0003 (+)
Part-P	0.14 +/- 0.14	No SR ^b	No ^b
TSS	17 +/- 19	p=0.0059 (-) ^b	No ^b

^a (+) = significantly increased; (-) = significantly reduced; SR = Wilcoxon signed rank test; paired t-test was used if not specified

^b Data were log-transformed for statistical analyses

Paired runoff/drainage samples from both monitoring periods were combined to analyze treatment from events with drainage from the SCL cell. Of the 11 events with paired samples, three were from the first monitoring period and eight were from the second monitoring period. In comparing the drainage and runoff concentrations, the SCL cell was able to significantly reduce the concentrations for NO_{2,3}-N, TKN, TAN, ON, TN, and TSS. No significant differences were measured for Ortho-P and TP, and the drainage was significantly higher for Part-P. Efficiency ratios (ERs) for these paired samples were calculated using Equation 2.3:

$$ER = \frac{EMC_{Influent} - EMC_{Effluent}}{EMC_{Influent}} \quad (2.3)$$

where EMC_{Influent} = event mean concentration of runoff and EMC_{Effluent} = event mean concentration of drainage. The SCL cell had ERs exceeding 0.5 for all nitrogen species and TSS. TP had an ER of -0.10 (concentration increase); however, the mean runoff concentration was 0.09 mg/L, which was lower than mean runoff concentration (0.18 mg/L) corresponding to events when grab samples were collected from the SCL cell (Table 2.6). A reason for the differences in TP performance for the SCL cell composite samples to the ones with grab samples are that the events with composite samples were larger, so the runoff concentrations were more diluted. The other runoff concentrations in Table 2.8 are lower than those in Table 2.6, so the ERs in Table 2.8 could be understating the potential of concentration reduction by the SCL cell because only concentrations from the larger events are considered.

Table 2.8: Summary of water quality results for events with drainage from SCL cell and statistical analyses of EMCs for runoff and SCL cell drainage samples.

Pollutant	Sample Location	ER^a	Average EMC	Range	Significant Difference vs. Runoff^b
TKN (n=11)	Runoff	0.58	0.74	0.33-1.61	p=0.0030 (-)
	SCL		0.31	0.13-0.77	
TAN (n=11)	Runoff	0.74	0.23	0.07-0.54	p=0.0017 (-)
	SCL		0.06	0.02-0.11	
ON (n=11)	Runoff	0.50	0.51	0.20-1.21	p=0.0177 (-)
	SCL		0.25	0.08-0.65	
NO _{2,3} -N (n=11)	Runoff	0.58	0.28	0.03-0.51	p=0.0069 (-)
	SCL		0.12	0.02-0.23	
TN (n=11)	Runoff	0.58	1.02	0.40-2.07	p=0.0015 (-)
	SCL		0.43	0.20-0.96	
TP (n=11)	Runoff	(0.10)	0.08	0.04-0.22	No ^c
	SCL		0.09	0.06-0.17	
Ortho-P (n=9)	Runoff	0.64	0.02	<RL-0.10	No ^c
	SCL		0.01	<RL-0.02	
Part-P (n=9)	Runoff	(0.35)	0.06	0.03-0.16	p=0.0438 (+)
	SCL		0.08	0.05-0.16	
TSS (n=11)	Runoff	0.58	40.6	6-184	p=0.0338 (-) ^c
	SCL		16.9	6-50	

^a Parentheses indicate an increase in effluent concentration, negative efficiency ratio

^b (+) = significantly increased; (-) = significantly reduced; SR = Wilcoxon signed rank test; paired t-test was used if not specified

^c Data were log-transformed for statistical analyses

Bioretention performance was also evaluated against ambient water quality concentrations associated with benthic health (McNett et al. 2010). TN and TP concentrations from the runoff and SCL cell grab samples were compared to concentrations that represented “good” and “fair” benthic health metrics in the Piedmont region of North Carolina (Table 2.9). This eco-region had more data, significant associations of TN and TP data to eco-region, and one monitoring station used in McNett et al.’s (2010) study was located within 1 km of the Rocky Mount bioretention site. Streams that were identified to have “good” benthic health had average TN and TP concentrations of 0.99 mg/L and 0.11 mg/L, respectively. Presence of intolerant benthic macroinvertebrate populations

(*Ephemeroptera*, *Plecoptera*, and *Trichoptera* [EPT]) characterize streams to be in “good” health. “Fair” benthic health had average TN and TP concentrations of 2.16 mg/L and 0.22 mg/L, respectively. Presence of more tolerant species (crayfish and crustaceans) distinguishes streams of “fair” benthic health. TN and TP runoff concentrations were significantly less polluted than the “fair” standard, but runoff TN was significantly more polluted and TP had no significant difference compared to the “good” standard. The concentrations of TN and TP for both grab and composite samples in the SCL cell were significantly less polluted than the “good” standard. The TN concentration of treated runoff from the Sand cell was not significantly different than the “good” standard but was significantly less polluted than the “fair” standard. For TP, the treated runoff was significantly more polluted than the “good” standard and no significant difference was present for the “fair” standard. These data indicate that the SCL cell was able to reduce/improve concentrations of TN and TP enough to meet the more rigorous “good” standard. However, the Sand cell had no impact on TN concentrations and a negative impact on TP to the point where the treated runoff from this system was no longer significantly cleaner than the “fair” standard.

Table 2.9: Comparison of runoff and Rocky Mount bioretention cell treated runoff concentrations to benthic health water quality metrics (McNett et al. 2010).

	vs. TN “good” ^a	vs. TN “fair” ^a	vs. TP “good” ^a	vs. TP “fair” ^a
In (n=40)	p=0.0282 (+) ^b	p<0.0001 (-) ^b	No SR ^b	p=0.0014 (-) SR ^b
SCL Cell Grab (n=29)	p<0.0001 (-)	p<0.0001 (-) ^b	p<0.0001 (-) ^b	p<0.0001 (-) ^b
SCL Cell Drainage (n=11)	p<0.0001 (-) ^b	p<0.0001 (-) ^b	p=0.0303 (-) SR ^b	p=0.0010 (-) SR ^b
Sand Cell (n=9)	No ^b	p=0.0118 (-) ^b	p=0.0010 (+) ^b	No ^b

^a (+) = significantly higher than standard; (-) = significantly lower than standard; SR = Wilcoxon signed rank test; paired t-test was used if not specified; “good” TN = 0.99 mg/L, “fair” TN = 2.16 mg/L, “good” TP = 0.11 mg/L, and “fair” TP = 0.22 mg/L.

^b Data were log-transformed for statistical analyses

2.5 DISCUSSION

Overall, given the two cells studied, the Sand cell outperformed the SCL cell from a hydrologic perspective. However, the short hydraulic residence time of runoff in the media of the Sand cell resulted in it releasing significantly higher concentrations of most nutrient species. The overall lack of nutrient treatment in the Sand cell raised concern for this system to be short circuiting nutrients to deeper subsoil and possibly shallow groundwater. Most of the runoff is entering into the subsoil at a depth of about 1.2 m (4 ft), which is below the root zone. The fate of nutrients after they exfiltrate into surrounding soils needs to be explored further to determine if any issues regarding groundwater contamination will be created. This is of particular interest for regions with sandy underlying soils because of the potentially large portion of exfiltration. This concern also holds for other infiltration-based practices that have sandy underlying soils and are in close proximity to sensitive waterbodies.

While the results from these sites identified that the IWS zone should be maximized to optimize hydrologic performance and pollutant load reduction, consideration should be given to avoid having the IWS zone discharge point too close to the surface of the media. Ideally, a small aerobic zone (i.e., 0.3 to 0.45 m) should still be maintained to prevent trapped pollutants (phosphorus and metals) from mobilizing under saturated conditions and to ensure plant survivability. Additionally, freezing of the IWS zone was not a concern in NC; however, this could potentially be problematic in colder climates with deeper frost lines.

Both measurements (drainage and rainfall) and calculations (runoff, overflow, ET, and exfiltration) were performed to determine the mass balance from these systems. Errors associated with measurements and calculations are inevitable; however, the outcome of the benefits of adding an IWS zone at sites with somewhat sandy underlying soils is robust enough to overcome these errors. Calculation of runoff had perhaps the largest source of error because it entered as diffuse flow along the cells' perimeter, so it was not able to be measured. Then, the exfiltration volume was calculated as the difference between this runoff volume and the volume of outflow and ET. As an example from the first monitoring period,

a 20 percent error in runoff volume calculation would have resulted in the annual exfiltration volume for the Sand and SCL cells to be $94\pm 1\%$ and $82\pm 4\%$, respectively.

Finally, examining the infiltration literature (Skaggs and Khaleel 1982) showed that the slower infiltration rate through the SCL cell's surface may have also been attributable to the underlying soil. With the slower exfiltration rate in the SCL cell, water could remain within the IWS zone at the start of the next event. Therefore, with no outlet to release the air within the media, air would become entrapped, thereby reducing the infiltration rate.

McWhorter (1971) measured that air pressure builds up faster in sand columns with shorter unsaturated zones than longer ones, thus resulting in a greater reduction in infiltration rate when the water table is closer to the surface.

2.6 SUMMARY AND CONCLUSIONS

Implications of this research that are important for design and management of bioretention cells are as follows:

- At sites with underlying soils that range from sand to sandy clay loam, the majority of runoff volume can be eliminated from the stormwater network when an IWS zone is included in the design. Volume reduction approached 100 percent for the Sand cell and was 87 and 75 percent for the SCL cell during the first and second monitoring periods, respectively. Due to the high outflow volume reduction, high pollutant load reductions were also achieved. To optimize the IWS zone depth for bioretention cells with sandier types of underlying soils, the IWS zone depth should be maximized, while still maintaining an aerobic zone in the media (ideally 0.3 to 0.45 m (1 to 1.5 ft)). The high outflow reduction from these cells was also due to the water storage availability within the IWS zones exceeding the surface storage volume.
- The three primary factors that dictate whether outflow (drainage and overflow) will occur are: (1) hydraulic conductivity of underlying soil, (2) IWS zone depth, and (3) surface infiltration rate. Higher hydraulic conductivity surrounding soils (as in the Sand cell) and deeper IWS zones (as in the first monitoring period) resulted in fewer

events with drainage and less drainage volume. Higher surface infiltration rates (Sand cell) resulted in fewer events with overflow and less overflow volume.

- Because the media and underlying soils were mostly sand, the hydraulic residence time in the Sand cell's media was short (less than three hours). This resulted in the bioretention cell media being unable to adequately treat nutrients. Only TAN had a significant concentration reduction.
- The IWS zone drainage configuration significantly reduced $\text{NO}_{2,3}\text{-N}$ because the hydraulic residence time was sufficiently long enough to create anaerobic conditions. When the IWS zone was full, runoff remained in the media of the SCL cell for up to seven days after the event ended. For events with drainage from the SCL cell, the ER for $\text{NO}_{2,3}\text{-N}$ was 0.58. However, the treated runoff from the Sand cell had no significant difference, and the average concentration was 15 percent higher after passing through its aerobic media.
- Another performance metric used to evaluate bioretention cell treatment was to compare runoff and treated runoff concentrations to concentrations consistent with "good" and "fair" benthic health in streams. Overall, in comparing the Rocky Mount site to the metrics presented in McNett et al. (2010), parking lot runoff achieved "fair" water quality for TN and TP; treated runoff from the Sand cell only achieved "fair" water quality for TN. However, treated runoff from the SCL cell met "good" water quality benchmarks for TN and TP. Despite a negative efficiency ratio for TP from the SCL cell during events with drainage, the SCL cell had concentrations significantly lower than the "good" benthic health water quality standard. This provides an example of how examining solely concentration reductions can be misleading.

2.7 ACKNOWLEDGEMENTS

The authors would like to acknowledge the Cooperative Institute for Coastal and Estuarine Environmental Technology (CICEET) for funding this project. Thanks to Dr. Aziz

Amoozegar, Dr. Gregory Jennings, and Dr. Wayne Skaggs for their review and input. Finally, thanks to Shawn Kennedy, Bill Lord, and Ryan Smith for assistance in setting up the site and installing monitoring equipment, and to Jenny James and Linda Mackenzie for water quality sample analyses.

2.8 REFERENCES

- Amatya, D. M., Skaggs, R. W., and Gregory, J. D. (1995). "Comparison of methods for estimating REF-ET." *Journal of Irrigation and Drainage Engineering*, 121(6), 427-435.
- Davis, A. P., Shokouhian, M., Sharma, H., and Minami, C. (2001). "Laboratory study of biological retention for urban stormwater management." *Water Environment Research*, 73(1), 5-14.
- Davis, A. P. (2007). "Field performance of bioretention: Water quality." *Environmental Engineering Science*, 24(8), 1048-1064.
- Davis, A. P. (2008). "Field performance of bioretention: Hydrology impacts." *Journal of Hydrologic Engineering*, 13(2), 90-95.
- Davis, A. P., Hunt, W. F., Traver, R. G., and Clar, M. (2009). "Bioretention technology: Overview of current practice and future needs." *Journal of Environmental Engineering*, 135(3), 109-117.
- Dietz, M. E., and Clausen, J. C. (2006). "Saturation to improve pollutant retention in a rain garden." *Environmental Science and Technology*, 40(4), 1335-1340.
- Eaton, A. D., Clesceri, L. S., and Greenberg, A. R. (1995). *Standard methods for the examination of water and wastewater*, American Public Health Association, American Water Works Association, and Water Environment Federation, Washington, D.C.
- Emerson, C. H., and Traver, R. G. (2008). "Multiyear and seasonal variation of infiltration from storm-water best management practices." *Journal of Irrigation and Drainage Engineering*, 134(5), 598-604.
- Gee, G. W., and Bauder, J. W. (1986). "Particle-size analysis." *Methods of soil analysis. Part 1: Physical and mineralogical methods*, A. Klute, ed., Soil Science Society of America, Madison, Wis., 383-411.

- Hardy, D. H., Tucker, M. R., and Stokes, C. E. (2007). "Crop fertilization based on North Carolina soil tests." *Circular No. 1*. North Carolina Department of Agriculture and Consumer Services, Agronomic Division, Raleigh, N.C.
- Hatt, B. R., Fletcher, T. D., and Deletic, A. (2009). "Pollutant removal performance of field-scale stormwater biofiltration systems." *Water Science and Technology*, 59(8), 1567-1576.
- Hsieh, C., and Davis, A. P. (2005). "Evaluation and optimization of bioretention media for treatment of urban storm water runoff." *Journal of Environmental Engineering*, 131(11), 1521-1531.
- Hunt, W. F., Jarrett, A. R., Smith, J. T., and Sharkey, L. J. (2006). "Evaluating bioretention hydrology and nutrient removal at three field sites in North Carolina." *Journal of Irrigation and Drainage Engineering*, 132(6), 600-608.
- Hunt, W. F., Smith J. T., Jadlocki S. J., Hathaway, J. M., and Eubanks, P. R. (2008). "Pollutant removal and peak flow mitigation by a bioretention cell in urban Charlotte, NC." *Journal of Environmental Engineering*, 134(5), 403-408.
- Kim, H., Seagren, E. A., and Davis, A. P. (2003). "Engineered bioretention for removal of nitrate from stormwater runoff." *Water Environment Research*, 75(4), 355-367.
- Ladson, A. R., Walsh, C. J., and Fletcher, T. D. (2006) "Improving stream health in urban areas by reducing runoff frequency from impervious surfaces." *Australian Journal of Water Resources*, 10(1), 23-32.
- Li, H., Sharkey, L. J., Hunt, W. F., and Davis, A. P. (2009). "Mitigation of impervious surface hydrology using bioretention in North Carolina and Maryland." *Journal of Hydrologic Engineering*, 14(4), 407-415.
- Lu, J, Sun, G., McNulty, S. G., and Amatya, D. M. (2005). "A comparison of six potential evapotranspiration methods for regional use in the southeastern United States." *Journal of the American Water Resources Association*, 41(3), 621-633.
- McNett, J. K., Hunt, W. F., and Osborne, J. A. (2010). "Establishing stormwater BMP evaluation metrics based upon ambient water quality associated with benthic macro-invertebrate populations." *Journal of Environmental Engineering*, 136(5), 535-541.
- McWhorter, D. B. (1971). "Infiltration affected by flow of air." *Hydrology paper No. 49*, Colorado State University, Fort Collins, Co.
- McWhorter, D. B., and Sunada, D. K. (1977). *Groundwater hydrology and hydraulics*, Water Resources Publications, Fort Collins, Co.

- N.C. Department of Environment and Natural Resources (NCDENR). (2009). "Chapter 12: Bioretention." *Stormwater best management practices manual*, North Carolina Department of Environment and Natural Resources, Division of Water Quality, Raleigh, N.C., 12.1-12.30.
- Newman, M. C., Dixon, P. M., Looney, B. B., and Pinder, J. E. (1989). "Estimating mean and variance for environmental samples with below detection limit observations." *Water Resources Bulletin*, 25(4), 905-916.
- Pandit, A., and Heck, H. H. (2009). "Estimations of soil conservation service curve numbers for concrete and asphalt." *Journal of Hydrologic Engineering*, 14(4), 335-345.
- Passeport, E., and Hunt, W. F. (2009). "Asphalt parking lot runoff nutrient characterization for eight sites in North Carolina, USA." *Journal of Hydrologic Engineering*, 14(4), 352-361.
- Passeport, E., Hunt, W. F., Line, D. E., Smith, R. A., and Brown, R. A. (2009). "Field study of the ability of two grassed bioretention cells to reduce storm-water runoff pollution." *Journal of Irrigation and Drainage Engineering*, 135(4), 505-510.
- Roseen, R. M., Ballesterro, T. P., Houle, J. J., Avelleneda, P., Widley, R., and Briggs, J. (2006). "Storm water low-impact development, conventional structural, and manufactured treatment strategies for parking lot runoff: Performance evaluations under varied mass loading calculations." *Transportation Research Record: Journal of the Transportation Research Board*, No. 1984, 135-147.
- Sharkey, L. J. (2006). "The performance of bioretention areas in North Carolina: A study of water quality, water quantity, and soil media." M.S. Thesis, North Carolina State University, Raleigh, N.C.
- Skaggs, R. W., and Khaleel, R. (1982). "Chapter 4: Infiltration." *Hydrologic modeling of small watersheds: Monograph No. 5*, American Society of Agricultural Engineers, St. Joseph, Mich., 121-166.
- State Climate Office (SCO). (2009). "1971-2000 climate normals." *Rocky Mount 8 ESE Station (Station #317400)*, State Climate Office of North Carolina, Raleigh, N.C. <<http://www.nc-climate.ncsu.edu/cronos/normals.php?station=317400>> (July 20, 2009).
- Strecker, E. W., Quigley, M. M., Urbonas, B. R., Jones, J. E., and Clary, J. K. (2001). "Determining urban storm water BMP effectiveness." *Journal of Water Resource Planning Management*, 127(3), 144-149.

- Thornthwaite, C. W. (1948). "An approach toward a rational classification of climate." *The Geographical Review*, 38(1), 55-94.
- U.S. Department of Agriculture – Natural Resources Conservation Service (USDA-NRCS). (2004a). "Chapter 9: Hydrologic soil-cover complexes." *Part 630 –Hydrology: National engineering handbook*, Washington D.C.
- U.S. Department of Agriculture – Natural Resources Conservation Service (USDA-NRCS). (2004b). "Chapter 10: Estimation of direct runoff from storm rainfall." *Part 630 – Hydrology: National engineering handbook*, Washington D.C.
- U.S. Environmental Protection Agency (USEPA). (1983). "Methods for chemical analysis of water and wastes." *Rep. No. EPA-600/4-79-020*, USEPA, Cincinnati, Oh.
- Walsh C. J., Fletcher T. D., and Ladson A. R. (2009). "Retention capacity: A metric to link stream ecology and storm-water management." *Journal of Hydrologic Engineering*, 14(4), 399-406.
- Zhang, L., Dawes, W. R., and Walker, G. R. (2001). "Response of mean annual evapotranspiration to vegetation changes at catchment scale." *Water Resources Research*, 37(3), 701-708.

3 IMPACTS OF MEDIA DEPTH ON EFFLUENT WATER QUALITY AND HYDROLOGIC PERFORMANCE OF UNDER-SIZED BIORETENTION CELLS

(This chapter was printed in a revised format)

Authors: R. A. Brown, W. F. Hunt III

Published: Journal of Irrigation and Drainage Engineering

Volume 137, Number 3, Pages 132-143

3.1 ABSTRACT

Fill media and excavation volume are the main costs in constructing bioretention cells, but the importance and impact of media depth in these systems is relatively unknown. Two sets of loamy sand filled-bioretention cells of two media depths (0.6 m and 0.9 m), located in Nashville, North Carolina, were monitored from March 2008 to March 2009 to examine the impact of media depth on their performance with respect to hydrology and water quality. Construction and design errors resulted in the surface storage volume being undersized for the design event (25 mm). The actual surface storage volume was only 28 percent and 35 percent of the design volume for the 0.6-m and 0.9-m media depth cells, respectively. Overflow (bypass) occurred at least three times more frequently than intended. The exfiltration volume was much higher in the deeper media cells, presumably attributable to greater storage volume in the media and more exposure to side walls. Evapotranspiration (ET) plus exfiltration accounted for 42 percent of the runoff in the 0.9-m media cells, while ET and exfiltration only accounted for 31 percent of the runoff in the 0.6-m media cells. With the increase in exfiltration, the deeper media depth met a previously defined low impact development (LID) hydrology goal of volume reduction more frequently than the shallower media system (44 percent of events compared to 21 percent). Larger outflow reduction consequently increased the reduction in pollutant loads. Estimated annual pollutant load

reduction for total nitrogen, total phosphorus, and total suspended solids were 21, 10, and 71 percent for the 0.6-m media cells and 19, 44, and 82 percent for the 0.9-m media cells, respectively. Overall, nitrogen reduction was poor due to suspected export of nitrate from fertilizer use, and phosphorus removal was hampered because of irreducible concentrations in the runoff. Pollutant reduction was limited due to the cells being undersized because of construction and design errors.

3.2 INTRODUCTION

Infiltration-based stormwater control measures (SCMs) are becoming widely used to reduce the negative impacts of urban stormwater runoff associated with increased impervious surfaces. As new stormwater rules focus on water quality and annual hydrologic balance, in addition to peak control, installing infiltration SCMs are necessary to obtain permits to construct developments. Bioretention is the most widely used low impact development (LID) SCM because of its versatility and level of performance. Bioretention functions to restore a site's natural hydrology by reducing runoff volume via ET and exfiltration. In addition to promoting natural hydrology, volume reduction is a very important component of pollutant load reduction. Bioretention also functions to capture or remove pollutants through adsorption, biological decomposition, filtration, and sedimentation. Bioretention combines a natural and engineered system to manage stormwater from developed areas. They are designed to improve the water quality of runoff before discharging into surface waters by capturing and treating runoff from a rainfall depth specified in design regulations.

Several years of intensive bioretention research and installation experience have assisted in the evolution of bioretention design guidelines. However, further research is required to continue to refine design criteria. Recently, Davis et al. (2009) evaluated the current knowledge of bioretention and what has been learned since the original concept was introduced over 18 years ago, in Prince George's County, Maryland. Fill media depth was identified as one of the design specifications in need of more research. For bioretention cells that require a specialized fill media that is mixed off-site, fill media represents one of the most expensive line items for construction. If performance of shallower systems were

comparable to that of deeper systems, shallower systems would be preferred because of savings in soil material and excavation costs.

Media depth requirements have changed since the initial concept was developed. The original guideline was 1.2 m so that adequate soil depth for tree and shrub roots was provided (Clar and Green 1993). However, with the eventual refinement of plant specifications, plants were chosen that could survive in shallower systems. Depending on the pollutant of concern, media depth selection could vary. Multiple studies have shown high removal of metals taking place in the top 0.2 m of media (Li and Davis 2008; Davis et al. 2001).

While field studies have monitored bioretention cells with different media depths, none of them has considered varying media depths with similar drainage area characteristics, drainage configurations, and in-situ soils in side-by-side plots (Davis 2008; Jones and Hunt 2009; Li et al. 2009; Passeport et al. 2009). Side-by-side bioretention cells will experience the same rainfall patterns and air temperatures, so the potential impact of these external variables on each storm will be avoided (Braga et al. 2007; Emerson and Traver 2008; Hunt et al. 2006). In North Carolina, vegetation governs media depth requirements. The minimum media depth is 0.6 m for cells vegetated with grass or shallow rooted plants and 0.9 m for cells vegetated with shrubs or trees (NCDENR 2009). In a comparison of six bioretention cells in North Carolina and Maryland, Li et al. (2009) showed that deeper media depths appeared to promote more exfiltration and ET, and the deeper media depths more closely mimicked predevelopment hydrology. They concluded that media depth may be a controlling design parameter to meet target hydrologic performance goals.

Previous field (Davis et al. 2006; Dietz and Clausen 2006; Hunt et al. 2006, 2008; Line and Hunt 2009; Roseen et al. 2006) and laboratory studies (Davis et al. 2001, 2006; Hsieh and Davis 2005a) have shown that bioretention overall has good removal rates and low effluent concentrations for heavy metals, oil/grease, total suspended solids (TSS), total nitrogen (TN), and total Kjeldahl nitrogen (TKN). However, in some of these studies, TN removal results have been mixed, attributable to poor bioretention media selection (Hunt et al. 2006), influx of groundwater into the underdrain (Line and Hunt 2009), and lack of an

anaerobic zone to promote denitrification for the reduction of nitrate plus nitrite ($\text{NO}_{2,3}\text{-N}$) (Kim et al. 2003). Conventionally drained bioretention cells, such as the ones presented in this study, lack an anaerobic zone, so “removal” of $\text{NO}_{2,3}\text{-N}$ has been poor, and in some cases, $\text{NO}_{2,3}\text{-N}$ effluent concentrations increased (Davis et al. 2001, 2006; Hsieh and Davis 2005b; Hunt et al. 2006, 2008; Line and Hunt 2009; Roseen et al. 2006).

The main objective of this research was to answer one of the critical questions associated with bioretention design and construction—the impact of fill media depth on bioretention performance. A second important study objective emerged post-construction: the impact on bioretention performance when cells have undersized surface storage volumes. This study assessed the performance of bioretention cells on a field scale that experienced the same rainfall depths and intensities under the same temperatures. Performance was measured both with respect to hydrology and water quality. With fill media comprising one of the major costs in bioretention cell construction, shallower media depth systems would be preferred if they were to function as well as deeper media systems. Furthermore, if bioretention cells are often under-constructed relative to design, what type of impact will this construction shortcoming have on annual performance?

3.3 SITE DESCRIPTION AND METHODS

The study site is located in the parking lot of a large commercial retail store in Nashville, NC (Fig. 3.1). Nashville is located in the Tar-Pamlico River Basin, and it lies on the edge of the Upper Coastal Plain. The site was constructed from June 2007 to February 2008, and for the data presented herein, monitoring took place from March 31, 2008 to March 10, 2009. During construction, 46,000 m^3 (60,000 yd^3) of soil was hauled from an off-site location, and 84,000 m^3 (110,000 yd^3) of soil was moved to another location on site because of the undulating topography at the original site. Heavy machinery compacted the soils at this site, which included the region where the bioretention cells were to be constructed. Since the quantity of soil hauled in and moved was so large, the in-situ soil lost its natural uniformity; therefore, bioretention performance measured at this site should be representative of many large-scale land development projects. Soil cores were taken of the

subsoil surrounding the bioretention cells (fill/haul soil) at depths ranging from 0.3 m (1 ft) to 0.9 m (3 ft) below the surface of the bowl. Particle size analysis was performed on 12 of the soil samples by the hydrometer method described in Gee and Bauder (1986). The texture of the underlying fill/haul soil samples ranged from sandy loam to loamy sand according to the U.S. Department of Agriculture (USDA) classification system. However, a few soil cores contained higher clay contents and were classified as sandy clay loam and clay loam. These samples were more frequently associated with the deeper samples of the 0.9-m media depth cells (collected from depths of 0.75 to 0.9 m below the bowl surface).

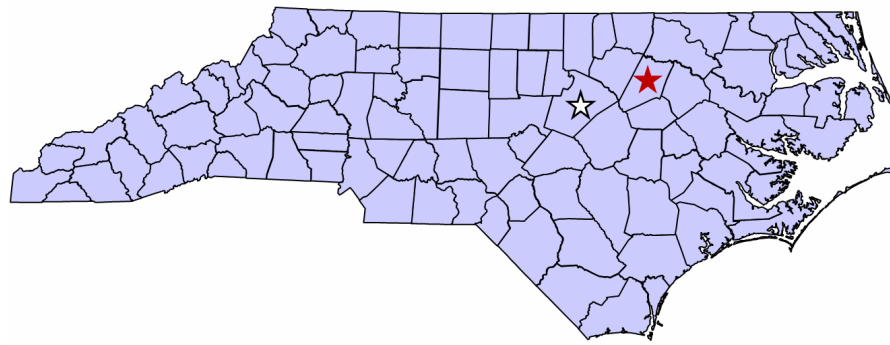


Figure 3.1: Location map of Nashville (solid star) with relation to Raleigh – NCSU campus (hollow star).

Seven bioretention cells treated runoff from the parking lot at this site (Fig. 3.2). Three cells were connected to one common outlet drain, and the other four cells were connected to a separate common outlet drain. Each of the cells acted in parallel. The set of three cells had a media depth of 0.9 m, and the set of four cells had a media depth of 0.6 m. Because of backwater constraints, the last cell in each set was not monitored (Fig. 3.2). The design specifications and actual characteristics of the cells monitored are presented in Table 3.1. According to the NC design standard, the discrete Soil Conservation Service-Curve Number (SCS-CN) method was used to design the bioretention cells to capture a 25 mm (1 in) event (NCDENR 2009). A specialized fill media consisting of 87.5 percent sand, 10 percent fines (silt and clay), and 2.5 percent certified compost was selected to have a design

infiltration rate of 25 mm/hr (1 in/hr). It was imported from a nearby sand mine, where it was thoroughly blended using large weighing scales. These bioretention cells were conventionally drained (no internal water storage zones) and vegetated with shrubs, perennials, and trees. Images of the bioretention cells after planting in February 2008 and after its first growing season in November 2008 are given in Figs. 3.3 and 3.4, respectively. Plant species in the cells include: red maple (*Acer rubrum*), sweet bay (*Magnolia virginica*), Virginia sweetspire (*Itea virginica*), liriop (Liriope sp.), verbena (*Verbena* sp.), and black-eyed Susan (*Rudbeckia hirta*). The asphalt parking lot, which drains to the bioretention cells, was observed to experience traffic typical of an active shopping center.

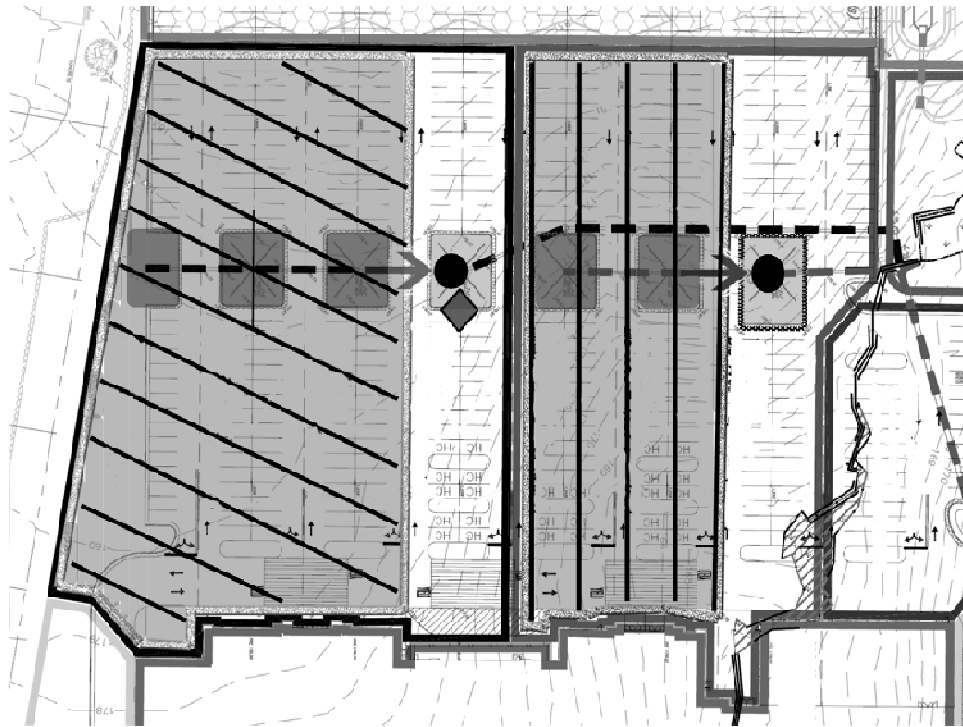


Figure 3.2: Layout of bioretention cells at the study site. The thick dashed lines represent the two outlet pipes, the arrow points to the weir location (solid black circle) in the outlet pipe where outflow was monitored, the diamond highlights the location of the representative runoff sampler, the cross-hatching highlights the drainage area for the 0.6-m media depth cells (left), the vertical lines highlight the drainage area for the 0.9-m media depth cells (right), the lighter shading represents the drainage area, and the darker shading represents the bioretention cell locations.



Figure 3.3: Bioretention cell shortly after planting and mulching were completed (February 2008).



Figure 3.4: Bioretention cell after a storm in November, 2008 (after 1 growing season).

Several months of monitoring data documented that the bioretention cells were not functioning according to design specifications. The ponding zone was not drawing down within 12 hours as required by regulations (NCDENR 2009); the surface drawdown time exceeded 48 hours. The bioretention cells were clogged with granite fines associated with the gravel base layer for the asphalt parking lot that washed into the cell during construction. Media for the cells was installed before the parking lot was paved, so the contractors protected the cells with a woven geotextile fabric to prevent fines from clogging the media (Fig. 3.5); however, the openings in the geotextile fabric were not small enough to prevent granite fines from passing through. An image of the fines clogging layer in the media is displayed in Fig. 3.6. The granite fines layer reduced the drawdown rate to a range of approximately 2.5 to 13 mm/hr, depending on season and individual bioretention cell, so minimal drawdown during an event in part led to overflow being generated more frequently than intended. Because of the high frequency of events with overflow, there was minimal peak flow mitigation; therefore, a discussion on peak flow will not be presented herein.



Figure 3.5: Woven geotextile fabric was placed on top of media (left) prior to the parking lot being paved with asphalt to prevent sediment from construction (right) from clogging the media.



Figure 3.6: Fines layer present within top layer (25 to 75 mm) of the media.

According to design, overflow should not have occurred for any rainfall event less than 25 mm. However, overflow was generated by rainfall events as small as 9 mm, meaning that this was the as-built water quality volume. After surveying the bioretention cells and their drainage catchment, it was determined that excessive overflow was created by the actual ponding depth and surface storage area of the bioretention cells being much less than the design specifications. The actual surface storage volume was only 28 percent and 35 percent of the designed surface storage volume for the 0.6-m and 0.9-m media depth cells, respectively (Table 3.1). These undersized cells were purposefully monitored for nearly one year, when they were repaired. All data presented herein were collected from the “undersized” cells. On March 11, 2009, the surface storage volume was increased to be closer to the design volume and the clogging layer was removed. Monitoring is planned to continue until March 2010 to compare the difference in performance of undersized and clogged cells to those that more closely resembled the design stated standards, which will be the subject of a future journal article. Watershed and bioretention characteristics are given in Table 3.1. Soil samples were collected from the top 0.3 m of media shortly after monitoring began and again after the end of the first monitoring period to analyze the media for chemical properties [P-Index and cation exchange capacity (CEC)]. The samples were analyzed by the North Carolina Department of Agriculture and Consumer Services.

Table 3.1: Summary of Nashville, NC bioretention cell characteristics.

Design Characteristics	0.6-m Media Depth	0.9-m Media Depth
Number of Cells Monitored	3	2
Drainage Area	0.68 ha (1.67 ac)	0.43 ha (1.07 ac)
Impervious Area	83%	97%
Design Cell Ponding Depth	0.3 m (12 in)	0.3 m (12 in)
Constructed Cell Ponding Depth	0.13 m (5 in)	0.15 m (6 in)
Design Cell Surface Area	425 m ² (4570 ft ²)	300 m ² (3250 ft ²)
Constructed Cell Surface Area	290 m ² (3120 ft ²)	206 m ² (2220 ft ²)
Design Cell Surface Storage Volume	124 m ³ (4380 ft ³)	91 m ³ (3210 ft ³)
Constructed Surface Storage Volume	37 m ³ (1240 ft ³)	32 m ³ (1120 ft ³)
Actual Storage Capacity vs. Design	28%	35%
Design Bioretention Infiltration Rate	25 mm/hr (1 in/hr)	
Actual Bowl Drawdown Rate	2.5-13 mm/hr (0.1-0.5 in/hr)	
P-Index (Fill Media) ^a	(Low): 11 to 18 (6/19/08); 3 to 6 (7/15/09)	
CEC (Fill Media) ^a	2.5 to 3.1	
Design Fill Media Specifications	87.5% Sand, 10% Fines ^b , 2.5% Certified Compost	
Actual Fill Media Composition ^c	86-89% Sand, 8-10% Silt, & 3-4% Clay	

^a Measured by NC Department of Agriculture & Consumer Services

^b Fines represent silt and clay sized particles

^c Determined by hydrometer method (Gee and Bauder, 1986)

3.4 FIELD DATA COLLECTION AND ANALYSIS

Automated samplers (ISCO 6712) with integrated flow meters (ISCO 730 Bubbler Module) were used to monitor runoff and outflow from the bioretention cells and collect flow-proportional samples. Two 90° v-notch weirs were installed in the common outlet pipe that collects overflow and underdrain flow from bioretention cells of similar media depth. The weirs were used in combination with the flow meters to measure outflow from the bioretention cells. Water levels measured by the flow meters were routinely checked during each field visit to verify accuracy. Within the typical range of underdrain flow (water level = 38.1 mm), the maximum error associated with the water level readings by the flow meter, including temperature influence, was ±3.4 mm, and it was ±6.1 mm at the maximum range of

the weir (water level = 381 mm). Including the maximum error of the water level reading, the range of discharge and maximum corresponding error for the low flow event (38.1 mm) were 0.311 L/s (21%) to 0.483 L/s (23%), and for the maximum range of the weir (381 mm), they were 118.8 L/s (4%) to 128.7 L/s (4%). The precision of the monitoring equipment is a potential source of error; however, it is relatively small.

A tipping bucket rain gauge (ISCO 674 Rain Gauge) was installed to measure rainfall intensity, while a manual plastic rain gauge measured rainfall depth. Runoff from the parking lot entered each bioretention cell through two curb cuts, one on either side (Fig. 3.3). A rectangular weir was installed at one of the curb cuts in one of the cells to monitor the water quality of the runoff from a representative section of parking lot by collecting flow-proportional samples. The concentrations from this one location (Fig. 3.2, diamond) were used to characterize runoff into all of the bioretention cells. The drainage area of this location is approximately one-eighth of the entire impervious asphalt parking lot that drains into the five monitored bioretention cells.

Flow-proportional storm samples were analyzed for nutrients and TSS. The nutrient species analyzed were orthophosphate (Ortho-P), total phosphorus (TP), total ammoniacal nitrogen (TAN), $\text{NO}_{2,3}\text{-N}$, Organic-N (ON), TKN, and TN. Samples were transferred to laboratory containers, placed on ice, and taken to the NCSU Center for Applied Aquatic Ecology (CAAE) laboratory (state-certified laboratory) within 24 hours to conduct chemical analyses as shown in Table 3.2. No preservation was used in the automated samplers; thus, samples that could not be recovered from the machine within 24 hours were discarded. Samples were collected from 20 events during the monitoring period.

Table 3.2: Summary of analytical methods for water quality analysis.

Abbreviation	Pollutant	Analytical Method	RL	Unit
NO _{2,3} -N	Nitrate + Nitrite nitrogen	SM 4500-NO ₃ -F ^a	0.0056	mg/L
TKN	Total Kjeldahl nitrogen	EPA 351.1 ^b	0.14	mg/L
TAN	Total ammoniacal nitrogen	SM 4500-NH ₃ -H ^a	0.007	mg/L
ON	Organic nitrogen	= TKN – TAN	N/A	mg/L
TN	Total nitrogen	= NO _{2,3} -N + TKN	N/A	mg/L
Ortho-P	Orthophosphate	SM 4500-P-F ^a	0.006	mg/L
TP	Total phosphorus	SM 4500-P-F ^a	0.01	mg/L
TSS	Total suspended solids	SM 2540 D ^a	1	mg/L

^a Source (Eaton et al. 1995)

^b Source (USEPA 1983)

3.5 CALCULATING RUNOFF, OUTFLOW, OVERFLOW, AND EVAPOTRANSPIRATION

3.5.1 Runoff

Runoff into each cell was calculated for each event by subtracting an initial abstraction depth from the rainfall depth measured in the plastic rain gauge and multiplying this depth by the drainage area. Initial abstraction values were calculated using curve numbers for the impervious asphalt parking lot and for the pervious surfaces (open space, poor conditions) (USDA-NRCS 2004a). The curve numbers varied based on antecedent moisture conditions at the site (USDA-NRCS 2004b). The range of the curve numbers and antecedent moisture conditions used in estimating runoff are presented in Table 3.3. Pandit and Heck (2009) found that nearly all of the rainfall on asphalt surfaces is transmitted to runoff. Discrete rainfall events were defined as those greater than 2.5 mm (0.10 in) and having an antecedent dry period of 6 hours or greater.

Table 3.3: Curve number and initial abstraction values for pervious and impervious land uses and varying antecedent moisture conditions.

Antecedent Moisture Condition	Curve Number (Initial Abstraction) for:		Antecedent Dry Period
	<i>Pervious Land Use</i>	<i>Impervious Land Use</i>	
1 (dry)	72 (19.8 mm)	97 (1.5 mm)	> 120 hours
2 (average)	86 (8.4 mm)	98 (1.0 mm)	48 to 120 hours
3 (wet)	94 (3.3 mm)	99 (0.5 mm)	6 to 48 hours

3.5.2 Outflow and Overflow

Outflow was measured with a 90° v-notch weir that was fixed into the 0.75-m diameter outlet concrete pipe connecting all cells of like media depth. The bioretention cells were constructed with overflow structures that mixed overflow with underdrain effluent into the same outlet pipe. Outflow was measured and water quality samples were collected from a combination of underdrain flow and overflow. Despite the underdrain flow and overflow being measured together, it was evident when overflow occurred by examining the outflow hydrograph. An example outflow hydrograph for an event with and without overflow is shown in Fig. 3.7. Underdrain flow appears as a relatively constant but gradually changing flow rate, where overflow can easily be identified by the rapid and short spikes in flow rate. To account for the volume of overflow, the outflow volume was calculated during the time period when the flow rate spiked. Then, the average of the flow rate before and after the spike (stable flow rate) was multiplied by the time period during which overflow occurred and this product was subtracted from the outflow volume to obtain the overflow volume. Underdrain flow was estimated by the difference between outflow volume and overflow. All of the runoff volume that did not leave through outflow was assumed to be lost through ET and exfiltration based on the water balance equation (Equation 3.1).

$$Vol_{in} = Vol_{Outflow} + \Delta S + Vol_{ET} + Vol_{EXF} \quad (3.1)$$

where Vol_{in} = runoff volume, $Vol_{outflow}$ = volume of underdrain flow and overflow, ΔS = change in subsurface and surface storage, Vol_{ET} = evapotranspiration volume, and Vol_{EXF} = exfiltration volume. Exfiltration is water leaving the bioretention media through the bottom and sides of the cell and entering the in-situ soil; it can also be referred to as seepage.

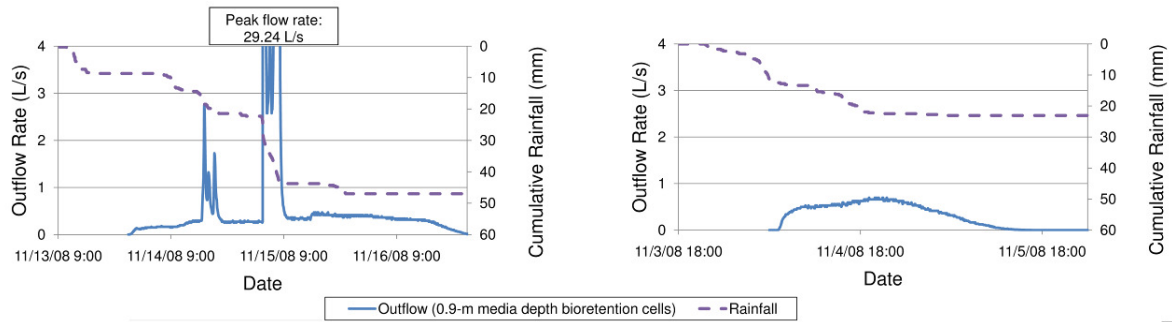


Figure 3.7: Outflow rate in the 0.9-m media depth cells and total rainfall amount versus time for an event with overflow [11/13/08-11/16/08] (left) and without overflow [11/3/08-11/5/08] (right). The periods of overflow are evident by the rapid spike in outflow rate (11/14/08, 3:30PM-8:00PM and 11/15/08, 4:30AM-9:30AM); peak outflow rate during overflow reached 29.24 L/s.

Statistical analyses were conducted using SAS version 8 (SAS Institute Inc., Cary, NC). Comparisons were made between inlet parameters and outlet parameters and among outlet parameters, and the level of significance used in all analyses was $\alpha = 0.05$. Four statistical tests for normality were used to check the validity of the assumption that the data were normal: Shapiro-Wilk, Kolmogorov-Smirnov, Creamer-von Mises, and Anderson-Darling. These tests showed better fits for normality when the data were log-transformed, so all the water quality data were log-transformed. Strecker et al. (2001) also reported that a valid approximation of water quality data for stormwater examined were lognormal distributions. To avoid issues with log-transforming data when samples for Ortho-P were below the reportable limit, a value of 0.001 mg/L was used (six times lower than the lowest recorded value). A paired t-test was used to determine significance if the data were normally distributed. Data were checked for outliers if the distribution was not normal and a

nonparametric test was performed to determine level of significance. A Wilcoxon signed-rank test was used to check significance if the data were symmetric. If the assumption of symmetry was not valid, a sign test was performed to determine significance.

3.5.3 Evapotranspiration

Evapotranspiration (ET) was estimated using the equation (Equation 3.2) developed by Zhang et al. (2001), where they correlated mean actual evapotranspiration (AET), annual precipitation (P), and potential evapotranspiration (PET), based on hydrologic data from over 250 watersheds across the world.

$$\frac{AET}{P} = \frac{1 + w \frac{PET}{P}}{1 + w \frac{PET}{P} + \frac{P}{PET}} \quad (3.2)$$

where w = the plant-available water coefficient, and it is representative of the way plants use soil-water for transpiration. A plant-available water coefficient of 0.5 was selected because this is the best fit for shortgrass and crops, which have similar root depths as the shrubs and perennials found in the bioretention cells of this study. Forested areas would have a plant-available water coefficient of 2.0.

PET was calculated using the Thornthwaite method (Thornthwaite 1948). Thornthwaite is the simplest method to calculate PET because it only requires one temperature term—average monthly temperature. Data for this term was found on the State Climate Office of NC website for the Nashville monitoring station—site ID: 316044 (SCO 2009). When the Thornthwaite method was compared to five other methods for estimating PET in Lu et al. (2005), it was found that Thornthwaite yielded the lowest annual values of PET. This can be attributed to the simplicity of the Thornthwaite equation, where the other methods have terms to account for radiation and other parameters. Since Thornthwaite underestimated PET, correction factors were included to provide a more reliable PET estimate (Amatya et al. 1995). Amatya et al. (1995) calculated correction factors for the Thornthwaite method at three sites in eastern North Carolina. The closest of these sites to

Nashville was Tarboro, North Carolina, which is approximately 35 km east of the bioretention research site.

3.6 RESULTS AND DISCUSSION

3.6.1 Hydrology

Sixty-four discrete runoff producing events were monitored for hydrology during the first phase of this study. The mean and median storm rainfall depths were 17.0 and 12.5 mm, respectively. Hydrologic performance was measured by examining the 24-hour effluent/influent volume ratio, as expressed by Equation 3.3—a LID hydrology goal first proposed in Davis (2008)

$$f_{V24} = \frac{V_{out-24}}{V_{in}} \quad (3.3)$$

where V_{out-24} = outflow volume leaving the cell within 24 hours and V_{in} = runoff volume into the bioretention cell. Davis (2008) suggested an LID site should have $f_{V24} < 0.33$. Two-thirds reduction was chosen because the rational method C coefficient of a highly impervious surface is often 0.9, and it is about 0.3 for an undeveloped (pervious) area (Davis 2008). Using this performance criterion, the bioretention cells with 0.9-m deep media met the LID hydrology goals more frequently (44 percent) compared to the 0.6-m deep cells (21 percent). There is a clear difference in 24-hour effluent/influent volume ratio between the 0.6-m and 0.9-m media depth cells (Fig. 3.8). In comparing the probability of achieving the target ratio (0.33) to the six bioretention cells in North Carolina and Maryland with varying media depths presented in Li et al. (2009), the 0.6-m media depth cells in Nashville met the LID goal less frequently than all six cells. The 0.9-m media depth cells only met the LID goal more frequently than one cell—a lined cell with 0.5–0.6 m media depth in Louisburg, North Carolina. The median f_{V24} was 0.56 and 0.39 for the 0.6-m and 0.9-m media depth cells, respectively. When this metric (median f_{V24}) was compared to data in Li et al. (2009), the 0.6-m media depth cells performed similarly to the lined cell at Louisburg (media depth: 0.5–

0.6 m) and a cell at College Park, Maryland (media depth: 0.5–0.8 m)—median $f_{V24} = 0.60$. The 0.9-m media depth cells performed better than both of these cells and was comparable to the unlined cell at Louisburg (media depth: 0.5–0.6 m)—median $f_{V24} = 0.36$. The cells that performed the best (lowest median f_{V24}) were the ones that were properly constructed and had the deepest media depths—two with 1.2-m media depths (Greensboro, North Carolina) and one with a 0.9-m media depth (Silver Spring, Maryland). All of the cells in Li et al. (2009) were properly constructed, so overflow was not as frequent. As overflow volume decreases, the potential improves for a larger volume of stormwater to be slowly filtered and either released as exfiltration or ET. The suspected reason the Nashville cells exported larger fractions of outflow is their being undersized attributable to poor construction.

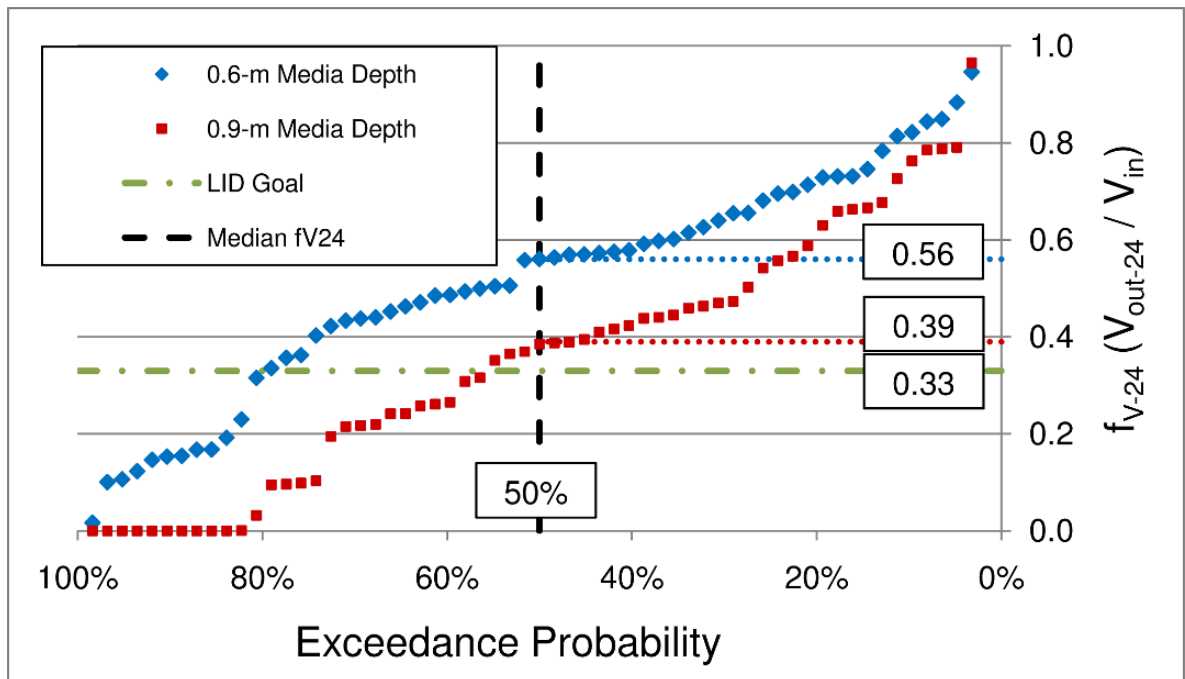


Figure 3.8: Exceedance probability of 24-hour effluent/influent volume ratio in Nashville bioretention cells.

The total PET calculated during the 11.5-month monitoring period using the Thornthwaite method with correction factors was 861 mm, and the precipitation during the

study period was 1,035 mm. To estimate actual ET, the PET and precipitation were substituted into Equation 3.2, along with a plant-available water coefficient of 0.5. The calculated depth of actual ET was 560 mm. Since ET only occurred in the bioretention cells, this depth was multiplied by the bioretention surface area to determine the volume of ET to be used in the water balance. Because the ratio of bioretention surface area to drainage area is small (approximately 4 to 5 percent), the contribution of ET is relatively small on an annual basis. The estimated percentage of runoff that left the bioretention cells as ET was approximately 3 percent. Since the cells have similar surface areas and vegetation, there is little difference in ET between the two sets of cells.

Combined underdrain and overflow were monitored as outflow. Excess runoff not measured in the outflow was calculated to be lost through exfiltration and ET (Equation 3.1). With ET being estimated as 3 percent of the annual runoff for both sets of cells, the rest of the runoff volume was attributed to exfiltration. In the 0.9-m media depth cells, 39 percent of runoff was lost through exfiltration compared to 28 percent for the 0.6-m media depth. This supports Jones and Hunt (2009) and Li et al. (2009), who suggest that deeper cells (or cells with more relatively more media volume) promote more exfiltration. When comparing the overflow volumes, the 0.9-m media depth had 35 percent of the runoff leaving as overflow; whereas, the 0.6-m media depth had 37 percent as overflow. The 0.6-m media depth cells had slightly more overflow because they had a smaller surface storage volume compared to that of the 0.9-m media depth cells. The remaining annual flow was released through the underdrains, as seen in the water balance in Fig. 3.9.

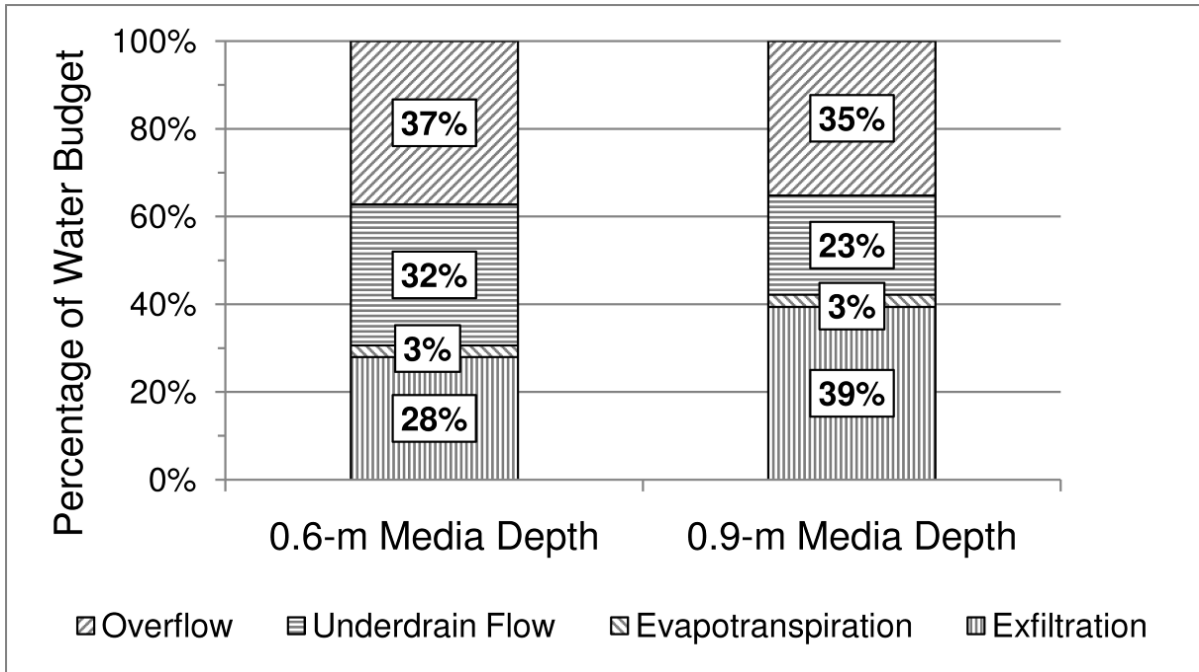


Figure 3.9: Water budget for 1 year monitoring period for Nashville bioretention cells.

The water balance was then broken down further to evaluate performance for various sized events (Table 3.4). From these data, the reduction of outflow is greatest for the smallest events, which would be expected. The design storm event was 25 mm, but inattentive construction management caused the brink overflow event to be less than one-half the design event—approximately 9 mm (rainfall depth). Some events larger than the brink overflow event could be captured without generating overflow, typically those of long duration and low intensity. Drawdown during an event would increase storage potential, allowing several events up to 13 mm to be captured by both sets of cells without generating overflow. One larger event (22 mm) was captured and produced no overflow in the 0.9-m media depth bioretention cells only, Fig. 3.7. For events smaller than half of the design event (2.5–13 mm), the total volume of runoff released through ET and exfiltration was 47 percent and 65 percent for the 0.6-m and 0.9-m media depth cells, respectively. This event size range is also consistent with events that could fully be captured in the bowl; however, even a few of these events generated some overflow. The large percentage of ET and exfiltration from

these events could be attributed to exfiltration into the sandy loam to loamy sand soils surrounding the bioretention media. For each range of rainfall depths presented in Table 3.4, the 0.9-m media depth cells have a substantially larger volume being released through ET and exfiltration, but the difference decreases as event size increases. The hypothesis for the deeper media depth cells being able to exfiltrate more water is that they have more media available to capture and store a larger portion of the more frequent, smaller storm events, as shown in Table 3.4. For larger storm events, the surface area of the bioretention cell exposed to in-situ soil is greater, creating the opportunity for increased exfiltration.

Table 3.4: Summary of water balance for various sized storm events.

Rainfall Depth (mm)	# of events	Estimated Underdrain Flow	Estimated Overflow	Total Outflow	Estimated ET & Exfiltration
		<i>0.6-m Media Depth Cells</i>			
2.5-13	33	42%	10%	53%	47%
13-25	18	38%	29%	67%	33%
25-38	6	22%	51%	74%	26%
>38	3	23%	59%	82%	18%
<hr/>					
<i>0.9-m Media Depth Cells</i>					
2.5-13	33	26%	8%	35%	65%
13-25	18	26%	27%	53%	47%
25-38	6	19%	50%	69%	31%
>38	3	16%	59%	75%	25%

Of the 64 monitored events, 11 exceeded the design storm (25 mm), so by design, no more than 11 events should have produced overflow (17% of the events monitored). However, because of the reduced surface storage, overflow was generated in 59% and 55% of the events monitored in the 0.6-m and 0.9-m deep cells, respectively. During the monitoring period, 26 events were smaller than the brink overflow event of 9 mm (0.35 in), which corresponded to the 26 and 29 events that had no overflow in the 0.6-m and 0.9-m media depth cells, respectively. Recall from Table 3.1, the 0.9-m media depth cells had a slightly larger surface storage volume. Table 3.5 highlights a summary of outflow conditions

for the events monitored. The 0.9-m media depth cells fully captured more events because they have a larger volume of media to store all the runoff from smaller rainfall events. Out of 64 events, the number of events fully assimilated (no outflow) by the 0.6-m and 0.9-m media depths were 0 and 11, respectively. The 11 events fully assimilated in the 0.9-m media depth were characterized as having dry to normal antecedent moisture conditions and precipitation less than 5 mm. Despite the reduced surface storage capacity in the first phase of this study, the data show that the deeper media cells are performing better than the shallower cells with respect to meeting the hydrologic goal of volume reduction.

Table 3.5: Characterization of forms of outflow monitored.

Media Depth	Events Monitored	Events with:			Events > 25 mm^a	Events > 9 mm^b
		<i>No Outflow</i>	<i>Underdrain Discharge Only</i>	<i>Overflow and Underdrain Drainage</i>		
0.6-m	64	0	26	38	11	26
0.9-m	64	11	18	35	11	26

^a 25 mm (rainfall depth) was the design event, but due to inadequate construction, this was not achieved

^b 9 mm (rainfall depth) is the brink overflow depth, approximate for the constructed storm depth

3.6.2 Water Quality

Average event mean concentrations (EMCs) were calculated for the parking lot runoff and outflow from the 0.6-m and 0.9-m media depth bioretention cells. The EMCs are summarized with the water quality results in Table 3.6. Efficiency ratios (ER) were calculated using Equation 3.4.

$$ER = \frac{(EMC_{Runoff} - EMC_{Outflow})}{EMC_{Runoff}} \quad (3.4)$$

where EMC_{Runoff} and $EMC_{Outflow}$ represent the mean of the EMCs across all storm events in the monitoring period for the parking lot runoff and bioretention outflow, respectively. Statistical analyses determined whether significant differences ($p < 0.05$) of pollutant

concentrations existed between: (1) the runoff and outflow from the 0.6-m media depth cells (In/0.6-m), (2) the runoff and outflow from the 0.9-m media depth cells (In/0.9-m), and (3) outflow from both media depths (0.6-m/0.9-m). For all water quality constituents, with the exception of Ortho-P, statistical analyses were performed on data for 19 runoff storm events and 20 outflow storm events for both media depth bioretention cells. Ortho-P results were based on 17 and 18 storm events for the runoff and outflow, respectively. A substantial portion of the runoff entering the bioretention cells were not treated by the bioretention media. The percentage of outflow that left the system as overflow was 54 percent and 61 percent for the 0.6-m and 0.9-m media depth cells, respectively. For this portion of the outflow monitored for water quality, sedimentation was the only pollutant removal mechanism. Since overtopping runoff entered the emergency overflow structure in the center of the bioretention cell, the water movement did slow and sedimentation occurred. With such a large percentage of the outflow consisting of overflow, concentration reductions were expected to be less than those of studies that only measure water quality of the drainage. Also, the impact of concentration reduction was not expected to be that great for pollutants that are not primarily treated through sedimentation because the volume of overflow present in the outflow was greater than the drainage volume.

Table 3.6: Average EMCs (mg/L), efficiency ratios, and statistical analyses for parking lot runoff and outflow from the 0.6-m and 0.9-m media depth bioretention cells.

Pollutant	Runoff (In) ^a	Outflow ^a		Efficiency Ratio ^b		Significant Differences (p-value)		
		0.6-m Media	0.9-m Media	0.6-m Media	0.9-m Media	In / 0.6-m	In / 0.9- m	0.6-m / 0.9-m
ON ^c	0.45 ± 0.39	0.49 ± 0.26	0.46 ± 0.31	(0.08)	(0.02)	No	No	No
TAN ^c	0.29 ± 0.48	0.05 ± 0.07	0.08 ± 0.08	0.82	0.74	Yes (<0.0001)	Yes (0.0002)	No
NO _{2,3} -N ^c	0.19 ± 0.11	0.59 ± 0.72	1.11 ± 1.36	(2.09)	(4.77)	Yes (0.0087)	Yes (< 0.0001)	Yes (< 0.0001)
TN ^c	0.94 ± 0.87	1.13 ± 0.91	1.64 ± 1.56	(0.21)	(0.75)	No	Yes (0.0297)	Yes (0.0016)
Ortho-P ^d	0.026 ± 0.085	0.029 ± 0.026	0.028 ± 0.026	(0.13)	(0.09)	Yes (Sign: 0.0127)	Yes (0.0002)	No
TP ^c	0.073 ± 0.105	0.074 ± 0.024	0.059 ± 0.024	(0.02)	0.19	Yes (0.0288)	No	Yes (0.0041)
TSS ^c	25 ± 14	9.9 ± 5.6	7.3 ± 6.5	0.60	0.71	Yes (0.0002)	Yes (< 0.0001)	Yes (0.0049)

^a Pollutant concentrations are presented as an average of the event mean concentrations +/- standard deviation

^b Parentheses and italics represent an increase in pollutant concentration

^c n=20 outflow; n=19 runoff

^d n=18 outflow; n=17 runoff

3.6.2.1 Nitrogen Species

Overall, the EMC was higher in the outflow for ON, NO_{2,3}-N, and TN, and it was lower for TAN. In comparing the outflow from each set of cells to the runoff, there was no significant change of ON, a significant reduction of TAN, and a significant increase of NO_{2,3}-N. Despite an increase in the outflow concentrations for TN from both sets of cells, there was no significant change between the runoff and outflow concentrations for the 0.6-m media depth cells; however, there was a significant increase for the 0.9-m media depth cells, when compared to runoff concentrations. When comparing the outflow concentrations to each other, there was no significant difference for ON and TAN, but a significant difference was

present for $\text{NO}_{2,3}\text{-N}$, and this led to a significant difference for TN. The average EMC of TN in the runoff was 0.94 mg/L, which is much lower than data presented in Passeport and Hunt (2009), where the average concentration reported for runoff from parking lots was 1.63 mg/L. Passeport and Hunt's (2009) reported parking lot runoff concentration is nearly identical to the average outflow EMC for the 0.9-m media (1.64 mg/L) and higher than the average outflow EMC from the 0.6-m media (1.13 mg/L). When compared to typical parking lot runoff, the TN outflow concentrations are not too high, but they are higher when compared to the runoff from this parking lot.

The cells studied at this site had excellent reductions of TAN, but no change for ON, and both sets of cells performed similarly. The biggest issue at this site was the large increase in $\text{NO}_{2,3}\text{-N}$, which consequently led to an increase in TN. Because of the conventional drainage configuration, in which no anaerobic portion of the cell is designed, a slight increase or no change in $\text{NO}_{2,3}\text{-N}$ was expected (Dietz and Clausen 2005; Hunt et al. 2008; Line and Hunt 2009).

Closer inspection of the $\text{NO}_{2,3}\text{-N}$ results showed little difference between runoff and outflow concentrations during the first two months of monitoring. Then, samples taken from July through November had outflow concentrations up to 20 times higher than runoff concentrations. During the final four months of monitoring, there was again no noticeable difference between the runoff and outflow concentrations, so the conditions appeared to be "back to normal." The results of this study were similar to the laboratory study by Hsieh and Davis (2005b), where stormwater was applied to bioretention media columns once a week for 12 weeks. Little difference was present for the first week, but $\text{NO}_{2,3}\text{-N}$ began to export at much higher rates for the next 4 weeks, with effluent concentrations then returning to concentrations measured in the first week from the 6th to 12th week. The reason for spiked effluent concentrations was attributable to exporting of $\text{NO}_{2,3}\text{-N}$ from mulch. Ninety-one percent of the original $\text{NO}_{2,3}\text{-N}$ contained in the mulch was lost (Hsieh and Davis 2005b). Chemical properties of the mulch were not measured at the Nashville site, so the extent of the contribution from the mulch as a nitrogen source is unclear. It is believed that it was a

contributing factor because of the rapid growth of plants, especially those on the sideslopes that do not contact and therefore receive nutrients from stormwater runoff (Figs. 3.3 and 3.4). The mulch in these cells was also spread exceptionally thick. When it was first applied in February 2008, there were portions of the cells where the mulch depth exceeded 20 cm. Another possible explanation for the increase in $\text{NO}_{2,3}\text{-N}$ could be attributable to fertilization of the plants upon planting. Unfortunately, this could not be verified with the landscaper at the site.

3.6.2.2 Phosphorus Species

Past studies have shown poor phosphorus sequestration when media saturated with phosphorus was used (Hunt et al. 2006). The media at this site had a low P-Index (Table 3.1), so good phosphorus entrapment was expected (Hardy et al. 2007). The average outflow concentrations for TP were very low: 0.074 mg/L and 0.059 mg/L for the 0.6-m and 0.9-m media depth cells, respectively. There was little reduction of phosphorus concentration compared to the runoff because the runoff concentration was also quite low—0.073 mg/L. Rarely have effluent concentrations from bioretention cells treating parking lots been as low as 0.07 mg/L (Hunt et al. 2006, 2008; Line and Hunt 2009). Therefore, an irreducible concentration (Strecker et al. 2001) of phosphorus may have entered the bioretention cells. When compared to an average TP concentration of 0.21 mg/L for eight other parking lots in North Carolina, this parking lot's concentration is quite low (Passeport and Hunt 2009). The runoff concentration (0.498 mg/L) for one event on September 17, 2008, was approximately nine times higher than the average event mean concentration; however, the outflow concentrations (0.123 and 0.077 mg/L) were relatively similar to their study averages. This one event illustrates that when this specialized media was exposed to runoff with relatively higher TP concentrations, the concentration present in the outflow was substantially lower.

Statistical analyses showed runoff and outflow concentrations of TP were not significantly different for the 0.9-m media depth, but the outflow concentrations were significantly higher than the runoff for the 0.6-m media depth. The 0.9-m media depth outflow had a significantly lower TP concentration than the 0.6-m media depth. The outflow

Ortho-P concentrations were both significantly higher than the runoff, but no significant difference was present when the two outflows were compared. Concentrations of Ortho-P were very low and were below the reportable limit in 10 of 17 and one of 18 samples for the runoff and 0.6-m media depth outflow, respectively. Since no difference was present in the Ortho-P, particle-bound phosphorus was the cause for the significant difference in TP for the two outflows. The 0.6-m media outflow had higher concentrations of TSS than the 0.9-m media.

3.6.2.3 Total Suspended Solids

Bioretention cells collect runoff and create conditions for sedimentation and filtration; thus, they have been shown to provide good capture of TSS and other total solids. However, sedimentation increases the risk of clogging, so bioretention cells need to be maintained. These bioretention cells were designed to overflow in the center of the cell as opposed to having excess water bypass the bioretention cell. Runoff from events with overflow was still exposed to sedimentation. There was a significant reduction in TSS for both media depth cells; however, the outflow in the 0.6-m media was significantly higher than the 0.9-m media outflow. An explanation for this could be attributable to more overflow volume in the 0.6-m media, so less sedimentation time occurred in these cells. Nonetheless, the difference was not substantial (< 3 mg/L).

3.6.3 Load Calculations

Pollutant load reduction is an important way to measure the performance of a SCM. With infiltration-based SCMs, such as bioretention, reducing outflow through ET and exfiltration can greatly improve performance. Loads were calculated for the 18 storm events that had reliable flow data and water quality samples at all three monitoring sites. These data were summed and the totals are shown in Table 3.7. The Ortho-P load reduction was only calculated for 16 events, because the laboratory did not analyze Ortho-P for two events attributable to exceedance of Ortho-P's 48-hour holding time. The sum of precipitation from the 18 events was slightly more than half of the normal annual rainfall (Table 3.8). Pollutant

loads presented in Table 3.9 are normalized by season. To estimate the annual pollutant loads, Equation 3.5 was used ('i' refers to season, 1 for spring and 4 for winter; Rf = rainfall):

$$Annual\ Load = \sum_{i=1}^4 Seasonal\ Load \times \frac{Rf_{Events\ monitored\ during\ season}}{Rf_{Normal\ seasonal\ depth}} \quad (3.5)$$

Table 3.7: Pollutant load calculations for the 18 events with available flow and water quality data.

Pollutant	0.6 m Cells			0.9 m Cells		
	<i>In</i> (kg/ha) ^a	<i>Out</i> (kg/ha) ^a	<i>Percent</i> <i>reduction or</i> <i>increase</i> ^b	<i>In</i> (kg/ha) ^a	<i>Out</i> (kg/ha) ^a	<i>Percent</i> <i>reduction or</i> <i>increase</i> ^b
TKN	2.91	1.78	39	3.26	1.37	58
ON	1.75	1.53	13	1.90	1.08	43
NO _{2,3} -N	0.84	1.52	(81)	0.95	2.30	(142)
TN	3.75	3.31	12	4.20	3.67	13
TAN	1.16	0.26	78	1.36	0.29	79
TP	0.27	0.26	5.3	0.30	0.17	44
Ortho-P	0.06	0.08	(37)	0.07	0.07	(5.1)
TSS	134.9	39.1	71	146.6	23.5	84

^a Calculated loading rates are presented as kg/ha of drainage area.

^b Parentheses denotes an increase in pollutant load.

Table 3.8: Seasonal summary of the precipitation depths of events used to calculate pollutant loads compared to normal seasonal precipitation depths.

	Percentage of events used to calculate loads compared to normal precipitation	Precipitation depth of events used to calculate loads (cm)	Normal precipitation depth^a (cm)
Spring 2008	47%	12.8	26.8
Summer 2008	65%	19.3	29.4
Fall 2008	61%	13.5	22.3
Winter 2009	34%	10.4	30.4
Year	51%	55.9	108.9

^a Normal precipitation data from 1971-2000 climate averages in Nashville, NC (SCO, 2009).

Table 3.9: Estimation of annual pollutant loads for the bioretention cells based on normal rainfall depths.

Pollutant	0.6 m Cells			0.9 m Cells		
	<i>In</i> (kg/ha/yr) ^a	<i>Out</i> (kg/ha/yr) ^a	<i>Percent reduction/increase^b</i>	<i>In</i> (kg/ha/yr) ^a	<i>Out</i> (kg/ha/yr) ^a	<i>Percent reduction/increase^b</i>
TKN	5.56	3.24	42	6.15	2.62	57
ON	3.32	2.75	17	3.59	2.03	43
NO _{2,3} -N	1.73	2.56	(48)	1.92	3.92	(104)
TN	7.30	5.80	21	8.07	6.55	19
TAN	2.24	0.49	78	2.57	0.59	77
TP	0.52	0.47	10	0.57	0.32	44
Ortho-P	0.10	0.14	(39)	0.11	0.12	(8.6)
TSS	244.8	72.0	71	264.5	46.4	82

^a Calculated annual loading rates are presented as kg/ha of parking lot.

^b Parentheses denotes an increase in annual pollutant load.

When the impact of volume reduction was included in the performance evaluation, the 0.9-m media had greater pollutant load reductions than the 0.6-m media for all the water quality constituents except NO_{2,3}-N, and the pollutant load reductions were essentially the same for TN and TAN. In North Carolina, bioretention is awarded credits for pollutant load

removals of 35, 45, and 85 percent for TN, TP, and TSS, respectively (NCDENR 2009). When these numbers were compared to the estimations for pollutant load reduction calculated for this site, the 0.9-m media appears to be more appropriate to be achieving these levels of reduction. The biggest difference between the cells is with respect to TP, where the 0.9-m media achieved a reduction of 44 percent, but only a 10 percent reduction occurred in the 0.6-m media. The amount of removal was 11 percentage points higher in the 0.9-m media for TSS, with a reduction of 82 percent. The TN performance was “underachieving” because the average EMC was significantly higher in the outflow than in the runoff. The increased TN concentrations were masked when the performance was measured on a load reduction scale because of the large volume reduction through exfiltration. The 0.9-m media achieved a TN reduction of 19 percent, where the 0.6-m media achieved a reduction of 21 percent. For both nutrients, but particularly for phosphorus, runoff concentrations were very low, thus making percent pollutant removal a poor metric for performance (Strecker et al. 2001).

3.7 CONCLUSIONS

A few major conclusions can be drawn from this study:

1. Care must be taken during bioretention cell construction. Under-sizing the surface storage volume has an important negative impact on bioretention performance. As overflow becomes a more frequent occurrence, a larger percentage of runoff goes untreated to the stormwater network. Poor performance from this site was attributable to a lack of surface storage. The 0.6-m and the 0.9-m media cells, as constructed, only held 28 percent and 35 percent of the designed storage capacity (25 mm) in their bowls. The brink overflow event from the bioretention cells was 9 mm. In the 0.6-m and 0.9-m media depth cells, overflow occurred in 59 percent and 55 percent of the events and accounted for 37 percent and 35 percent of the annual water balance, respectively. Designers who specifically undersize bioretention bowl capture volumes must “beware” as well that purposeful under-sizing the bowl volume may have substantial negative impacts on cell performance.

2. Similar to data found in the literature, the deeper media depths promote more exfiltration and less outflow volume. With more media present to store runoff and more area exposed to the in-situ soil to exfiltrate water, the deeper media depths released less outflow. The data show that a LID hydrology goal of 24-hour volume reduction is met more frequently in the deeper (0.9-m) media depth (44 percent of events) compared to the shallower (0.6-m) media depth (21 percent of events). Since the bioretention cells were undersized, volume reduction was measured for the annual runoff associated with the events that could be typically captured in the surface storage zone of the bioretention cells (up to 13 mm). Approximately 65 percent and 48 percent of the annual runoff from these events left as exfiltration and ET from the 0.9-m and 0.6-m media depth cells, respectively.
3. The primary reason for pollutant load reduction of TN and TP was significant outflow reduction. In the 0.6-m and 0.9-m media depth bioretention cells, 31 percent and 42 percent of the runoff measured during the monitoring period was eliminated from potential outflow (exfiltration and ET), respectively. Despite significantly higher concentrations of TN in the outflow of the 0.9-m media depth compared to the 0.6-m media depth, the annual pollutant load reduction in the 0.9-m media depth (19 percent) was similar to the annual pollutant load reduction in the 0.6-m media depth cells (21 percent). The reasons were attributable to greater outflow reduction in the deeper media depth and a higher efficiency ratio for ON.
4. Based on the annual estimate that ET contributed roughly three percent to the water balance, exfiltration is the major contributor of outflow reduction, with the deeper media depth exfiltrating a larger portion of the annual runoff (39 percent versus 28 percent). The large volume reduction can be attributed to the sandy loam to loamy sand soils surrounding the bioretention media.
5. The degree to which TN concentrations increased was somewhat surprising, in particular $\text{NO}_{2,3}\text{-N}$ concentrations. This raises the issue of important implications on the role of maintenance in nutrient removal, which is a subject for future research.

Initial fertilizer use promotes rapid vegetation growth, which improves aesthetics of bioretention cells; however, these maintenance steps are unnecessary sources of nitrogen.

3.8 ACKNOWLEDGEMENTS

The writers would like to acknowledge North Carolina Department of Environment and Natural Resources (NCDENR) and the Cooperative Institute for Coastal and Estuarine Environmental Technology (CICEET) for funding this project. Thanks to Dr. Aziz Amoozegar, Dr. Gregory Jennings, Dr. Wayne Skaggs, and Mr. Dan Line for their review and input. Finally, thanks to Shawn Kennedy and Bill Lord for assistance in setting up the site and installing monitoring equipment, and to Jenny James, Linda Mackenzie, and Eric Morris for water quality sample analyses.

3.9 REFERENCES

- Amatya, D. M., Skaggs, R. W., and Gregory, J. D. (1995). "Comparison of methods for estimating REF-ET." *Journal of Irrigation and Drainage Engineering*, 121(6), 427-435.
- Braga, A., Horst, M., and Traver, R. G. (2007). "Temperature effects on the infiltration rate through an infiltration basin BMP." *Journal of Irrigation and Drainage Engineering*, 133(6), 593-601.
- Clar, M. L., and Green, R. (1993). *Design manual for use of bioretention in stormwater management*, Department of Environmental Resources, Prince George's County, Md.
- Davis, A. P., Shokouhian, M., Sharma, H., and Minami, C. (2001). "Laboratory study of biological retention for urban stormwater management." *Water Environment Research*, 73(1), 5-14.
- Davis, A. P., Shokouhian, M., Sharma, H., and Minami, C. (2006). "Water quality improvement through bioretention media: Nitrogen and phosphorus removal." *Water Environment Research*, 78(3), 284-293.
- Davis, A. P. (2008). "Field performance of bioretention: Hydrology impacts." *Journal of Hydrologic Engineering*, 13(2), 90-95.

- Davis, A. P., Hunt, W. F., Traver, R. G., and Clar, M. (2009). "Bioretention technology: Overview of current practice and future needs." *Journal of Environmental Engineering*, 135(3), 109-117.
- Dietz, M. E., and Clausen, J. C. (2005). "A field evaluation of rain garden flow and pollutant treatment." *Water Air and Soil Pollution*, 167(1), 123-138.
- Dietz, M. E., and Clausen, J. C. (2006). "Saturation to improve pollutant retention in a rain garden." *Environmental Science and Technology*, 40(4), 1335-1340.
- Eaton, A. D., Clesceri, L. S., and Greenberg, A. R. (1995). *Standard methods for the examination of water and wastewater*, American Public Health Association, American Water Works Association, and Water Environment Federation, Washington, D.C.
- Emerson, C. H., and Traver, R. G. (2008). "Multiyear and seasonal variation of infiltration from storm-water best management practices." *Journal of Irrigation and Drainage Engineering*, 134(5), 598-605.
- Gee, G. W., and Bauder, J. W. (1986). "Particle-size analysis." *Methods of soil analysis. Part 1: Physical and mineralogical methods*, A. Klute, ed., Soil Science Society of America, Madison, Wis., 383-411.
- Hardy, D. H., Tucker, M. R., and Stokes, C. E. (2007). "Crop fertilization based on North Carolina soil tests." *Circular No. 1*. North Carolina Department of Agriculture and Consumer Services, Agronomic Division, Raleigh, N.C.
- Hsieh, C., and Davis, A. P. (2005a). "Evaluation and optimization of bioretention media for treatment of urban storm water runoff." *Journal of Environmental Engineering*, 131(11), 1521-1531.
- Hsieh, C., and Davis, A. P. (2005b). "Multiple-event study of bioretention for treatment of urban storm water runoff." *Water Science and Technology*, 51(3-4), 177-181.
- Hunt, W. F., Jarrett, A. R., Smith, J. T., and Sharkey, L. J. (2006). "Evaluating bioretention hydrology and nutrient removal at three field sites in North Carolina." *Journal of Irrigation and Drainage Engineering*, 132(6), 600-608.
- Hunt, W. F., Smith J. T., Jadlocki S. J., Hathaway, J. M., and Eubanks, P. R. (2008). "Pollutant removal and peak flow mitigation by a bioretention cell in urban Charlotte, NC." *Journal of Environmental Engineering*, 134(5), 403-408.
- Jones, M. P., and Hunt, W. F. (2009). "Bioretention impact on runoff temperature in trout sensitive waters." *Journal of Environmental Engineering*, 135(8), 577-585.

- Kim, H., Seagren, E. A., and Davis, A. P. (2003). "Engineered bioretention for removal of nitrate from stormwater runoff." *Water Environment Research*, 75(4), 355-367.
- Li, H., and Davis, A. P. (2008). "Heavy metal capture and accumulation in bioretention media." *Environmental Science and Technology*, 42(14), 5247-5253.
- Li, H., Sharkey, L. J., Hunt, W. F., and Davis, A. P. (2009). "Mitigation of impervious surface hydrology using bioretention in North Carolina and Maryland." *Journal of Hydrologic Engineering*, 14(4), 407-415.
- Lu, J, Sun, G., McNulty, S. G., and Amatya, D. M. (2005). "A comparison of six potential evapotranspiration methods for regional use in the southeastern United States." *Journal of the American Water Resources Association*, 41(3), 621-633.
- Line, D. E., and Hunt, W. F. (2009). "Performance of a bioretention area and a level-spreader-grass filter strip at two highway sites in North Carolina." *Journal of Irrigation and Drainage Engineering*, 135(2), 217-224.
- N.C. Department of Environment and Natural Resources (NCDENR). (2009). "Chapter 12: Bioretention." *Stormwater best management practices manual*, North Carolina Department of Environment and Natural Resources, Division of Water Quality, Raleigh, N.C., 12.1-12.30.
- Pandit, A., and Heck, H. H. (2009). "Estimations of soil conservation service curve numbers for concrete and asphalt." *Journal of Hydrologic Engineering*, 14(4), 335-345.
- Passeport, E., and Hunt, W. F. (2009). "Asphalt parking lot runoff nutrient characterization for eight sites in North Carolina, USA." *Journal of Hydrologic Engineering*, 14(4), 352-361.
- Passeport, E., Hunt, W. F., Line, D. E., Smith, R. A., and Brown, R. A. (2009). "Field study of the ability of two grassed bioretention cells to reduce storm-water runoff pollution." *Journal of Irrigation and Drainage Engineering*, 135(4), 505-510.
- Roseen, R. M., Ballester, T. P., Houle, J. J., Avelleneda, P, Widley, R., and Briggs, J. (2006). "Storm water low-impact development, conventional structural, and manufactured treatment strategies for parking lot runoff: Performance evaluations under varied mass loading calculations." *Transportation Research Record: Journal of the Transportation Research Board*, No. 1984, 135-147.
- State Climate Office (SCO). (2009). "1971-2000 climate normals." *Nashville Station (Station #316044)*, State Climate Office of North Carolina, Raleigh, N.C. <<http://www.nc-climate.ncsu.edu/cronos/normals.php?station=316044>> (July 20, 2009).

- Strecker, E. W., Quigley, M. M., Urbonas, B. R., Jones, J. E., and Clary, J. K. (2001). "Determining urban storm water BMP effectiveness." *Journal of Water Resource Planning Management*, 127(3), 144-149.
- Thornthwaite, C. W. (1948). "An approach toward a rational classification of climate." *The Geographical Review*, 38(1), 55-94.
- U.S. Department of Agriculture – Natural Resources Conservation Service (USDA-NRCS). (2004a). "Chapter 9: Hydrologic soil-cover complexes." *Part 630 –Hydrology: National engineering handbook*, Washington D.C.
- U.S. Department of Agriculture – Natural Resources Conservation Service (USDA-NRCS). (2004b). "Chapter 10: Estimation of direct runoff from storm rainfall." *Part 630 – Hydrology: National engineering handbook*, Washington D.C.
- U.S. Environmental Protection Agency (USEPA). (1983). "Methods for chemical analysis of water and wastes." *Rep. No. EPA-600/4-79-020*, USEPA, Cincinnati, Oh.
- Zhang, L., Dawes, W. R., and Walker, G. R. (2001). "Response of mean annual evapotranspiration to vegetation changes at catchment scale." *Water Resources Research*, 37(3), 701-708.

4 IMPACT OF MAINTENANCE AND IM(PROPERLY) SIZING BIORETENTION ON HYDROLOGIC PERFORMANCE

4.1 ABSTRACT

To ensure proper bioretention functionality, qualified construction oversight and routine maintenance are necessary both during and after construction. Two sets of bioretention cells of varying media depths (0.6-m and 0.9-m) were monitored for two, 12-month periods, in Nashville, NC. During the pre-repair (first) monitoring period, the bioretention cells were (1) clogged with fine sediment from construction and (2) severely undersized. Complete drawdown of the surface storage zone took 48 hours or more, as compared to the recommended 12 hours. Initially, the surface storage volumes for the 0.6-m and 0.9-m media depth cells were only 28 and 35 percent of the design storage volume, respectively. The design event for the bioretention cells was 25 mm (1 in), but the system was frequently overwhelmed, with overflow occurring for events as small as 9 mm (0.35 in). After the first year of monitoring, the top 75 mm (3 in) of media was removed (including the fines layer), which nearly doubled the surface storage volume of both sets of cells. With the increased surface storage volume, more annual runoff was treated and fewer events had overflow. In the repaired cells, the smallest event with overflow was 19 mm (0.75 in), but some events up to 28 mm (1.10 in) were fully captured without generating overflow. The reduction in overflow directly resulted in an additional 25 percent of annual runoff being treated through the media. Moreover, removal of the clogging fines layer increased the surface infiltration rate by nearly a factor of 10. The results of this study illustrate that improperly constructed and maintained bioretention cells have reduced performance. Therefore, even a minor construction error, such as incorrectly setting the target elevation for top of the media or the emergency overflow structure, can dramatically reduce the surface storage volume, which will consequently reduce performance. Despite still being relatively undersized with respect to the design event during the post-repair (second) monitoring period (between one-half to two-thirds of the design capacity), the bioretention cells were able to

treat almost 90 percent of the annual runoff, which is typically the target water quality volume used in the design of low impact development practices. If treating 90 percent of annual runoff is the goal for bioretention, current design standards for calculating surface storage volume may be overly conservative, which will result in increased construction and land opportunity costs. This study demonstrates the importance for designers and regulators to account for infiltration *during* events when calculating annual runoff treatment.

4.2 INTRODUCTION

Stormwater management has been linked to stream health. Walsh et al. (2005) measured ecological condition in urban streams that had varying degrees of connected impervious landscape and determined that ecological condition in streams decreased as connected imperviousness increased. Ecological condition was measured as a function of algal biomass density, diatom and macroinvertebrate composition, concentrations of dissolved organic carbon and filterable reactive phosphorus, and electrical conductivity. One of the causes for impaired stream health is increased runoff volume and flow rates being conveyed to streams as connected impervious area increases. If management practices do not release outflow from the smallest and most frequent events, such as those with precipitation depth less than 15 mm, the number of events with runoff and magnitude of flow rates will more closely resemble the pre-developed condition. Such hydrologic mitigation will help maintain and improve stream health in urban areas (Ladson et al. 2006; Walsh et al. 2005, 2009). In urban catchments with a large fraction of connected impervious areas, flow rate and flow frequency increase, which causes urban streams to become flashy and flood-prone (Paul and Meyer 2001). Increased peak flow rates and frequency of high flow rates cause conditions that are detrimental to in-stream biota (Paul and Meyer 2001; Walsh et al. 2005; Wheeler et al. 2005). As less runoff infiltrates into the landscape, the flow rate between events (baseflow) is reduced (Nelson et al. 2006; Rose and Peters 2001).

Infiltration-based stormwater control measures (SCMs) are becoming widely used to achieve more stringent stormwater regulations that focus on water quality and an annual hydrologic balance of pre-developed conditions. However, they are more susceptible to

construction or maintenance complications than traditional SCMs (i.e., retention/detention basin), resulting in less than ideal performance. One of the major issues impacting long-term performance of these systems is clogging from fine soil particles associated with unstable drainage areas. This phenomenon has been observed in permeable pavement systems and bioretention cells (Bean et al. 2007; Brown and Hunt 2011; Li and Davis 2008b). Laboratory and field studies on bioretention cells have shown sediment and particulate-bound pollutants accumulate primarily in the top 0.05 to 0.2 m (Li and Davis 2008a, 2008b).

Infiltration is one of the primary mechanisms for functionality of bioretention cells. Thus, to ensure long-term success, maintenance must be performed to sustain a permeable surface. In addition to soil particles clogging the surface layer, compaction can also play a role in reduced surface infiltration capacity (Pitt et al. 2008). Periodic inspection of bioretention cells should be performed to ensure continuous functionality (Asleson et al. 2009). Assessment measures can include: (1) visual inspection after a rain event to ensure proper drawdown time and (2) soil and plant identification to verify that hydric soils and wetland vegetation are not present. Some additional assessment measures include infiltration rate testing and synthetic drawdown testing, but inspection after a rainfall event is the easiest means to ensure adequate drawdown time (Asleson et al. 2009).

Another issue influencing bioretention function is having qualified construction oversight. Retention and detention basins are typically designed to store several meters of water, so if the target elevation for the base of the system or a drawdown orifice is off by 0.1 m, it would result in an error of storage by only 2-3 percent. Additionally, with freeboard included in these designs, the inaccurate elevation would likely have no effect on overall storage capacity. In contrast, if target elevations for a bioretention cell or stormwater wetland are off by 0.1 m, this could result in reduced storage capacity of over 30 percent because these systems are designed with much shallower surface storage depths prior to releasing runoff as overflow (maximum depths are typically 0.3 m). Since these systems are designed with shallower surface storage depths, minor oversights in construction can lead to

major negative impacts on functionality. Such an oversight would result in more overflow volume and less runoff treated in the system than intended.

The major issues to ensure proper functionality of bioretention cells are maintenance and qualified construction oversight. Bioretention cells from the study presented herein had both poor construction oversight and improper maintenance. Brown and Hunt (2011) examined the performance of the clogged and undersized bioretention cells for one year. The same systems were then re-examined after the clogging layer was removed and the surface storage volume was increased. The objective of this study was to assess the change in hydrologic performance by restoring the surface infiltration rate and increasing the surface storage volume for two sets of clogged and undersized bioretention cells that had varying media depths (0.6-m and 0.9-m).

4.3 METHODOLOGY

4.3.1 Site Description

The study site was located in the parking lot of a large commercial retail store in Nashville, NC. Nashville is in the upper Tar-Pamlico River Basin and lies on the edge of the Upper Coastal Plain (a region generally described as somewhat flat and sandy). Construction took place from June 2007 to February 2008, and monitoring began on March 31, 2008. Seven bioretention cells treated runoff from an asphalt parking lot (Fig. 4.1), with cells configured in parallel. Three cells (0.9-m media depth) were connected to one outlet drain, and the other four cells (0.6-m media depth) were connected to a different outlet drain. Due to backwater constraints, the last cell in each set was not monitored (Fig. 4.1). The design event for these bioretention cells was 25 mm (1 in), in adherence to NCDENR (2009) design guidance. The bioretention cells were conventionally drained and vegetated with shrubs, perennials, and trees. An image of the bioretention cells in July 2010, over two years after construction, is shown in Fig. 4.2. More detailed site specific information is available in Brown and Hunt (2011).

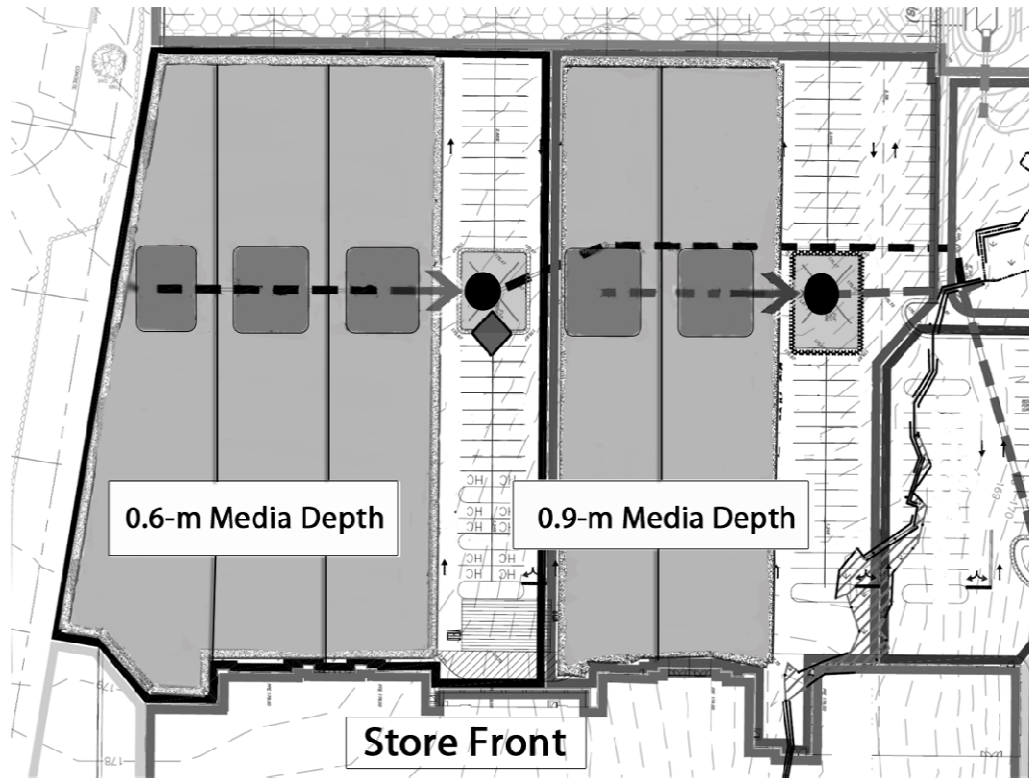


Figure 4.1: Bioretention cell layout diagram. The thick dashed lines represent the two outlet pipes. The arrow points to the weir location in the outlet pipe where outflow was monitored (represented by the circles), and the diamond highlights the location of the representative runoff sampler. The hatching highlights the drainage areas for each set of cells.



Figure 4.2: Image of the bioretention cells after two years (July 2010).

After several months, it was observed that the bioretention cells were not functioning according to design specifications. The surface storage zone was not draining within 12 hours after the event's conclusion, as required by state guidance (NCDENR 2009). It usually took 48 hours or more to drain. Upon closer inspection, it was observed that the bioretention cells were clogged with granite fines associated with the asphalt parking lot gravel base layer that washed into the cell during construction (Fig. 4.3). Because the bioretention media was installed prior to paving the parking lot, the contractors attempted to protect the media from clogging by using a woven geotextile fabric. However, the openings in the geotextile fabric were not small enough to prevent granite fines from passing through. Above the granite fines layer, the bioretention media was bleached white because this portion of the media remained saturated for extended periods of time, allowing the iron (Fe^{3+}) in the soil to become reduced (Fe^{2+}) (Fig. 4.3).

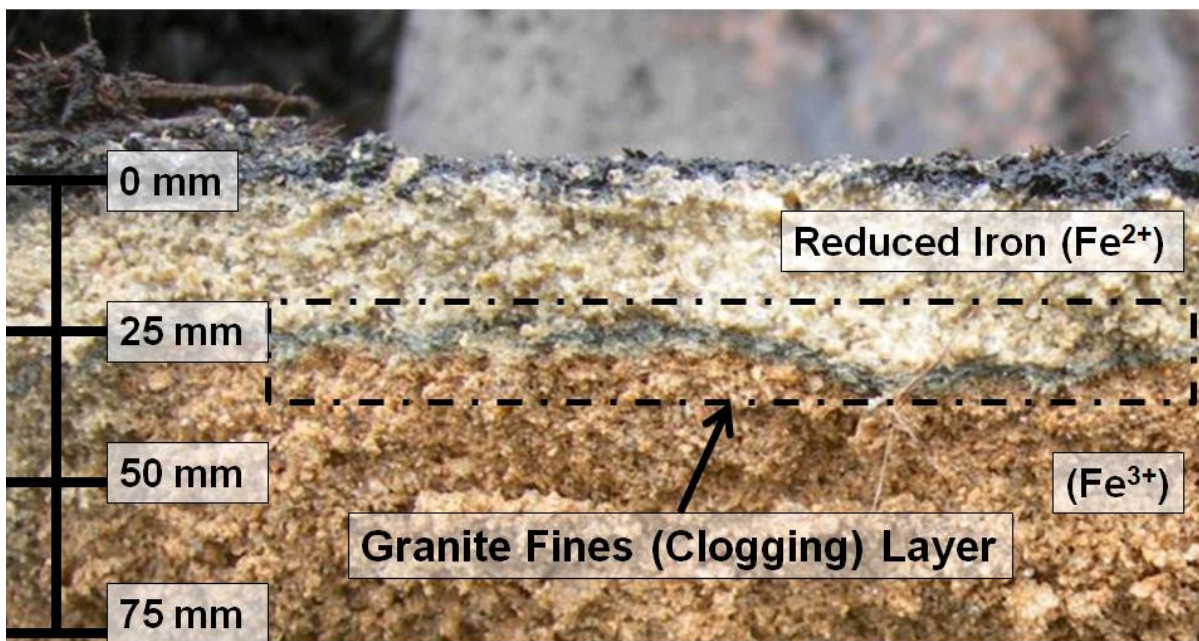


Figure 4.3: Image highlighting the granite fines (clogging) layer (dashed box) present in top 25 to 75 mm (1 to 3 in) of the media. Regions with ferrous (Fe^{2+}) and ferric (Fe^{3+}) iron are also noted.

In addition, overflow was generated more frequently than intended. During the pre-repair period, overflow occurred for rainfall events as small as 9 mm (0.35 in), which was identified as the brink overflow depth. This depth equates to the minimum rainfall depth over the drainage area needed to cause overflow when assuming that no infiltration occurs in the bioretention cell. Per design specifications, overflow should not have occurred for any rainfall event less than 25 mm (1 in). After surveying the bioretention cells and their respective drainage areas, it was determined that the actual ponding depth and surface storage area of the bioretention cells were less than the design specifications. The actual surface storage volume was only 28 and 35 percent of the design surface storage volume for the 0.6-m and 0.9-m media depth cells, respectively. Brown and Hunt (2011) monitored these undersized and clogged cells for nearly one year. On March 11, 2009, they were repaired by removing the clogging layer present in the top 75 mm (3 in) of the media. In an effort to further increase the surface storage volume, the side slopes were steepened to modestly increase the surface area. This increased the surface storage volume by 89 percent for both cells; however, they were still relatively undersized with respect to the design event (between one-half to two-thirds of the design capacity). After the repair, the brink overflow depth for the bioretention cells was estimated per re-survey to be 17 mm (0.67 in). Monitoring of the repaired bioretention cells that more closely resembled the design standards continued through March 24, 2010. Drainage area and bioretention cell characteristics both pre- and post-repair are highlighted in Table 4.1.

Table 4.1: Summary of Nashville, NC bioretention cell characteristics.

Design Characteristics	0.6-m Media Depth	0.9-m Media Depth
Number of Cells Monitored	3	2
Drainage Area	0.68 ha (1.67 ac)	0.43 ha (1.07 ac)
Impervious Area	83%	97%
Design Cell Ponding Depth	0.3 m (12 in)	0.3 m (12 in)
Pre-Repair Cell Ponding Depth	0.13 m (5 in)	0.15 m (6 in)
Post-Repair Cell Ponding Depth	0.2 m (8 in)	0.27 m (10 in)
Design Cell Surface Area	425 m ² (4570 ft ²)	300 m ² (3250 ft ²)
Pre-Repair Cell Surface Area	290 m ² (3120 ft ²)	206 m ² (2220 ft ²)
Post-Repair Cell Surface Area	322 m ² (3470 ft ²)	226 m ² (2430 ft ²)
Design Cell Surface Storage Volume	124 m ³ (4380 ft ³)	91 m ³ (3210 ft ³)
Pre-Repair Surface Storage Volume	35 m ³ (1240 ft ³)	32 m ³ (1120 ft ³)
Post-Repair Cell Storage Volume	66 m ³ (2340 ft ³)	60 m ³ (2120 ft ³)
Pre-Repair Storage Capacity Relative to Design	28%	35%
Post-Repair Storage Capacity Relative to Design	53%	66%
Surface Infiltration Rate (pre-repair)	2.5 – 12.7 mm/hr (0.1 – 0.5 in/hr)	2.5 – 6.4 mm/hr (0.1 – 0.25 in/hr)
Surface Infiltration Rate (post-repair)	10 – 115 mm/hr (0.4 – 4.5 in/hr)	11 – 51 mm/hr (0.45 – 2.0 in/hr)
K _{Sat} of Bioretention Media ^a	45 mm/hr (1.75 in/hr)	
Bioretention Media Composition ^b	86-89% Sand, 8-10% Silt, & 3-4% Clay	

^a Determined by constant head permeability test on five, 75 mm (3 in) diameter soil cores taken from the top 0.3 m of the media (Klute 1986). Cores were taken from below observed clogged portion.

^b Determined by hydrometer method (Gee and Bauder 1986).

4.3.2 Field Data Collection Methods

Automated samplers (ISCO 6712TM) with integrated bubbler modules (ISCO 730TM) were used to continuously monitor runoff and outflow rates. A tipping bucket rain gauge (ISCO 674 Rain GaugeTM) was installed to measure rainfall intensity, while a manual plastic rain gauge measured rainfall depth. Runoff from the parking lot entered each bioretention cell through two curb cuts on opposite sides of the cell. A 0.75-m (2.5-ft) wide rectangular

weir with end contractions was installed at one of the curb cuts in one of the cells to continuously monitor runoff and peak flow rates from a section of parking lot that was entirely asphalt. During the two-year monitoring period, several events were not monitored due to battery and bubbler errors, so outflow was estimated using rainfall events with similar depths, intensities, and antecedent dry periods. On May 14, 2009, water level loggers, manufactured by Infinities USA, were installed to record water levels in the surface storage zone to measure surface infiltration rates. Measurements were taken every ten minutes. Initial soil-water content prior to rainfall has a major influence on infiltration rate (Skaggs and Khaleel 1982). In order to have similar soil-water contents when calculating infiltration rate, only the tail ends of large events (events greater than 25 mm (1 in)) that occurred throughout the year were used to calculate the infiltration rates listed in Table 4.1. The infiltration ranges were not identical for both media depths because two of the three 0.6-m media depth bioretention cells had infiltration rates which were normally twice as fast as the other bioretention cells. It is believed that this was due to the surface area being less affected by the clogging layer for these cells. Since the water level loggers were not installed until the post-repair period, the surface infiltration rate was estimated during the pre-repair period by measuring the depth between the overflow structure and the top of the water in the surface storage zone and dividing by the time since overflow last occurred.

4.3.3 Statistical Methods

Nonparametric statistical tests were used to compare how the different media depths and monitoring periods impacted peak flow rate ratios and 24-hour effluent/influent volume ratios and to compare the rainfall characteristics between the two monitoring periods. These tests were run using the statistical package, SAS, version 9.1.3. When comparisons were made during the same monitoring period, only paired events were included, so the Wilcoxon signed-rank test was used. When the pre-repair and post-repair datasets were compared, a Wilcoxon rank-sum test was used. Two-sided tests and a significance level of $\alpha = 0.05$ were used in analysis. One result of including all events is that the numerous small events can have a large contribution to the statistical results. From a receiving stream perspective, the

most influential events are the larger ones that generate higher flow rates. For this reason, a subset analysis was performed for events greater than the brink overflow event from the pre-repair period – 9 mm (0.35 in). This allowed the impact of the increased surface storage volume to be evaluated for events that were typically large enough to generate overflow prior to the repair and for events that were large enough to impact the receiving stream.

4.3.4 Mass Balance Calculations

Runoff into the bioretention cells was calculated for each event by subtracting an initial abstraction depth from the rainfall depth and multiplying by the drainage area. Initial abstraction values were calculated using curve numbers for the impervious asphalt parking lot and for the pervious surfaces (open space, poor conditions) (USDA-NRCS 2004a). The curve numbers were varied based on antecedent moisture conditions at the site (USDA-NRCS 2004b). The curve numbers and antecedent moisture conditions used in estimating runoff are presented in Table 4.2. Pandit and Heck (2009) found that nearly all of the rainfall on asphalt surfaces is transmitted to runoff. Discrete rainfall events were defined as those greater than 2.5 mm (0.10 in) and having an antecedent dry period of 6 hours or greater.

Table 4.2: Curve number and initial abstraction values for pervious and impervious land uses and varying antecedent moisture conditions (USDA-NRCS 2004a, 2004b).

Antecedent Moisture Condition	Curve Number (and Initial Abstraction) for:		Antecedent Dry Period
	<i>Pervious Land Use</i>	<i>Impervious Land Use</i>	
1 (dry)	72 (19.8 mm)	97 (1.5 mm)	> 120 hours
2 (average)	86 (8.4 mm)	98 (1.0 mm)	48 to 120 hours
3 (wet)	94 (3.3 mm)	99 (0.5 mm)	6 to 48 hours

Peak runoff rates were calculated using the Rational Method (Equation 4.1).

$$Q_{Peak} = C \times i \times A \quad (4.1)$$

where, Q_{Peak} = peak flow rate (cfs), C = rational coefficient, i = rainfall intensity for the time of concentration (in/hr), and A = area (acres) (Malcolm 1989). The rational coefficients used for asphalt surfaces and surrounding pervious areas (lawns with heavy soil on a 2-5 percent slope) were 0.95 and 0.20, respectively (Malcolm 1989). The rational coefficients used for the 0.6-m and 0.9-m media depth cell drainage areas were 0.85 and 0.95, respectively. The time of concentration was calculated using the Kirpich equation (Equation 4.2):

$$t_c = \frac{\left(\frac{L^3}{H}\right)^{0.385}}{128} \quad (4.2)$$

where, t_c = time of concentration (min), L = hydraulic length of the watershed (ft), H = elevation change in the watershed (ft) (Malcolm 1989). The time of concentration for both drainage areas was calculated to be approximately 4 minutes. With rainfall depths being recorded on 2 minute intervals, peak 4 minute intensities were recorded for each event. Since runoff was only monitored at one of the bioretention cell inlets, the runoff data was used to verify that the rational coefficient selection and time of concentration calculation were reasonable.

Outflow was measured with a 90° sharp-crested, v-notch weir fixed in the 0.75-m diameter outlet concrete pipe connecting all cells of similar media depth. The bioretention cells were constructed with overflow structures that combined overflow and drainage, so outflow was measured as a combination of both treated and untreated water. Despite measuring drainage and overflow together, it was evident when overflow occurred by examining the outflow hydrograph. A detailed example is provided in Brown and Hunt (2011). Drainage was characterized by a gradually changing flow rate, whereas overflow could easily be identified by the short, rapid spikes in flow rate.

As described in Brown and Hunt (2011), evapotranspiration (ET) was estimated using an equation developed by Zhang et al. (2001), where mean actual evapotranspiration (AET), annual precipitation (P), and potential evapotranspiration (PET) were correlated, based on hydrologic data from over 250 watersheds across the world. PET was calculated using the

Thornthwaite method (Thornthwaite 1948). Since the Thornthwaite method is not data intensive, it tends to underestimate PET (Lu et al. 2005). Thus, correction factors were included to provide a more reliable PET estimate (Amatya et al. 1995). Amatya et al. (1995) calculated correction factors for the Thornthwaite method at three sites in eastern North Carolina. The closest site to Nashville was Tarboro – 35 km to the east.

Runoff that did not leave through outflow or ET was assumed to be lost through exfiltration based on the water balance equation (Equation 4.3).

$$Vol_{Runoff} = Vol_{outflow} + Vol_{ET} + Vol_{EXF} \quad (4.3)$$

where Vol_{Runoff} = runoff volume, $Vol_{outflow}$ = outflow volume (sum of drainage and overflow), Vol_{ET} = evapotranspiration volume, and Vol_{EXF} = exfiltration volume. Exfiltration is water leaving the bioretention media through the bottom and sides of the cell and entering the in-situ soil; it can also be referred to as seepage.

4.4 RESULTS

4.4.1 Flow Characterization and Annual Water Balance

The rainfall distributions of both monitoring periods were quite similar. The mean rainfall depths for the pre-repair (first) and post-repair (second) periods were 16.1 mm (0.63 in) and 15.9 mm (0.62 in), respectively. During the pre-repair and post-repair periods, 17 and 18 percent of the events were greater than 25 mm (1 in), respectively. The pre-repair period had a higher median rainfall depth (11.6 mm (0.46 in)) compared to the post-repair period (10.3 mm (0.40 in)), but the post-repair period had the larger maximum event – 136.9 mm (5.39 in) versus 92.9 mm (3.66 in). Overall, there was no significant difference between rainfall depths for the pre-repair and post-repair periods (p-value = 0.58). Although the average 30-minute rainfall intensity was greater during the pre-repair period (14.3 versus 11.1 mm/hr), there was no significant difference (p-value = 0.108). The average rainfall duration was longer during the post-repair period (8.8 versus 8.0 hours), but again, there was no significant difference (p-value = 0.77).

One of the major differences between the two monitoring periods was the frequency of events with overflow, as evidenced in Table 4.3. During the pre-repair period, events with overflow occurred more than three times more frequently than events greater than the design event (11 events). Out of 64 events, overflow occurred in 38 and 35 for the 0.6-m and 0.9-m media depth bioretention cells, respectively. After the surface storage volume in both sets of bioretention cells was increased by 89 percent during the repair phase, overflow events only occurred in 18 of 76 events for both sets of cells. This was greater than the number of events exceeding the design event (14 events); however, the surface storage volume in both cells was still less than the design capacity. Despite the surface storage volume during the post-repair period being only 53 (0.6-m media depth) and 66 (0.9-m) percent of the design volume, the smallest event with overflow was 19 mm (0.75 in), an increase from 9 mm (0.35 in). The increased surface infiltration rate (Table 1) also allowed more runoff to infiltrate during events. This had the greatest impact on low intensity events. The largest event fully captured from both sets of cells, without generating overflow, in the post-repair period was 28 mm (1.10 in), an increase from 13 mm (0.51 in) during the pre-repair period. Several other studies have shown unclogged bioretention cells were able to fully capture runoff (no overflow) from events approximately two times larger than the design event because of the infiltration that occurs during an event (Hunt et al. 2008; Li et al. 2009).

Table 4.3: Characterization of forms of outflow monitored.

Media Depth	Events Monitored	Events with:			Events > 25 mm ^a
		No Outflow	Drainage Only	Overflow and Drainage	
0.6-m Pre-Repair	64	0	26	38	11
0.6-m Post-Repair	76	0	58	18	14
0.9-m Pre-Repair	64	11	18	35	11
0.9-m Post-Repair	76	6	52	18	14

^a 25-mm was the design event, but due to inadequate construction, this event's volume of runoff was not able to be captured.

By repairing the cells, which nearly doubled the surface storage volume, the annual overflow volume was reduced by nearly 70 percent. In the 0.6-m media depth cells, the annual overflow volume was reduced from 37 percent to 12 percent. In the 0.9-m media depth cells, the annual overflow volume was reduced from 35 percent to 11 percent (Fig. 4.4). By increasing the surface storage volume, an additional 25 percent of annual runoff was treated by the bioretention media. As more runoff passed through the media, the potential for biological, chemical, and physical treatment increased. Also, by delaying the release of runoff, there was more opportunity for exfiltration into the surrounding soils to take place. As a result, annual exfiltration modestly increased from 28 to 32 percent and 39 to 42 percent in the 0.6-m and 0.9-m media depth cells, respectively.

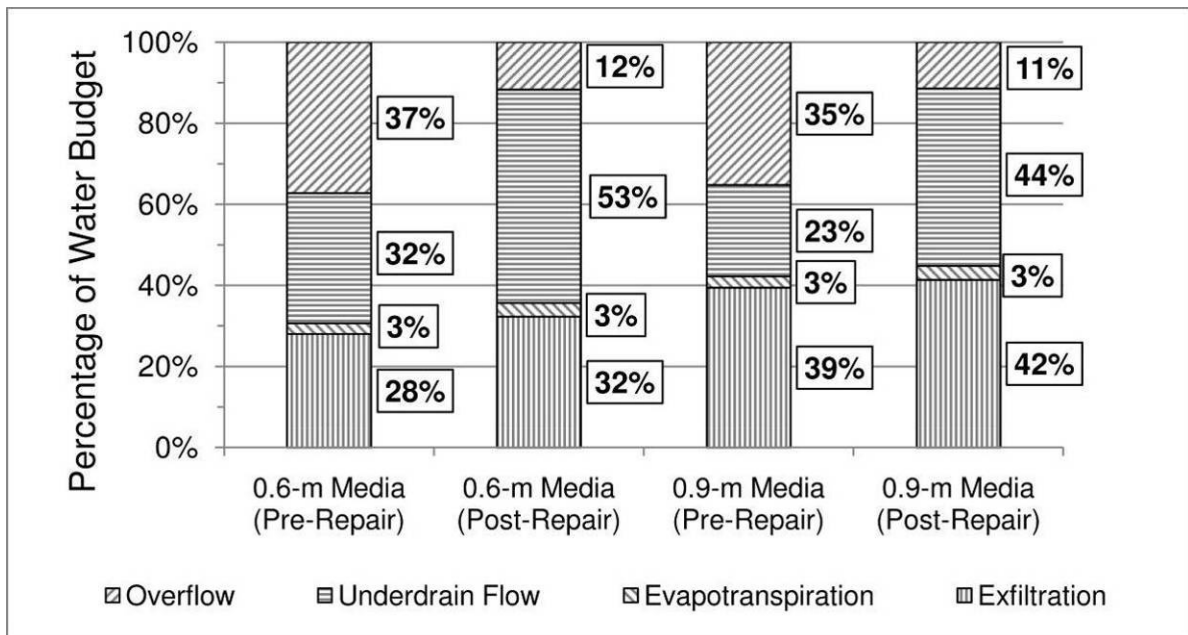


Figure 4.4: Fate of runoff in bioretention cells for both pre- and post-repair monitoring periods.

The water balance was dissected further to evaluate bioretention performance for various sized events (Table 4.4). For small events (2.5-12.7 mm), the percentage of outflow and the sum of ET and exfiltration were within two percentage points on an annual basis.

However, drainage volume increased in the post-repair period because there was no overflow from these events. The biggest difference between the two monitoring periods is the decrease in overflow volume after the cells were repaired. As the event size range increased, the difference in ET and exfiltration between the two monitoring periods increased because more runoff passed through the media in the post-repair period, which allowed for more runoff to have a chance to leave as exfiltration. The large percentage of exfiltration was attributed to the sandy loam to loamy sand soils surrounding the bioretention media (Brown and Hunt 2011). For each range of rainfall depths presented in Table 4.4, the 0.9-m media depth cells had a substantially larger volume being released through ET and exfiltration, but with diminishing returns as event size increases, as shown in Table 4.4. Hypothetically, the deeper media depth cells are able to exfiltrate more water due to more media volume being available to capture and store a larger portion of runoff and more exposed area to surrounding soils. In addition, the hydraulic head is larger for a bioretention cell with deeper media depth, so it would force more runoff to exfiltrate into the underlying in-situ soil.

Table 4.4: Partitioning of hydrologic fates for various sized storm events

<i>Event Size (mm)</i>	<i>n</i>	0.6-m Pre-Repair				0.9-m Pre-Repair			
		<i>Drain</i>	<i>Over-flow</i>	<i>Outflow</i>	<i>ET & Exfil</i>	<i>Drain</i>	<i>Over-flow</i>	<i>Outflow</i>	<i>ET & Exfil</i>
2.5-12.7	33	42%	10%	53%	47%	26%	8%	35%	65%
12.7-25.4	18	38%	29%	67%	33%	26%	27%	53%	47%
25.4-38.1	6	22%	51%	74%	26%	19%	50%	69%	31%
> 38.1	3	23%	59%	82%	18%	16%	59%	75%	25%
		0.6-m Post-Repair				0.9-m Post-Repair			
2.5-12.7	42	53%	0%	53%	47%	33%	0%	33%	67%
12.7-25.4	21	55%	6%	61%	39%	50%	5%	55%	45%
25.4-38.1	7	53%	14%	66%	34%	49%	15%	64%	36%
> 38.1	6	51%	23%	74%	26%	42%	24%	65%	35%

4.4.2 Volume and Flow Reduction

Two low impact development (LID) hydrologic impact parameters proposed by Davis (2008) were analyzed for the Nashville site: 24-hour effluent/influent volume ratio and peak flow rate ratio. The 24-hour effluent/influent volume ratio is expressed by Equation 4.4:

$$f_{V24} = \frac{V_{out-24hr}}{V_{in}} \quad (4.4)$$

where $V_{out-24hr}$ = outflow volume leaving the cell within 24 hours and V_{in} = runoff volume into the bioretention cell. Davis (2008) suggested an LID site should have $f_{V24} < 0.33$. Two-thirds reduction was chosen because the rational method C coefficient of a highly impervious surface is often 0.9, and it is about 0.3 for an undeveloped (pervious) area (Davis 2008). Using this performance criterion, the bioretention cells with deeper media depth (0.9 m) performed significantly better than the shallower systems (0.6 m) for both monitoring periods (p-value < 0.0001 for both monitoring periods). These results were in agreement with findings by Li et al. (2009). Despite the *increase* in surface storage volume post-repair, the frequency of meeting the LID goal actually dropped from 44 to 37 percent in the 0.9-m media depth cells. In the 0.6-m media depth cells, the frequency of meeting the LID goal essentially remained constant (at 20 to 21 percent). For nearly all of the events that met the LID goal, the corresponding fate of runoff for each event could be characterized as those that did not generate overflow, so in comparing the two monitoring periods, the same volume of runoff was infiltrating into the media. Therefore, the lack of overall improvement when using this metric can be explained by the fact that infiltration rate was almost ten times faster during the post-repair period, so more drainage would occur within 24 hours after an event commenced. During the pre-repair period, it would take the surface storage zone approximately two days to drain, so outflow would typically still be occurring well after 24 hours. However, post-repair, both media depths reduced the mean f_{V24} values because more runoff was infiltrating into the media and leaving as exfiltration. Yet, there was still no significant difference in the 24-hour effluent/influent volume ratio from either the 0.6-m (p-value = 0.24) or 0.9-m (p-value = 0.70) media depth bioretention cells. A graph and

summary table of the 24-hour effluent/influent volume ratio are shown in Fig. 4.5 and Table 4.5, respectively.

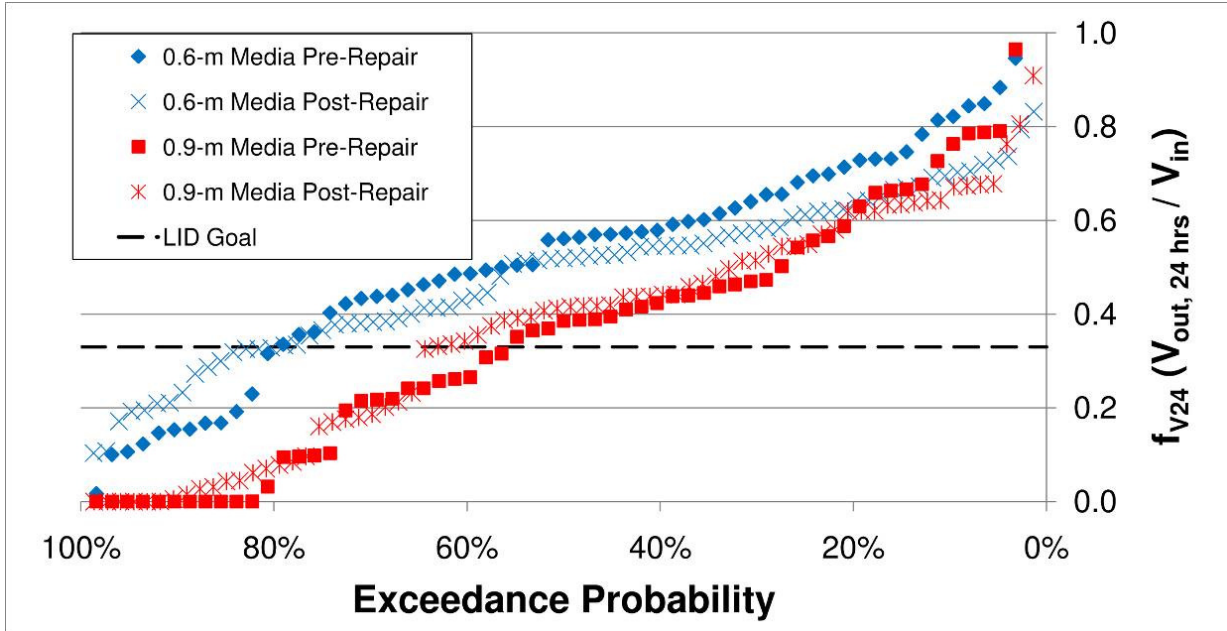


Figure 4.5: Exceedance probability plots for 24-hour effluent/influent volume ratios.

Table 4.5: Summary table of 24-hour effluent/influent volume ratios.

Monitoring Period	0.6-m Media Depth			0.9-m Media Depth		
	Mean	Median	LID Goal ^b	Mean	Median	LID Goal ^b
Pre-Repair (n=61)	0.53	0.56	20%	0.38	0.39	44%
Post-Repair (n=75,72) ^a	0.48	0.52	21%	0.37	0.41	37%

^a Event numbers for the 0.6-m and 0.9-m media depths, respectively.

^b Percentage of storms where $f_{V24} < 0.33$.

The peak flow rate ratio is expressed in Equation 4.5:

$$R_{Peak} = \frac{Q_{Peak-out}}{Q_{Peak-in}} \quad (4.5)$$

where $Q_{\text{Peak-out}}$ = outflow peak rate and $Q_{\text{Peak-in}}$ = runoff peak rate. Davis (2008) suggested an LID site should have $R_{\text{Peak}} < 0.33$. Two-thirds reduction was chosen again because of the ratio of rational C coefficients (Davis 2008). Using this performance criterion, the bioretention cells that had been repaired (surface storage increased) met the LID goal more frequently. In the 0.6-m media depth cells, the frequency of meeting the goal increased from 77 to 85 percent, and in the 0.9-m media depth cells, the frequency of meeting the goal increased from 73 to 87 percent. Post-repair outflow was characterized by a higher percentage of drainage, a direct result of having larger surface storage volumes. Because overflow was occurring less frequently, peak outflow rates were lower. Additionally, the duration of higher flow rates was reduced because the time period in which overflow occurred was reduced. This is expected to minimize the negative impacts that higher flow rates have on receiving streams. When considering peak flow rate ratios from all events, there was no significant difference between the pre- and post-repair periods for the 0.6-m (p-value = 0.23) and 0.9-m (p-value = 0.30) media depth bioretention cells. The lack of significance was due to the influence of the numerous, small events, which contribute minimal outflow to receiving streams. In order to truly quantify the impact of increasing the surface storage volume, only events greater than the brink overflow event (9 mm (0.35 in)) from the pre-repair period were considered. This subset analysis of the larger events showed that both the 0.6-m (p-value = 0.032) and 0.9-m (p-value = 0.015) media depth bioretention cells had significantly lower peak flow rate ratios during the post-repair period. The ability to achieve lower peak flow rate ratios is independent of media depth, but appears to be completely dependent on surface storage volume and infiltration potential. The peak flow rate ratios were significantly lower for the 0.9-m compared to the 0.6-m media depth bioretention cells during both the pre-repair (p-value = 0.0002) and post-repair (p-value < 0.0001) periods. The 0.9-m media depth bioretention cells had significantly lower peak flow rate ratios because it had more surface storage volume relative to the design volume for both monitoring periods and there were fewer events without outflow from the deeper media depth cells. A graph and summary table of the peak flow rate ratios are shown in Fig. 4.6 and Table 4.6, respectively. With adequate surface storage volume to minimize occurrence

of events with overflow, bioretention has been extremely effective at reducing peak flow rates for all events other than those that overwhelm the surface storage (Hunt et al. 2008; Li et al. 2009). Surface storage volume determination appears to be a very important parameter in the bioretention design process.

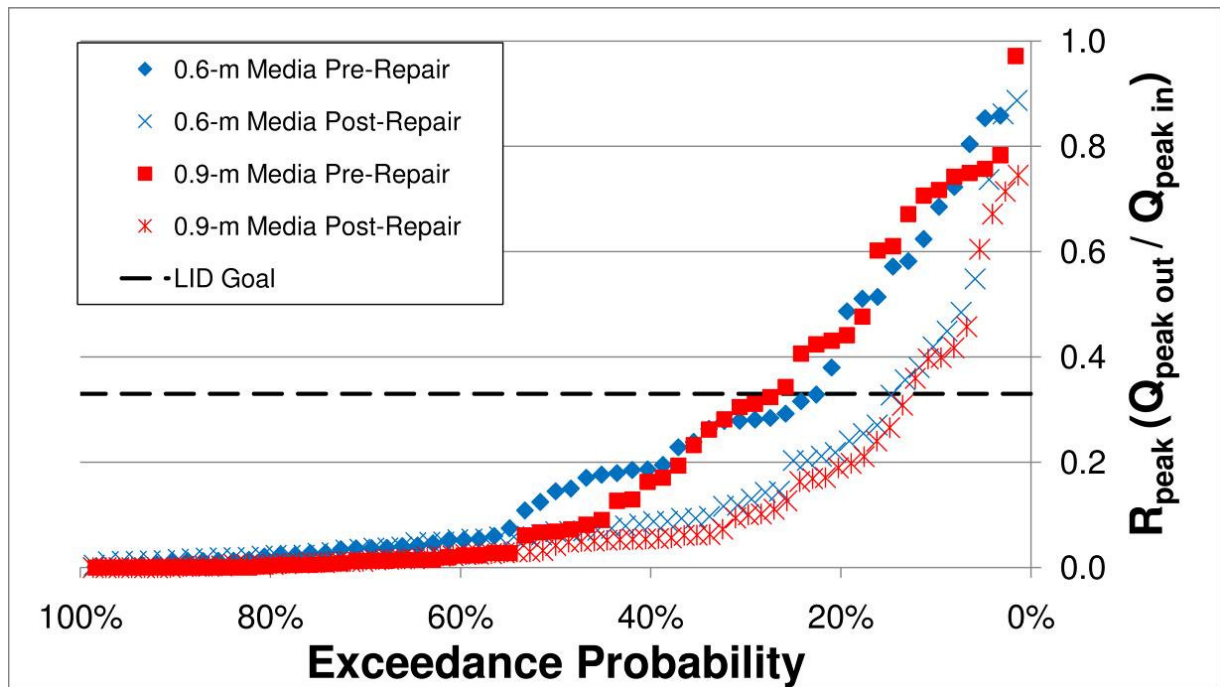


Figure 4.6: Exceedance probability plots for peak flow rate ratios.

Table 4.6: Summary table of peak flow rate ratios.

Monitoring Period	0.6-m Media Depth			0.9-m Media Depth		
	Mean	Median	LID Goal ^b	Mean	Median	LID Goal ^b
Pre-Repair (n=61)	0.23	0.14	77%	0.21	0.07	73%
Post-Repair (n=67/73) ^a	0.15	0.07	85%	0.12	0.04	87%

^a Event numbers for the 0.6-m and 0.9-m media depths, respectively.

^b Percentage of storms where $R_{Peak} < 0.33$.

Flow duration curves over the entirety of both monitoring periods were created as another way to describe the impact of reduced surface storage volume and infiltration rate.

As impervious surfaces increase, flow rates become higher and the durations of these higher rates occur for longer periods. These effects have been shown to cause increased erosion potential, and they create conditions that are detrimental to in-stream biota (Paul and Meyer 2001; Walsh et al. 2005; Wheeler et al. 2005). Therefore, the goal is to minimize high flow rates and durations in which higher flow rates occur to minimize the negative impacts that stormwater has on stream condition and health. Characteristics of monitoring, flow, and rainfall durations are presented in Table 4.7. To compare flow duration curves between and among both monitoring periods, flow rate durations were normalized to average annual rainfall, as described in Equation 4.6:

$$T_{Q,Normal} = T_{Q,Actual} \times \frac{P_{Ave,Annual}}{P_{Measured}} \quad (4.6)$$

where, $T_{Q,Normal}$ = normalized flow rate duration, $T_{Q,Actual}$ = actual flow rate duration, $P_{Ave,Annual}$ = average annual precipitation, and $P_{Measured}$ = precipitation measured during the monitoring period. Since the monitoring stations and periods did not have the exact same rainfall depths, the runoff volumes were not the same. In order to compare flow duration curves between the monitored data, similar runoff volumes needed to be compared, so each of the stations and periods were normalized with respect to average annual rainfall depth. It was assumed that the time periods in which events were not monitored had a similar distribution of flow rates as those monitored during the specific period. The average annual rainfall depth from 1970-2000 in Nashville, NC was 1089 mm (42.9 in) (SCO 2010). Both monitoring periods were within 41 mm (1.6 in) of each other, which provide additional support that the two monitoring periods had similar rainfall characteristics that were also similar to the average rainfall in the area.

Table 4.7: Flow duration and rainfall characteristics during both monitoring periods.

Media Depth	Monitoring Period	Flow Monitoring Duration	Flow Duration > 0.01 L/s	Rainfall Duration	Rainfall Depth During Monitoring
		Days	Days	Days	mm
0.6-m	Pre-Repair	333	116.4	18.8	983
0.6-m	Post-Repair ^a	348	69.4	23.5	1062
0.9-m	Pre-Repair ^b	331	75.4	18.3	958
0.9-m	Post-Repair ^c	382	52.8	24.0	1123

^a Eight events were not monitored due to battery failure and bubbler module errors.

^b A portion of one event was not monitored due to battery failure.

^c A portion of one event and two entire events were not monitored due to battery failure.

Based on Equation 4.6, annual durations in which flow rates (in L/s/ha) were greater than the following values were calculated: 0.1, 0.5, 1.0, 2.5, 5, 10, 15, 25, 50, and 100 – as described in Fig. 4.7 and Table 4.8. Data analysis showed the pre-repair period had the longest duration of the smallest flows (0.1 L/s/ha) and of the largest flows (greater than 10 L/s/ha). The clogging, fines layer caused longer durations of flow at low rates because infiltration was greatly reduced, leading to flow persisting for extended periods of time at very low rates. The longer duration of high flow rates was due to the pre-repaired surface storage volume being approximately one-half that of the repaired cells, causing three times more overflow volume to occur. Coincidentally, the higher flow rates (10 through 100 L/s/ha) occurred approximately two to three times more often during the pre-repair period. This suggests that the pre-maintenance bioretention cells discharged erosive flows to the receiving stream for approximately two to three times longer than post-maintenance cells. The actual rate that would determine if erosion occurs depends on characteristics of the receiving water body (stream substrate and channel dimension). High discharge rates from a bioretention cell would more likely impact a smaller stream channel, one with smaller particle size substrate, or a stream that has a high percentage of impervious areas in the watershed. Higher flow rates increase shear stress on the streambed and banks, leading to erosion and disturbance of in-stream biota (Paul and Meyer 2001; Wheeler et al. 2005). After the repair, both sets of cells had longer durations of moderate flow rates (1.0 and 2.5

L/s/ha), because drainage, not overflow, became the more common form of outflow. These rates were consistent with the typical flow rates for the repaired cells under saturated conditions. An additional 20 percent of annual runoff left via drainage during the post-repair period. Another contributing factor to the increase in the moderate flow rates was the rapidly infiltrating surface layer, which increased the drainage rate when the bioretention cells were saturated. In comparing runoff flow rates, the pre-repair period had a longer duration of higher runoff rates and shorter duration of lower runoff rates. This could be due to the average 30-minute rainfall intensity being larger and rainfall duration being smaller during this period; however, since neither of these terms was significantly different, it was assumed that similar rainfall patterns were present in both periods.

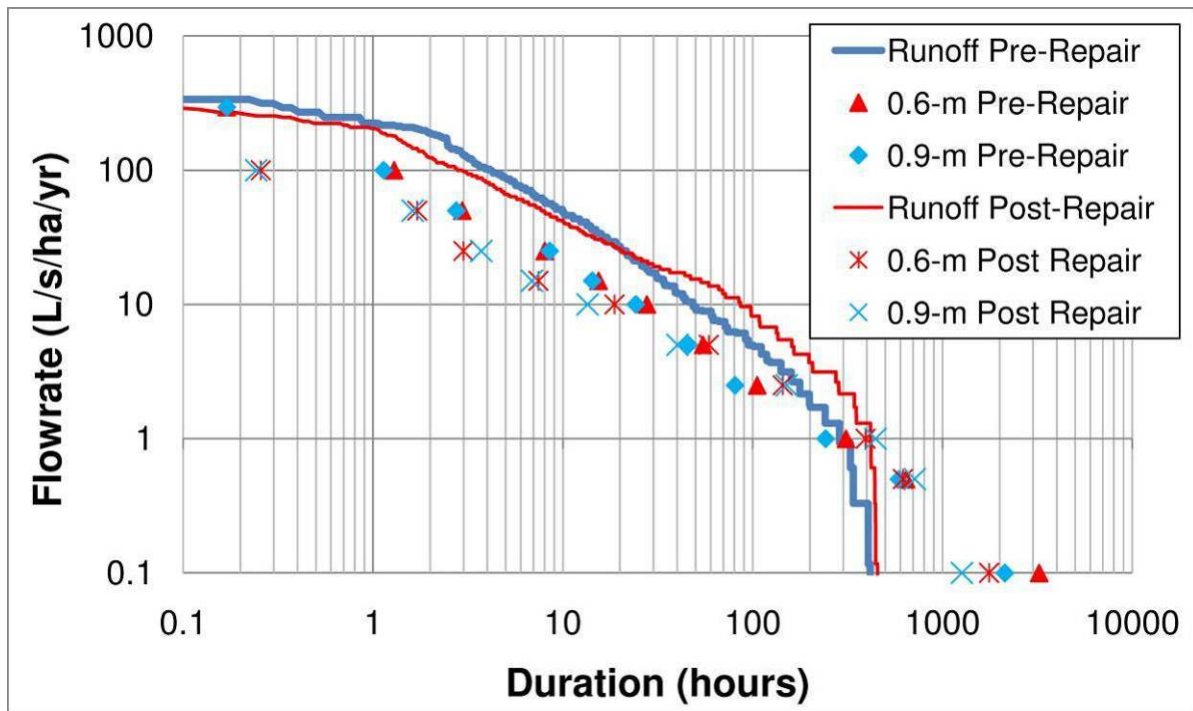


Figure 4.7: Exceedance durations for specified precipitation-normalized flow rates for both monitoring periods.

Table 4.8: Durations of precipitation-normalized flow rates greater than specified values.

Station	Monitoring Period	Flow Rate Duration > _____ L/s/ha (hours/yr)				
		0.1 L/s/ha	0.5 L/s/ha	1.0 L/s/ha	2.5 L/s/ha	5 L/s/ha
Runoff	Pre-Repair	417	339	287	177	94.9
Runoff	Post-Repair	456	440	417	284	161
0.6-m	Pre-Repair	3228	642	310	106	54.8
0.6-m	Post-Repair	1760	618	393	144	58.7
0.9-m	Pre-Repair	2132	590	242	80.9	46.0
0.9-m	Post-Repair	1267	715	444	151	40.1
		10 L/s/ha	15 L/s/ha	25 L/s/ha	50 L/s/ha	100 L/s/ha
Runoff	Pre-Repair	48.5	33.9	21.6	10.0	4.2
Runoff	Post-Repair	86.2	53.3	20.7	7.7	2.9
0.6-m	Pre-Repair	27.7	15.4	8.0	3.0	1.3
0.6-m	Post-Repair	18.7	7.4	3.0	1.7	0.3
0.9-m	Pre-Repair	24.3	14.3	8.5	2.8	1.1
0.9-m	Post-Repair	13.5	6.9	3.7	1.6	0.2

4.5 DISCUSSION

After the bioretention cells were repaired, there was little, if any, improvement in the 24-hour effluent/influent volume ratio; however, the deeper media depth cells still performed significantly better than the shallower media depth cells. As more runoff infiltrated into the surface of the bioretention cells, annual exfiltration volume increased by three to four percent. The most notable difference in performance pre- and post- repair was with respect to percent runoff treated and reduction in peak flow rates. An additional 25 percent of the annual runoff that had previously left as overflow was now infiltrating and being treated by the media. This allowed for a slower release of more runoff, which reduced peak flows and the durations of high flow rates. If this set of undersized and poorly maintained systems is commonplace, current performance assessments may be too generous.

Despite that the surface storage volume was still not fully sized with respect to NC regulatory design specifications after the repair was made, the bioretention cells fully

captured runoff from two events larger than the design event. This was due to the increase in infiltration rate resulting from the removal of the clogging layer. The frequency of overflow was still slightly more common (18 events) than the number of events greater than the design event (14 events); however, almost 90 percent of runoff was treated by the bioretention media. This raises a question of whether the design community is required to overdesign the surface storage volume in bioretention cells. The implications of overdesigning the surface storage volume are increased construction and opportunity cost from having a larger footprint.

As advised in many state stormwater manuals, the surface storage zone is sized to completely capture and store runoff from a specified water quality event (first flush). In the Piedmont region of NC, this is 25 mm (1 in) (NCDENR 2009). When sizing the surface storage volume, infiltration during the event is not taken into account. Over a 30-year period (1974-2003) in Raleigh, NC, approximately 70 km (43 miles) west of Nashville, NC, it was determined that 85 and 90 percent of annual runoff could be stored if stormwater control measures (SCMs) captured the first 29.4 mm (1.16 in) and 36.5 mm (1.44 in) of rainfall, respectively (Bean 2005). However, in an infiltrating system (like a bioretention cell), the intra-event infiltration volume can be substantial, especially if the surface is not clogged. During the pre-repair period, the surface capture volume (runoff volume required to completely fill the surface storage zone, assuming no infiltration) was only 9 mm (0.35 in) of rainfall over the drainage area, yet the bioretention cells treated approximately 65 percent of annual runoff. During the post-repair period, the surface capture volume was increased to about 17 mm (0.67 in) of rainfall, and the bioretention surface infiltration rate was restored. Under these conditions, almost 90 percent of annual runoff was treated. If the goal is to capture and treat 80 to 90 percent of annual runoff, setting the surface capture volume to be that which stores runoff from a 25 mm (1 in) event may be excessive for North Carolina (and states with similar rainfall patterns and amounts).

The previously presented water quality event depths were calculated in Bean (2005) by using long-term weather stations to find discrete rainfall depths for each event over the

30-year period. The rainfall event depth that corresponds to capturing 85 and 90 percent of the rainfall was calculated by assuming that any event less than the target depth would be fully captured. For events greater than the target depth, only the target depth was assumed to be captured, and the remainder was assumed to be untreated (overflow). A similar exercise was performed for the Nashville bioretention cells. However, in this exercise, the target depth was calculated for the monitored amount of runoff treated on an annual basis for each monitoring period (Fig. 4.4).

During the pre-repair period, the actual surface capture volume was approximately 9 mm (0.35 in); however, the cells functioned as if they had a water quality depth of 15 mm (0.59 in) because they treated approximately 65 percent of the runoff. Substantial infiltration occurred during events even when the surface of the media was partially clogged. The repaired cells treated almost 90 percent of runoff, so they effectively performed as if they had a water quality depth of 37 mm (1.46 in); however, the actual surface capture volume was only 17 mm (0.67 in). Once the clogging layer was removed, the impact of intra-event infiltration was substantial on treating runoff for a system that remained relatively undersized. Had the bioretention cells been constructed in accordance with the design surface capture volume of 25 mm (1 in) and if they did not infiltrate during the events, these cells should have only captured (and treated) approximately 82 percent of runoff, noticeably less than what actually occurred during the post-repair period. Therefore, to accurately determine the surface capture volume needed to treat 90 percent of runoff, a long-term (i.e., 10 or more years) continuous computer simulation model that calculates infiltration on at least an hourly basis is necessary to make sufficient designs. With multiple years of continuous weather data, the model would be able to account for infiltration during events, which will more accurately estimate the amount of runoff treated.

4.6 CONCLUSIONS

This study demonstrated the importance of properly constructing and maintaining bioretention cells. If a somewhat slight construction error is made regarding the target elevation for the top of the media or the invert elevation for the emergency overflow

structure, the cell could be undersized, substantially impacting performance. Improperly sizing a bioretention cell leads to increased effluent pollutant loads. First, increased overflow volume results in a larger percentage of runoff exiting the system with only minimal treatment (sedimentation). Secondly, less runoff entering the media reduces the potential for exfiltration of runoff carrying pollutants. Increased overflow frequency also results in higher peak outflow rates and longer durations of high outflow rates.

This study showed that despite the bioretention cells being undersized (one-half to two-thirds of design capacity), they were still able to treat almost 90 percent of the annual runoff. With this percentage typically being the target water quality volume, it was suggested that current bioretention design standards could be over-sizing these systems by not accounting for intra-event infiltration. The volume of infiltration during an event can be substantial, especially if the surface is not clogged with fine sediment. Oversized systems would increase the material cost for construction and incur a spatial opportunity cost.

With respect to peak flow mitigation, surface storage volume is clearly the most important design parameter. No apparent gain was observed by having a deeper media depth. Surface storage volume is potentially a more important design parameter than media depth from a stream channel protection perspective, provided a minimum media depth (i.e., 0.6 m) is provided. However, deeper media does promote more exfiltration volume and better performance in regard to outflow reduction.

Finally, this study has shown that it is essential to have qualified construction oversight to ensure that bioretention cell design and installation are consistent. If bioretention media has been placed in the cell while the drainage area is still unstable, it is important to protect the media from fine sediment. Routine maintenance is also essential to ensure adequate long-term performance. A clogged bioretention cell will overflow more frequently, leading to higher peak flow rates, longer durations of high flow rates, and less treated runoff.

4.7 ACKNOWLEDGEMENTS

The authors would like to acknowledge NC Department of Environment and Natural Resources (NCDENR) and the Cooperative Institute for Coastal and Estuarine Environmental Technology (CICEET) for funding this project. Also, thanks to Dr. Aziz Amoozegar, Dr. Greg Jennings, and Dr. Wayne Skaggs for their input; Dr. Jon Hathaway for his review; Shawn Kennedy for assistance in setting up the site and installing monitoring equipment; and Bill Lord, Mitch Woodward, Dan Line, Cole Ammons, Trisha Moore, and Fred Ammons for the labor involved in repairing the bioretention cells.

4.8 REFERENCES

- Amatya, D. M., Skaggs, R. W., and Gregory, J. D. (1995). "Comparison of methods for estimating REF-ET." *Journal of Irrigation and Drainage Engineering*, 121(6), 427-435.
- Asleson, B. C., Nestingen, R. S., Gulliver, J. S., Hozalski, R. M., and Nieber, J. L. (2009). "Performance assessment of rain gardens." *Journal of the American Water Resources Association*, 45(4), 1019-1031.
- Bean, E. Z. (2005). "A field study to evaluate permeable pavement surface infiltration rates, runoff quantity, runoff quality, and exfiltrate quality." M.S. Thesis, North Carolina State University, Raleigh, N.C.
- Bean, E. Z., Hunt, W. F., and Bidelspach, D. A. (2007). "Field survey of permeable pavement surface infiltration rates." *Journal of Irrigation and Drainage Engineering*, 133(3), 249-255.
- Brown, R. A., and Hunt, W. F. (2011). "Impacts of media depth on effluent water quality and hydrologic performance of under-sized bioretention cells." *Journal of Irrigation and Drainage Engineering*, 137(3), 132-143.
- Davis, A. P. (2008). "Field performance of bioretention: Hydrology impacts." *Journal of Hydrologic Engineering*, 13(2), 90-95.
- Gee, G. W., and Bauder, J. W. (1986). "Particle-size analysis." *Methods of soil analysis. Part 1: Physical and mineralogical methods*, A. Klute, ed., Soil Science Society of America, Madison, Wis., 383-411.

- Hunt, W. F., Smith, J. T., Jadlocki, S. J., Hathaway, J. M., and Eubanks, P. R. (2008). "Pollutant removal and peak flow mitigation by a bioretention cell in urban Charlotte, N.C." *Journal of Environmental Engineering*, 134(5), 403-408.
- Klute, A. (1986). "Water retention: Laboratory methods." *Methods of soil analysis. Part 1: Physical and mineralogical methods*, A. Klute, ed., Soil Science Society of America, Madison, Wis., 635-662.
- Ladson, A. R., Walsh, C. J., and Fletcher, T. D. (2006) "Improving stream health in urban areas by reducing runoff frequency from impervious surfaces." *Australian Journal of Water Resources*, 10(1), 23-32.
- Li, H., and Davis, A. P. (2008a). "Heavy metal capture and accumulation in bioretention media." *Environmental Science and Technology*, 42(14), 5247-5253.
- Li, H., and Davis, A. P. (2008b). "Urban particle capture in bioretention media I: Laboratory and field studies." *Journal of Environmental Engineering*, 134(6), 409-418.
- Li, H., Sharkey, L. J., Hunt, W. F., and Davis, A. P. (2009). "Mitigation of impervious surface hydrology using bioretention in North Carolina and Maryland." *Journal of Hydrologic Engineering*, 14(4), 407-415.
- Lu, J, Sun, G., McNulty, S. G., and Amatya, D. M. (2005). "A comparison of six potential evapotranspiration methods for regional use in the southeastern United States." *Journal of the American Water Resources Association*, 41(3), 621-633.
- Malcolm, H. R. (1989). *Elements of urban stormwater design*. North Carolina State University, Raleigh, N.C.
- N.C. Department of Environment and Natural Resources (NCDENR). (2009). "Chapter 12: Bioretention." *Stormwater best management practices manual*, North Carolina Department of Environment and Natural Resources, Division of Water Quality, Raleigh, N.C., 12.1-12.30.
- Nelson, R. A., Smith, J. A., and Miller, A. J. (2006). "Evolution of channel morphology and hydrologic response in an urbanizing drainage basin." *Earth Surface Processes and Landforms*, 31(9), 1063-1079.
- Pandit, A., and Heck, H. H. (2009). "Estimations of soil conservation service curve numbers for concrete and asphalt." *Journal of Hydrologic Engineering*, 14(4), 335-345.
- Paul, M. J., and Meyer, J. L. (2001). "Streams in the urban landscape." *Annual Review of Ecology and Systematics*, 32(1), 333-365.

- Pitt, R., Chen, S., Clark, S., Swenson, J., and Ong, C. (2008). "Compaction's impacts on urban storm-water infiltration." *Journal of Irrigation and Drainage Engineering*, 134(5), 652-658.
- Rose, S., and Peters, N. E. (2001). "Effects of urbanization on streamflow in the Atlanta area (Georgia, USA): A comparative hydrological approach." *Hydrological Processes*, 15(8), 1441-1457.
- Skaggs, R. W., and Khaleel, R. (1982). "Chapter 4: Infiltration." *Hydrologic modeling of small watersheds: Monograph No. 5*, American Society of Agricultural Engineers, St. Joseph, Mich., 121-166.
- State Climate Office (SCO). (2009). "1971-2000 climate normals." *Nashville Station (Station #316044)*, State Climate Office of North Carolina, Raleigh, N.C. <<http://www.nc-climate.ncsu.edu/cronos/normals.php?station=316044>> (July 20, 2009).
- Thornthwaite, C. W. (1948). "An approach toward a rational classification of climate." *The Geographical Review*, 38(1), 55-94.
- U.S. Department of Agriculture – Natural Resources Conservation Service (USDA-NRCS). (2004a). "Chapter 9: Hydrologic soil-cover complexes." *Part 630 –Hydrology: National engineering handbook*, Washington D.C.
- U.S. Department of Agriculture – Natural Resources Conservation Service (USDA-NRCS). (2004b). "Chapter 10: Estimation of direct runoff from storm rainfall." *Part 630 – Hydrology: National engineering handbook*, Washington D.C.
- Walsh C. J., Fletcher T. D., and Ladson A. R. (2005). "Stream restoration in urban catchments through re-designing stormwater systems: Looking to the catchment to save the stream." *Journal of the North American Benthological Society*, 24(3), 690-705.
- Walsh C. J., Fletcher T. D., and Ladson A. R. (2009). "Retention capacity: A metric to link stream ecology and storm-water management." *Journal of Hydrologic Engineering*, 14(4), 399-406.
- Wheeler, A. P., Angermeier, P. L., and Rosenberger, A. E. (2005). "Impacts of new highways and subsequent landscape urbanization on stream habitat and biota." *Reviews in Fisheries Science*, 13(3), 141-164.
- Zhang, L., Dawes, W. R., and Walker, G. R. (2001). "Response of mean annual evapotranspiration to vegetation changes at catchment scale." *Water Resources Research*, 37(3), 701-708.

5 ANALYSIS OF CLIMATIC FACTORS AND CONSECUTIVE EVENTS FOR FIELD MONITORED BIORETENTION CELLS

5.1 ABSTRACT

Previous research has shown that nutrient treatment in conventionally drained bioretention cells has been dependent upon varying wetting and drying regimes in the media and other environmental factors. This study examines these factors more in-depth by correlating them to runoff and outflow concentrations and by collecting water quality samples from four to six consecutive events during three different periods for a set of field monitored bioretention cells. To analyze performance from consecutive events, the evolution of cumulative pollutant loads is presented by plotting cumulative load versus cumulative volume. This new way of presenting water quality data allows for the direct analysis of event mean concentrations (EMCs), load reduction, and volume reduction with one graph, as well as describing the seasonal impacts and impacts from consecutive events. Two sets of bioretention cells of varying media depths (0.6-m and 0.9-m) were monitored for two, 12-month periods, in Nashville, NC. During the pre-repair (first) monitoring period, the bioretention cells were (1) clogged with fine sediment from construction and (2) severely undersized. During the pre-repair period, overflow occurred three times more frequently than it should have per design specifications. The clogging layer present in the top 75 mm (3 in) was removed after the first year. This repair restored the design infiltration rate and increased the surface storage volume to allow for the target annual runoff volume to infiltrate into the media during the post-repair (second) monitoring period. The overall results of this study showed that conventionally drained bioretention cells mainly convert organic nitrogen, the predominant source of nitrogen in runoff, to nitrate in the aerobic environment present in the media. Nitrate is then exported from the media during subsequent events. The highest export occurred during the warmer months because of the influence that higher media temperature had on increasing microbial activity. Based on these results, it would be highly

encouraged for future bioretention designs to include a zone that can provide potential for denitrification, such as an internal water storage zone. Indicative of a first flush response, precipitation depth was negatively correlated to runoff and outflow concentrations. In comparing the outflow concentrations from both sets of cells, the water quality treatment between 0.6-m and 0.9-m media depth bioretention cells was not different enough to warrant a suggestion of using the deeper media depth for better water quality treatment. However, the deeper media depth did provide substantial improvement in the volume of runoff leaving via exfiltration. An additional ten percent of annual runoff left via exfiltration for the deeper media depth cells, so this set of cells had higher pollutant load reductions.

5.2 INTRODUCTION

In the most recent National Water Quality Inventory, 44 percent of river and stream miles, 64 percent of lake acres, and 30 percent of estuary square miles were identified as impaired. For all of these waterbodies, nutrients were identified as a top five cause for impairment, with urban stormwater runoff being a top ten source of impairment (USEPA 2009). Additionally, the Wadeable Streams Assessment found that 42 percent of U.S. stream miles were in poor biological condition, with the top two most widespread stressors being nitrogen and phosphorus (USEPA 2009). One method to reduce the impacts of nutrients on sensitive watersheds is through implementing total maximum daily load (TMDL) standards. One of the non-point sources of pollution regulated with TMDLs is urban stormwater runoff. A wide variety of stormwater control measures (SCMs) can be used to reduce pollutant loads of stormwater runoff, with one of the more effective SCMs to treat stormwater runoff quality being bioretention.

Bioretention is an infiltration-based SCM that is becoming more widely used because of its ability to improve water quality and restore the hydrologic condition of the pre-developed landscape. Research on bioretention cells have shown they are effective at removing many pollutants (sediment, heavy metals, oil/grease, nitrogen, phosphorus, pathogen indicator species, and thermal pollution) from urban runoff depending on design and soil media composition (Bratieres et al. 2008; Davis et al. 2001, 2003, 2006; Dietz and

Clausen 2006; Hatt et al. 2009; Hsieh and Davis 2005a; Hunt et al. 2006, 2008; Jones and Hunt 2009; Kim et al. 2003). However, in some of these studies, total nitrogen (TN) removal has been absent due to poor bioretention media selection (Hunt et al. 2006) and lack of an anaerobic zone to promote denitrification for the reduction of nitrite and nitrate ($\text{NO}_{2,3}\text{-N}$) (Kim et al. 2003). For nutrient sensitive watersheds with TMDLs, such as the one for the study site presented herein, phosphorus and nitrogen are pollutants of particular concern.

Many questions regarding phosphorus treatment in bioretention cells have been addressed. Laboratory and field studies have shown that total suspended solids (TSS) cannot significantly penetrate past the top 0.2 m (Li and Davis 2008); therefore, particulate-bound phosphorus (Part-P) should be easily removed through filtration. Removal of orthophosphate (Ortho-P), a major form of dissolved phosphorus, is controlled by the media properties and vegetation. Hunt et al. (2006) showed phosphorus removal efficiency increased as phosphorus content in the media decreased. Phosphorus sorption is increased when the media is comprised of more available aluminum or iron oxide binding sites. In a predominantly sand-based media, mixtures that include aluminum and iron oxides can improve phosphorus binding potential. The major source of these binding sites is in the clay composition of the media. Additional binding sites are located in the organic matter in the media and mulch. Other studies demonstrated that with the addition of fly ash (Zhang et al. 2008) or aluminum based water treatment residuals (O'Neil and Davis 2010) the phosphorus sorption potential increases. Lucas and Greenway (2008) also showed that presence of vegetation increased phosphorus removal efficiency, and Bratieres et al. (2008) found that the vegetation that had a more extensive root system and the presence of root hairs had the highest concentration reductions. However, reduction of total phosphorus (TP) concentrations exceeded 77 percent for various vegetation types and when vegetation was absent because the influent phosphorus composition was predominantly particulate-bound phosphorus (approximately 70 percent) (Bratieres et al. 2008).

Nitrogen treatment has been a more complex issue to comprehend for bioretention cells because they are natural systems and the primary treatment mechanisms result from

microorganisms in the soil and vegetation. Nitrogen reduction provided by bioretention cells have varied due to media composition, vegetation, and drainage configuration (Bratieres et al. 2008; Hunt et al. 2006; Kim et al. 2003; Lucas and Greenway 2008). The media in conventionally drained bioretention cells is primarily aerobic, so microbial processes in the media mineralize organic nitrogen (ON) into ammonium and convert ammonium to $\text{NO}_{2,3}\text{-N}$ through nitrification. Stormwater runoff is a continuous source of nitrogen. The media can be another source of nitrogen, but it is dependent on the sources of the materials used in the mixture, namely the organic sources used. Although fertilizers do not need to be applied due to the influx of nitrogen from runoff, they present additional nitrogen sources, especially if the landscaper is unaware of bioretention functionality.

The changing soil-moisture conditions in a conventionally drained bioretention cell make the processes of nitrification and subsequent leaching of $\text{NO}_{2,3}\text{-N}$ difficult to control. Under aerobic conditions during extended dry periods, $\text{NO}_{2,3}\text{-N}$ builds up in the media, only to be leached/flushed out during subsequent events. This is one of the reasons why conventionally drained bioretention cells have had poor “removal” of $\text{NO}_{2,3}\text{-N}$, and in some cases, effluent nitrate concentrations increased (Brown and Hunt 2011a; Davis et al. 2001, 2006; Hatt et al. 2009; Hsieh and Davis 2005b; Hunt et al. 2006, 2008; Line and Hunt 2009; Roseen et al. 2006). Hatt et al. (2007) documented how treatment efficiencies have been impacted by different wetting and drying regimes in the media. Effluent TN and $\text{NO}_{2,3}\text{-N}$ concentrations immediately following a dry period were up to seven times higher than during wet periods (Hatt et al. 2007). Blecken et al. (2007) also documented in a bioretention column study that temperature had an influence on nitrogen treatment efficiency. In this study, higher temperatures resulted in higher effluent concentrations of $\text{NO}_{2,3}\text{-N}$. This is a result of increased nitrification as temperatures increased. Contrasting this study, the removal efficiencies and efficiency ratios for dissolved inorganic nitrogen ($\text{NO}_{2,3}\text{-N}$ and total ammoniacal nitrogen (TAN)) in two bioretention cells in New Hampshire were higher in the summer months than the winter months (Roseen et al. 2009). Also, for two bioretention cells with internal water storage in North Carolina, $\text{NO}_{2,3}\text{-N}$ concentration removals were higher in

the spring and summer months than in the autumn and winter months, which was believed to be affected by increased microbial degradation and plant uptake (Passeport et al. 2009).

In order to promote denitrification, it was first proposed and successfully documented in Kim et al. (2003) that elevating the underdrain (internal water storage layer) created an anoxic zone. Later field studies had mixed results for including an internal water storage zone to improve denitrification (Brown and Hunt 2011b; Davis 2007; Dietz and Clausen 2006; Hunt et al. 2006; Passeport et al. 2009). One cause for the mixed results was due to the impact of the underlying soils which controlled the duration of saturation within the media (Brown and Hunt 2011b; Passeport et al. 2009). Another could be related to the influent $\text{NO}_{2,3}\text{-N}$ concentrations used in Kim et al. (2003), which were approximately seven times higher than average parking lot runoff concentrations from eight sites in North Carolina (Passeport and Hunt 2009).

The objective of this study was to measure the water quality treatment for an adequately sized set of bioretention cells that had been monitored previously when they were severely undersized (Brown and Hunt 2011a). Since this was a continuation of a previous field study, more detailed analysis and data collection were completed to better understand treatment in field bioretention cells. One method was to collect water quality samples from consecutive events, in contrast to most field studies which sporadically collect water quality samples throughout the monitoring period. This type of analysis allowed for a more in-depth and detailed look at how climatic and environmental factors and previous events influence nitrogen treatment for bioretention cells. Some laboratory studies have examined individual factors but were not able to represent all of the variations that occur in the field (Blecken et al. 2007; Bratieres et al. 2008; Hatt et al. 2007). Laboratory studies are advantageous in that the researcher has more control over external factors; however, they don't represent the variability of climate and rainfall patterns that occur in the field.

5.3 METHODOLOGY

5.3.1 Site Description

The study site was located in the parking lot of a large commercial retail store in Nashville, NC. Detailed site specific information is available in Brown and Hunt (2011a). Nashville is located in the upper Tar-Pamlico River Basin, a nutrient sensitive watershed, and lies on the edge of the Upper Coastal Plain (a region generally described as somewhat flat and sandy). The site was constructed from June 2007 to February 2008, and monitoring began on March 31, 2008. Seven bioretention cells treated runoff from an asphalt parking lot (Fig. 5.1), with cells configured in parallel. Outflow from the three cells with 0.9-m media depth was conveyed with one pipe, while outflow from the other four cells with 0.6-m media depth was conveyed with a separate pipe. Due to backwater constraints near the outlet of each pipe, the last cell in each set was not monitored. Therefore, the weir was installed immediately upstream of where outflow entered from the last cell in the set (Fig. 5.1). This allowed for the outflow to travel uninterrupted for 20 m (66 ft) on a 0.5 percent slope before reaching the weir, which created more uniform flow conditions near the weir. The three monitored 0.6-m media depth cells treated an 83 percent impervious, 0.68 ha (1.67 ac) watershed, while the two monitored 0.9-m media depth cells treated a 97 percent impervious, 0.43 ha (1.07 ac) watershed. The bioretention cells were conventionally drained (no internal water storage zones) and were vegetated with shrubs, perennials, and trees. Images of the vegetation progression during the first growing season and after the study was complete are presented in Fig. 5.2.

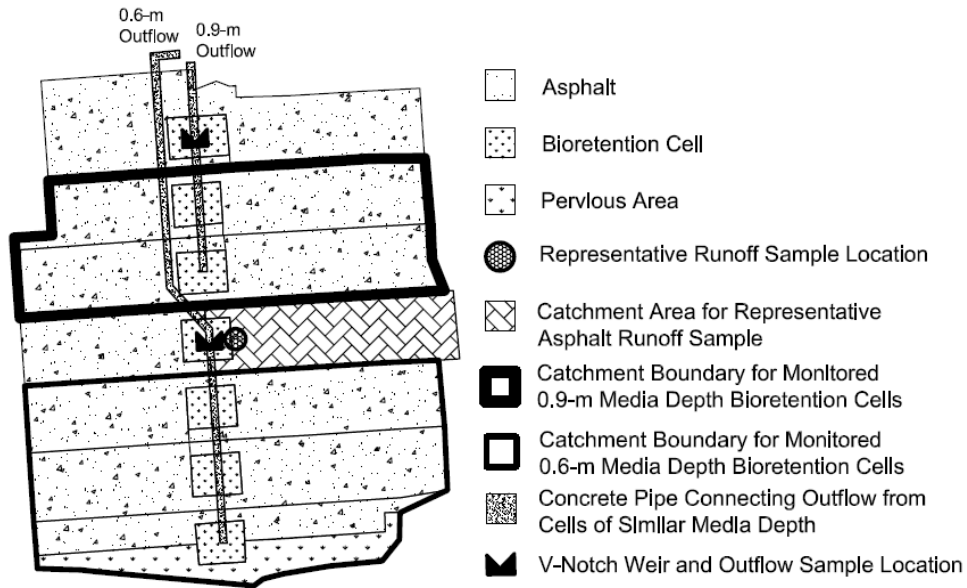


Figure 5.1: Bioretention cell layout diagram.



Figure 5.2: Images of the bioretention cells clockwise from top left: start of first growing season (4/14/08), middle of first growing season (9/6/08), end of first growing season (11/15/08), and middle of third growing season (7/19/10).

After several months, it was observed that the bioretention cells were not functioning according to design specifications. The surface storage zone was not draining within 12 hours after the event's conclusion, as recommended by state guidance (NCDENR 2009). It usually took 48 hours or more to drain. Upon closer inspection, it was observed that the bioretention cells were clogged with granite fines associated with the asphalt parking lot gravel base layer that washed into the cell during construction (Brown and Hunt 2011a). After the fines layer was removed, the range of infiltration rates increased from 2.5 – 12.7 mm/hr (0.1 – 0.5 in/hr) to 10 – 115 mm/hr (0.4 – 4.5 in/hr) (Chapter 4). Another issue was that overflow occurred three times more frequently than intended, which led to a smaller percentage of runoff infiltrating into the engineered media. Overflow occurred for rainfall events as small as 9 mm (0.35 in) during the pre-repair monitoring period. Per design specifications, overflow should not have occurred for any rainfall event less than 25 mm (1 in). After surveying the bioretention cells, it was determined that the actual surface storage volumes were only 28 and 35 percent of the design surface storage volume for the 0.6-m and 0.9-m media depth cells, respectively. Brown and Hunt (2011a) monitored the hydrologic response and water quality treatment of these undersized and clogged cells for nearly one year. On March 11, 2009, they were repaired by removing the clogging layer present in the top 75 mm (3 in) of the media. Monitoring of the repaired bioretention cells that more closely resembled the design standards continued through March 24, 2010. The repair increased the surface storage volume by 89 percent for both sets of cells; however, they were still relatively undersized with respect to the design event (between one-half to two-thirds of the design capacity). Despite being relatively undersized, the percentage of annual runoff treated by the media during the post-repair monitoring period was nearly 90 percent, an increase from approximately 65 percent during the pre-repair monitoring period (Chapter 4).

5.3.2 Field Data Collection Methods

Flow-proportional storm samples were collected with automated samplers (ISCO 6712TM) and flow rates were measured with integrated bubbler modules (ISCO 730TM) in combination with sharp-crested weirs. Runoff entered each bioretention cell through two

curb cuts on opposite sides of the cell, so a 0.75-m (2.5-ft) wide rectangular weir with end contractions was installed at one of the curb cuts in one of the cells for monitoring runoff water quality and flow rates from a representative section of asphalt parking lot (Fig. 5.1). The bioretention cells were constructed with overflow structures that combined overflow and drainage into a 0.75-m diameter concrete pipe that connected all cells of similar media depth, so a 90° v-notch weir was fixed into this pipe for measuring outflow rates and collecting outflow samples from each set of cells. A tipping bucket rain gauge (ISCO 674™) was installed to measure rainfall intensity, while a manual plastic rain gauge measured cumulative rainfall depth.

Runoff volume was calculated for each event by subtracting an initial abstraction depth from the rainfall depth and multiplying by the drainage area. The specific initial abstraction depths for the different land uses and antecedent moisture conditions are presented in Brown and Hunt (2011a). As described in Brown and Hunt (2011a), a discrete rainfall event occurred when the rainfall depth exceeded 2.5 mm (0.10 in) and the antecedent dry period (ADP) exceeded six hours. Some water quality events included multiple discrete rainfall events because the surface storage still had runoff ponded and/or the outflow rate was still high. Of 41 water quality events collected during both monitoring periods, 11 had combined discrete events, but only two had an ADP exceeding 12 hours.

Flow-proportional storm samples were analyzed for nutrients and TSS. The nutrient species analyzed were Ortho-P, TP, TAN, NO_{2,3}-N, and total Kjeldahl nitrogen (TKN). The ON was calculated as the difference between TKN and TAN, TN was calculated as the sum of TKN and NO_{2,3}-N, and Part-P was calculated as the difference between TP and Ortho-P. Samples were transferred to laboratory containers, placed on ice, and delivered to the NCSU Center for Applied Aquatic Ecology (CAAE) laboratory (state-certified laboratory) within 24 hours to conduct chemical analyses as shown in Table 5.1 (Eaton et al. 1995; USEPA 1983). No preservation was used in the automated samplers; thus, samples that could not be recovered from the sampler within 24 hours were discarded.

Table 5.1: Summary of analytical methods for water quality analysis.

Pollutant	Pollutant	Analytical Method	Reportable Limit (mg/L)
NO _{2,3} -N	Nitrate + Nitrite nitrogen	SM 4500-NO ₃ -F ^a	0.0056
TKN	Total Kjeldahl nitrogen	EPA 351.1 ^b	0.14
TAN	Total ammoniacal nitrogen	SM 4500-NH ₃ -H ^a	0.007
ON	Organic nitrogen	= TKN – TAN	N/A
TN	Total nitrogen	= NO _{2,3} -N + TKN	N/A
Ortho-P	Orthophosphate	SM 4500-P-F ^a	0.006
Part-P	Particulate-bound phosphorus	= TP – Ortho-P	N/A
TP	Total phosphorus	SM 4500-P-F ^a	0.01
TSS	Total suspended solids	SM 2540 D ^a	1

^a Source (Eaton et al. 1995)

^b Source (USEPA 1983)

During the pre-repair period, samples were collected from 20 events for both sets of bioretention cells, and during the post-repair period, 25 and 24 events were collected from the 0.6-m and 0.9-m media depth bioretention cells, respectively. For the representative runoff monitoring location (Fig. 5.1), 19 and 23 events were sampled during the pre- and post-repair periods, respectively. As a result of Hatt et al.'s (2007) bioretention column study that showed differences in nitrogen treatment under varying wetting and drying regimes, attempts were made during the post-repair period to collect water quality samples from successive events to better characterize the nitrogen treatment in field bioretention cells under varying soil-moisture regimes and other climatic and environmental factors. Four to six consecutive events were collected during three different periods – early spring (13Mar09 – 7May09), late summer (29July09 – 31Aug09), and middle autumn (26Oct09 – 19Nov09).

Temperature of the media was measured with air/water/soil temperature sensors (TMCX-HD) attached to HOBO 4 channel loggers (U12-008). The loggers were manufactured by Onset Computer Corporation (Bourne, Mass.). In each of the 0.6-m and 0.9-m bioretention cells, media temperature was measured at the following depths: 0.05, 0.3, and 0.6 m (2, 12, and 24 in). Media temperature was also measured at 0.9 m (36 in) in the 0.9-m bioretention cells. Average media temperature during an event was calculated from

the 0.3 m and 0.6 m depths in the 0.6-m and 0.9-m media depth cells, respectively. These depths were approximately one-half of the depth of the cell (including the gravel layer). The media temperature was calculated as the average temperature during 24 hours after the runoff infiltrated to the respective depth. For events exceeding 24 hours, a 48-hour average was used. Temperature sensors were installed on June 26, 2008, so data were collected for the final 21 months of the 24-month study.

5.3.3 Statistical Methods

Statistical analyses were conducted using SAS® 8.2 and JMP® 7.0 (SAS Institute Inc., Cary, NC). The level of significance used in all analyses was $\alpha = 0.05$. Initially, the water quality data were checked for the assumption of normality. The four statistical tests used to check the validity of this assumption were Shapiro-Wilk, Kolmogorov-Smirnov, Creamer-von Mises, and Anderson-Darling. These tests usually showed better fits for normality when the data were log-transformed; therefore, most of the water quality data were log-transformed to run parametric statistical tests. Strecker et al. (2001) showed that lognormal distributions were a valid approximation for influent and effluent event mean concentration data. To avoid complications from using Ortho-P concentration data that were below the reportable limit, one-half of the reportable limit was used (Newman et al. 1989).

For normally distributed datasets, a paired t-test was used to make comparisons between runoff and outflow from both sets of cells and between outflow concentrations from each set of cells. A Wilcoxon signed-rank test was used if the datasets were not normally distributed. As a means to determine whether similar runoff concentrations were entering the bioretention cells during the two monitoring periods, runoff concentrations were analyzed using a two sample t-test or Wilcoxon rank sum test if the datasets were normally distributed or symmetrically distributed, respectively. Event sizes were compared using a Wilcoxon rank sum test to determine whether there was a difference in the magnitude of events from each period. Finally, environmental factors from each event were correlated to event mean concentrations (EMCs) to determine the influence that precipitation depth, ADP, average

media temperature, and percent of runoff infiltrating into the cell had on runoff and outflow concentrations. Spearman rank correlation coefficients were calculated for these parameters because the non-transformed datasets were not normally distributed.

5.4 RESULTS

5.4.1 Consecutive Events

To further explore (1) the treatment under the varying wetting and drying regimes present at a field site and (2) the impact of other environmental and climatic factors, water quality samples were collected from successive events during three different periods from the post-repair monitoring period. Typical analysis of water quality performance for field monitored bioretention cells have included percent concentration reduction and load removal rates calculated from a variety of randomly sampled events (Hatt et al. 2009; Hunt et al. 2006, 2008; Passeport et al. 2009; Roseen et al. 2009). These types of analyses were still conducted at this site, but are described in later sections. To display the evolution of cumulative pollutant loads in runoff and outflow from consecutive events, cumulative pollutant load was plotted as a function of cumulative volume, similar to results presented in Peu et al. (2007). The EMC is represented as the slope for each event, so this one graph visually represents the EMC, pollutant load reduction, and volume reduction. Information on seasonality and the impact of previous events can be inferred as well. An example evolution of cumulative pollutant load graph is displayed in Fig. 5.3. For the first four events (up to cumulative volume 2000 m³/ha), the line formed by the points from these events is mostly linear, so the pollutants are exported proportionally to the runoff/outflow volume. It also describes that export is consistent for events of different sizes. However, at the fifth event, which is highlighted with an arrow, a sharp increase in slope becomes present. This indicates that some external factor caused the system to change the export rate. This is an example of why collecting water quality samples from consecutive events and using this type of graph is beneficial. Through incorporation of knowledge about previous and subsequent events, it

will allow researchers to move away from the “black box” analysis of field monitored stormwater control measures.

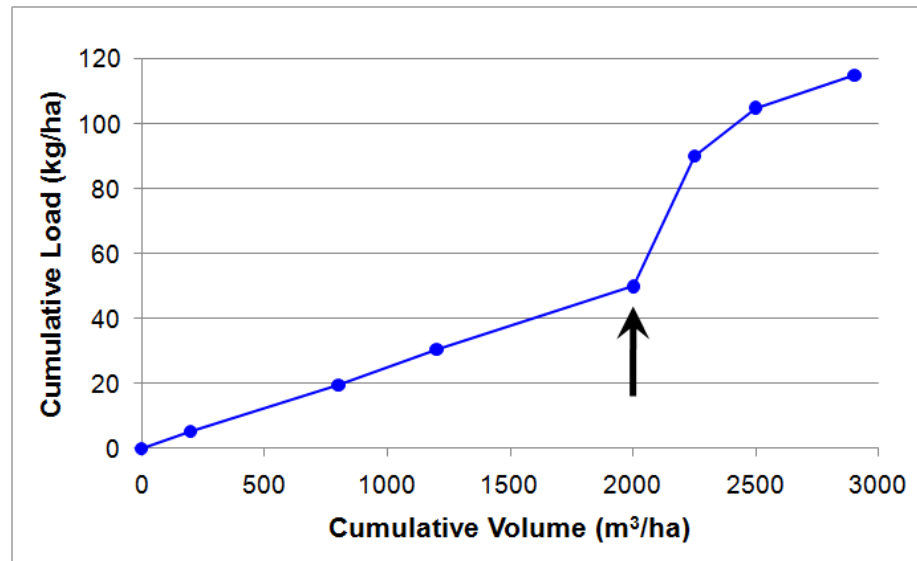


Figure 5.3: Example of evolution of cumulative pollutant load graph. (Arrow indicates the start of an event with a sharp change in pollutant export rate.)

The evolution of cumulative pollutant loads were plotted on the same graph for runoff and outflow from each cell for the three post-repair monitoring periods for TSS, TP, Part-P, and Ortho-P. Only events that had data from all three locations were plotted. In these graphs (Figs. 5.4-5.7), a circle represents runoff, a square represents 0.6-m media depth outflow, and a diamond represents 0.9-m media depth outflow. To distinguish between the different monitoring periods, a variation of the shape was used (small solid shapes are early spring, large hollow shapes are late summer, and large solid shapes are middle autumn), and the cumulative flow volume was reset to the nearest 1000 m³/ha for each period, also indicated with a solid vertical line. The main results displayed in the evolution of TSS load in Fig 5.4 were high reduction of TSS load from both cells, and the outflow relationships were mostly linear, except during events that had a high percentage of overflow. This indicates that as long as overflow does not occur, the TSS export rate is generally constant. The impact of

overflow on TSS export is evident during the second event of the late summer period, where approximately 40 percent of runoff left via overflow. With less infiltration and subsequent filtration and retention time in the surface storage zone, more suspended sediment was discharged in the outflow, so the slope from this event was steeper. Another discovery was that the 0.6-m media depth cells consistently had a higher export rate of TSS than the 0.9-m media depth cells. Despite similar cumulative outflow volumes for the events shown in Fig. 5.4, the 0.6-m media depth cells had almost two times the cumulative load. A possible explanation is preferential flow in the 0.6-m media depth cells. Preferential flow would lead to washout of more sediment and particulate-bound pollutants. Peak drainage rates and surface infiltration rates were compared between the cells to determine the likelihood that preferential flow occurred. The median, 75th percentile, and maximum peak drainage rates were approximately two times higher in the 0.6-m media depth cells for the 49 monitored events that had no overflow and data from both sets of cells. The median, 75th percentile, and maximum peak outflow rates for the 0.6-m media depth cells were 1.83, 3.73, and 8.79 L/s/ha, respectively, and in the 0.9-m media depth cells, they were 0.85, 1.88, and 5.51 L/s/ha, respectively. Infiltration rates were only compared between the five monitored cells when events were greater than 25 mm and when all cells had valid data (6 events). On average, two of the 0.6-m media depth cells had an average infiltration rate that was approximately double the other 0.6-m media depth cell and both 0.9-m media depth cells. The 0.6-m media depth cells had average infiltration rates of 25, 45, and 56 mm/hr (1.0, 1.8, and 2.2 in/hr), and the 0.9-m media depth cells had average infiltration rates of 26 and 27 mm/hr (1.0 and 1.1 in/hr). All five cells had the same mixture of media, so the higher infiltration rates in the 0.6-m media depth cells was best explained by preferential flow through macropores that were present in the shallower media depth cells.

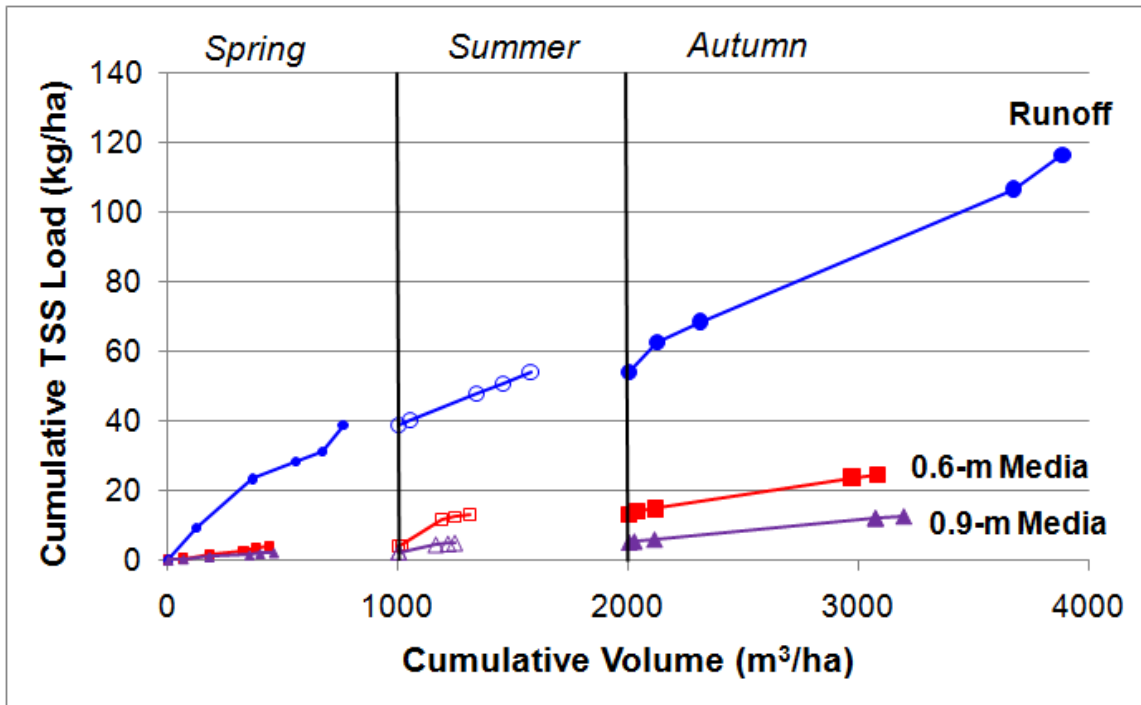


Figure 5.4: Cumulative load versus cumulative volume graph for TSS.

The evolution of total phosphorus load (Fig. 5.5) illustrates the buffering capacity of the bioretention cells because there is less variation in the slope for outflow as compared to runoff. Despite a more constant slope with respect to the outflow concentrations, the slopes were on average steeper than those for the runoff. However, the outflow had a lower overall cumulative load when compared to the runoff load, because of the large volume reduction. It appears that an additional source of phosphorus in the profile contributed to the export of phosphorus in the outflow. There are two distinct periods with elevated TP concentrations in the runoff, and these occurred during the end of the spring period and in the autumn months. At the end of spring, high levels of pollen were present on the pavement and in the water quality samples. In the autumn months, leaves had begun to fall. Therefore, the elevated runoff concentrations appear to occur because of two main external environmental inputs, pollen and leaves. The TP analysis is broken down for the species of Part-P and Ortho-P in Figs. 5.6 and 5.7, respectively. The majority of TP in runoff was in the form Part-P; outflow was more balanced between the two phosphorus forms. For the plotted events, the ratios of

Part-P to Ortho-P for the 0.6-m and 0.9-m media depths were 1.7 and 0.6, respectively, while it was 7.2 for runoff. With preferential flow being a concern for the 0.6-m media depth cells, the 0.9-m media depth cells would have a more tortuous flow path which would increase pore water contact and could lead to more leaching of Ortho-P from the media. Both Part-P and Ortho-P had elevated runoff concentrations due to inputs from pollen and leaves, but the impact on total load was more substantial for Part-P. In Knight et al. (1972), average mineral composition of 58 species of pollen and leaves were measured to determine that these substances provide a source of phosphorus. The composition of phosphorus for monocotyledonous species was 18 and 22 milliequivalents / 100 g in pollen and leaves, respectively, and dicotyledonous species was 19 and 31 milliequivalents / 100 g in pollen and leaves, respectively (Knight et al. 1972). The outflow relationships for Part-P and Ortho-P were mostly linear, with Ortho-P having a more linear trend. Consistent with the TSS results, the 0.6-m media depth cells also had a greater total contribution of Part-P, and the event in late summer (2Aug09) with overflow had one of the highest outflow EMCs for Part-P. The slope for outflow load of Ortho-P flattened after the first three events. In Fig 5.6, the third and fourth events occurred on March 28th and April 14th, respectively. Based on the timing of these events and the Ortho-P response, the decrease in Ortho-P could either be a result of increased plant uptake or a reduction in the pollutant source present in the profile though dilution.

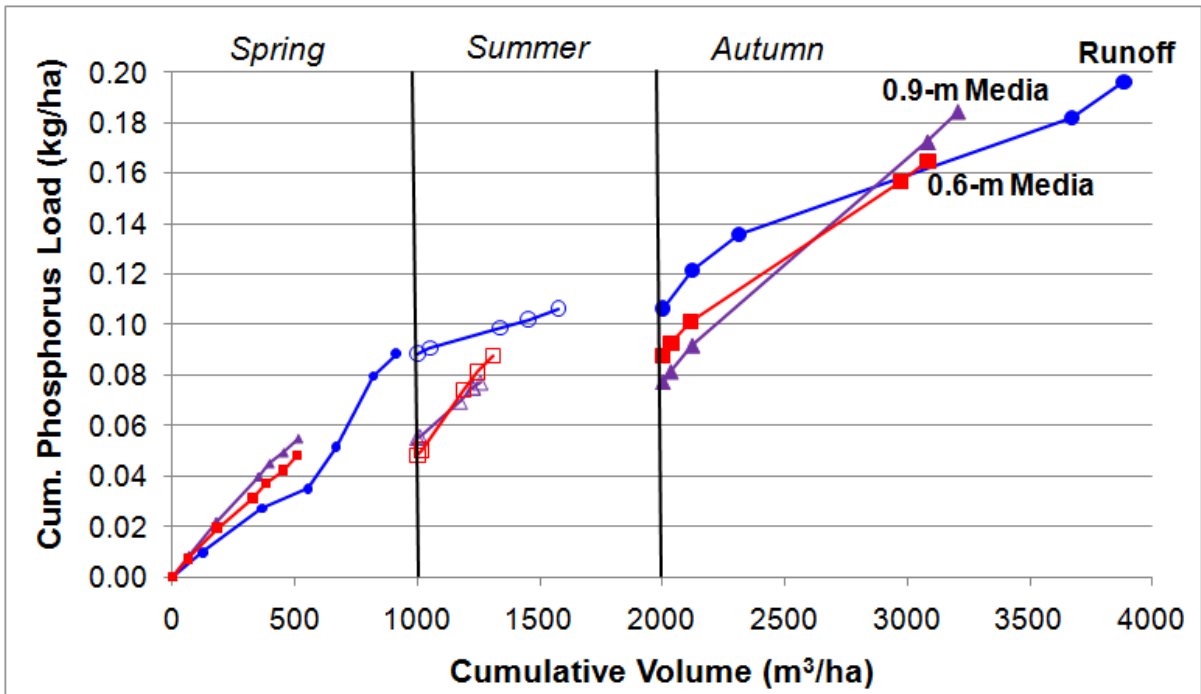


Figure 5.5: Cumulative load versus cumulative volume graph for TP.

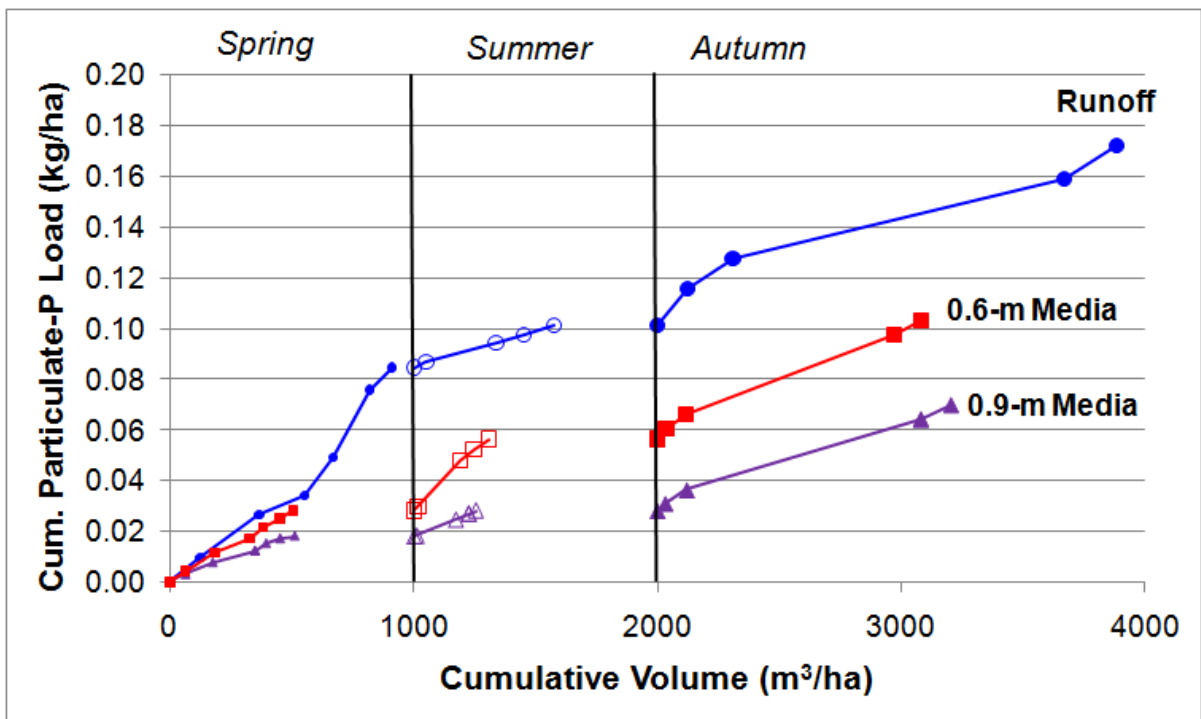


Figure 5.6: Cumulative load versus cumulative volume graph for Part-P.

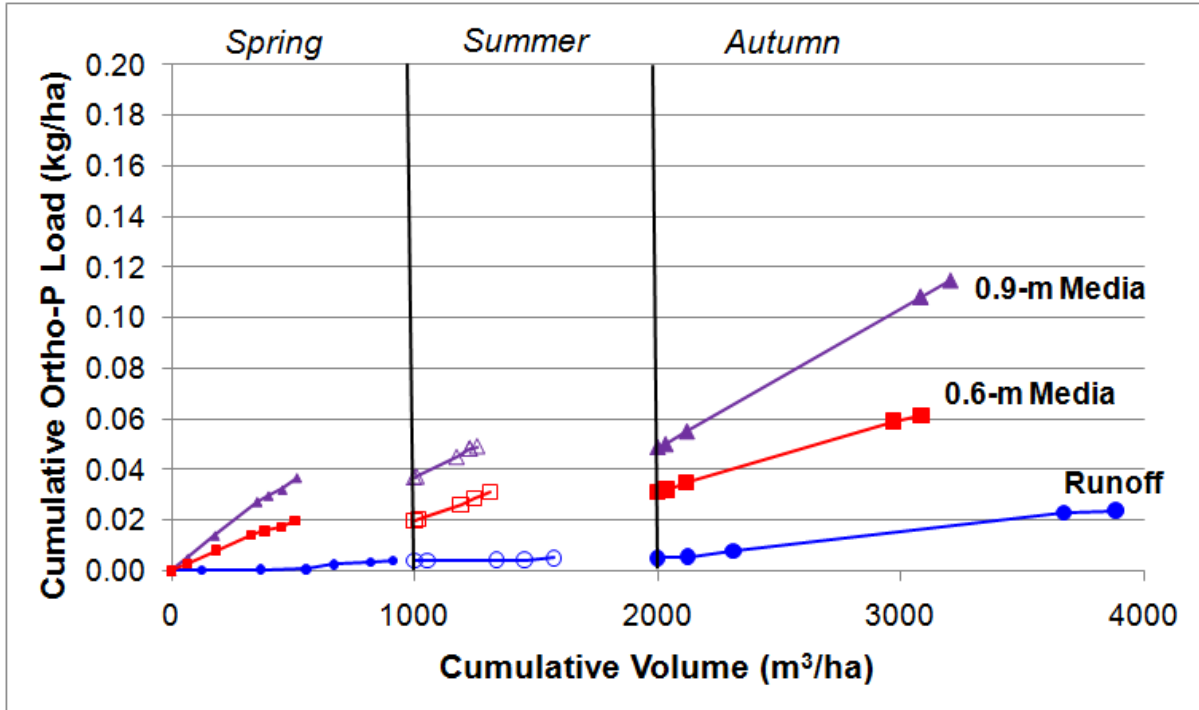


Figure 5.7: Cumulative load versus cumulative volume graph for Ortho-P.

For the nitrogen species, all of the species were plotted on graphs that were separated based on runoff (Fig. 5.8) and outflow from the 0.6-m (Fig 5.9) and 0.9-m (Fig. 5.10) media depth cells. Organic nitrogen is represented with triangles, TAN with diamonds, and $\text{NO}_{2,3}\text{-N}$ with circles. For Figs. 5.9 and 5.10, average media temperature is plotted on a secondary axis and is represented with a cross. Through evaluation of the evolution of pollutant loads, it revealed that TAN loads were buffered and greatly reduced in the outflow. This occurred because the filter media is predominantly an aerobic environment. The cumulative TAN load discharged from the 0.6-m media depth cells was 53 percent higher than from the 0.9-m media depth cells. Similar to the elevated TP concentrations in the runoff, elevated ON concentrations in the runoff occurred during the same periods, so the pollen and leaves are suspected to have provided a source of ON as well. In Knight et al. (1972), average mineral composition of 58 species of pollen and leaves were measured to determine that these substances provide a source of nitrogen as well. The composition of nitrogen for

monocotyledonous species was 260 and 159 milliequivalents / 100 g in pollen and leaves, respectively, and dicotyledonous species was 278 and 225 milliequivalents / 100 g in pollen and leaves, respectively (Knight et al. 1972). The elevated ON concentrations in the runoff were buffered in the outflow. However, due to the ON influx and subsequent transformations, outflow $\text{NO}_{2,3}\text{-N}$ concentrations increased dramatically. In the early spring period, the pollen was first detected for the fourth event (14Apr09). Then there was a 480-hour ADP before the next event (5May09), which also had pollen detected. The input of ON was linear for these two events; however, the export of $\text{NO}_{2,3}\text{-N}$ in the outflow was higher for the fifth event. This occurred because of the influx of ON from the previous event and the long ADP, which provided time for mineralization and nitrification in the aerobic media. Also, during this time period, the media temperature was increasing, which stimulated more microbial activity. In comparison to the runoff, the outflow from both cells had steeper slopes (higher EMCs) at different times. The slopes for $\text{NO}_{2,3}\text{-N}$ and ON were the largest during the end of the spring season and into the summer season. The media temperatures during these time periods were the highest, so this confirmed the laboratory results from Blecken et al. (2007), where elevated media temperatures led to increased $\text{NO}_{2,3}\text{-N}$ export. During this time period, the export of $\text{NO}_{2,3}\text{-N}$ was greater than that of ON. For runoff and 0.6-m media depth cells, the largest contributing nitrogen species was ON, while it was $\text{NO}_{2,3}\text{-N}$ for the 0.9-m media depth cells. The cumulative ON load for outflow from both sets of cells was approximately one-half that of the runoff, but the 0.6-m media depth cells were 10 percent higher than the 0.9-m media depth cells. This could once again be as a result of the higher suspended sediment load being released from the 0.6-m media depth cells. The biggest difference between the outflow cumulative loads from the two cells was $\text{NO}_{2,3}\text{-N}$. The $\text{NO}_{2,3}\text{-N}$ load discharged from the 0.9-m media depth cells was more than twice that from the 0.6-m media depth cells; similar to the results with Ortho-P. This could be attributable to either a larger nutrient source in the 0.9-m media depth cells or a more tortuous flow path that flushed out more of these dissolved pollutants from the porewater.

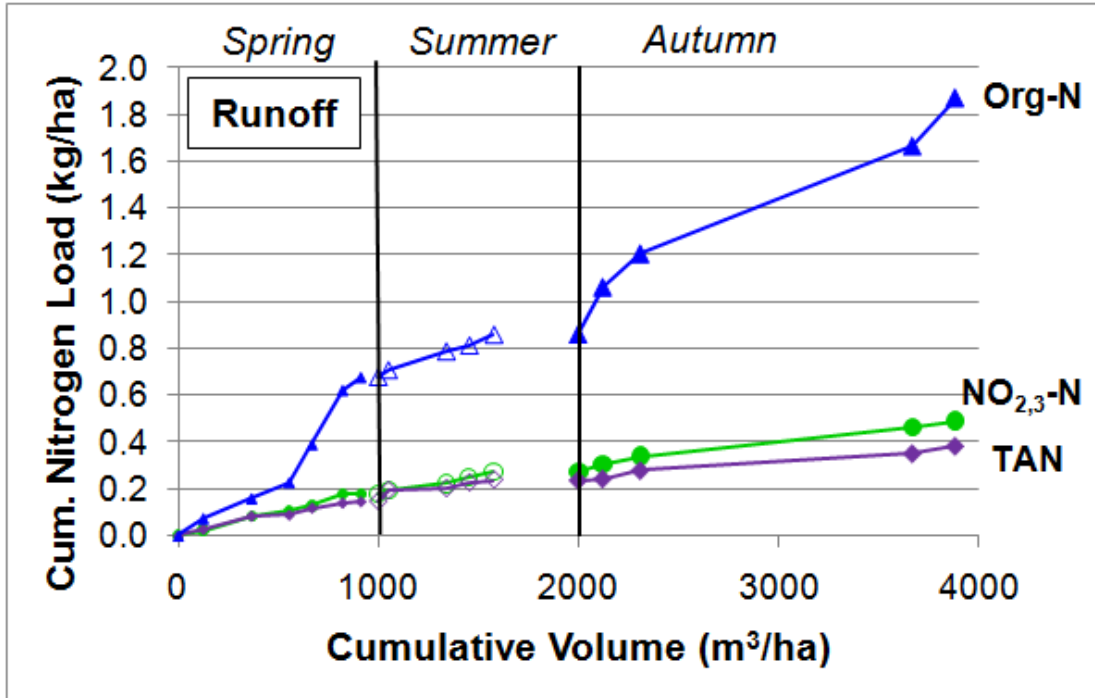


Figure 5.8: Cumulative load versus cumulative volume graph for nitrogen species in runoff.

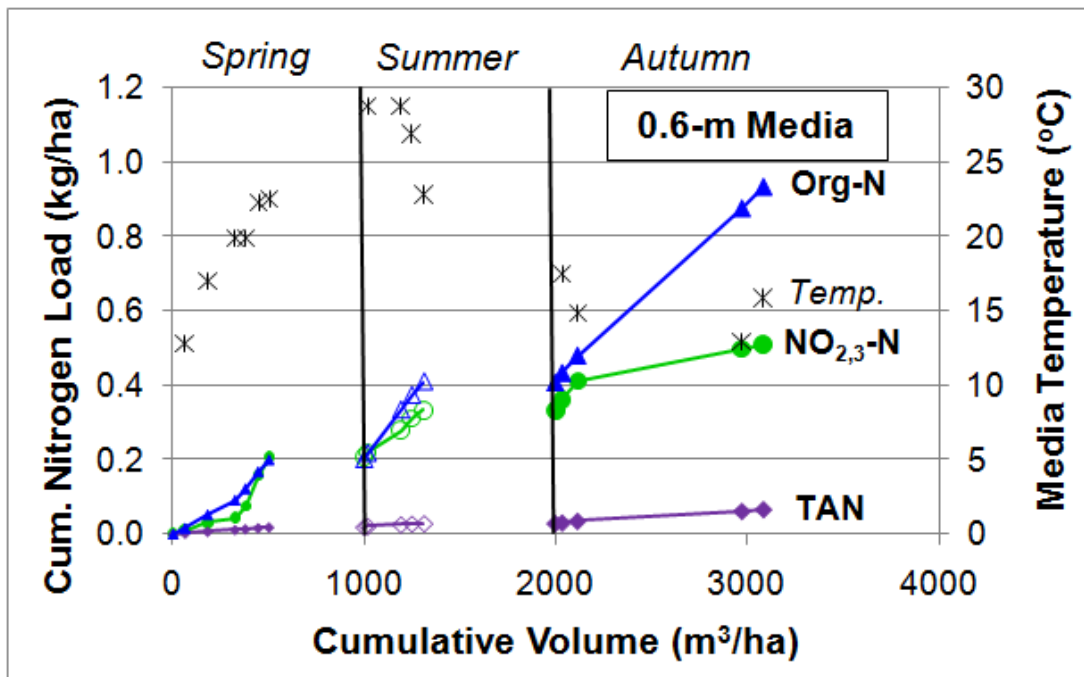


Figure 5.9: Cumulative load versus cumulative volume graph for nutrient species in outflow from the 0.6-m media depth cells.

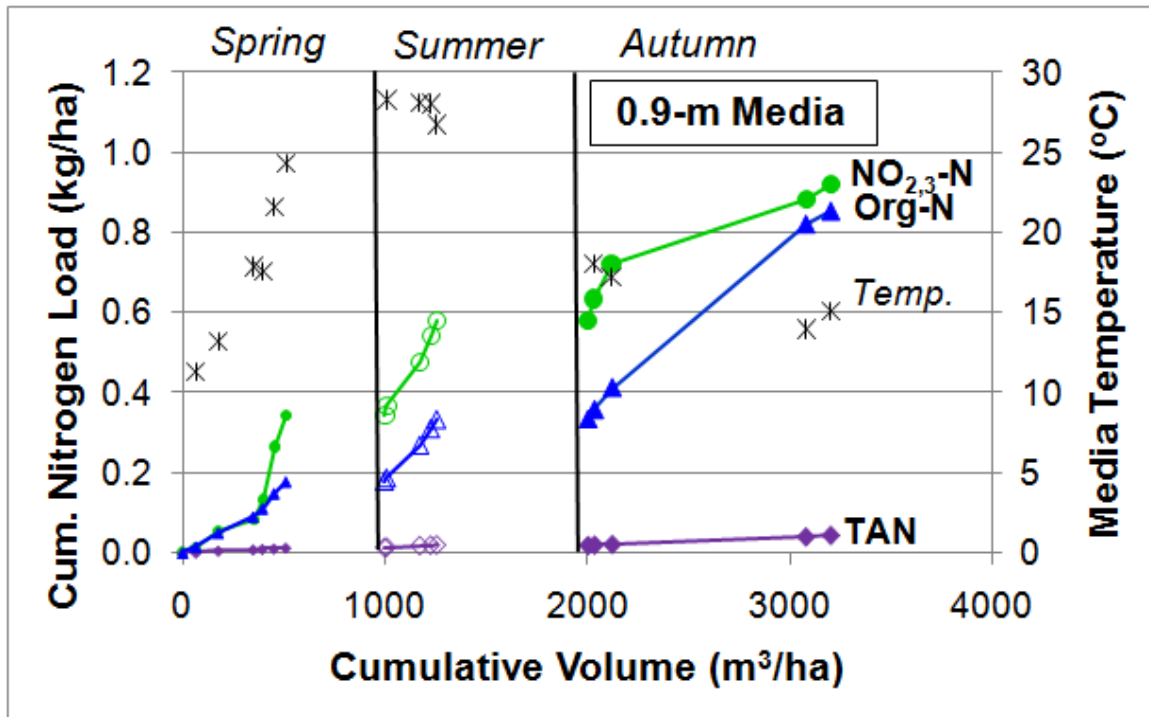


Figure 5.10: Cumulative load versus cumulative volume graph for nutrient species in outflow from the 0.9-m media depth cells.

Some additional results not presented in the previous figures were that during the middle of the autumn season, a 137-mm event occurred and outflow was sampled halfway through the event and then again at the end. The EMCs were lower during the later sample for all pollutants. Also, immediately after the repair had taken place, two events were sampled from the 0.6-m media depth cells only, and these events had an initial spike in all pollutants with the exception of TAN. During the repair, the mulch was moved and the media was raked around, similar to plowing. Similar results were noted in Peu et al. (2007), where plowing events triggered mineralization that resulted in an increase in nitrate load released in drainage water from a reconstituted soil. Specific characteristics of each event are provided in Table 5.2.

Table 5.2: Characteristics for events sampled consecutively.

Date	Num. of Discrete Events	Ant. Dry Period	Precip. Depth	Runoff Vol. ^a	0.6-m Media Depth			0.9-m Media Depth		
					Vol.	Percent Runoff Infil. ^b	Ave. Media Temp.	Vol.	Percent Runoff Infil. ^b	Ave. Media Temp.
					hr	mm	m ³ /ha	m ³ /ha		°C
Period 1 – Early Spring (denoted by small solid shapes in Figs. 5.4-5.10)										
3/19/09	1	68	13.5	125	64	100%	12.8	66	100%	11.3
3/26/09 ^c	1	148	3.3	0	0	N/A	N/A	0	N/A	N/A
3/27/09	1	14	21.8	208	119	88%	17.0	112	86%	13.2
3/28/09	1	10	19.8	188	145	71%	19.9	173	81%	17.9
4/2/09 ^c	1	115	2.5	0	0	N/A	N/A	0	N/A	N/A
4/6/09 ^d	1	73	26.7	257	188	58%	21.7	207	61%	18.3
4/14/09	1	191	12.4	114	55	100%	19.9	46	100%	17.6
5/5/09	1	480	16.3	153	68	100%	22.2	57	100%	21.6
5/7/09	1	39	10.2	91	57	100%	22.5	60	100%	24.3
Period 2 – Late Summer (denoted by large hollow shapes in Figs. 5.4-5.10)										
7/29/09	1	96	6.1	51	18	100%	28.8	10	100%	28.3
7/31-8/2/09	2	44	5.4 / 24.3 ^e	287	173	63%	28.8	153	60%	28.1
8/6/09	1	82	12.4	115	56	100%	26.9	53	100%	28.1
8/14/09 ^d	1	205	11.9	109	N.S.	N/A	N/A	N.S.	N/A	N/A
8/22-23/09 ^d	2	189	12.9 / 40.0 ^e	518	N.S.	N/A	N/A	325	59%	28.1
8/31/09	1	170	13.2	122	64	100%	22.8	30	100%	26.7
Period 3 – Middle Autumn (denoted by large solid shapes in Figs. 5.4-5.10)										
10/26-28/09	2	271	3.4 / 9.8 ^e	122	36	100%	17.5	32	100%	18.0
11/1/09	1	99	19.8	188	79	100%	14.9	88	100%	17.3
11/10-13/09	1a	215	136.9	1360	454	74%	13.0	480	74%	14.0
	1b				402		13.0	481		14.0
11/13/09 ^c	1	13	3.0	0	0	N/A	N/A	0	N/A	N/A
11/18-19/09	1	117	22.4	214	112	100%	15.9	124	100%	15.1

^a Runoff volume per area from impervious surface only. Water quality samples of runoff were not collected from cells that are highlighted, bold, and italicized.

^b Percentage of runoff that infiltrated into the surface

^c Event not sampled due to lack of runoff generated (precipitation depth < 3.3 mm)

^d Event not included on graph because samples were not collected at all locations

^e Two discrete rainfall events that were combined as one water quality event, (first event depth / second event depth)

Note: N.S. = Not Sampled;

5.4.2 Precipitation Characterization of Water Quality Events

Overall, there were 19 and 22 water quality events with paired samples at each location (runoff and outflow from both sets of bioretention cells) that were collected during the pre- and post-repair periods, respectively. Rainfall characteristics for these events are presented in Table 5.3. Overall, the median and 75th percentile events were substantially larger during the pre-repair period, but the post-repair period had the largest maximum event. The two periods had comparable 25th percentile events, and a Wilcoxon rank sum test determined the rainfall depths between the two periods were not significantly different (p-value = 0.136); however, the authors level of confidence in this conclusion is low. More water quality events during the pre-repair period were comprised of combined discrete events due to occasions where runoff was ponded in the surface storage zone at the time of a subsequent event. A similar statistical comparison was made solely on discrete events. The Wilcoxon rank sum test on the discrete events depths proved the discrete rainfall events comprising the water quality events for the two periods were more similar (p-value = 0.601). In examining the discrete events, the mean, 25th percentile, and median events were nearly identical.

Table 5.3: Rainfall characteristics for both monitoring periods where samples were collected from all three locations.

Monitoring Period	WQ vs. Discrete Events	Rainfall Characteristics for Water Quality Events				
		Mean	25% Event	Median	75% Event	Max
Pre-Repair (n=19)	Water Quality	31.5 mm (1.24 in)	13.2 mm (0.52 in)	27.4 mm (1.08 in)	45.8 mm (1.81 in)	68.1 mm (2.68 in)
Post-Repair (n=22)	Water Quality	25.1 mm (0.99 in)	12.6 mm (0.50 in)	19.6 mm (0.77 in)	28.2 mm (1.11 in)	136.9 mm (5.39 in)
Pre-Repair (n=29)	Discrete	20.7 mm (0.81 in)	9.3 mm (0.37 in)	16.3 mm (0.64 in)	28.3 mm (1.12 in)	66.3 mm (2.61 in)
Post-Repair (n=25)	Discrete	21.9 mm (0.86 in)	9.8 mm (0.39 in)	16.3 mm (0.64 in)	22.2 mm (0.88 in)	136.9 mm (5.39 in)

5.4.3 Correlation of Environmental Factors

To determine if any environmental factors influenced the water quality results, Spearman rank correlation coefficients (ρ) were computed for all pollutants. Correlations between ADP and precipitation depth were computed for runoff concentrations (Table 5.4). Additionally, correlations between average media temperature and percent of runoff infiltrated were computed for outflow concentrations from the 0.6-m (Table 5.5) and 0.9-m (Table 5.6) media depth bioretention cells. These relationships showed that precipitation depth was negatively correlated to water quality concentrations for runoff and outflow from both sets of cells, with the exception of Ortho-P from runoff and 0.6-m media depth cells and TSS from the 0.9-m media depth cells. The correlations from runoff concentrations were only significant for TKN, TAN, ON, NO_{2,3}-N, and TN. These results indicate parking lots have a first flush. A concentration-based first flush is described as having high initial concentrations followed by a rapid concentration decline with relatively low and constant concentrations for the remainder of the event (Sansalone and Cristina 2004). In collecting one flow-weighted composite sample from each event, a larger event has rapid wash-off associated with the first portion of large events, and then once the initial load is washed off, later samples from the event have lower concentrations, which dilute the overall composite sample. The correlations between precipitation depth and outflow concentrations for both sets of cells were also only significant for TKN, ON, NO_{2,3}-N, and TN. These statistics indicate that large events have lower average concentrations of these pollutants. The reasons for these results are due to: (1) large events having a lower average runoff concentration and (2) large events tending to have a higher percentage of overflow volume. Overflow occurs during the tail-end of the event, when the runoff concentrations are lower. All four nitrogen species had correlation coefficients exceeding 0.30 for the factor 'percent of runoff infiltrated,' while NO_{2,3}-N was significant in both cell depths and ON and TN were only significant in the 0.9-m media depth cells. This suggests large events with overflow will have lower average concentrations of nitrogen species, especially NO_{2,3}-N. These results also indicate the initial NO_{2,3}-N wash-out has a smaller contribution during larger events,

leading to lower outflow concentrations. During the drying regime from the previous event, NO_{2,3}-N is produced via nitrification.

Table 5.4: Spearman rank correlation coefficients (ρ) between runoff and environmental factors (n = 23, except for TSS, n = 22).

Pollutant	Antecedent Dry Period		Precipitation Depth	
	Spearman ρ	p-value	Spearman ρ	p-value
TKN	0.21	0.337	-0.58	0.004
TAN	0.09	0.675	-0.53	0.009
ON	0.18	0.404	-0.48	0.021
NO _{2,3} -N	0.15	0.510	-0.55	0.006
TN	0.17	0.427	-0.64	0.001
TP	0.38	0.070	-0.32	0.132
Ortho-P	0.63	0.001	0.09	0.690
TSS	0.06	0.795	-0.10	0.671

Note: Significant relationships are highlighted and in bold.

Table 5.5: Spearman rank correlation coefficients (ρ) between 0.6-m media depth outflow and environmental factors (n = 25).

Pollutant	Antecedent Dry Period		Precipitation Depth		Percent of Runoff Infiltrated		Media Temperature	
	ρ	p-value	ρ	p-value	ρ	p-value	ρ	p-value
TKN	0.24	0.251	-0.57	0.003	0.32	0.115	0.50	0.011
TAN	0.30	0.143	-0.26	0.218	0.06	0.777	0.14	0.499
ON	0.23	0.274	-0.58	0.002	0.35	0.090	0.52	0.007
NO _{2,3} -N	0.16	0.453	-0.70	0.0001	0.41	0.041	0.63	0.001
TN	0.26	0.213	-0.66	0.0004	0.39	0.056	0.59	0.002
TP	-0.19	0.361	-0.13	0.541	-0.01	0.983	0.49	0.014
Ortho-P	-0.46	0.021	0.14	0.517	-0.08	0.702	0.11	0.594
TSS	0.19	0.369	-0.19	0.376	-0.15	0.463	0.69	0.0001

Note: Significant relationships are highlighted and in bold.

Table 5.6: Spearman rank correlation coefficients (ρ) between 0.9-m media depth outflow and environmental factors ($n = 24$, except for TSS, $n = 23$).

Pollutant	Antecedent Dry Period		Precipitation Depth		Percent of Runoff Infiltrated		Media Temperature	
	ρ	p-value	ρ	p-value	ρ	p-value	ρ	p-value
TKN	0.02	0.939	-0.58	0.003	0.40	0.051	0.67	0.0003
TAN	0.06	0.765	-0.03	0.900	-0.16	0.460	-0.10	0.653
ON	0.03	0.878	-0.57	0.004	0.41	0.047	0.68	0.0003
NO _{2,3} -N	0.13	0.533	-0.63	0.001	0.48	0.018	0.73	0.0001
TN	0.15	0.486	-0.62	0.001	0.48	0.016	0.71	0.0001
TP	-0.20	0.351	-0.09	0.689	0.11	0.625	0.12	0.573
Ortho-P	-0.40	0.054	-0.05	0.806	0.03	0.905	0.16	0.470
TSS	0.19	0.379	0.11	0.609	-0.35	0.106	0.22	0.316

Note: Significant relationships are highlighted and in bold.

Outflow concentrations of nitrogen species were positively correlated to media temperature, with the highest correlation to NO_{2,3}-N. Higher media temperatures made microbial communities more active, thus leading to more mineralization and nitrification. Interestingly, TP and TSS concentrations from the 0.6-m media depth cells were also positively correlated to media temperature. There was no significant correlation for Ortho-P, so the correlation of TP was due to the particulate-bound form. These data provide additional support that preferential flow occurred in the 0.6-m media depth cells. Measured infiltration and drainage rates were the highest during the summer months, so the likelihood of sediment washout during these warmer months was higher. With respect to antecedent dry period, only Ortho-P had a significant correlation. It was positively correlated for runoff and negatively correlated for outflow from both cells. All other pollutants were positively correlated for runoff and outflow from both cells, with the exception of TP in outflow from both sets of cells (due to Ortho-P), but these lacked statistical significance.

In Brown and Hunt (2011a), there was little difference between runoff and outflow concentrations of NO_{2,3}-N during the first two months of monitoring. Then, samples taken from July through November had outflow concentrations up to *20 times* higher than runoff concentrations. During the final four months of monitoring, there was again no noticeable

difference between the runoff and outflow concentrations, so the conditions appeared to be “back to normal.” It was originally thought that this was an initial flush of $\text{NO}_{2,3}\text{-N}$ caused by the $\text{NO}_{2,3}\text{-N}$ present in the mulch, similar to that from the laboratory study by Hsieh and Davis (2005b). However, the mulch used in their study was comprised of grass clippings and municipal collected leaves. In Nashville, triple shredded hardwood bark mulch was used, and this material has less readily available nitrogen upon decomposition. In Hsieh and Davis (2005b), 91 percent of the original nitrate contained in the grass clippings and leaf mulch was lost during the study. However, this level of nitrate release from hardwood bark mulch would not be expected because bark and woodchips have a carbon to nitrogen ratio that is at least 10 times greater than grass clippings, so there is less available nitrogen (Barker 1997). During the post-repair period (the following year), it was discovered that elevated concentrations of $\text{NO}_{2,3}\text{-N}$ occurred again over a similar period (April through November). Therefore, initial leaching could only partially explain what happened. Blecken et al. (2007) found that temperature had a major influence on nutrient treatment efficiency, especially for $\text{NO}_{2,3}\text{-N}$. When the columns were at 2°C and 8°C , the average $\text{NO}_{2,3}\text{-N}$ concentrations increased by 198 and 265 percent, respectively; when the columns were tested at 20°C , the $\text{NO}_{2,3}\text{-N}$ concentration increased by 1461 percent. Based on the negative correlations between outflow concentration and media temperature, as shown in Tables 5.5 and 5.6, the field study presented herein had similar results to this laboratory study. Nitrogen properties of the mulch and media were not measured at the Nashville site, so the extent of the contribution from these sources is unknown. A more likely candidate for the nitrogen source could have been from an unknown application of slow-release fertilizer applied during the first growing season. The priming effect, from agronomy research, could potentially be another explanation. The definition of the priming effect is that easily available organic substances stimulate microorganism activity, which will accelerate mineralization. Factors that can cause this to occur include: input of organic or mineral fertilizers, input of organic substances, mechanical treatment of soil, or drying/rewetting (Kuzyakov et al. 2000).

5.4.4 Concentration Analysis

More runoff infiltrated into the media during the post-repair period because of the larger surface storage volume and faster infiltration rate. For the events sampled for water quality, the percentage of runoff that infiltrated into the media for the 0.6-m media depth cells increased from 46 to 85 percent. Likewise, the percentage of runoff that infiltrated into the 0.9-m media depth cells increased from 43 to 84 percent. This increased the potential for biological, chemical, and physical treatment of runoff.

Statistical analyses of comparing EMCs between runoff and outflow from each set of bioretention cells, average EMCs, and efficiency ratios for runoff and outflow during the post-repair period are presented in Table 5.7. These statistical analyses and basic performance measurements reiterate the findings already presented by analyzing the evolution of cumulative pollutant loads for runoff and outflow from consecutive events. In comparing the two monitoring periods, there were several changes in the statistical conclusions between runoff and outflow EMCs. During the post-repair period, outflow EMCs of TKN from both sets of cells were now significantly lower than runoff EMCs. Additionally, outflow EMCs of TKN, ON, and TAN were now significantly lower for the 0.9-m media depth cells compared to the 0.6-m media depth cells. However, the differences in average EMCs for both media depth cells were not large; the differences in average EMCs for TKN, ON, and TAN were 16, 14, and 55 percent, respectively. While 55 percent may seem large for TAN, the difference in average EMCs was only 0.015 mg/L. These changes in statistical conclusions could have occurred as a result of more runoff infiltrating into the media or the plant/rhizosphere community becoming more established. In the post-repair period, outflow EMCs of Ortho-P were now significantly higher for the 0.9-m media depth cells compared to the 0.6-m media depth cells. The elevated Ortho-P concentrations in the 0.9-m media depth cells resulted in the outflow EMCs of TP to be significantly greater than the runoff EMCs. However, the outflow TP concentrations from both sets of cells were still relatively low (0.10 mg/L). The average runoff and outflow EMCs were less than one-half of the average TP concentration from eight other parking lots monitored in NC (0.21 mg/L)

(Passeport and Hunt 2009). Therefore, it is possible that an irreducible concentration (Strecker et al. 2001) of TP entered the bioretention cells. Ortho-P and TP were the only two pollutants that had decreases in efficiency ratios for both cells. Average outflow EMCs of Ortho-P were almost four and six times greater than runoff in the post-repair period for the 0.6-m and 0.9-m cells, respectively.

Table 5.7: Average EMCs (mg/L), efficiency ratios, and statistical analyses for parking lot runoff and outflow from the 0.6-m and 0.9-m media depth bioretention cells (paired data from post-repair period only, n=22, unless otherwise noted).

Pollutant	Runoff (In) ^a	Outflow ^a		Efficiency Ratio ^b		Significant Differences (p-value) ^c		
		0.6-m Media	0.9-m Media	0.6-m Media	0.9-m Media	In / 0.6-m	In / 0.9-m ^d	0.6-m / 0.9-m ^d
TKN	0.87 ± 0.52	0.62 ± 0.28	0.54 ± 0.22	0.28 [0.28]	0.38 [0.28]	Yes ^e (0.0263)	Yes (0.0068)	Yes (0.0052)
ON	0.69 ± 0.46	0.58 ± 0.27	0.51 ± 0.22	0.16 [(0.08)]	0.26 [(0.02)]	No ^e	No (SR)	Yes (0.0129)
TAN	0.18 ± 0.20	0.04 ± 0.02	0.03 ± 0.01	0.76 [0.82]	0.84 [0.74]	Yes (<0.0001)	Yes (<0.0001)	Yes (<0.0001)
NO _{2,3} -N	0.18 ± 0.10	0.46 ± 0.38	0.94 ± 0.80	<i>(1.55)</i> [(2.09)]	<i>(4.25)</i> [(4.77)]	Yes (SR: 0.0004)	Yes (<0.0001)	Yes (<0.0001)
TN	1.05 ± 0.57	1.08 ± 0.59	1.48 ± 1.00	<i>(0.03)</i> [(0.21)]	<i>(0.41)</i> [(0.75)]	No ^e	Yes ^e (0.0187)	Yes (0.0002)
Ortho-P	0.008 ± 0.009	0.036 ± 0.015	0.053 ± 0.023	<i>(3.57)</i> [(0.13)]	<i>(5.70)</i> [(0.09)]	Yes ^e (<0.0001)	Yes (<0.0001)	Yes ^e (0.0009)
TP	0.08 ± 0.04	0.10 ± 0.03	0.10 ± 0.03	<i>(0.26)</i> [(0.02)]	<i>(0.22)</i> [0.19]	Yes (0.0397)	Yes (0.0266)	No
TSS ^f	45 ± 21	14 ± 9	8 ± 3	0.68 [0.60]	0.82 [0.71]	Yes ^e (<0.0001)	Yes (<0.0001)	Yes (<0.0001)

^a Pollutant concentrations are presented as an average of the EMCs +/- standard deviation

^b Parentheses and italics represent an increase in pollutant concentration. Brackets indicate efficiency ratios for pre-repair period, and no brackets indicate efficiency ratios for the post-repair period.

^c Bold indicates conclusion is different from pre-repair period. Log-transformed, paired t-test was run for all instances unless otherwise noted (SR = Wilcoxon signed-rank test).

^d n = 23, except TSS, n = 22

^e normally distributed without log-transformation

^f n=21 for runoff and 0.9-m media depth outflow

The buffering ability for pollutants in the filter media as described with the cumulative load versus cumulative volume graphs is supported in Table 5.7 by comparing the standard deviation to the average EMC. Pollutants with a small standard deviation as compared to the average EMC display a buffering capacity. Examples from the outflow for both sets of cells are ON, TAN, Ortho-P, and TP. In contrast, the standard deviations for these pollutants in the runoff were much larger in comparison to the average EMCs, which describe the higher variability of runoff concentrations for these pollutants.

One cause for concern from these results was the elevated outflow EMCs of NO_{2,3}-N, TN, and Ortho-P. It is likely that an unknown source of nitrogen and phosphorus was added to the bioretention cells such as fertilizer. Average EMC values for TN were comparable for runoff and outflow from the 0.6-m media depth cells; however, for the 0.9-m media depth cells, the average EMC for TN was approximately 40 percent higher. Since the media is primarily aerobic, little denitrification was expected to occur, so most of the NO_{2,3}-N generated in the bioretention cells via mineralization and nitrification was expected to be released through drainage and exfiltration. The average EMC for NO_{2,3}-N in the 0.9-m media depth outflow (0.94 mg/L) was more than double that of the 0.6-m media depth outflow (0.46 mg/L), and these were much greater than the 0.18 mg/L measured in the runoff.

Efficiency ratios for most of the pollutants improved during the post-repair period. This occurred either as a result of more runoff infiltrating into the media or higher runoff concentrations occurring during the post-repair period. From the pre-repair to post-repair periods, runoff concentrations for several pollutants had increased, as presented in Table 5.8. The increases occurred primarily for ON, TP, and TSS. These pollutants had median EMCs that were 69, 43, and 90 percent higher during the post-repair period, respectively. The results for TP and TSS were significant. The increase in TSS was likely responsible for the increases in ON and TP. There was less than 25 percent difference in median EMCs for all of the dissolved pollutants: TAN, NO_{2,3}-N, and Ortho-P. The parking lot was monitored within two months after it was paved during the pre-repair period, so runoff during that

period might not have been representative of typical runoff from an aged asphalt surface. As the shopping center experienced more use, including the import of sediment on vehicles, more particulates could have been carried off with runoff, thus increasing ON, TP (predominantly in the particulate form), and TSS. Despite the increase in runoff concentrations during the post-repair period, the concentrations were still less than the average from eight parking lots monitored in NC (Passeport and Hunt 2009). While the increases in concentrations between the two periods were significant for several pollutants, it was still not substantial enough to classify this site as having runoff more polluted than typical parking lots. The median concentrations from both periods and comparisons between the two periods are described in Table 5.8. In one event that was monitored from the pre-repair period (16Sept2008), an abnormally high runoff concentration was reported (Brown and Hunt 2011a). This is why Table 5.8 examines changes in median and not mean concentrations. In comparing the event with an elevated concentration to the median EMCs during the period, the Ortho-P, TP, TAN, and TKN concentrations were 50, 10, 13, and 8 times higher, respectively. Since this event was in September when there was no deicing substances applied, high pollen counts, or leaves falling, and the TSS concentration was in line with the median concentrations, this event did not seem representative of typical runoff concentrations. The high concentration could have been due to a localized source that only entered this one cell, in which case it would not be representative of runoff entering the other cells. Additionally, this event was 13.2 mm (0.52 in), had only three samples taken, and occurred five days after the previous event. Since the results from this event didn't seem representative of typical runoff, an additional analysis was done with the outlier removed. Removal of this outlier reclassified the TKN and ON concentrations during the post-repair as significantly higher than compared to the pre-repair period. The TP and TSS concentrations remained significantly different between the two periods.

Table 5.8: Comparing runoff concentrations from the pre-repair to post-repair periods.

Pollutant	Median Runoff EMC (mg/L)		Change in Median EMC	Sig. Diff. ^a (p-value)	Sig. Diff. with Pre- Repair period outlier removed ^b (p-value)
	<i>Pre-Repair Period</i>	<i>Post-Repair Period</i>			
TKN	0.52	0.69	+ 33%	No (0.206)	Yes (0.047)
ON	0.33	0.56	+ 69%	No (0.065)	Yes (0.014)
TAN	0.17	0.13	- 23%	No (0.363)	No (0.625)
NO _{2,3} -N	0.17	0.18	+ 10%	No (0.604)	No (0.892)
TN	0.64	0.86	+ 33%	No (0.337)	No (0.098)
Ortho-P	0.006	0.005	+ 10%	No (1.00)	No (0.747)
TP	0.051	0.073	+ 43%	Yes (0.049)	Yes (0.016)
TSS	21	40	+ 90%	Yes (0.001)	Yes (0.003)

^a Wilcoxon rank sum test run to compare the two distributions.

^b All data were log-transformed to be normally distributed and a two sample t-test was used.

Note: Bolded items are significantly different.

5.4.5 Load Analysis

As another metric for performance, pollutant loads were calculated for 22 water quality events (comprised of 25 discrete rainfall events) throughout the course of the year to account for seasonal differences. A variety of storm sizes and intensities were monitored. The calculated cumulative loads and removal percentages are presented in Table 5.9. The 22 water quality events accounted for approximately one-third of the discrete rainfall events (25 out of 76) and nearly one-half of the total rainfall depth (558 mm out of 1190 mm) measured during the post-repair period. In comparing the post-repair period to the pre-repair period, load reductions improved for all pollutants except for Ortho-P in both sets of cells and TP in the 0.9-m media depth cells. In the post-repair period, Ortho-P was exported at rates two to three times higher than the runoff load. During the pre-repair period the net export rate was less than 40 percent.

Table 5.9: Summary of the cumulative pollutant loads calculated for 22 water quality events.

Pollutant	0.6 m Cells			0.9 m Cells		
	<i>In</i> (kg/ha) ^a	<i>Out</i> (kg/ha) ^a	<i>Percent reduction or increase</i> ^b	<i>In</i> (kg/ha) ^a	<i>Out</i> (kg/ha) ^a	<i>Percent reduction or increase</i> ^b
TKN	3.44	1.79	48 [39]	3.65	1.40	62 [58]
ON	2.86	1.66	42 [13]	3.03	1.32	56 [43]
TAN	0.58	0.13	78 [78]	0.62	0.08	87 [79]
NO _{2,3} -N	0.75	0.93	(25) [(81)]	0.79	1.60	(103) [(142)]
TN	4.18	2.72	35 [12]	4.44	3.00	32 [13]
Ortho-P	0.04	0.12	(184) [(37)]	0.05	0.17	(274) [(5.1)]
TP	0.34	0.30	12 [5.3]	0.36	0.29	19 [44]
TSS ^c	204	43.5	79 [71]	213	23.6	89 [84]

^a Calculated loading rates are presented as kg/ha of drainage area.

^b Parentheses denote an increase in pollutant load. Brackets denote percent reduction during the pre-repair period.

^c n = 21 for 0.6-m media, and n = 20 for 0.9-m media.

To make comparisons between the monitoring periods, similar methods for estimating annual loads from Brown and Hunt (2011a) were used. The pollutant load reductions were normalized by season to account for the seasonal differences in treatment and the differences in total precipitation depth of all the events sampled for water quality in each season. These precipitation depths and the normal seasonal precipitation depths are shown in Table 5.10. Equation 5.1 was used to calculate annual pollutant loads (where ‘i’ refers to season, so 1 = spring and 4 = winter; Rf = rainfall):

$$Annual\ Load = \sum_{i=1}^4 Seasonal\ Load \times \frac{Rf_{Events\ monitored\ during\ season}}{Rf_{Normal\ seasonal\ depth}} \quad (5.1)$$

Table 5.10: Seasonal summary of the precipitation depths of events used to calculate pollutant loads compared to normal seasonal precipitation depths.

	Percentage of events used to calculate loads compared to normal precipitation	Precipitation depth of events used to calculate loads (mm)	Normal precipitation depth^a (mm)
Spring 2009	51%	136	268
Summer 2009	28%	81	294
Fall 2009	105%	233	223
Winter 2010	36%	108	304
Year	51%	558	1089

^a Normal precipitation data from 1971-2000 climate averages in Nashville, NC (SCO, 2009).

Based on the calculations of annual pollutant loads (Table 5.11), the post-repair period had improved annual pollutant removal rates for all pollutants except NO_{2,3}-N, Ortho-P, and TP in the 0.9-m media depth cells and Ortho-P in the 0.6-m media depth cells. Percent removal of pollutant loads improved during the post-repair period because more runoff infiltrated into the media and the average runoff EMCs were higher. Additionally, as described in Chapter 4, the annual percentage of exfiltration was slightly higher during the post-repair period. The annual outflow loads of Ortho-P and NO_{2,3}-N were higher than the runoff loads, which indicates that there is a source of these pollutants within the soil profile. Overall, the 0.9-m media depth cells had better load reductions to the stormwater network for TKN, ON, TAN, and TSS because these cells had more exfiltration and significantly lower concentrations. On an annual basis, the amount of runoff that left via exfiltration was 32 and 42 percent for the 0.6-m and 0.9-m media depth cells, respectively. The influence of NO_{2,3}-N export from the 0.9-m media depth cells resulted in a lower net removal rate of TN compared to the 0.6-m media depth cells. The 0.9-m media depth cells still had a higher reduction of TP load, a direct result of higher TSS removal, but it now exported more Ortho-P than the 0.6-m media depth cells.

Table 5.11: Estimation of annual pollutant loads for the bioretention cells based on normal rainfall depths.

Pollutant	0.6 m Cells			0.9 m Cells		
	<i>In</i> (kg/ha/yr) ^a	<i>Out</i> (kg/ha/yr) ^a	<i>Percent reduction or increase</i> ^b	<i>In</i> (kg/ha/yr) ^a	<i>Out</i> (kg/ha/yr) ^a	<i>Percent reduction or increase</i> ^b
TKN	6.36 [5.56]	3.41 [3.24]	46 [42]	6.83 [6.15]	2.64 [2.62]	61 [57]
ON	5.06 [3.32]	3.17 [2.75]	37 [17]	5.42 [3.59]	2.48 [2.03]	54 [43]
TAN	1.30 [2.24]	0.25 [0.49]	81 [78]	1.40 [2.57]	0.16 [0.59]	89 [77]
NO _{2,3} -N	1.58 [1.73]	2.07 [2.56]	(31) [(48)]	1.69 [1.92]	3.70 [3.92]	(119) [(104)]
TN	7.94 [7.30]	5.48 [5.80]	31 [21]	8.52 [8.07]	6.34 [6.55]	26 [19]
Ortho-P	0.08 [0.10]	0.23 [0.14]	(189) [(39)]	0.08 [0.11]	0.30 [0.12]	(259) [(8.6)]
TP	0.69 [0.52]	0.61 [0.47]	11 [10]	0.74 [0.57]	0.55 [0.32]	26 [44]
TSS	410 [245]	94 [72]	77 [71]	429 [265]	49 [46]	88 [82]

^a Calculated annual loading rates are presented as kg/ha of parking lot. Brackets denote annual loading rates during the pre-repair period.

^b Parentheses denote an increase in annual pollutant load. Brackets denote percent reduction during the pre-repair period.

5.5 CONCLUSIONS

As a result of studying this site for an additional year, with repaired bioretention cells, more detailed monitoring, and a more well-established plant/rhizosphere community, several conclusions can be made about conventionally drained bioretention cells. They are as follows:

- Examining water quality results from consecutive events in a field study allowed for a better understanding of the processes that took place between events that led to changes in treatment efficiency. This was measured by plotting cumulative load versus cumulative volume as a means to present the evolution of cumulative pollutant loads. Deposition of pollen in the spring and leaves in autumn led to elevated runoff concentrations of ON, TP, and Ortho-P. The influx of ON from pollen and an extended antecedent dry period led to a high export rate of NO_{2,3}-N in a subsequent event.

- Media temperature was positively correlated to outflow concentrations of nitrogen in these conventionally drained bioretention cells. This resulted in higher outflow concentrations of NO_{2,3}-N during warmer months. To reduce TN and NO_{2,3}-N concentrations, bioretention cells should be constructed with an internal water storage zone feature (as recommended by Kim et al. (2003) and Passeport et al. (2009)) to promote denitrification during these periods when microbial activity would normally be high.
- Other environmental factors that significantly influenced runoff and outflow concentrations were precipitation and percent of runoff infiltrated. Larger precipitation events resulted in lower runoff EMCs, a characteristic of a first flush response. Larger precipitation also resulted in lower outflow EMCs due to runoff overflowing during the tail-end of the storm when concentrations were lower. The correlation was significant for NO_{2,3}-N because smaller events had a larger contribution of initial leaching of NO_{2,3}-N, which was created via nitrification during the drying regime in the media.
- While, the deeper media depth cells (0.9-m) had significantly lower EMCs when compared to the shallower systems (0.6-m) for TKN, ON, and TAN, none of which had average EMC differences greater than 0.08 mg/L. For the additional cost required to construct deeper bioretention cells, there did not appear to be enough concentration reduction to warrant using deeper media depths in conventionally drained bioretention cells. However, the major benefit of deeper media depth exists in the additional outflow reduction that these systems can provide. The deeper media depth cells had an additional ten percent of annual runoff leave via exfiltration, which further reduced the pollutant loads released by the bioretention cells.
- The TSS and Part-P loads released by the 0.6-m media depth cells were approximately twice that from the 0.9-m media depth cells, and the outflow EMCs were both significantly higher from the 0.6-m media depth cells. These particulate-bound pollutants were exported at higher rates for the cells that had approximately

double the median, 75th percentile, and maximum peak flow rates for drainage only and double the infiltration rates. This implies that preferential flow pathways carrying sediment may have been responsible for the decreased treatment efficiency of these particulate-bound pollutants. Organic nitrogen was also exported at a higher rate and had a significantly higher EMC in the 0.6-m media depth cells. If the 0.6-m media depth cells had more preferential flow, the 0.9-m media depth cells would have a more tortuous flow path, which could increase the leaching potential for dissolved pollutants (Ortho-P and NO_{2,3}-N) present in the pore water. For these dissolved pollutants, the 0.9-m media depth cells had significantly higher EMCs than the 0.6-m media depth cells and released approximately two times the load compared to the 0.6-m media depth cells.

- The outflow loads of Ortho-P and NO_{2,3}-N were higher than the runoff loads, indicating a source present within the profile. Although the source is unknown, it was likely from an application of fertilizer, which is a potential concern from a maintenance perspective. No additional nutrient sources are needed for vegetation due to the influx of nutrients from runoff. Nitrate and nitrite export was expected because of the aerobic environment in the media of a conventionally drained bioretention cell, which would transform nitrogen found in runoff into NO_{2,3}-N. However, the increase in average EMC for TN was not expected.

5.6 ACKNOWLEDGEMENTS

The authors would like to acknowledge NC Department of Environment and Natural Resources (NCDENR) and the Cooperative Institute for Coastal and Estuarine Environmental Technology (CICEET) for funding this project. Also, thanks to Francois Birgand, Aziz Amoozegar, Greg Jennings, and Wayne Skaggs for their input; Jenny James and Linda Mackenzie for water quality sample analyses; Shawn Kennedy for assistance in setting up the site and installing monitoring equipment; and Bill Lord, Mitch Woodward,

Dan Line, Cole Ammons, Trisha Moore, and Fred Ammons for the labor involved in repairing the bioretention cells.

5.7 REFERENCES

- Barker, A. V. (1997). "Chapter 10: Composition and uses of compost." *Agricultural uses of by-products and wastes, Vol. 668*, J. E. Rechcigl and H. C. MacKinnon, eds., American Chemical Society, Washington, DC, 140-162.
- Blecken, G. T., Zinger, Y., Muthanna, T. M., Deletic, A., Fletcher, T. D., and Viklander, M. (2007). "The influence of temperature on nutrient treatment efficiency in stormwater biofilter systems." *Water Science and Technology*, 56(10), 83-91.
- Bratieres, K., Fletcher, T. D., Deletic, A., and Zinger, Y. (2008). "Nutrient and sediment removal by stormwater biofilters: A large-scale design optimization study." *Water Research*, 42(14), 3930-3940.
- Brown, R. A., and Hunt, W. F. (2011a). "Impacts of media depth on effluent water quality and hydrologic performance of under-sized bioretention cells." *Journal of Irrigation and Drainage Engineering*, 137(3), 132-143.
- Brown, R. A., and Hunt, W. F. (2011b). "Underdrain configuration to enhance bioretention infiltration to reduce pollutant loads." *Journal of Environmental Engineering*, (under review).
- Davis, A. P., Shokouhian, M., Sharma, H., and Minami, C. (2001). "Laboratory study of biological retention for urban stormwater management." *Water Environment Research*, 73(1), 5-14.
- Davis, A. P., Shokouhian, M., Sharma, H., Minami, C., and Winogradoff, D. (2003). "Water quality improvement through bioretention: Lead, copper, and zinc removal." *Water Environment Research*, 75(1), 73-82.
- Davis, A. P., Shokouhian, M., Sharma, H., and Minami, C. (2006). "Water quality improvement through bioretention media: Nitrogen and phosphorus removal." *Water Environment Research*, 78(3), 284-293.
- Davis, A. P. (2007). "Field performance of bioretention: Water quality." *Environmental Engineering Science*, 24(8), 1048-1064.
- Dietz, M. E., and Clausen, J. C. (2006). "Saturation to improve pollutant retention in a rain garden." *Environmental Science and Technology*, 40(4), 1335-1340.

- Eaton, A. D., Clesceri, L. S., and Greenberg, A. R. (1995). *Standard methods for the examination of water and wastewater*, American Public Health Association, American Water Works Association, and Water Environment Federation, Washington, D.C.
- Hatt, B. E., Fletcher, T. D., and Deletic, A. (2007). "Hydraulic and pollutant removal performance of stormwater filters under variable wetting and drying regimes." *Water Science and Technology*, 56(12), 11-19.
- Hatt, B. E., Fletcher, T. D., and Deletic, A. (2009). "Pollutant removal performance of field-scale stormwater biofiltration systems." *Water Science and Technology*, 59(8), 1567-1576.
- Hsieh, C., and Davis, A. P. (2005a). "Evaluation and optimization of bioretention media for treatment of urban storm water runoff." *Journal of Environmental Engineering*, 131(11), 1521-1531.
- Hsieh, C., and Davis, A. P. (2005b). "Multiple-event study of bioretention for treatment of urban storm water runoff." *Water Science and Technology*, 51(3-4), 177-181.
- Hunt, W. F., Jarrett, A. R., Smith, J. T., and Sharkey, L. J. (2006). "Evaluating bioretention hydrology and nutrient removal at three field sites in North Carolina." *Journal of Irrigation and Drainage Engineering*, 132(6), 600-608.
- Hunt, W. F., Smith J. T., Jadlocki S. J., Hathaway, J. M., and Eubanks, P. R. (2008). "Pollutant removal and peak flow mitigation by a bioretention cell in urban Charlotte, NC." *Journal of Environmental Engineering*, 134(5), 403-408.
- Jones, M. P., and Hunt, W. F. (2009). "Bioretention impact on runoff temperature in trout sensitive waters." *Journal of Environmental Engineering*, 135(8), 577-585.
- Kim, H., Seagren, E. A., and Davis, A. P. (2003). "Engineered bioretention for removal of nitrate from stormwater runoff." *Water Environment Research*, 75(4), 355-367.
- Knight, A. H., Crooke, W. M., and Shepherd H. (1972). "Chemical composition of pollen with particular reference to cation exchange capacity and uronic acid content." *Journal of the Science of Food and Agriculture*, 23(3), 263-274.
- Kuzyakov, Y., Friedel, J. K., and Stahr, K. (2000). "Review of mechanisms and quantification of priming effects." *Soil Biology and Biochemistry*, 32(11-12), 1485-1498.
- Li, H., and Davis, A. P. (2008). "Urban particle capture in bioretention media I: Laboratory and field studies." *Journal of Environmental Engineering*, 134(6), 409-418.

- Line, D. E., and Hunt, W. F. (2009). "Performance of a bioretention area and a level-spreader-grass filter strip at two highway sites in North Carolina." *Journal of Irrigation and Drainage Engineering*, 135(2), 217-224.
- Lucas, W. C., and Greenway, M. (2008). "Nutrient retention in vegetated and non-vegetated bioretention mesocosms." *Journal of Irrigation and Drainage Engineering*, 134(5), 613-623.
- Newman, M. C., Dixon, P. M., Looney, B. B., and Pinder, J. E. (1989). "Estimating mean and variance for environmental samples with below detection limit observations." *Water Resources Bulletin*, 25(4), 905-916.
- N.C. Department of Environment and Natural Resources (NCDENR). (2009). "Chapter 12: Bioretention." *Stormwater best management practices manual*, North Carolina Department of Environment and Natural Resources, Division of Water Quality, Raleigh, N.C., 12.1-12.30.
- O'Neil, S. W., and Davis, A. P. (2010). "Analysis of bioretention media specifications and relationships to overall performance." *Proceedings, 2010 International Low Impact Development Conference*, K. Lichten and S. Struck, eds., ASCE, San Francisco, Ca.
- Passeport, E., and Hunt, W. F. (2009). "Asphalt parking lot runoff nutrient characterization for eight sites in North Carolina, USA." *Journal of Hydrologic Engineering*, 14(4), 352-361.
- Passeport, E., Hunt, W. F., Line, D. E., Smith, R. A., and Brown, R. A. (2009). "Field study of the ability of two grassed bioretention cells to reduce storm-water runoff pollution." *Journal of Irrigation and Drainage Engineering*, 135(4), 505-510.
- Peu, P., Birgand, F., and Martinez, J. (2007). "Long term fate of slurry derived nitrogen in soil: A case study with a macro-lysimeter experiment having received high loads of pig slurry (Solepur)." *Bioresource Technology*, 98(17), 3228-3234.
- Roseen, R. M., Ballesterro, T. P., Houle, J. J., Avelleneda, P., Widley, R., and Briggs, J. (2006). "Storm water low-impact development, conventional structural, and manufactured treatment strategies for parking lot runoff: Performance evaluations under varied mass loading calculations." *Transportation Research Record: Journal of the Transportation Research Board*, No. 1984, 135-147.
- Roseen, R. M., Ballesterro, T. P., Houle, J. J., Avelleneda, P., Briggs, J., Fowler, G., and Widley, R. (2009). "Seasonal performance variations for storm-water management in cold climate conditions." *Journal of Environmental Engineering*, 135(3), 128-137.

- Sansalone, J. J., and Cristina, C. M. (2004). "First flush concepts for suspended and dissolved solids in small impervious watersheds." *Journal of Environmental Engineering*, 130(11), 1301-1314.
- State Climate Office (SCO). (2009). "1971-2000 climate normals." *Nashville Station (Station #316044)*, State Climate Office of North Carolina, Raleigh, N.C. <<http://www.nc-climate.ncsu.edu/cronos/normal.php?station=316044>> (July 20, 2009).
- Strecker, E. W., Quigley, M. M., Urbonas, B. R., Jones, J. E., and Clary, J. K. (2001). "Determining urban storm water BMP effectiveness." *Journal of Water Resource Planning Management*, 127(3), 144-149.
- U.S. Environmental Protection Agency (USEPA). (1983). "Methods for chemical analysis of water and wastes." *Rep. No. EPA-600/4-79-020*, USEPA, Cincinnati, Oh.
- U.S. Environmental Protection Agency (USEPA). (2009). "National water quality inventory: Report to Congress—2004 reporting cycle." *Rep. No. EPA 841-R-08-001*, USEPA, Washington, D.C.
- Zhang, W., Brown, G. O., Storm, D. E., and Zhang, H. (2008). "Fly ash amended sand as filter media in bioretention cells to improve phosphorus retention." *Water Environment Research*, 80(6), 507-516.

6. LID TREATMENT TRAIN: PERVIOUS CONCRETE WITH SUBSURFACE STORAGE IN SERIES WITH BIORETENTION AND CARE WITH SEASONAL HIGH WATER TABLES

6.1 ABSTRACT

Two infiltrating low impact development (LID) practices configured in series, pervious concrete and bioretention (PC-B), were monitored for 17 months to examine the hydrologic and water quality response of this LID treatment train design. For the first LID practice, 0.53 ha of pervious concrete was installed to treat direct rainfall and runoff from 0.36 ha of contributing asphalt parking lot. The pervious concrete was installed over a gravel subsurface storage basin, which was designed to store 25 mm (1 in) of runoff from the parking lot before draining into the second LID practice – a 0.05 ha bioretention cell. The bioretention cell also received additional runoff from 0.19 ha of surrounding pervious landscape. The bioretention cell was conventionally drained, had a media depth of 0.5 m (1.6 ft), and was constructed at a location with a high water table. Rational C coefficients associated with peak flow rates were calculated for all events with rainfall intensities greater than 2.5 cm/hr (1 in/hr). The mean and median rational C coefficients were 0.012 and 0.001, respectively. During the entire monitoring period, exfiltration and evapotranspiration accounted for 71 percent of the total runoff volume. Of 80 monitored events, 33 had outflow. The large outflow reduction subsequently led to high pollutant load reductions for total nitrogen (51%), total phosphorus (50%), and total suspended solids (89%). However, when the contribution of baseflow was included in the calculation, the total nitrogen load discharged from the bioretention cell was 63% *higher* than that of the runoff load because of nitrate and nitrite (NO_{2,3}-N) present in the baseflow. The total nitrogen (TN) loads of runoff, outflow [storm flow (total outflow minus baseflow)], outflow (baseflow), and outflow (total) were 7.70, 3.76, 8.76, and 12.53 kg/ha/yr, respectively. Of the 8.76 kg/ha/yr TN in the

baseflow, 92 percent was in the form of $\text{NO}_{2,3}\text{-N}$. This study demonstrated the hydrologic benefits (peak flow and volume reduction) gained by having two infiltration LID practices in series. The performance was substantially better than that of a single treatment practice (bioretention) that was monitored at the same site. However, the water quality results were not as promising due to the influx of groundwater in the bioretention cell and the lack of denitrifying conditions in either the bioretention cell or pervious concrete system. This study also demonstrated the potential negative impact of increased TN and $\text{NO}_{2,3}\text{-N}$ export to surface water from bioretention cells sited in an area with a high water table.

6.2 INTRODUCTION

As impervious surfaces increase, detrimental impacts on stormwater runoff are observed, including increased runoff volume, peak discharge, and pollutant export (Lee and Bang 2000; Line et al. 2002; Line and White 2007; Makepeace et al. 1995). The focus of stormwater management has shifted from peak flow rate reduction to the reduction of pollutant export and restoration of pre-developed hydrologic conditions. Low impact development (LID) practices, such as bioretention cells and permeable pavement, can be installed to achieve these goals. LID practices target stormwater treatment near the source by promoting infiltration and evapotranspiration (ET) using natural approaches (Davis 2005).

In most published studies, only a single LID practice has been evaluated (Brattebo and Booth 2003; Brown and Hunt 2011a; Collins et al. 2008; Hatt et al. 2009). A notable exception to this is Rushton (2001). Rarely have multiple LID practices in series been studied, despite that most LID guidelines recommend installing these practices in series. The objective for placing two different practices in series should be to align different treatment mechanisms to increase groundwater recharge, improve water quality treatment, and reduce pollutant export. Because performance of practices in series is not well documented, questions persist regarding how to size individual practices so that (1) water quality and hydrological benefits are achieved and (2) whether practices in series are financially worthwhile.

One concern regarding implementation of multiple stormwater control measures (SCMs) in series is the potential for limited pollutant removal if similar treatment mechanisms are employed by all systems (USEPA 2002). Additionally, systems with similar treatment mechanisms may approach irreducible concentrations after treatment through one system (Hathaway and Hunt 2010; Schueler and Holland 2000; Strecker et al. 2001). In a study of three stormwater wetlands in series, Hathaway and Hunt (2010) found that more than 80 percent of the concentration reduction for all pollutants measured occurred after treatment through the first wetland. The first wetland significantly reduced all pollutant concentrations, yet there was no significant difference for any pollutant concentration between the outlet of the second and outlet of the third wetland. This suggests it would have been better to install an SCM that utilized different treatment mechanisms to provide greater hydrologic benefits and possibly additional water quality treatment.

Permeable pavement is designed to reduce runoff by allowing rainwater to pass through to the underlying soil. At sites with underlying soils that have low permeability, underdrains are typically installed. The various types of permeable pavement include: pervious concrete (PC), concrete grid pavers (CGP), permeable interlocking concrete pavers (PICP), and plastic reinforcing grid pavers. When designed, sited, and maintained properly, a variety of permeable pavements have been shown to dramatically reduce surface runoff volumes and peak flow rates (Bean et al. 2007; Brattebo and Booth 2003; Collins et al. 2008; Fassman and Blackbourn 2010). Permeable pavement has also been shown to significantly reduce runoff concentrations of zinc, copper, and phosphorus (Bean et al. 2007; Brattebo and Booth 2003; Rushton 2001). Results for total nitrogen (and nitrate) removal have been mixed (Bean et al. 2007; Collins et al. 2010; Tota-Maharaj and Scholz 2010). Collins et al. (2010) specifically found that, with the exception of concrete grid pavers, most permeable pavement types (including pervious concrete) conveyed the total nitrogen concentration that was atmospherically deposited into the effluent. Pollutant load reductions improved when an elevated underdrain was installed (Collins et al. 2010) and when underlying soils had high

permeability (Bean et al. 2007; Rushton 2001) because of the increase in exfiltration/seepage volume.

Depending on design and media composition, bioretention cells have been effective at removing many pollutants from urban runoff (Bratieres et al. 2008; Davis et al. 2003; Dietz and Clausen 2005; Hatt et al. 2009; Hunt et al. 2006; Kim et al. 2003). Media composition and depth are critical to the effectiveness of bioretention cells. Hunt et al. (2006) found that the phosphorus removal efficiency increased when the media had less phosphorus present. Deeper media depths released less outflow; consequently, these systems had higher pollutant load reduction (Brown and Hunt 2011a; Li et al. 2009). Nitrogen treatment provided by bioretention cells has varied due to media composition, vegetation, and drainage configuration (Bratieres et al. 2008; Hunt et al. 2006; Kim et al. 2003; Lucas and Greenway 2008). The media in conventionally drained bioretention cells is primarily aerobic, so microbial processes in the media convert ammonium to nitrate through nitrification which is then released as such in the outflow. Laboratory (Kim et al. 2003) and field (Brown and Hunt 2011b; Davis 2007; Passeport et al. 2009) studies have shown that elevating the underdrain to create an anaerobic environment promoted denitrification. Additionally, influx of groundwater from a seasonally high water table was identified as a factor causing elevated outflow concentrations of nitrate (Line and Hunt 2009).

The purpose of this study was to examine how a pervious concrete – bioretention in-series treatment system impacted site hydrology and water quality. Does linking these two “stalwarts” of LID in series provide cost-effective treatment?

6.3 METHODOLOGY

6.3.1 Site Description

The study site was a parking lot at a large commercial retail store, in Nashville, NC. The SCMs installed to treat the parking lot runoff were 0.53 ha of pervious concrete (with subsurface storage) and a 0.05 ha bioretention cell receiving the pervious concrete outflow

(Fig. 6.1). The pervious concrete also treated an additional 0.36 ha of surrounding asphalt parking lot with two concrete driving lanes. The pervious concrete was 0.2 m (8 in) thick and was poured over a subsurface storage basin filled with washed #67 stone (approximately 13 mm (0.5 in) diameter). According to the design, the storage basin, which occupied 0.18 ha and was 0.45 m deep (Fig. 6.2), could store/retain runoff from a 25-mm (1-in) rainfall event over the entire drainage area (0.89 ha). Observations confirmed that outflow from the subsurface storage basin only occurred for events approximately equal to or greater than 25 mm (1 in). Outflow from the basin flowed into the bioretention cell through a perforated PVC pipe positioned along the side of the bioretention cell (Fig. 6.1).



Figure 6.1: Images of the pervious concrete (A) and bioretention cell that received drainage from pervious concrete site (B).

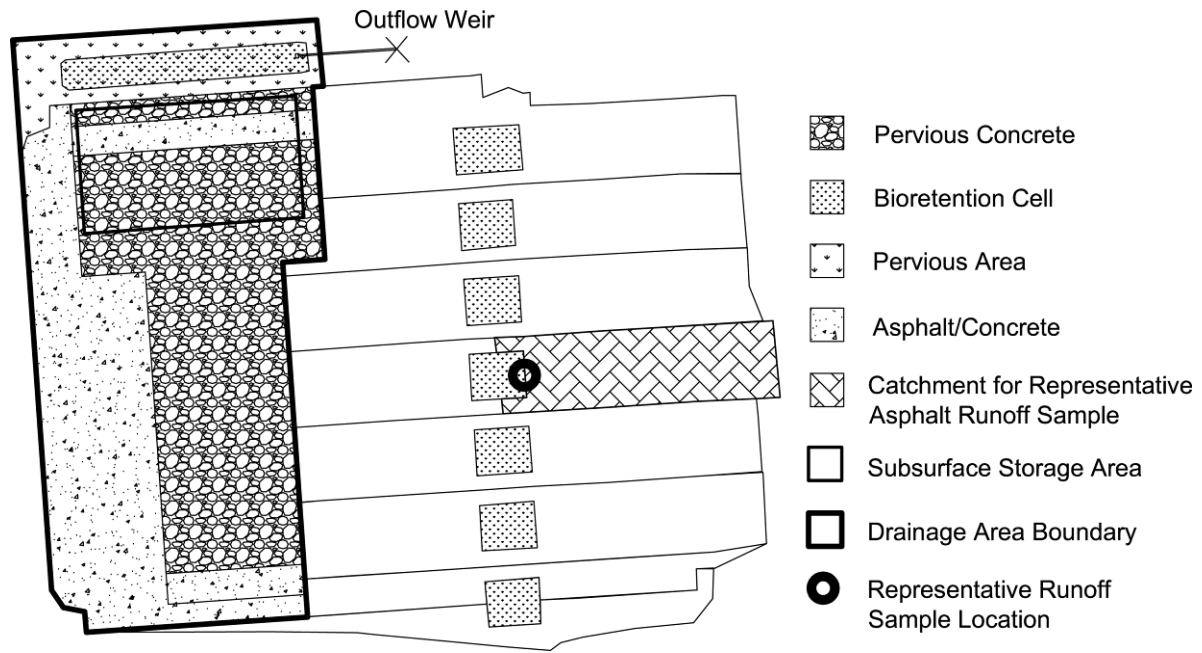


Figure 6.2: Site layout of the parking lot and SCMs.

The bioretention cell was conventionally drained (pipe placed along bottom of cell with no storage zone) with a media depth of 0.5 m (1.6 ft) and surface area of 0.05 ha. In addition to the pervious concrete drainage area, 0.19 ha of surrounding grassed and landscaped area drained to the cell, for a total watershed area of 1.13 ha. The media was comprised of approximately 88% sand, 10% clay and silt, and 2% certified compost. The phosphorus index of the media was low (P-Index = 12 to 19), providing the potential for phosphorus sorption (Hardy et al. 2007). Beneath the media was a 0.10-m (4-in) layer of washed sand, a 0.05 m (2-in) layer of choking stone, and a 0.15 m (6-in) layer of washed #57 stone with underdrains embedded in it. The bioretention cell was planted with loblolly pines (*Pinus taeda*) and had no mulch on the surface. During the study, volunteer grass and weeds were evident on the surface. The surface storage volume of the bioretention cell was *designed* to detain runoff from a 25-mm (1-in) event; however, it was undersized by 75% because either the target elevation for the top of the media or the overflow structure was not met. However, it is likely that the lack of storage did not negatively affect overall performance because the pervious concrete SCM metered the runoff, unlike if impervious

surfaces had drained directly to the bioretention cell. With the low runoff rates and high infiltration rate at the bioretention surface, overflow from the bioretention cell was only observed for six percent of the events.

Another important issue with the construction of the bioretention cell was its placement in soil with a high water table. During excavation in 2007, the soil at the base of the bioretention cell was dry due to a severe drought in the region, but indications of hydric soils were observed. Designers suspected that there might be a seasonally high water table, so the cell was lined with an impermeable liner to prevent water from passing through the interface between the bioretention media and in-situ soil. Despite this effort, the liner failed, as groundwater flowed almost continuously from the underdrains throughout the entire monitoring period. The pervious concrete was never maintained during the study period. Despite a lack of maintenance, ponding was never present on the surface of the pervious concrete.

6.3.2 Sampling Methods

Automated samplers (ISCO 6712TM) with integrated bubbler modules (ISCO 730TM) were used to collect flow-proportional composite samples of runoff from a section of asphalt (Fig. 6.2) and outflow from the bioretention cell. No monitoring was conducted between the pervious concrete and the bioretention cell. Both sites were monitored for 17 months – March 26, 2008 to September 2, 2009. A 120°, sharp-crested, v-notch weir was used in combination with the sampler's flow module to monitor outflow from the pervious concrete-bioretention (PC-B) system (Fig. 2). Water levels measured by the bubbler module were routinely field verified during site visits. For each event, baseflow was subtracted from the total monitored flow to calculate the storm flow. The baseflow volume was calculated as the duration of outflow multiplied by the average of the baseflow rate before and after the event.

The asphalt parking lot runoff station (described in Brown and Hunt 2011a) was used to measure a representative sample of runoff from the same parking lot. It was also used to continuously monitor runoff flow rates from a section that was entirely asphalt using a 0.75-

m (2.5-ft) wide rectangular weir with end contractions. This portion of the parking lot had more traffic than the pervious concrete section, so it may represent higher runoff pollutant concentrations, especially for total phosphorus (TP) and total suspended solids (TSS). However, most of the total nitrogen (TN) was likely atmospherically deposited, as has been found in a study done in the same region (Collins et al. 2010). The annual TN load from the runoff monitoring location was 7.7 kg/ha/yr, which is in the range of reported atmospheric deposition from six monitoring stations in central North Carolina – 6.2 to 10.7 kg/ha/yr (Line et al. 2002). At the site, a tipping bucket rain gauge (ISCO 674 Rain Gauge™) measured rainfall intensity, while a manual plastic rain gauge measured rainfall depth.

For storms during which outflow measurements were not recorded due to loss of sampler power supply, outflow was estimated using rainfall versus discharge regression relationships that were developed based on monitored events. This is described in more detail later. Regressions were made for two categories, events with (1) more than and (2) less than five days antecedent dry period (ADP) per USDA-NRCS (2004a) guidance. The outflow regressions were divided into these two categories because, if the ADP was less than five days, the subsurface storage basin may not be fully available to store incoming runoff, so the likelihood of outflow was greater. Since there was a long delay in hydrologic response for the PC-B system, individual events were characterized as those where the ADP was greater than 24 hours.

6.3.3 Water Quality Methods

Flow-proportional samples from each monitored event and grab samples of non-storm flow (baseflow) were collected and analyzed for nutrients and TSS. The samplers were programmed with an enable level to prevent sampling of baseflow between events. Storm samples were composited into one 10-L container in the automated sampler. The composite sample was mixed thoroughly, transferred to laboratory containers, placed on ice, and delivered to the NCSU Center for Applied Aquatic Ecology laboratory (state-certified laboratory) within 24 hours and analyzed (Table 6.1) within recommended maximum holding times (Eaton et al. 1995; USEPA 1983). No preservation was used in the automated

samplers; thus, samples that could not be recovered from the machine within 24 hours were discarded. Samples were analyzed for orthophosphate (Ortho-P), TP, total ammoniacal nitrogen (TAN), nitrite plus nitrite (NO_{2,3}-N), and total Kjeldahl nitrogen (TKN). Organic-nitrogen (ON) was calculated as the difference of TKN and TAN, and TN was calculated as the sum of TKN and NO_{2,3}-N (Table 1). For events when outflow was not sampled (less than one-half of the events with outflow), concentrations from monitored storms close in time (same season) and similar in rainfall accumulation were utilized in the annual load calculation.

Table 6.1: Summary of analytical methods for water quality analysis.

Abbreviation	Pollutant	Analytical Method	Reportable Limit (RL)	Unit
NO _{2,3} -N	Nitrate + Nitrite nitrogen	SM 4500-NO3-F ^a	0.0056	mg/L
TKN	Total Kjeldahl nitrogen	EPA 351.1 ^b	0.14	mg/L
TAN	Total ammoniacal nitrogen	SM 4500-NH3-H ^a	0.007	mg/L
ON	Organic nitrogen	= TKN – TAN	N/A	mg/L
TN	Total nitrogen	= NO _{2,3} -N + TKN	N/A	mg/L
Ortho-P	Orthophosphate	SM 4500-P-F ^a	0.006	mg/L
TP	Total phosphorus	SM 4500-P-F ^a	0.01	mg/L
TSS	Total suspended solids	SM 2540 D ^a	1	mg/L

^a Source (Eaton et al. 1995)

^b Source (USEPA 1983)

6.3.4 Runoff Calculation

Runoff from the site was calculated for each event by subtracting an initial abstraction depth from the rainfall depth and multiplying by the drainage area for each land use. Initial abstraction depths were calculated using curve numbers (CN), which varied based on antecedent moisture conditions at the site (USDA-NRCS 2004a). Under average antecedent moisture condition, a CN of 98 was used for paved surfaces and a CN of 86 was used for the pervious landscape (open space with poor condition; hydrologic soil group C) (USDA-NRCS 2004b).

6.3.5 Statistical Methods

Statistical analyses of water quality results for paired samples of outflow and runoff were conducted using SAS[®] version 8 (SAS Institute Inc., Cary, NC). The level of significance used in all analyses was $\alpha = 0.05$. Four statistical tests for normality (Shapiro-Wilk, Kolmogorov-Smirnov, Creamer-von Mises, and Anderson-Darling) were used to check the validity of the assumption that the data were normal. In cases where the normality assumption was weak, the data were log-transformed. If the data were normally distributed, a paired t-test was used to determine if the concentrations were significantly different. If the data were not normally distributed but had symmetry, a Wilcoxon signed-rank test was used, and a sign test was used if none of these assumptions were valid. Water quality data were analyzed for events with paired samples of runoff and outflow.

For loads, statistical analysis was limited by the fact that outflow from PC-B occurred for less than half of the events monitored, while runoff occurred for every event at the representative asphalt parking lot station. Thus, a comparison between the rainfall-pollutant load relationships was conducted using the least square means (LS means) test (SAS 1985). This test uses the pooled variance of the relationships to evaluate the pollutant load at the average value of rainfall for both relationships combined. Hence, LS means evaluated the dependent variable at the midpoint of the range of the combined set of independent variables (rainfall). The value of the dependent variable for each relationship can then be used to compute a percent reduction.

6.4 RESULTS AND DISCUSSION

6.4.1 Precipitation Characterization and Hydrology

Throughout the 17-month monitoring period, 80 discrete events occurred. Of these events, 33 produced outflow at the weir of the PC-B system and 17 were sampled for water quality. Rainfall characteristics are described in Table 6.2. For four events, outflow was not monitored due to power failure, but the events were large enough that outflow should have

been generated. Linear relationships of outflow volume versus rainfall were used to estimate outflow from these events. Separating the relationships between those with more than and less than five days since the previous rainfall, the coefficient of determination, r^2 , increased from 0.77 (regression of all data) to 0.87 and 0.89, respectively (Fig. 6.3). The relationship of estimated runoff from the entire site under the normal antecedent moisture condition is depicted. From this graph, it is evident that when the antecedent dry period is longer, outflow is substantially less because there is more storage available in the subsurface storage basin. Based on the linear relationships for the two categories, the line crosses the x-axis at 11.2 mm (0.44 in) and 21.3 mm (0.84 in) for ADP less than and greater than 5 days, respectively. These depths equate to the estimated rainfall depth needed to start to generate outflow from the PC-B system.

Table 6.2: Rainfall characteristics of all events, events with outflow, and events sampled for water quality.

	All Events	Events with Outflow	Events Sampled for Water Quality
Number	80	33	17
Mean	19.3 mm (0.76 in)	34.6 mm (1.36 in)	39.0 mm (1.53 in)
Median	12.6 mm (0.50 in)	29.3 mm (1.16 in)	40.6 mm (1.60 in)
Range	2.5 – 111.3 mm (0.10 – 4.38 in)	8.5 – 111.3 mm (0.34 – 4.38 in)	10.4 – 68.1 mm (0.41 – 2.68 in)

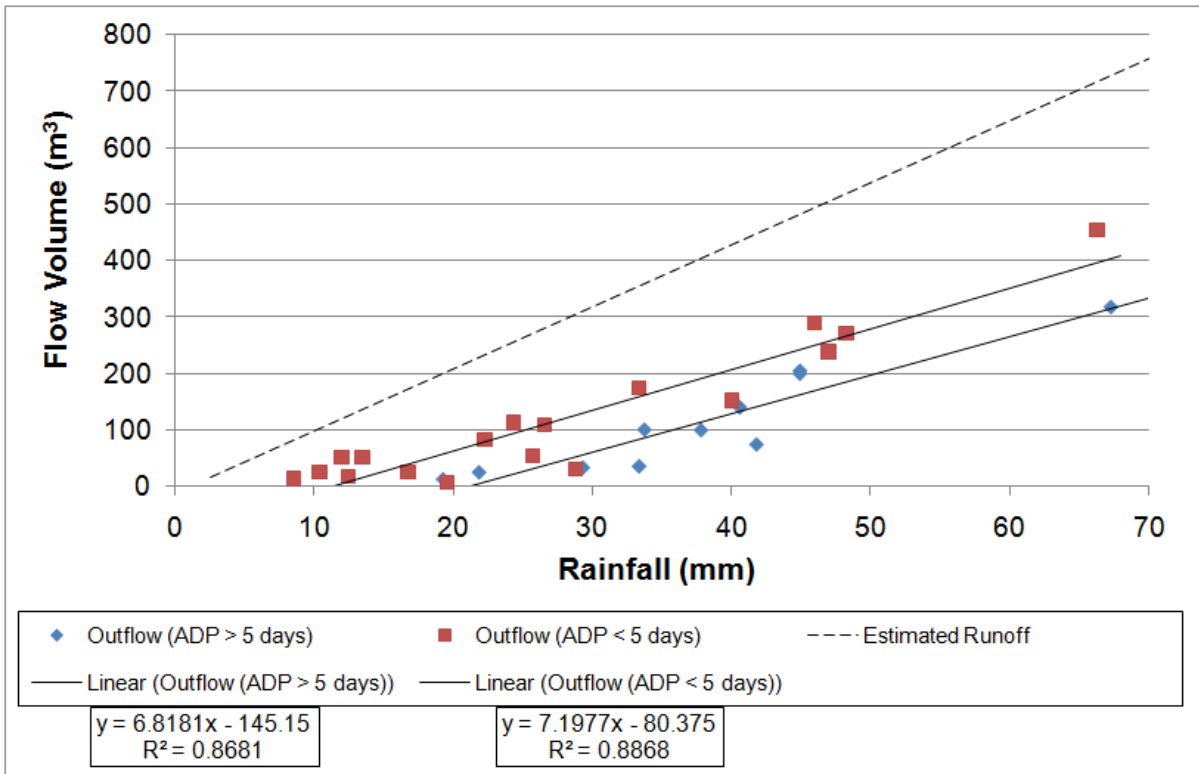


Figure 6.3: Relationship of flow volume versus rainfall depth for runoff and outflow, which was separated by length of time since previous rainfall (less than and greater than 5 days); the equation corresponding to each line is immediately below the line label.

The PC-B system also provided peak flow mitigation. Rational C coefficients were computed from the peak outflow rates and rainfall intensities for all events that had intensities greater than 2.5 cm/hr (1 in/hr) for the duration of the time of concentration. The minimum rainfall intensity of 2.5 cm/hr was chosen because this intensity has been used for the design of some SCMs (level spreader/filter strips) in North Carolina (NCDENR 2010). It was assumed that the time of concentration for the pervious concrete was equal to what it would have been had the lot been entirely asphalt, which was approximately six minutes based on the Kirpich equation (USDA-NRCS 2010). The rational C coefficient was computed from the peak outflow rate and rainfall intensity by using the rational equation (Equation 6.1):

$$C = \frac{Q_{Peak}}{i \times A} \quad (6.1)$$

where, C = calculated rational C coefficient, Q_{Peak} = peak outflow rate from PC-B (cfs), i = rainfall intensity for the time of concentration (in/hr), and A = area (acres) (Malcolm 1989). The mean and median rational C coefficients for the 42 events with rainfall intensities greater than 2.5 cm/hr were 0.012 and 0.001, respectively. The highest rational C coefficient was 0.14, but this was slightly inflated due to occurrence of overflow from the bioretention cell. As a comparison, a paved surface and wooded area have rational C coefficients of 0.90-0.95 and 0.05-0.15, respectively (Malcolm 1989). In general, the rational C coefficients were highest for the events with overflow because these events were larger and generally had lower rainfall intensities. These factors resulted in smaller differences between the runoff and outflow peaks as compared to events with higher rainfall intensities, which were generally from smaller events that did not produce overflow.

The maximum flow rate from the bioretention cell (in the absence of overflow) was approximately 5 L/s/ha (0.07 ft³/s/ac), and the maximum monitored outflow rate from PC-B (including overflow) was 12.5 L/s/ha (0.18 ft³/s/ac). On an annual basis, the outflow rate only exceeded 5 L/s/ha for 23 hours. The flow duration curve for runoff presented in Fig. 6.4 is from the 0.13 ha representative section of asphalt, which represents runoff from an entirely impervious asphalt surface. Even though the PC-B drainage area was eight times larger than the representative section of asphalt, the representative section of asphalt was assumed to represent runoff from the PC-B drainage area under the condition where no SCMs were installed. In assuming both areas were 100 percent impervious, the time of concentrations for both were small and comparable (approximately two and six minutes); therefore, the difference in drainage areas should not have a major impact on the portrayal of runoff flow rates in Fig. 6.4. On an annual basis, the flow rate from parking lot runoff exceeded the highest outflow rate from PC-B (12.5 L/s/ha) and the rate in which overflow from the bioretention cell was occurring (5 L/s/ha) for 64 hours and 116 hours, respectively.

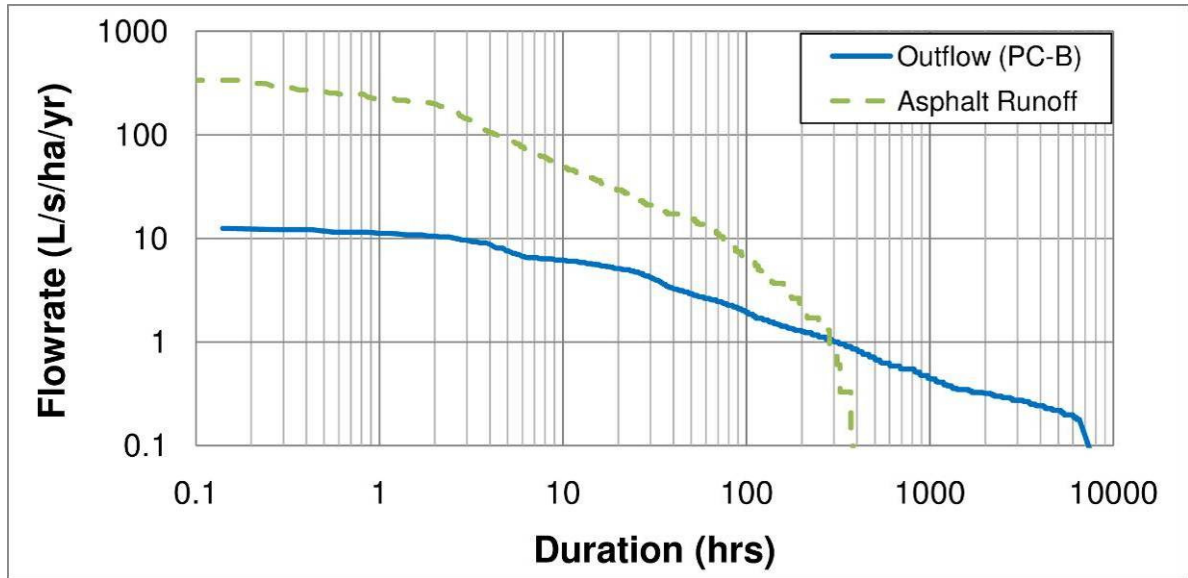


Figure 6.4: Annual flow duration curve for outflow from the PC-B system and parking lot runoff from a 100 percent impervious asphalt surface.

The highest 6-minute rainfall intensity monitored at this site was 109 mm/hr (4.29 in/hr), which is slightly less than the 1-year, 6-minute intensity (114 mm/hr (4.49 in/hr)) (NOAA 2010). Using the rational equation for the highest rainfall intensity monitored (109 mm/hr (4.29 in/hr)) over this drainage area and assuming the site was entirely impervious, the peak runoff rate would have been 285 L/s/ha (4.1 ft³/s/ac). This particular event had a rainfall depth of 19.6 mm (0.77 in), yet only had a peak outflow rate of 0.19 L/s/ha (0.003 ft³/s/ac). The peak outflow rate was approximately 0.07% of the peak runoff rate for an entirely impervious surface. This demonstrates that, provided there is enough storage volume to prevent overflow, peak outflow reduction was substantial from the PC-B system.

6.4.2 Water Quality

Outflow was only generated for larger events, so the events sampled for water quality had mean and median rainfall depths approximately two and three times higher than all of the runoff events monitored, respectively (Table 6.2). The average event mean concentrations (EMCs) of runoff appear to be low because only runoff samples from events with outflow

were included. When a wider range of event sizes was included in the calculation of average EMCs of runoff, average EMCs were larger, as presented in Brown and Hunt (2011a). Mean runoff nutrient concentrations for events with paired outflow samples were less than all eight parking lots monitored by Passeport and Hunt (2009) in North Carolina. Mean, median, and ranges of runoff and outflow concentrations are described in Table 6.3, and efficiency ratios (ER) are calculated using Equation 6.2:

$$ER = 1 - \frac{EMC_{Ave,Out}}{EMC_{Ave,In}} \quad (6.2)$$

where, $EMC_{Ave,Out}$ = average EMC of the outflow and $EMC_{Ave,In}$ = average EMC of the runoff. Only ON, $NO_{2,3-N}$, and TP fit a normal distribution, while TAN fit a normal distribution after being log-transformed. Since TKN and TN were symmetric, the nonparametric Wilcoxon signed-rank test was used. TSS had neither normality nor symmetry, so a nonparametric sign test was used. As evidenced in Table 6.3, many pollutant's concentrations actually increased significantly. However, TAN and TSS had significant reductions.

Table 6.3: Water quality concentrations for paired samples of asphalt parking lot runoff and outflow from the PC-B. (All concentrations are in units mg/L)

Pollutant	Asphalt Parking Lot Runoff			PC-B Outflow			Efficiency
	Mean	Median	Range	Mean	Median	Range	Ratio
TAN ^a	0.17	0.16	0.03 - 0.45	0.04	0.03	0.01 - 0.16	0.74*
ON ^a	0.32	0.31	0.02 - 0.60	0.57	0.59	0.16 - 1.06	-0.77*
TKN ^a	0.49	0.47	0.27 - 0.86	0.61	0.62	0.17 - 1.08	-0.25
$NO_{2,3-N}$ ^a	0.18	0.15	0.03 - 0.48	0.78	0.83	0.37 - 1.32	-3.41*
TN ^a	0.67	0.62	0.30 - 1.34	1.39	1.37	0.82 - 2.05	-1.09*
TP ^a	0.05	0.05	0.02 - 0.08	0.09	0.09	0.04 - 0.18	-0.92*
Ortho-P ^b	< RL	< RL	< RL - 0.01	0.03	0.02	0.01 - 0.11	N/A ^c
TSS ^b	28.8	21.0	2 - 75	10.3	10.7	2 - 23	0.64*

^a n = 17

^b n = 16

^c Runoff concentrations were below the reportable limit too frequently to run statistical test for this pollutant.

* indicates significance at the 0.05 level

The results from this site were complicated due to influx of groundwater into the bioretention cell. This caused large increases in concentrations of $\text{NO}_{2,3}\text{-N}$ and TN, and the fate of nitrogen appeared to be similar to that reported for the pervious concrete section in Collins et al. (2010). Significant reduction of TAN through nitrification was expected because both systems were primarily aerobic environments. Prior to analysis, it was expected that $\text{NO}_{2,3}\text{-N}$ would increase somewhat in the PC-B because outflow from the subsurface storage basin was drawn from the top of the basin, instead of from the bottom, where denitrifying conditions could have potentially been present. However, $\text{NO}_{2,3}\text{-N}$ concentration more than tripled, which doubled the TN concentration in the outflow, attributable to the groundwater influx. Other potential causes are (1) the bioretention cell was conventionally drained instead of having an internal water storage zone and (2) the initial lack of vegetation in the bioretention cells (Bratieres et al. 2008; Lucas and Greenway 2008).

Both practices filtered runoff, leading to the significant reduction of TSS. The TP concentration significantly increased, and the Ortho-P concentration increased as well. Statistical tests were not performed on the Ortho-P data because the runoff concentrations were below the reportable limit in 14 out of 16 events. Overall, the outflow TP concentrations were still relatively low. The mean and median TP concentrations were 0.09 mg/L which is approximately one-half of the proposed irreducible concentration for TP (0.15 to 0.20 mg/L) from stormwater best management practices (Schueler and Holland 2000).

Baseflow samples were collected on four occasions throughout the monitoring period, and the water quality characteristics of these samples are highlighted in Table 6.4. The grab sample concentrations showed that baseflow was comprised mainly of $\text{NO}_{2,3}\text{-N}$. The mean $\text{NO}_{2,3}\text{-N}$ concentration was higher in the baseflow than in the outflow from the PC-B system. In examining the ranges, most of the other constituents were commonly below the reportable limits (RL). The baseflow load was calculated by multiplying the grab sample concentration for the specific season by the volume of baseflow during that period.

Table 6.4: Comparison of PC-B outflow and baseflow water quality concentrations.

	TAN	TKN	NO_{2,3}-N	TN	Ortho-P	TP	TSS
Mean ^a	0.04	0.61	0.78	1.39	0.02	0.09	10.3
Mean ^b	0.011	0.07	1.11	1.18	0.007	0.011	0.6
Median ^b	0.013	0.07	0.98	1.02	0.008	0.011	0.8
Range ^b	< RL [1 of 4] - 0.018	All < RL	0.67 - 1.83	0.75 - 1.94	< RL [1 of 4] - 0.006	< RL [1 of 4] - 0.016	All < RL
RL	0.007	0.14	0.006	N/A	0.006	0.01	1

^a PC-B outflow concentrations (n=17 for all except TSS and Ortho-P [n=16])

^b Baseflow concentrations (n=4)

Pollutant loads were divided into load from storm flow and baseflow (Table 6.5) and these were summed to determine total outflow load. In looking solely at storm flow, estimated annual load reductions were high for all pollutants except Ortho-P and NO_{2,3}-N, which increased slightly. The reductions were primarily due to the estimated 71 percent reduction in annual outflow volume. Percent reductions in storm event loads computed using the least squares means statistical analysis are also included in Table 6.5. This analysis also provided an assessment of the statistical significance of the difference based on the pooled variances. As shown, the increases in NO_{2,3}-N and Ortho-P were not statistically significant, while all of the reductions were. When storm flow and baseflow were combined, the total export of NO_{2,3}-N and TN from the PC-B increased by 464 and 63 percent compared to estimated export from an asphalt parking lot.

Table 6.5: Annual pollutant loads for parking lot runoff (computed) and monitored outflow.

	Pollutant Load							Volume (m ³)
	TAN	TKN	NO _{2,3} -N	TN	Ortho-P	TP	TSS	
Asphalt Parking Lot Runoff (kg/ha/yr)	1.99	5.93	1.77	7.70	0.10	0.58	278	15,353
Storm Outflow (kg/ha/yr)	0.15	1.80	1.96	3.76	0.13	0.29	30.3	4,525
Reduction (%) ^a	92	70	-11	51	-25	50	89	71
Reduction (%) ^b	90*	48*	-35	39*	-51	39*	86*	67*
Baseflow (kg/ha/yr)	0.09	0.73	8.03	8.76	0.05	0.12	5.7	11,469
Total Outflow (kg/ha/yr)	0.25	2.54	9.99	12.53	0.17	0.41	35.9	15,994
Reduction (%) ^a	88	57	-464	-63	-70	29	87	-4

^a Arithmetic reduction computed from differences in annual export

^b Reduction in storm event loads computed statistically using the least squares means analysis

* indicates significance at the 0.05 level

6.4.3 Comparison to Single Practices

In comparing how well the LID practices in series performed versus a single LID practice, the results from this study were compared to results presented in Chapter 4. Both studies occurred at the same research location and over a similar time period, so the soils and rainfall patterns were similar. Chapter 4 analyzed the hydrologic performance of the maintained bioretention cells that treated runoff from the front portion of the parking lot at this site (Fig. 6.2). By every metric available, the PC-B installation outperformed the individual bioretention cells (Table 6.6). As another example of the impact that LID practices in series have on outflow reduction, Rushton (2001) showed the average amount of runoff from porous pavement draining to a swale was reduced by 32 percent, as compared to runoff from concrete and asphalt draining to a swale.

Table 6.6: Comparison of performance for PC-B to a single LID practice – bioretention with 0.6-m and 0.9-m media depth (Chapter 4).

Metric	PC-B	Bioretention: 0.6-m Media Depth	Bioretention: 0.9-m Media Depth
Annual Volume Reduction (seepage/exfiltration and ET)	71%	35%	45%
Annual Untreated Runoff (overflow/bypass)	1%	12%	11%
Maximum Outflow Rate (L/s/ha/yr)	12.5	115	115
Duration Exceeding 12.5 L/s/ha/yr (hr)	0	12	10
Duration Exceeding 5 L/s/ha/yr (hr) ^a	23	59	40

^a Approximate maximum flow rate in PC-B in which outflow could be categorized as drainage only (no overflow from the bioretention cell).

6.5 CONCLUSIONS

Two infiltration LID practices in series (pervious concrete and bioretention) proved to be effective at reducing the hydrologic impact (volume and peak flow reduction) of parking lot runoff. In comparing the PC-B system to a single treatment practice (bioretention) that was monitored at the same research site, hydrologic performance was substantially improved. The PC-B system had nearly double the amount of volume reduction (seepage/exfiltration and ET). The amount of untreated surface runoff (overflow) was reduced from 11 and 12 percent to one percent. This reduced the duration of high outflow rates, and the maximum monitored peak outflow rate was about one-tenth that of the individual practices (12.5 versus 115 L/s/ha/yr). The outflow rate exceeded 5 L/s/ha for 23 hours, which was the approximate rate in which the outflow could be characterized as drainage only. The outflow rate at this threshold for the single treatment systems occurred approximately two to three times longer. Mean and median rational C coefficients calculated for the peak outflow and rainfall rates of events with rainfall intensities greater than 2.5 cm/hr (1 in/hr) were 0.012 and 0.001, respectively, which was less than forested areas (0.05-0.15). The hydrologic improvement could have been greater had the bioretention cell not intercepted groundwater. However, to

achieve these benefits, approximately five times more money was spent for stormwater treatment per hectare than the bioretention-only treatment at this site.

Overall, there was a lack of water quality treatment (concentration reduction) due to LID selection and construction. Only TSS and TAN concentrations were significantly reduced. Because care was not taken to avoid locating a bioretention cell in an area with a seasonally high water table, average $\text{NO}_{2,3}\text{-N}$ concentrations quadrupled and average TN concentrations doubled. It is crucial to keep bioretention cells from being installed in areas with high water tables, *even if liners are installed*. Outflow from the bioretention cell occurred almost year-round. Despite the relatively low baseflow rate [0.25 L/s (4 gal/min)], annual outflow loads of $\text{NO}_{2,3}\text{-N}$ from baseflow were higher than those from storm flow. Draining surrounding groundwater through a bioretention cell not only adds pollutants directly to the stream, but it could negatively impact local hydrology (i.e., draining wetlands or lowering groundwater levels below the root zones of riparian buffers). Given the high water table at this site, it may have been more beneficial from a water quality (and even a hydrologic perspective) to have installed a small stormwater wetland. This practice would have had more potential to reduce $\text{NO}_{2,3}\text{-N}$, and it would not have contributed as much baseflow because the water table in the wetland would have been about 0.6 to 0.9 m (2 to 3 ft) higher than that of the bioretention cell.

This study opens the door to new questions on employing SCMs in series. Was the improvement in hydrology worth the extra expense? Had pervious concrete been used independently would similar results be realized? What if only one practice was used, but it was oversized? In future studies, it is imperative that SCMs are constructed and installed properly and follow the most up-to-date design recommendations from research.

6.6 ACKNOWLEDGEMENTS

This project was funded by an EPA Section 319 Grant (EW07076) administered by the NCDENR- Division of Water Quality. The authors also acknowledge the efforts of Shawn Kennedy for monitoring station installation and project maintenance, Dr. Jon

Hathaway for his insightful review, and Bill Lord for his presence during construction. Also, thanks to Jenny James and Linda Mackenzie at the Center for Applied Aquatic Ecology Laboratory for sample analyses.

6.7 REFERENCES

- Bean, E. Z., Hunt, W. F., and Bidelspach, D. A. (2007). "Evaluation of four permeable pavement sites in eastern NC for runoff reduction and water quality impacts." *Journal of Irrigation and Drainage Engineering*, 133(6), 583-592.
- Bratieres, K., Fletcher, T. D., Deletic, A., and Zinger, Y. (2008). "Nutrient and sediment removal by stormwater biofilters: A large-scale design optimisation study." *Water Research*, 42(14), 3930-3940.
- Brattebo, B. O. and Booth, D. B. (2003). "Long term stormwater quantity and quality performance of permeable pavement systems." *Water Research*, 37(18), 4369-4376.
- Brown, R. A., and Hunt, W. F. (2011a). "Impacts of media depth on effluent water quality and hydrologic performance of under-sized bioretention cells." *Journal of Irrigation and Drainage Engineering*, 137(3), 132-143.
- Brown, R. A., and Hunt, W. F. (2011b). "Underdrain configuration to enhance bioretention infiltration and pollutant load reduction." *Journal of Environmental Engineering* (under review).
- Claytor, R. A., and Schueler, T. R. (1996). *Design of stormwater filtering systems*, Center for Watershed Protection, Silver Spring, Md.
- Collins, K. A., Hunt, W. F., and Hathaway, J. M. (2008). "Hydrologic comparison of four types of permeable pavement and standard asphalt in eastern North Carolina." *Journal of Hydrologic Engineering*, 13(12), 1146-1157.
- Collins, K. A., Hunt, W. F., and Hathaway, J. M. (2010). "Side-by-side comparison of nitrogen species removal at four types of permeable pavements and standard asphalt in eastern North Carolina." *Journal of Hydrologic Engineering*, 15(6), 512-521.
- Davis, A. P., Shokouhian, M., Sharma, H., Minami, C., and Winogradoff, D. (2003). "Water quality improvement through bioretention: Lead, copper, and zinc removal." *Water Environment Research*, 75(1), 73-75
- Davis, A. P. (2005). "Green engineering principles promote low-impact development." *Environmental Science and Technology*, 39(16), 338A-344A.

- Davis, A. P. (2007). "Field performance of bioretention: Water quality." *Environmental Engineering Science*, 24(8), 1048-1064.
- Dietz, M. E. and Clausen, J. C. (2005). "A field evaluation of rain garden flow and pollutant treatment." *Water Air and Soil Pollution*, 167, 123-138.
- Eaton, A. D., Clesceri, L. S., and Greenberg, A. R. (1995). *Standard methods for the examination of water and wastewater*, American Public Health Association, American Water Works Association, and Water Environment Federation, Washington, D.C.
- Fassman, E. A., and Blackbourn, S. (2010). "Urban runoff mitigation by a permeable pavement system over impermeable soils." *Journal of Hydrologic Engineering*, 15(6), 475-485.
- Hardy, D. H., Tucker, M. R., and Stokes, C. E. (2007). "Crop fertilization based on North Carolina soil tests." *Circular No. 1*. North Carolina Department of Agriculture and Consumer Services, Agronomic Division, Raleigh, N.C.
- Hathaway, J. M., and Hunt, W. F. (2010). "Evaluation of storm-water wetlands in series in Piedmont North Carolina." *Journal of Environmental Engineering*, 136(1), 140-146.
- Hatt, B. E., Fletcher, T. D., and Deletic, A. (2009). "Hydrologic and pollutant removal performance of stormwater biofiltration systems at the field scale." *Journal of Hydrology*, 365(3-4), 310-321.
- Hunt, W. F., Jarrett, A. R., Smith, J. T., and Sharkey, L. J. (2006). "Evaluating bioretention hydrology and nutrient removal at three field sites in North Carolina." *Journal of Irrigation and Drainage Engineering*, 132(6), 600-608.
- Kim, H., Seagren, E. A., and Davis, A. P. (2003). "Engineered bioretention for removal of nitrate from stormwater runoff." *Water Environment Research*, 75(4), 355-367.
- Lee, J. H. and Bang, K. W. (2000). "Characterization of urban stormwater runoff." *Water Research*, 34(6), 1773-1780.
- Li, H., Sharkey, L. J., Hunt, W. F., and Davis, A. P. (2009). "Mitigation of impervious surface hydrology using bioretention in North Carolina and Maryland." *Journal of Hydrologic Engineering*, 14(4), 407-415.
- Line, D. E., White, N. M., Osmond, D. L., Jennings, G. D., and Mojonner, C. B. (2002). "Pollutant export from various land uses in the upper Neuse River basin." *Water Environment Research*, 74(1), 100-108.

- Line, D. E. and White, N. M. (2007). "Effects of development on runoff and pollutant export." *Water Environment Research*, 79(2), 185-190.
- Line, D. E. and Hunt, W. F. (2009). "Performance of a bioretention area and a level spreader-grass filter strip at two highway sites in North Carolina." *Journal of Irrigation and Drainage Engineering*, 135(2), 217-224.
- Lucas, W. C. and Greenway, M. (2008). "Nutrient retention in vegetated and non-vegetated bioretention mesocosms." *Journal of Irrigation and Drainage Engineering*, 134(5), 613-623.
- Makepeace, D. K., Smith, D. W., and Stanley, S. J. (1995). "Urban stormwater quality: Summary of contaminant data." *Critical Reviews in Environmental Science and Technology*, 25(2), 93-139.
- Malcolm, H. R. (1989). *Elements of urban stormwater design*. North Carolina State University, Raleigh, N.C.
- National Oceanic and Atmospheric Administration (NOAA). (2010). *Precipitation data frequency server*, National Weather Service, Silver Spring, Md., <http://hdsc.nws.noaa.gov/hdsc/pfds/orb/nc_pfds.html> (Sept. 3, 2010).
- N. C. Department of Environment and Natural Resources (NCDENR). (2010). "Chapter 8: Level spreader – vegetated filter strip system." *Stormwater best management practices manual*, North Carolina Department of Environment and Natural Resources, Division of Water Quality, Raleigh, N.C., 8.1–8.25.
- Passeport, E., Hunt, W. F., Line, D. E., Smith, R. A., and Brown, R. A. (2009). "Field study of the ability of two grassed bioretention cells to reduce storm-water runoff pollution." *Journal of Irrigation and Drainage Engineering*, 135(4), 505-510.
- Passeport, E. and Hunt, W. F. (2009). "Asphalt parking lot runoff nutrient characterization for eight sites in North Carolina." *Journal of Hydrologic Engineering*, 14(4), 352-361.
- Rushton, B. (2001). "Low-impact parking lot design reduces runoff and pollutant loads." *Journal of Water Resources Planning Management*, 127(3), 172-179.
- SAS. (1985). "SAS/STAT guide for personal computers, version 6." SAS Institute Inc., Cary, N.C.
- Schueler, T. R. and Holland, H. K. (2000). "Article 65: Irreducible pollutant concentrations discharged from stormwater practices." *The practice of watershed protection*, The Center for Watershed Protection, Ellicott City, Md., 377–380.

- Strecker, E. W., Quigley, M. M., Urbonas, B. R., Jones, J. E., and Clary, J. K. (2001). "Determining urban storm water BMP effectiveness." *Journal of Water Resource Planning Management*, 127(3), 144-149.
- Tota-Maharaj, K., and Scholz, M. (2010). "Efficiency of permeable pavement systems for the removal of urban runoff pollutants under varying environmental conditions." *Environmental Progress and Sustainable Energy*, 29(3), 358-369.
- U.S. Department of Agriculture – Natural Resources Conservation Service (USDA-NRCS). (2004a). "Chapter 10: Estimation of direct runoff from storm rainfall." *Part 630 – Hydrology: National engineering handbook*, Washington D.C.
- U.S. Department of Agriculture – Natural Resources Conservation Service (USDA-NRCS). (2004b). "Chapter 9: Hydrologic soil-cover complexes." *Part 630 –Hydrology: National engineering handbook*, Washington D.C.
- U.S. Department of Agriculture – Natural Resources Conservation Service (USDA-NRCS). (2010). "Chapter 15: Time of concentration." *Part 630 –Hydrology: National engineering handbook*, Washington D.C.
- U.S. Environmental Protection Agency (USEPA). (1983). "Methods for chemical analysis of water and wastes." *Rep. No. EPA-600/4-79-020*, USEPA, Cincinnati, Oh.
- U.S. Environmental Protection Agency (USEPA). (2002). "Considerations in the design of treatment Best Management Practices (BMPs) to improve water quality." *Rep. No. EPA 600/R-03/103*, USEPA, Office of Research and Development, Cincinnati, Oh.

7. MODELING BIORETENTION HYDROLOGY WITH DRAINMOD

7.1 ABSTRACT

Previous field studies have shown that the hydrologic performance of bioretention cells varies greatly because of the impact of underlying soil, physiographic region, drainage configuration, surface storage volume, drainage area to bioretention surface area ratio, and media depth. To more accurately describe the hydrologic response to predict pollutant loads and to determine whether a site meets low impact development (LID) hydrology criteria, a long-term hydrologic model that generates a water balance is needed. Models that are currently available either: (1) are unable to run continuous simulations, (2) do not accurately model underdrain flow for typical designs of bioretention cells, or (3) do not properly account for the volumetric water content in the profile. DRAINMOD, a widely-accepted drainage model, was used to simulate the hydrologic response of runoff entering a bioretention cell. The concepts of water movement in bioretention cells are very similar to agricultural fields with drainage pipes, so many bioretention design specifications corresponded directly to DRAINMOD inputs. Detailed hydrologic data were collected from two bioretention field sites for 24 months to calibrate and test the model. Each field site had two sets of bioretention cells with varying media depths, media types, drainage configurations, underlying soils, and surface storage volumes. Runoff into the cell was modeled for three combinations of impervious percentage and consistency of the impervious area (depressions versus smoothly graded asphalt); Nash-Sutcliffe coefficients exceeded 0.99 for all cases during both the calibration and validation periods. At Nashville, during the post-repair period, the Nash-Sutcliffe coefficients for drainage and exfiltration/evapotranspiration (ET) both exceeded 0.8 during the calibration and validation periods. During the pre-repair period, the Nash-Sutcliffe coefficients for drainage, overflow, and exfiltration/ET were all in the range of 0.6-0.9 during both the calibration and validation periods. DRAINMOD is also unique compared to other bioretention models in that it accounts for evapotranspiration (ET),

and it can simulate performance from a cell with an internal water storage (IWS) zone. The bioretention cells at Rocky Mount included an IWS zone. For both the calibration and validation periods, the predicted (modeled) volume of exfiltration/ET was within one and five percent of the estimated volume for the cells with sand (Sand cell) and sandy clay loam (SCL cell) underlying soils, respectively. Nash-Sutcliffe coefficients for the SCL cell during both the calibration and validation periods were 0.92. One of the controlling factors in DRAINMOD is the drainage configuration. The model is capable of simulating hydrologic response based on hourly rainfall data for long periods of meteorological records. Hydrologic outputs from the model include: volume of runoff, overflow, drainage, exfiltration (seepage), and ET. Sixty-year simulations (1950-2009) were run using hourly rainfall records to determine the impacts that media type, drainage configuration, surface storage depth, surface storage volume, and drainage area to bioretention area ratio had on the annual hydrologic response to runoff for a bioretention cell designed to capture the 25-mm design event. Long-term simulations were also run to evaluate the performance from cells with one-half or double the surface storage volume. Finally, long-term simulations were run to determine the relationship between the surface storage capacity needed to treat 90 percent of annual runoff and the design event. Results from a cell that followed current NC design standards, with a design event of 25 mm, an average surface storage depth of 0.23 m, and a media saturated hydraulic conductivity of 25 mm/hr, will treat 95 percent of annual runoff. In order to treat 90 percent of annual runoff, the required surface storage capacity for this cell was only 70 percent of the design event. Similar results were obtained for Wilmington, NC, where the design event was 38 mm. Again, the required surface storage capacity was only 70 percent of the design event.

7.2 INTRODUCTION

Increased land development and the stormwater runoff it contributes have been identified as reasons for impairment of surface waters in the U.S. (USEPA 2007). As the focus of new stormwater rules shifts to prioritize water quality and annual hydrologic balance, in addition to peak flow reduction and flood control, incorporating infiltration-based

stormwater control measures (SCMs) is becoming necessary. These low impact development (LID) practices help to restore a site's natural hydrology and reduce the negative effects caused from increased impervious areas in urbanized watersheds. Bioretention cells are one of the most commonly used LID practices.

Intensive research and installation experience have assisted in the evolution of bioretention design recommendations. For unlined bioretention cells, one common theme has been a large variation in hydrologic performance based on a number of design characteristics and the site's location. This is mostly attributable to design configurations, underlying soils, physiographic region, and climate conditions. Deeper media depth increased exfiltration and reduced outflow volume and frequency (Li et al. 2009; Brown and Hunt 2011a). Also, as the ratio of bioretention surface area to drainage area increased, outflow volume was reduced (Hatt et al. 2009; Jones and Hunt 2009). These studies imply that as volume of bioretention media is increased, outflow is reduced. Site location impacts rainfall patterns and underlying soils. Some regions have in-situ soils with a higher sand content than others. Bioretention cells constructed at sites with sandier underlying soils have greater exfiltration than those with tighter underlying soils (Brown and Hunt 2011a, 2011b; Passeport et al. 2009). Brown and Hunt (2011b) and Li et al. (2009) also determined that an internal water storage (IWS) zone design feature can further reduce runoff volumes; results were magnified in locations with sandy underlying soils. Additionally, Hunt et al. (2008) identified a steep hydraulic gradient from the bottom of the bioretention cell as being responsible for enhancing hydrologic performance. Despite these generalized conclusions about hydrologic performance, it is difficult to apply concrete numbers for volume and pollutant load reduction to bioretention designs because of the variety of site and design variables.

The long term effectiveness of bioretention cells can be evaluated by using a field tested, reliable model to continuously simulate its hydrologic performance for a variety of design configurations. One model that can be used for this purpose is DRAINMOD, a long-term, continuous simulation drainage model that was first developed in the 1970s at North

Carolina State University. DRAINMOD has been used to model agricultural drainage systems, controlled drainage, subirrigation, wetland hydrology, nitrogen dynamics and losses from drained soils, impacts of drainage system and irrigation management on soil salinity in irrigated arid soils, on-site wastewater treatment, forest hydrology, and other applications (Skaggs 1978, 1982, 1999; Youssef et al. 2005). The model continues to be improved and extended, and bioretention hydrology is one of the new applications.

Increasing the confidence of predicting hydrologic performance of bioretention cells could lead to the development of a “sliding scale” performance credit system. This would allow designers to alter their plans to better fit site constraints, and this will invariably allow for better, more appropriate designs. The current North Carolina state standard, like most regulatory authorities, uses a “one size fits all” approach for designing and awarding credit for bioretention cells (NCDENR 2009). Two drivers for developing a “flexible” bioretention design methodology are: (1) a site’s physical constraints could force undersized or oversized designs, such as in retrofits, and (2) monitored bioretention cells have been shown to have large variations in hydrologic performance.

A benefit of a long-term continuous model is that it uses multiple years of historic rainfall and temperature data to calculate an annual water balance. A water balance allows quantification of groundwater recharge (exfiltration). It can also be used to determine the degree to which bioretention cells are able to restore the pre-developed hydrologic condition of the landscape. Finally, by determining the fraction of runoff that (1) receives full treatment (drainage), (2) receives minimal treatment (overflow), and (3) does not reach the stormwater network (exfiltration and ET), pollutant loads released by bioretention cells can be estimated.

Currently, no widely accepted long-term model exists for bioretention. Bioretention models that are currently available either: (1) are unable to run continuous simulations, (2) do not accurately model underdrain flow for typical designs of bioretention cells, or (3) do not properly account for the volumetric water content in the profile.

Initial modeling studies did not include underdrains (Brander et al. 2004; Dussaillant et al. 2004, 2005; Heasom et al. 2006). Brander et al. (2004) and Heasom et al. (2006) used single-event models to predict overflow from bioinfiltration cells (no underdrain). Single-event models are useful to assist in bioretention design by routing a design event; however, they do not account for antecedent soil moisture conditions which can have a large effect on performance. Continuous simulation models are beneficial because they account for antecedent conditions and can factor in periods of wet weather or droughts. Periods of wet weather are especially important because the system is more likely to be overwhelmed hydraulically. Continuous simulation models predict both day-by-day and the annual performance of the system.

Dussaillant et al. (2004) developed a long-term, continuous simulation, numerical model that was based on the mixed formulation of the one-dimensional Richards equation (RECHARGE). Later, Dussaillant et al. (2005) developed a simplified numerical model, RECARGA, based on the Green-Ampt infiltration equation. When compared to the more complex RECHARGE, RECARGA had good results (Dussaillant et al. 2005). However, at the time, an option to include underdrains was not available for either model. RECARGA has since been modified, and the most updated version available online, Version 2.3, has an option to include an underdrain. However, RECARGA's method of including an underdrain is not commensurate with typical field installations, and underdrain flow is calculated using the orifice equation after the user enters the diameter for only one drain.

He and Davis (2011) recently developed a two-dimensional variable saturated flow model, based on the Richards equation to explore general impacts of using different media types, surrounding soils, initial water content in the media, drainage to bioretention area ratios, and cell widths. However, the model simulations were based on a variety of single events, so it did not compute a water balance for a continuous period of record, and therefore, was not capable of evaluating the effect of wet periods or sequence of weather events on performance. In some of the simulations presented, the He and Davis (2011) model included two drains.

Palhegyi (2010) developed a computation bioretention hydrology model to assist with sizing bioretention cells to meet flow duration criteria. The model used a soil moisture computational procedure based on the algorithms used in Hydrologic Engineering Center Hydrologic Modeling System (HEC-HMS) (USACE 2000). This algorithm follows the principle that water will move through the profile via ET, percolation (exfiltration), and drainage (if underdrains are installed) until the water content equals the field capacity. Then water will only leave via ET until the water content equals the wilting point. Underdrain flow is modeled using an algorithm solving Bernoulli's equation for a user-specified pipe length and diameter. The model showed good results when field verified to a biofiltration cell in Villanova, PA; however, this cell did not include an underdrain, so its applicability to bioretention cells with underdrains was not evaluated.

In Lucas (2010), a bioretention planter system was modeled for a design storm using HydroCAD and then for a continuous weather data set using SWMM 5.0.014 to determine impacts on combined sewer overflows. Both models gave comparable results when modeling a single synthetic rainfall event; however, neither model was field tested. These models used an orifice to control inflow rates into the media and once the media was saturated it used Darcy's Law. "Dummy" nodes, areas, and cylinders were added in the models to route water through the system (Lucas 2010).

Some other models with continuous simulation capabilities, currently available to designers to model bioretention hydrology include: Storm Water Management Model (SWMM) 5.0, windows-based Source Loading and Management Model (WinSLAMM) 9.4, and Model for Urban Stormwater Improvement Conceptualism (MUSIC) 3.1. However, the processes used by these models and some of the ones presented earlier to model water movement through the media and into the drains are not as comprehensive as those in DRAINMOD.

DRAINMOD calculates drainage rates as a function of soil properties and drainage configuration, and it incorporates the impact of having the water level close to the surface. The other previously described bioretention models either calculate available water storage

by subtracting field capacity from total porosity or by using a constant, user-input, void ratio of the media. However, the water stored in the media profile varies with water table depth. Using field capacity to calculate the amount of water stored in the profile is not appropriate when the water table is close to the surface. As an example, the volume of water drained based on the water table depth in the media was calculated per the soil-water characteristic curve and by subtracting the field capacity (volumetric water content at a suction of -1.0 m) from the saturated volumetric water content (Table 7.1). Results are given for two types of media, both of which were subsequently used in the calibration of DRAINMOD. One was predominantly sand (Rocky Mount site), while the other had a mixture that was more typical of current N.C. design recommendations (Nashville site). Table 7.1 shows that the largest errors occur when the water table is closest to the surface and for the Nashville media, which has a more gradual soil-water characteristic curve. The Nashville media has a higher fraction of fine particles, so it holds more water in the media at larger suctions. DRAINMOD requires inputs for the soil-water characteristic and related functions that allow the model to account for the variation in water present in the media based on the water table depth, a more accurate representation of the water present in the media. This concept is especially important for modeling bioretention cells with an IWS zone because the water level could likely remain within the profile for the entire inter-event period. A representative calculation of this concept is presented in Table 7.1. For a cell with a water table 0.6 m below the soil surface, the error associated with neglecting the soil water characteristic curve is 88 percent (Nashville). This is an inherent error in models that use the field capacity concept for shallow water table systems. An illustration of this example is presented in Fig. 7.1. Additionally, none of the available models include an option to create an elevated underdrain outlet to model the performance for a bioretention cell with an IWS zone drainage configuration.

Table 7.1: Comparison of calculating volume of water drained from media based on water table depth by using soil-water characteristic curve or by subtracting field capacity from saturated volumetric water content.

Water Table Depth	Volume Drained (cm ³ /cm ²)		Saturation Minus Field Capacity		Percent Error	
	Rocky Mount Media	Nashville Media	Rocky Mount Media	Nashville Media	Rocky Mount Media	Nashville Media
m	cm	cm	cm	cm		
0.1	0.008	0.0003	0.031	0.017	-273%	-6017%
0.3	0.056	0.013	0.092	0.052	-65%	-289%
0.6	0.147	0.055	0.184	0.103	-25%	-88%
1.0	0.269	0.120	0.306	0.172	-14%	-43%

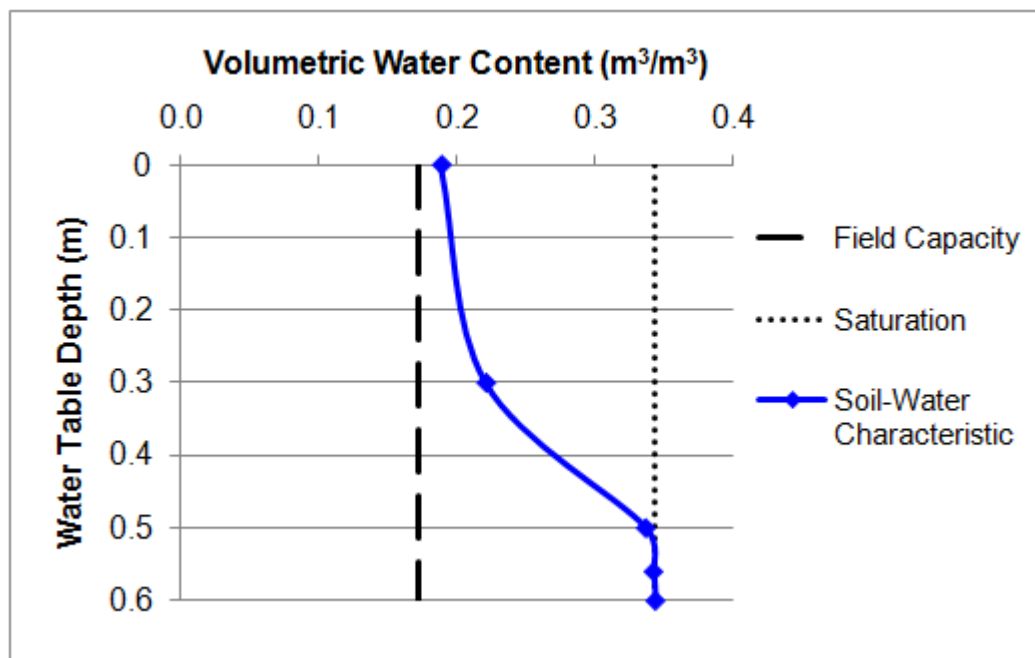


Figure 7.1: Description of volumetric water content present in profile for Nashville media when the water table depth is 0.6 m, where the soil-water characteristic (solid line) and field capacity (long dashes) are presented.

With the large variation in hydrologic performance from bioretention cells, a continuous, long-term model, such as DRAINMOD, could make bioretention designs more

reliable. DRAINMOD could be another tool to help answer design questions that still persist regarding minimum fill media depth, fill media composition, maximum ponding depth, and underdrain configuration (Davis et al. 2009). If successful, DRAINMOD could be used as a predictive tool for new design configurations that have not been installed or monitored. It could also be used to determine the hydrologic impact of a wide variety of design configurations that differ from those currently stated in design manuals. All these applications will help advance the practice of bioretention design towards a “sliding scale” performance metric of evaluating hydrologic performance. The objective of this project is to field test DRAINMOD to determine its reliability for describing the hydrologic response and performance of bioretention cells.

7.3 MODEL DESCRIPTION AND APPLICATION

7.3.1 DRAINMOD Description

As presented by Skaggs (1978, 1982, 1999), the governing equations for DRAINMOD are based on two water balances: (1) in the soil profile (Equation 7.1) and (2) at the soil surface (Equation 7.2). In the soil profile, the water balance is computed for a section of soil of unit surface area, located at the midpoint between adjacent drains, and extending from the impermeable layer to the soil surface:

$$\Delta V_a = D + ET + DS - F \quad (7.1)$$

where ΔV_a = change in the air volume, D = lateral drainage from the section, ET = evapotranspiration, DS = deep seepage, and F = infiltration entering the section in Δt (time increment). DRAINMOD uses the Green and Ampt equation to calculate the rate of infiltration. The water balance at the surface is computed per unit surface area by:

$$P = F + \Delta S + RO \quad (7.2)$$

where P = precipitation, F = infiltration, ΔS = change in volume of water stored on the surface, and RO = runoff during time period Δt .

DRAINMOD computes each water balance for a time increment Δt , with all units expressed in terms of depth (cm). The time increment is normally 1 hour; however, when the rainfall rate exceeds the infiltration capacity, Δt decreases to 0.05 hours or less. When there is no rainfall and the drainage rate is rapid, Δt is increased to 2 hours, and when the drainage and ET rates are slow, Δt is further increased to daily.

To solve for the losses via drainage, DRAINMOD uses Hooghoudt's equation (Equation 7.3) to compute drainage flux when the water table is below the surface. The flux is evaluated in terms of the water table at the midway point between the drains and the hydraulic head in the drains.

$$q = \frac{8Kd_e m + 4Km^2}{L^2} \quad (7.3)$$

where, K = effective lateral hydraulic conductivity, L = drain spacing, m = water table height above the drains at the midpoint, and d_e = equivalent drain depth. To correct for convergence near the drain, an equivalent depth is calculated using equations developed in Moody (1967). For typical bioretention installations, the drain depth to drain spacing ratio will likely be less than 0.3, so Equation 7.4 is used to calculate the equivalent depth.

$$d_e = \frac{d}{1 + \frac{d}{L} \left[\frac{8}{\pi} \ln\left(\frac{d}{r}\right) - \left(3.55 - \frac{1.6d}{L} + 2\left(\frac{2}{L}\right)^2 \right) \right]} \quad (7.4)$$

In this equation, r = drain radius and d = drain depth. If the depth to spacing ratio exceeds 0.3, a different equation is used. When the surface is ponded and the profile is saturated, drainage rate is calculated with the Kirkham equation (Equation 7.5) (Kirkham 1957).

$$q = \frac{4\pi K(t + d - r)}{GL} \quad (7.5)$$

In this equation, t = ponding depth and G is a term dependent on drain depth and spacing and depth of the profile. It is called Kirkham's coefficient G in DRAINMOD and is defined in Equation 7.6.

$$G = 2 \ln \left[\frac{\tan(\pi(2d-r)/4h)}{\tan(\pi r/4h)} \right] + 2 \sum_{m=1}^{\infty} \ln \left[\frac{\cosh(\pi mL/2h) + \cos(\pi r/2h)}{\cosh(\pi mL/2h) - \cos(\pi r/2h)} \cdot \frac{\cosh(\pi mL/2h) - \cos(\pi(2d-r)/2h)}{\cosh(\pi mL/2h) + \cos(\pi(2d-r)/2h)} \right] \quad (7.6)$$

In this equation, h = depth of profile. If the drainage rate is limited by pipe size, valves or other structural features, a user-specified drainage coefficient is used by DRAINMOD to limit the maximum drainage flux from the system.

There are multiple ways to calculate potential evapotranspiration (PET), with some methods requiring more meteorological data than others. Under the most basic application, DRAINMOD uses the Thornthwaite method (with monthly correction factors) to calculate daily PET (Thornthwaite 1948). PET is distributed daily for the 12 hours between 6:00 a.m. and 6:00 p.m., and PET is set equal to zero when rainfall occurs. ET is calculated based on the soil water conditions. If the conditions are not limiting, ET is set equal to PET. However, as the soil water conditions become limiting (dry zone depth exceeds root depth), ET is set equal to the upward flux from the water table. More detailed information about DRAINMOD's governing equations, model components, how various model utilities function, and ways to measure model input parameters are provided in Skaggs (1999) and in the DRAINMOD Reference Report (Skaggs 1980).

A general description of the modeling procedure for bioretention cells using DRAINMOD is that the model is run to simulate runoff from the contributing area. Since the contributing area is typically highly impervious and will generate a large portion of runoff, the model input parameters have wide drain spacing, shallow surface storage, and low infiltration rate. The contributing area runoff file is created from this initial simulation, and it is included in the simulation for the bioretention design. The model input parameters for the bioretention design are entered based on the various design configurations and site conditions. Appendix A provides a step-by-step description of using DRAINMOD for this application. One drawback of the model is that inputs are held constant for the entire period

of the simulation. Emerson and Traver (2008) and Braga et al. (2007) have shown that seasonal variation of infiltration SCMs occurred because the temperature variation throughout the year affected the infiltration rates.

7.3.2 Comparison of Bioretention Design Specifications to DRAINMOD Inputs

The concepts of water movement in bioretention cells when installed with underdrains are very similar to agricultural fields drained by tiles. Because of the similarities, many DRAINMOD inputs corresponded directly to bioretention cell design specifications. A comparison of these inputs is presented in Table 7.2. DRAINMOD is unique for bioretention models because an option exists to create an elevated underdrain outlet through the model input for controlled drainage, and it can simulate multiple drains of various spacing distances and diameters. Other models to date have been unable to simulate these types of drainage configurations. In Table 7.3, examples of DRAINMOD outputs are related to bioretention cell applications.

Table 7.2: DRAINMOD inputs are compared to typical bioretention design parameters.

Bioretention Design Parameters	DRAINMOD Inputs
Drain depth	Depth from soil surface to drain (B)
Drain size	Effective radius of drains (Re)
Drain spacing	Spacing between drains (L)
Average surface storage depth	Maximum surface storage (Sm)
Depth from surface to bottom of gravel	Distance from surface to impermeable layer (H)
Drainage coefficient	Drainage rate as limited by hydraulic capacity of the drainage system in bioretention cell
Media / gravel characteristics and depths	Inputs for soil-water characteristic curve and saturated hydraulic conductivity for each layer
Internal water storage zone design	Weir setting for controlled drainage
Drainage area : bioretention area ratio	Field ratio of contributing land area
Vegetation root depth	Vegetation root depth
Exfiltration rate of subsoil	Vertical or deep seepage parameters
Weather conditions	Rainfall and temperature files
Evapotranspiration	Either enter a file of calculated PET or use Thornthwaite method (with or without adjusted parameters)

Table 7.3: Relating DRAINMOD outputs applicable to bioretention cells.

DRAINMOD Outputs	Potential Meaning for Bioretention
ET	Evapotranspiration (volume eliminated)
Drainage	Underdrain flow volume (treated portion)
Runoff	Overflow volume (untreated portion)
Seepage	Exfiltration (volume eliminated)
Wet stress	Vegetation stress indicator
Dry stress	Vegetation stress indicator
Rank files for each of the above outputs	Quantify impact of severe events or large consecutive events (i.e. 1 in 10 years)

7.4 DETERMINATION OF INPUT PARAMETERS

7.4.1 Site Description

DRAINMOD was calibrated and validated for bioretention cells located in Nashville and Rocky Mount, NC. These sites are described in detail in Chapters 2 – 5. At each site, there were two different bioretention cells that were monitored for approximately 24 months. One of the main differences between the two sites was drainage configuration. The Nashville site was conventionally drained and the Rocky Mount site had an elevated underdrain outlet, which created an IWS zone. Bioretention cell characteristics varied between the two cells at each site. At Nashville, the cells had varying media depths (0.6 m versus 0.9 m), while at Rocky Mount, the underlying soil varied (sandy clay loam versus sand). Among them, the bioretention cells had a variety of different underlying soils, media depths, drainage configurations, surface storage volumes, design events, and drainage area to bioretention surface area ratios.

After the first year, one of the design specifications was altered at each site to measure the impact of the change. From year 1 to year 2, the surface storage zone was increased and a clogging layer was removed at the Nashville site (year 1 – pre-repair period, year 2 – post-repair period). At the Rocky Mount site, the IWS zone was decreased by 0.3 m (year 1 – deep IWS period, year 2 – shallow IWS period). Since more detailed water table

and soil water content measurements were collected during the second monitoring period, this period was used for calibration. The only adjustment to the model necessary to simulate the first year of the study at Rocky Mount was to increase the IWS zone depth. At Nashville, the surface storage depth was decreased and a clogging layer was added to the surface of the profile. All other cell properties remained constant between the two years.

7.4.2 Monitoring Methods

The hydrologic monitoring methods are described for each site in detail in Chapters 2 – 5. In general, runoff, drainage, and overflow volumes were measured or estimated for each site. Because each site was highly impervious, runoff was estimated using an initial abstraction method that assumed that shallow depressions were filled first and then the rest of the rainfall was transmitted as runoff. For asphalt on a shallow slope, Pandit and Heck (2009) found that nearly all of the rainfall on an asphalt surface would be transmitted as runoff. At the Nashville site, overflow and drainage were measured together using a sharp-crested 90° v-notch weir. Based on the outflow hydrograph, overflow could be separated from drainage to allow for each to be summed separately. At Rocky Mount, drainage was measured with a sharp-crested 30° v-notch weir, and overflow was estimated based on rainfall intensity, bioretention cell surface storage characteristics, drainage area characteristics, and measured surface infiltration rates that varied by month. An Excel spreadsheet was created to estimate overflow volume on an hourly basis. Based on a water balance, all of the runoff that did not exit via overflow or drainage was assumed to be lost via exfiltration or ET. At each site, estimations of ET suggested that water was primarily released through exfiltration, attributable to the relatively sandy underlying soils.

Water level loggers, manufactured by Infinities USA, were installed during the second year of the monitoring period to measure the water levels in the surface storage zone of all cells and in the IWS zone at the cells in Rocky Mount. The IWS zone drawdown rates were 7-11 mm/hr (0.28-0.43 in/hr) and 200-300 mm/hr (8-12 in/hr) for the Sandy Clay Loam (SCL) and Sand cells, respectively. To calculate the exfiltration rate, the IWS drawdown rate was multiplied by the effective drainable porosity, which was estimated to be 0.30. This

equated to an exfiltration rate of 2.1-3.3 mm/hr (0.08-0.13 in/hr) in the SCL cell and 60-90 mm/hr (2.4-3.6 in/hr) in the Sand cell. Initial soil-water content prior to rainfall has a major influence on infiltration rate (Skaggs and Khaleel 1982). In order to assume that the measured infiltration rate (drawdown rate of surface storage zone) would represent the final constant infiltration rate that occurs under fully saturated conditions, only the tail ends of large events (events greater than 25 mm (1 in)) that occurred throughout the year were used. These infiltration rates were used to determine the Green and Ampt infiltration parameters used in DRAINMOD. The average, measured final constant infiltration rate from each set of cells was assumed to be equivalent to the saturated hydraulic conductivity of the entire profile, which is used in determining both of the Green and Ampt infiltration parameters.

At the Nashville site, there was no internal water storage zone and the soil had a high saturated hydraulic conductivity, so drainage rarely occurred for more than 12 hours after runoff ceased. This made it difficult to take water table readings within the media to compare to the daily output of water table depth in DRAINMOD, so HOBO soil moisture sensors were installed to measure soil water content in the media. Four Soil Moisture smart sensors (model: S-SMC-M005) were used in a HOBO Micro Station (manufacturer: Onset Computer Corporation) to measure volumetric soil water content in one 0.6-m and one 0.9-m media depth cell. In the 0.9-m media depth cell, sensors were installed at the following depths: 0.05, 0.3, 0.6, and 0.9 m, and in the 0.6-m media depth cell, sensors were installed at the following depths: 0.05, 0.2, 0.4, and 0.56 m. This type of soil moisture sensor uses time-domain reflectometry (TDR) to measure volumetric soil-water content by measuring the velocity of a voltage pulse passing between the two parallel rods. Volumetric water content was measured at each depth for two separate occasions to confirm the readings of the soil moisture sensors, which had an average absolute error of 5.9 percent and a range of error of 11.5 to 11.3 percent. The volumetric water content measurements were used to assist in selecting the vertical seepage parameters. This was done by comparing predicted water table depths, when the level was beneath the bottom of the bioretention cell, to the measured

volumetric water content of the media and its resulting negative pressure head as determined by the soil-water characteristic.

At each site, the drainage area, bioretention cell area and average surface storage zone depth, media depth, drain depth, and depth to drain outlet (for IWS designs) were surveyed. The bioretention design specifications were entered in the model per surveyed data and measurements (described later) taken of the media's soil-water characteristic curves, saturated hydraulic conductivities, and infiltration and exfiltration rates. Once these properties were determined, they were entered into DRAINMOD to simulate the hydrologic response of the systems.

7.4.3 Drainage Coefficient

The drainage coefficient is the maximum hydraulic capacity of the drainage network in cm/day. If the drainage coefficient exceeds the flux calculated by the Kirkham equation when the surface is fully ponded and the media is fully saturated, the maximum drainage rate would be the rate calculated by the Kirkham equation. If the drainage coefficient is less than the rate calculated by the Kirkham equation, the capacity of the drainage network limits the drainage rate, so the maximum drainage rate predicted by the model is set equal to the drainage coefficient. The drainage coefficient was determined by examining the maximum drainage rate from the largest events from each monitoring period. The largest events were selected because it was likely that the entire profile would be saturated and the surface storage zone would be full. Based on the maximum observed drainage rates from each set of cells at the Nashville site, the drainage coefficients for the 0.6-m and 0.9-m media depth cells were set at 85 and 60 cm/day, respectively. The maximum drainage rate at the Rocky Mount site occurred during the shallow IWS period because of the larger difference in hydraulic head between the surface storage zone and IWS outlet. Based on the maximum observed drainage rate at Rocky Mount, the drainage coefficient was set at 75 cm/day.

7.4.4 Soil

To create a new soil file in DRAINMOD, two parameters are required: (1) a soil-water characteristic curve and (2) saturated hydraulic conductivity. To determine these inputs, six, 77-mm diameter soil cores were collected from each type of bioretention media. The soil-water characteristic curves were measured using a pressure plate apparatus, which measured the water released from a saturated soil core under various pressures. The average volumetric water contents at the various pressures for the two media are presented in Table 7.4. Saturated hydraulic conductivity was measured with a constant head permeability test, as described in Klute (1986).

Table 7.4: Soil-water characteristics for Rocky Mount and Nashville media.

Pressure head (m)	Volumetric Water Content (m ³ /m ³)	
	<i>Rocky Mount Media</i>	<i>Nashville Media</i>
0	0.350	0.344
-0.04	0.291	0.342
-0.1	0.175	0.337
-0.3	0.05	0.221
-0.6	0.045	0.189
-1.0	0.044	0.172
-2.0	0.044	0.151
-3.0	0.044	0.139
-4.0	0.044	0.131
-6.0	N/A	0.117
Notes	Too sandy (96% sand) ^a	Typical N.C. Composition ^a

^a per NCDENR (2009) standards

Additionally, soil samples were collected of the surrounding soil with an auger to determine the soil particle distribution. Soil particle size distribution was measured with a hydrometer and followed the procedure in Gee and Bauder (1986). These measurements confirmed the underlying soil texture with that listed for the soil series described in the Nash County soil survey. In the description of each soil series, information about the saturated

hydraulic conductivity of the most limiting layer and depth to water table was presented. These numbers were a guideline for entering the deep seepage parameters for the Nashville site because the conventional drainage configuration did not allow for a more exact exfiltration rate to be measured on site.

7.4.5 Climate

7.4.5.1 Temperature

Maximum and minimum daily air temperatures are climate inputs for DRAINMOD. These measurements were obtained for both the Rocky Mount and Nashville sites from the State Climate Office of NC monitoring station, “NRKM – Rocky Mount,” in Rocky Mount, NC (SCO 2011). This monitoring station was the closest available weather station to either site. It was within 12 km (7.5 mi) and 2.5 km (1.5 mi) of the Nashville and Rocky Mount sites, respectively.

7.4.5.2 Precipitation

Precipitation depths were measured every 2 minutes using an ISCO 674 tipping bucket rain gage. Since DRAINMOD precipitation can be entered as hourly depths, the measured rainfall depths were summed on an hourly basis throughout the entire monitoring period for each site.

A major benefit of DRAINMOD is its ability to simulate long-term hydrology, so in addition to the weather datasets during the monitoring periods, two sets of long-term weather files were created from weather stations in Raleigh and Wilmington, NC. The Raleigh station is located at the Raleigh-Durham International Airport – station call sign “KRDU.” The Wilmington station is located at the Wilmington International Airport – station call sign “KILM.” These stations are cooperative weather stations and are automated surface observation systems managed by the National Weather Service (ASOS-NWS). Sixty years of hourly precipitation data (1950-2009) were obtained from the National Climatic Data Center (NOAA 2011). Daily maximum and minimum air temperatures for the same stations and period (1950-2009) were obtained from the State Climate Office of North Carolina (SCO

2011). “KRDU” was selected as the site to be used for a long-term weather dataset because it had a more complete and longer dataset. “KILM” was used to serve as a representative weather profile for a coastal region of NC. The design event for bioretention cells was 25 mm (1.0 in) for the Nashville, Rocky Mount, and Raleigh locations. For the 20 coastal counties of NC it is increased to 38 mm (1.5 in) because of the larger annual rainfall depths in this region (NCDENR 2009).

7.4.5.3 Potential Evapotranspiration

PET can be incorporated into the model by entering a file of daily PET depths based on any type of PET method that is possible for the available meteorological data. If PET is not calculated separately, the option in DRAINMOD is to use the Thornthwaite method based on the daily maximum and minimum air temperatures. This is the simplest method to calculate PET because it only requires mean monthly air temperature as its sole input, so it is not as precise as other options. As a result, DRAINMOD has an option to include PET correction factors. The mean monthly air temperature is used to calculate the heat index from the site. The calculation of heat index (I) is described in Equation 7.7, where T_i is the mean monthly temperature in degrees Celsius. For the Nashville and Rocky Mount sites, mean monthly air temperatures from 1971-2000 were reported from station “316044 – Nashville” and “317400 – Rocky Mount 8 ESE,” respectively (SCO 2011). Based on these temperatures, the calculated heat indices for Nashville and Rocky Mount were 71.2 and 73.9, respectively. The calculated heat index and daily temperatures are then used to calculate daily PET.

$$I = \sum_{i=1}^{12} \left(\frac{T_i}{5} \right)^{1.514} \quad (7.7)$$

To improve accuracy of PET, monthly correction factors for the Thornthwaite method were used to correct the daily PET estimate. Amatya et al. (1995) calculated correction factors for three sites in eastern North Carolina (Tarboro, Carteret, and Plymouth). Tarboro is within 35 km of both field sites, so its correction factors were used.

7.5 MODEL RESULTS

With the exception of the deep seepage parameters for the Nashville site, the DRAINMOD input parameters were either measured on site or in the Soil and Water Laboratory at Weaver Laboratory on N.C. State University campus. Inputs were determined and DRAINMOD was used to simulate the hydrology of all bioretention cells. The methods used to quantify the calibration and validation of the model were calculating percent error of runoff and each outflow variable and comparing the measured and predicted depths of runoff and the outflow variables (in terms of cm per bioretention surface area). At Rocky Mount, measured and predicted water table depths were also compared. Finally, Nash-Sutcliffe coefficients and coefficients of determination (r^2) were calculated. Nash-Sutcliffe coefficients were calculated on an event-basis using Equation 7.8.

$$R_{NS}^2 = 1 - \frac{\sum_{i=1}^N (Q_{i,measured} - Q_{i,predicted})^2}{\sum_{i=1}^N (Q_{i,measured} - Q_{average})^2} \quad (7.8)$$

where, $Q_{i,measured}$ = measured volume for event i , $Q_{i,predicted}$ = predicted volume for event i , $Q_{average}$ = average measured volume for N events, N = total number of events for the monitoring period, and R_{NS}^2 = Nash-Sutcliffe coefficient (Nash and Sutcliffe 1970).

Contributing area runoff was the first process calibrated. It was calibrated by adjusting the drain spacing, drain depth, surface storage depth, and Green and Ampt infiltration parameters for the soil file created for asphalt. At each site, data from the second monitoring period and first monitoring period were used to calibrate and validate DRAINMOD, respectively. Once predicted runoff was in agreement with the estimated runoff, the different forms of outflow were calibrated from the various bioretention cells based on their site and design characteristics. Since the change between monitoring periods at Rocky Mount was relatively minor (reducing the IWS outlet), data collected for the entire shallow IWS period were used to calibrate DRAINMOD for these bioretention cells. Data

collected for the deep IWS period were used to test or validate the model. At Nashville, the presence of a clogging layer in the pre-repair period made the transition between modeling the two periods more complex than solely changing an outlet depth. For this reason, both monitoring periods were split into two equal (6 month) periods to calibrate and validate the model. The post-repair period was calibrated first because the profile was more uniform and not impacted by a restricting layer. The same vertical seepage parameters and drain characteristics from the post-repair period were used for the pre-repair period.

7.5.1 Contributing Area Runoff

There were three combinations of impervious percentage and consistency in the impervious area (depressions versus smoothly graded asphalt) in the four separate bioretention cells. The parking lot at the Rocky Mount site had larger depressions compared to Nashville site, which was smoothly graded. Therefore, less runoff per unit area was generated at the Rocky Mount site. Also, the impervious portion of the drainage area at Rocky Mount was approximately 75 percent for the two bioretention cells, where, in Nashville, it was 83 percent and nearly 100 percent for the 0.6-m and 0.9-m media depth cells, respectively. A constant surface storage depth was initially used to model runoff from the contributing area. Then the field ratio (drainage area to bioretention area ratio) was altered to set the annual estimated and predicted (modeled) runoff volumes equal to each other for modeling the performance of the bioretention cell. However, this approach resulted in an over-prediction of runoff for smaller events and an under-prediction of runoff from larger events for the sites that had larger portions of pervious areas and larger depression storage in the impervious areas. Overall, this approach inaccurately represented the depression storage of the drainage area. Therefore, in the model setup to predict runoff from the contributing area, the surface storage parameter was increased for the sites with larger depression storage in the impervious sections and larger portions of pervious area. The Nashville site with nearly 100 percent impervious area had a surface storage parameter equal to 0.01 cm. This was increased to 0.07 cm for the Nashville site with 83 percent impervious

area and 0.28 cm for the Rocky Mount sites with approximately 75 percent impervious area and several shallow depressions in the asphalt surface.

The period with a deep IWS zone at Rocky Mount and the post-repair period at Nashville were used as the calibration periods. Nash-Sutcliffe coefficients during the calibration period were 0.99 at Rocky Mount and 1.00 for both sites at Nashville. In the validation period (shallow IWS period at Rocky Mount and pre-repair period at Nashville), Nash-Sutcliffe coefficients were 0.99 and 1.00 for the Rocky Mount site and both Nashville sites, respectively. For runoff from each site and period, Nash-Sutcliffe coefficients exceeded 0.99. Also, a linear trend was calculated for the predicted (modeled) versus estimated data and the slope ranged between 0.99 and 1.01, with the coefficient of determination (r^2) exceeding 0.99 for all sites and periods. The predicted runoff volumes for each event were in excellent agreement with the method that was used to estimate runoff volume. An example of the predicted (modeled) versus estimated runoff data for the 0.6-m media depth cells at Nashville during the validation (pre-repair) period is presented in Fig 7.2. The linear trend and coefficient of determination (r^2) are also presented.

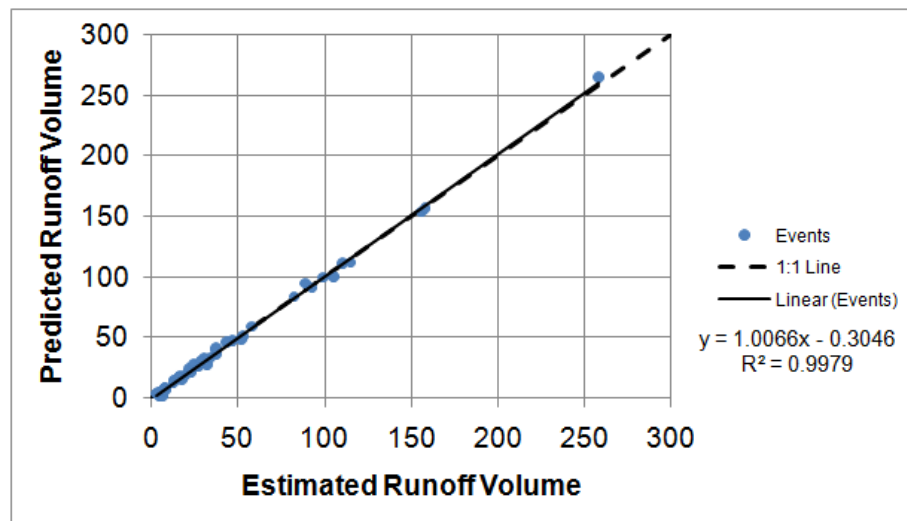


Figure 7.2: Predicted (modeled) versus estimated runoff volume data for pre-repair (validation) period of the 0.6-m media depth bioretention cells at Nashville. Also presented are the linear trend of these data and coefficient of determination (r^2). (All units are in cm per bioretention surface area).

7.5.2 Nashville Site – Conventional Drainage Configuration

7.5.2.1 Post-Repair Monitoring Period (Year 2)

As described in Table 7.5, the predicted data at the Nashville site were in good agreement with the measured and estimated data for both the calibration and validation periods, during the post-repair monitoring period. Of the forms of outflow, drainage had the strongest agreement between measured and predicted data; Nash-Sutcliffe coefficients and coefficients of determination exceeded 0.9. Nash-Sutcliffe coefficients for exfiltration/ET were approximately 0.9 and 0.8 during the calibration and validation periods, respectively. Nash-Sutcliffe coefficients for overflow during the calibration period were 0.82 and 0.71 for the 0.6-m and 0.9-m media depth cells, respectively. The weakest model agreement occurred during the validation period for overflow, where Nash-Sutcliffe coefficients were 0.58 and 0.40 for the 0.6-m and 0.9-m media depth cells, respectively. However, the error between predicted and measured volumes from each set of cells during the validation period was less than 10 percent. The cumulative water balance is displayed in Figs. 7.3–7.4 for the 0.6-m and 0.9-m media depth cells, respectively.

Table 7.5: Comparison of measured/estimated and predicted (modeled) results for the Nashville bioretention cells, during the post-repair period.

Cell Description	Method of Comparison	Fate of Runoff: (cm per bioretention surface area per monitoring period [percent of annual runoff])			
		Runoff	Drainage	Overflow	Exfiltration/ET
Calibration Period [0.6-m Media Depth Cells] (11Mar09-16Sept09)	Measured/estimated volume [percent of annual runoff]	1005	470 [46.8%]	120 [11.9%]	415 [41.3%]
	Predicted volume [percent of annual runoff]	1010	538 [53.3%]	100 [9.9%]	372 [36.8%]
	Difference between measured and predicted volumes	5	68	-20	-43
	Percent difference between measured and predicted volumes	0.6%	14.5%	-16.5%	-10.4%
	Nash-Sutcliffe Coefficient	1.00	0.90	0.82	0.87
	Coefficient of determination (r^2)	1.00	0.99	0.85	0.96
	Validation Period [0.6-m Media Depth Cells] (16Sept09-24Mar10)	Measured/estimated volume [percent of annual runoff]	1300	744 [57.3%]	150 [11.5%]
Predicted volume [percent of annual runoff]		1292	652 [50.4%]	165 [12.8%]	475 [36.8%]
Difference between measured and predicted volumes		-8	-92	15	69
Percent difference between measured and predicted volumes		-0.6%	-12.4%	10.5%	17.1%
Nash-Sutcliffe Coefficient		1.00	0.96	0.58	0.81
Coefficient of determination (r^2)		1.00	0.97	0.88	0.86

Table 7.5 (continued)

Cell Description	Method of Comparison	Fate of Runoff: (cm per bioretention surface area per monitoring period [percent of annual runoff])			
		Runoff	Drainage	Overflow	Exfiltration/ET
Calibration Period [0.9-m Media Depth Cells] (11Mar09-16Sept09)	Measured/estimated volume [percent of annual runoff]	974	418 [42.9%]	108 [11.0%]	448 [46.0%]
	Predicted volume [percent of annual runoff]	981	454 [46.3%]	63 [6.4%]	464 [47.3%]
	Difference between measured and predicted volumes	7	36	-45	16
	Percent difference between measured and predicted volumes	0.6%	8.5%	-41.7%	3.5%
	Nash-Sutcliffe Coefficient	1.00	0.94	0.71	0.88
	Coefficient of determination (r^2)	1.00	0.95	0.77	0.91
	Validation Period [0.9-m Media Depth Cells] (16Sept09-24Mar10)	Measured/estimated volume [percent of annual runoff]	1257	564 [44.8%]	147 [11.7%]
Predicted volume [percent of annual runoff]		1254	540 [43.0%]	141 [11.3%]	574 [45.7%]
Difference between measured and predicted volumes		-3	-24	-6	27
Percent difference between measured and predicted volumes		-0.2%	-4.3%	-3.6%	4.9%
Nash-Sutcliffe Coefficient		1.00	0.93	0.40	0.81
Coefficient of determination (r^2)		1.00	0.93	0.77	0.83

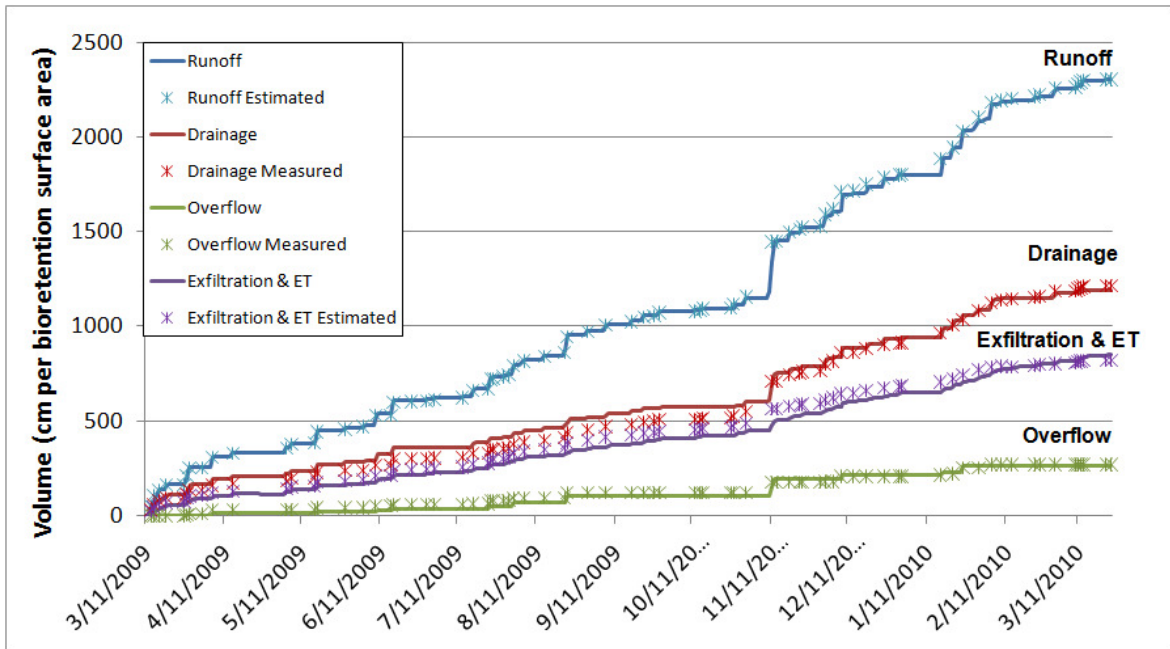


Figure 7.3: Cumulative fate of runoff for 0.6-m media depth cells at Nashville, during the post-repair monitoring period.

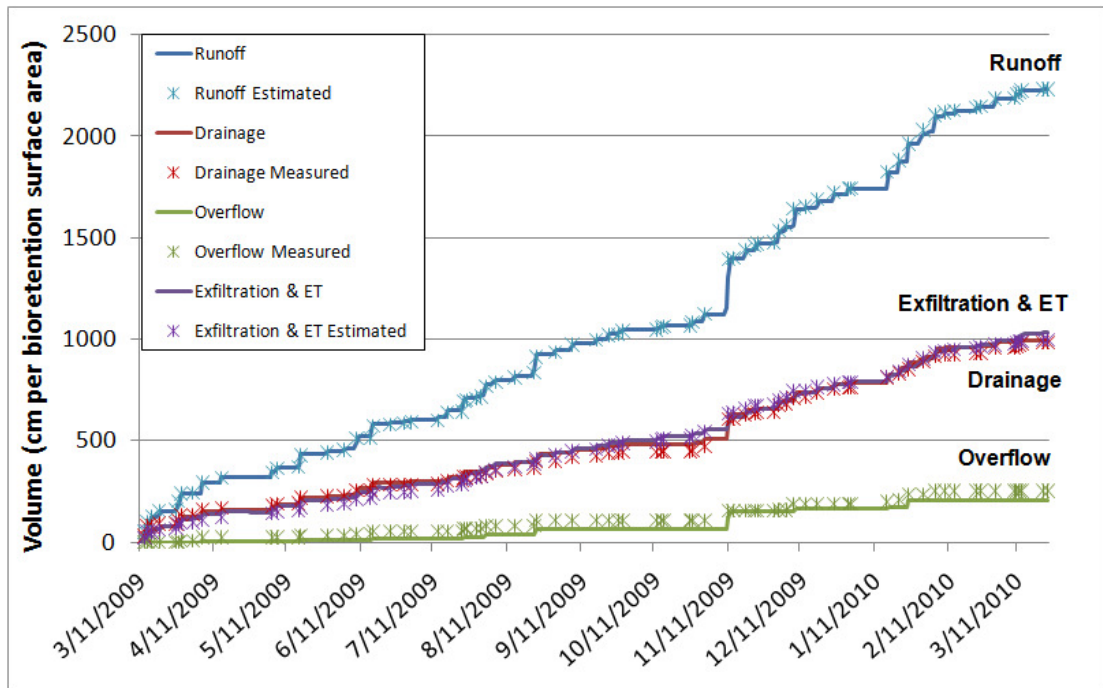


Figure 7.4: Cumulative fate of runoff for 0.9-m media depth cells at Nashville, during the post-repair monitoring period.

7.5.2.2 Pre-Repair Monitoring Period [Clogged and Undersized] (Year 1)

Modeling the performance of the Nashville bioretention cells for the pre-repair period was difficult because of the thin restrictive layer that formed at the 20-cm depth, as discussed in Chapters 3-4. Infiltration parameters were finally determined based on the effective saturated hydraulic conductivity of the entire profile, which was approximately equal to the upper range of the final constant infiltration rate that was measured under fully saturated conditions. With these inputs, results predicted by the model were in good agreement with the measured/estimated data for the pre-repair monitoring period, as shown in Table 7.6. Nash-Sutcliffe coefficients during the calibration and validation periods ranged from 0.81-0.88, 0.70-0.73, and 0.62-0.73, for overflow, drainage, and exfiltration/ET, respectively, showing that the model agreement was similar between the calibration and validation periods for the pre-repair monitoring period. The cumulative water balance is displayed in Figs. 7.5–7.6 for the 0.6-m and 0.9-m media depth cells, respectively.

Table 7.6: Comparison of measured/estimated and predicted (modeled) results for the Nashville bioretention cells, during the pre-repair period.

Cell Description	Method of Comparison	Fate of Runoff: (cm per bioretention surface area per monitoring period [percent of annual runoff])			
		Runoff	Drainage	Overflow	Exfiltration/ET
Calibration Period [0.6-m Media Depth Cells] (7Apr08-29Sept08)	Measured/estimated volume [percent of annual runoff]	1357	426 [31.4%]	576 [42.4%]	355 [26.2%]
	Predicted volume [percent of annual runoff]	1355	375 [27.7%]	634 [46.8%]	346 [25.5%]
	Difference between measured and predicted volumes	-2	51	58	-9
	Percent difference between measured and predicted volumes	-0.1%	-11.8%	10.1%	-2.8%
	Nash-Sutcliffe Coefficient	1.00	0.70	0.87	0.62
	Coefficient of determination (r^2)	1.00	0.71	0.97	0.64
	Validation Period [0.6-m Media Depth Cells] (30Sept08-10Mar09)	Measured/estimated volume [percent of annual runoff]	742	250 [33.6%]	205 [27.6%]
Predicted volume [percent of annual runoff]		744	292 [39.3%]	191 [25.7%]	261 [35.0%]
Difference between measured and predicted volumes		2	42	-14	-27
Percent difference between measured and predicted volumes		0.2%	17.2%	-6.8%	-9.5%
Nash-Sutcliffe Coefficient		1.00	0.73	0.86	0.69
Coefficient of determination (r^2)		1.00	0.84	0.89	0.81

Table 7.6 (continued)

Cell Description	Method of Comparison	Fate of Runoff: (cm per bioretention surface area per monitoring period [percent of annual runoff])			
		Runoff	Drainage	Overflow	Exfiltration/ET
Calibration Period [0.9-m Media Depth Cells] (7Apr08-29Sept08)	Measured/estimated volume [percent of annual runoff]	1295	299 [23.1%]	501 [38.7%]	495 [38.2%]
	Predicted volume [percent of annual runoff]	1292	290 [22.4%]	546 [42.3%]	457 [35.3%]
	Difference between measured and predicted volumes	-3	-9	45	-38
	Percent difference between measured and predicted volumes	-0.2%	-3.0%	9.0%	-7.7%
	Nash-Sutcliffe Coefficient	1.00	0.72	0.88	0.73
	Coefficient of determination (r^2)	1.00	0.73	0.97	0.75
	Validation Period [0.9-m Media Depth Cells] (30Sept08-10Mar09)	Measured/estimated volume [percent of annual runoff]	725	157 [21.6%]	209 [28.8%]
Predicted volume [percent of annual runoff]		729	227 [31.1%]	156 [21.5%]	345 [47.4%]
Difference between measured and predicted volumes		4	70	-53	-14
Percent difference between measured and predicted volumes		0.5%	44.5%	-25.1%	-3.8%
Nash-Sutcliffe Coefficient		1.00	0.71	0.81	0.72
Coefficient of determination (r^2)		1.00	0.89	0.85	0.72

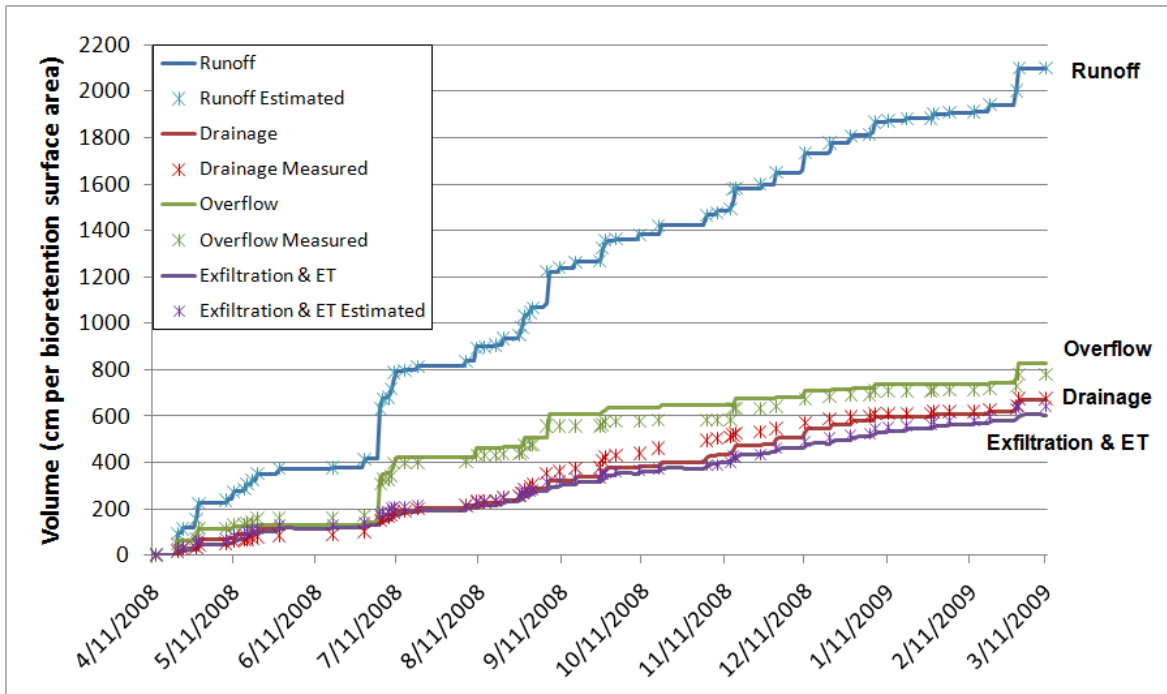


Figure 7.5: Cumulative fate of runoff for 0.6-m media depth cells at Nashville, during the pre-repair monitoring period.

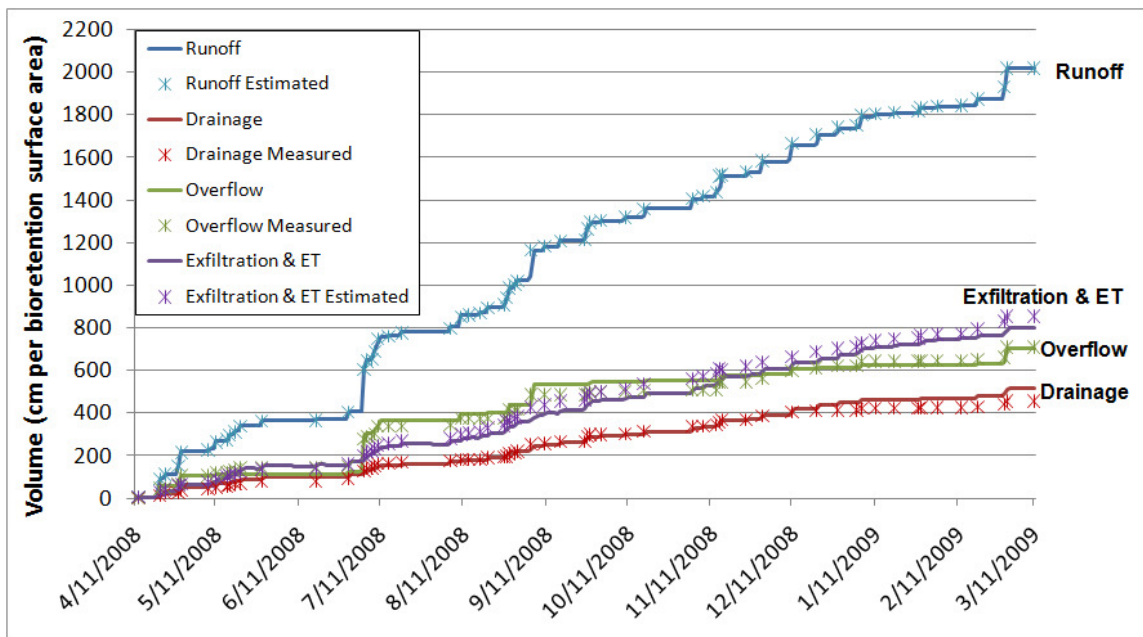


Figure 7.6: Cumulative fate of runoff for 0.9-m media depth cells at Nashville, during the pre-repair monitoring period.

7.5.3 Rocky Mount Site – IWS Drainage Configuration

7.5.3.1 Sandy Clay Loam (SCL) Cell

Results for the SCL cell at Rocky Mount are provided in Table 7.7. Overall, model predictions for the Rocky Mount site were in good agreement with the measured data. During the calibration period (shallow IWS period), Nash-Sutcliffe coefficients were 0.92 for drainage and exfiltration/ET and 0.88 for overflow. The error between the cumulative predicted and estimated overflow volume and exfiltration/ET volume were less than one percent, and the error between the cumulative predicted and measured drainage volume was 16 percent. Initial inspection of the results indicates that predicted drainage and overflow were not in good agreement with measured/estimated values during the validation period (deep IWS period). The reason for the poor agreement was attributable to the shallow slope of the parking lot and the emergency bypass stormwater drop inlet not being installed at the proper elevation. These two factors caused runoff to bypass the bioretention cell and immediately enter the emergency bypass prior to flowing into the surface storage zone for extreme, intense events. These events were more prevalent during the validation period (deep IWS period). It did not matter if there was still storage available, flow bypassed the cell. DRAINMOD will not predict overflow to occur until the surface storage zone has been exceeded. Therefore, for this site that allowed bypass prior to filling the surface storage zone to maximum capacity, DRAINMOD cannot accurately predict overflow. Had the storage volume been available, the bypass water would have entered the cell and left via drainage, thus improving agreement between predicted and measured flows. Although the bypass flow problem prevented the model from accurately predicting outflows, model prediction of the portion leaving as exfiltration/ET was in good agreement with measured results. In the validation period, the error between the cumulative predicted and estimated exfiltration/ET volumes was five percent, and the Nash-Sutcliffe coefficient and coefficient of determination were both 0.92. While the agreement for outflow from the validation period was weaker, the Nash-Sutcliffe coefficient for overflow was still 0.69. Also, despite a negative Nash-Sutcliffe coefficient for drainage, the net difference in predicted and measured volumes was

only 7.9 percent of the cumulative runoff volume (124 cm/bioretenion surface area out of 1559 cm/bioretenion surface area of runoff). The evolution of the cumulative water balance is displayed in Figs. 7.7–7.8 for the shallow (calibration) and deep (validation) IWS monitoring periods, respectively.

Table 7.7: Comparison of measured/estimated and predicted (modeled) results for the SCL cell at Rocky Mount.

Monitoring Period	Method of Comparison	Fate of Runoff: (cm per bioretention surface area per monitoring period [percent of annual runoff])			
		<i>Runoff</i>	<i>Drainage</i>	<i>Overflow</i>	<i>Exfiltration/ET</i>
Calibration Period [Shallow IWS Zone Period] (13Jan09 – 11Jan10)	Measured/estimated volume [percent of annual runoff]	1251	231 [20.5%]	88 [7.1%]	932 [72.5%]
	Predicted volume [percent of annual runoff]	1272	269 [21.2%]	88 [7.0%]	930 [71.9%]
	Difference between measured and predicted volumes	21	38	0	-2
	Percent difference between measured and predicted volumes	2%	16%	<1%	<1%
	Nash-Sutcliffe Coefficient	0.99	0.92	0.88	0.92
	Coefficient of determination (r^2)	0.99	0.96	0.90	0.92

Table 7.7 (continued)

Monitoring Period	Method of Comparison	Fate of Runoff: (cm per bioretention surface area per monitoring period [percent of annual runoff])			
		Runoff	Drainage	Overflow	Exfiltration/ET
Validation Period [Deep IWS Zone Period] (14Sept07 – 13Jan09)	Measured/estimated volume [percent of annual runoff]	1562	31 [2.0%]	175 [11.2%]	1353 [86.8%]
	Predicted volume [percent of annual runoff]	1559	155 [9.9%]	111 [7.1%]	1292 [83.0%]
	Difference between measured and predicted volumes	-3	124	-64	-61
	Percent difference between measured and predicted volumes	<1%	407%	-36%	-5%
	Nash-Sutcliffe Coefficient	0.99	< 0	0.69	0.92
	Coefficient of determination (r^2)	0.99	0.61	0.72	0.92

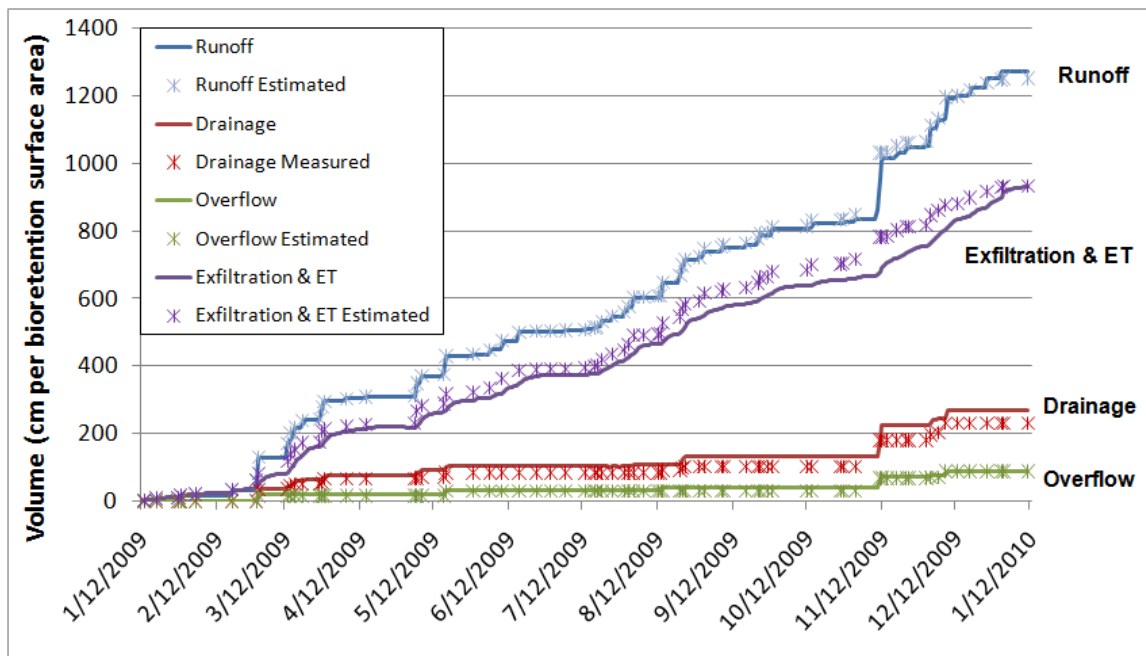


Figure 7.7: Cumulative fate of runoff for SCL cell at Rocky Mount, during the calibration period (shallow IWS zone monitoring period).

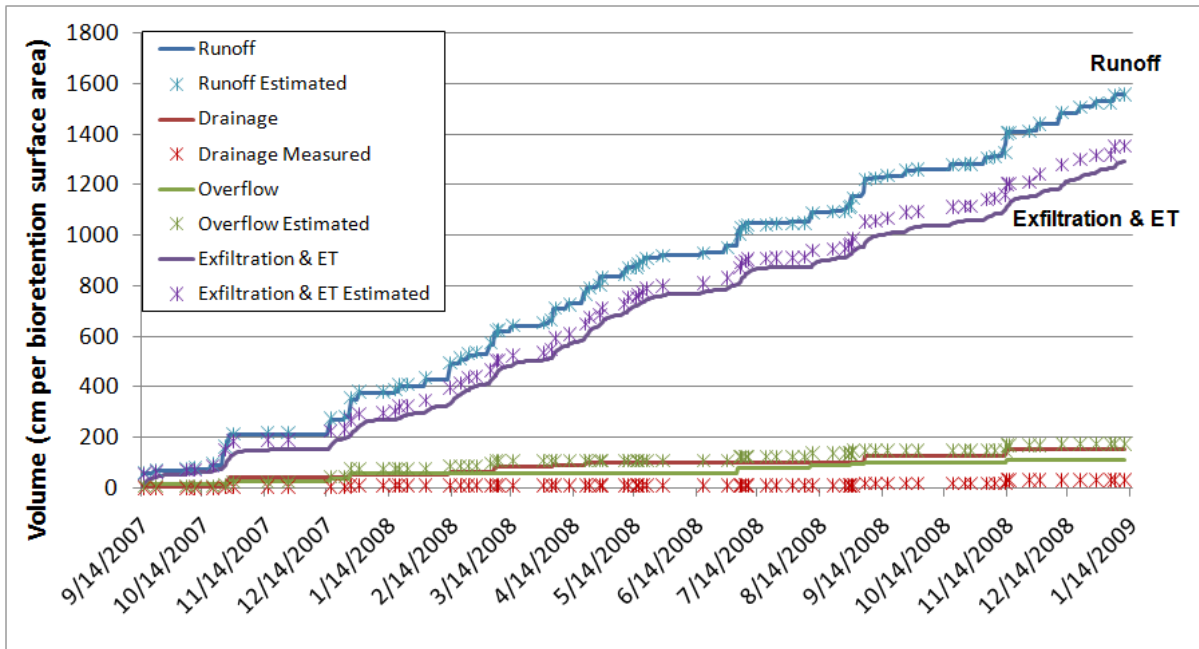


Figure 7.8: Cumulative fate of runoff for SCL cell at Rocky Mount, during the validation period (deep IWS zone monitoring period).

Measured water table depths were also used in calibrating DRAINMOD during the shallow IWS period. DRAINMOD predicts water table depth at the end of each day. These depths were compared to the measured depths for the SCL cell during the shallow IWS period. Of 320 daily readings, the water table was too deep to take an actual reading for 178, and drainage was occurring for 7, so in comparing 135 daily water table depths, the average absolute error was 7.8 cm (3.1 in), and the interquartile range of the absolute error was -7.9 to 3.5 cm (-3.1 to 1.4 in). The 135 daily water table depths that had valid measurements were compared to the predicted results in Fig 7.9. A linear trendline was added to this plot, which had a coefficient of determination of approximately 0.82 and a slope of approximately 1.04, which was nearly in line with the 1:1 line of perfect agreement. The plot of the entire period in which water table measurements were recorded is presented in Figs. 7.10–7.12. The range of valid water table depths is presented as the data points between the two dashed lines (bottom of drain pipe and top of IWS outlet). Overall, model prediction matched well with observations during each event and drawdown was accurately modeled within the IWS zone.

It was most accurate in the period between May and October (most of the growing season). From February to April and November to January (most of the dormant season), the measured drawdown was slower than the predicted drawdown rate. This was likely due to the water table underlying the bioretention cell rising closer to the bottom of the cell reducing the downward hydraulic gradient and slowing the exfiltration rate. During these months, local water tables often rise due to reduced ET. In the period between June and July, the measured water table drawdown was slightly faster than the predicted drawdown. This could be due to a deeper water table beneath the bioretention cell and increased hydraulic gradient and exfiltration rate. There was a slight variation in the actual measured exfiltration/seepage rate for the SCL cell 2.1-3.3 mm/hr (0.08-0.13 in/hr). In order to balance the faster and slower rates during calibration, 3.0 mm/hr (0.12 in/hr) was selected to be used in the model.

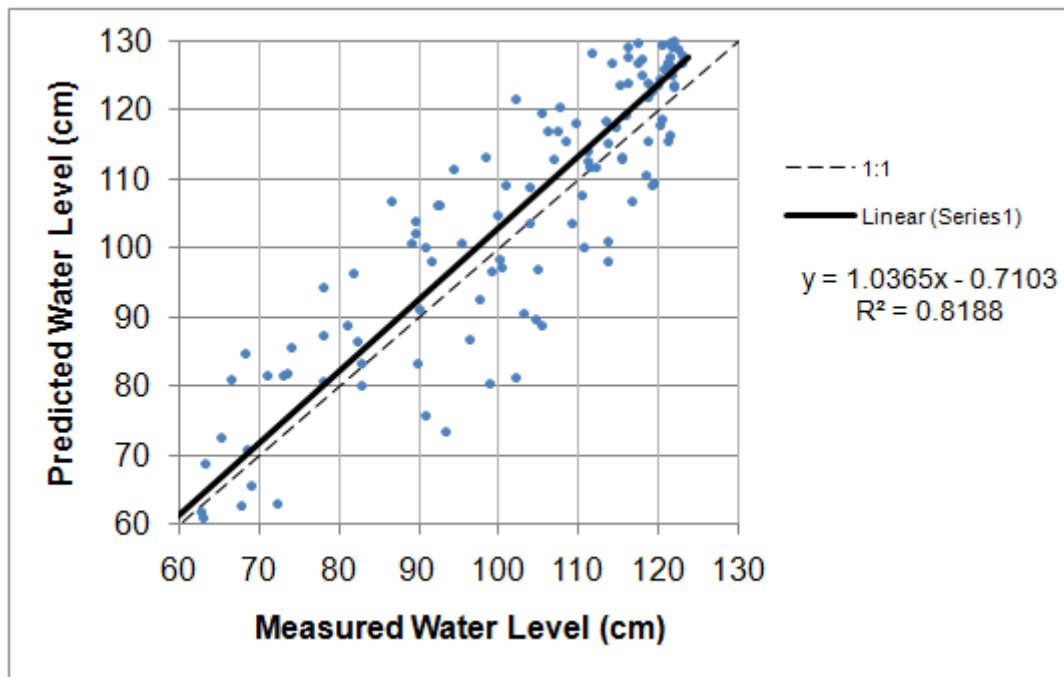


Figure 7.9: Comparison of predicted versus measured water table depths for SCL cell at Rocky Mount, during the calibration period (shallow IWS zone monitoring period).

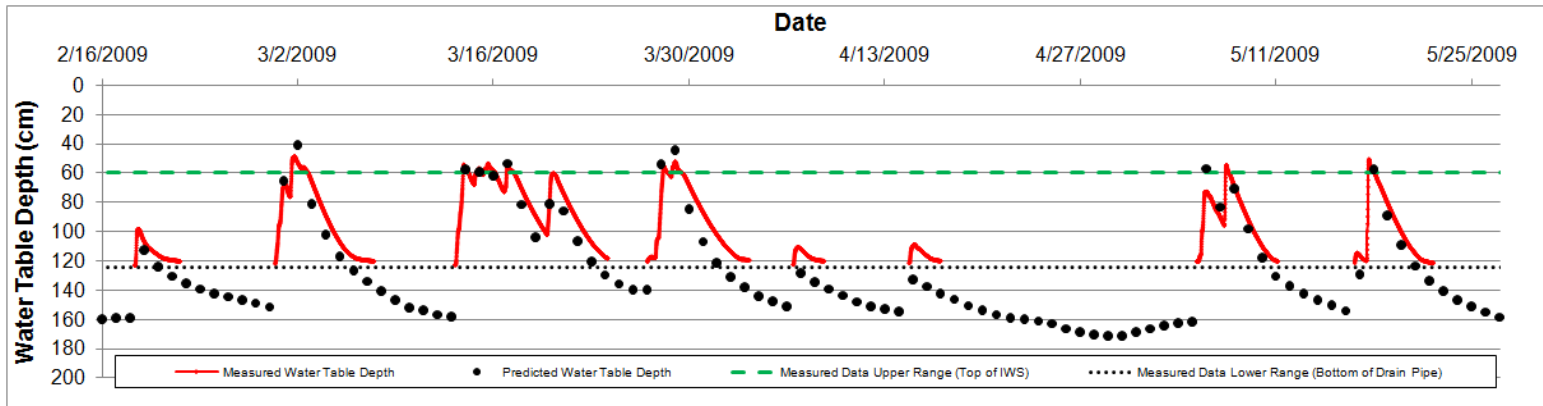


Figure 7.10: Comparison of predicted versus measured water table depths for SCL cell [February to May 2009].

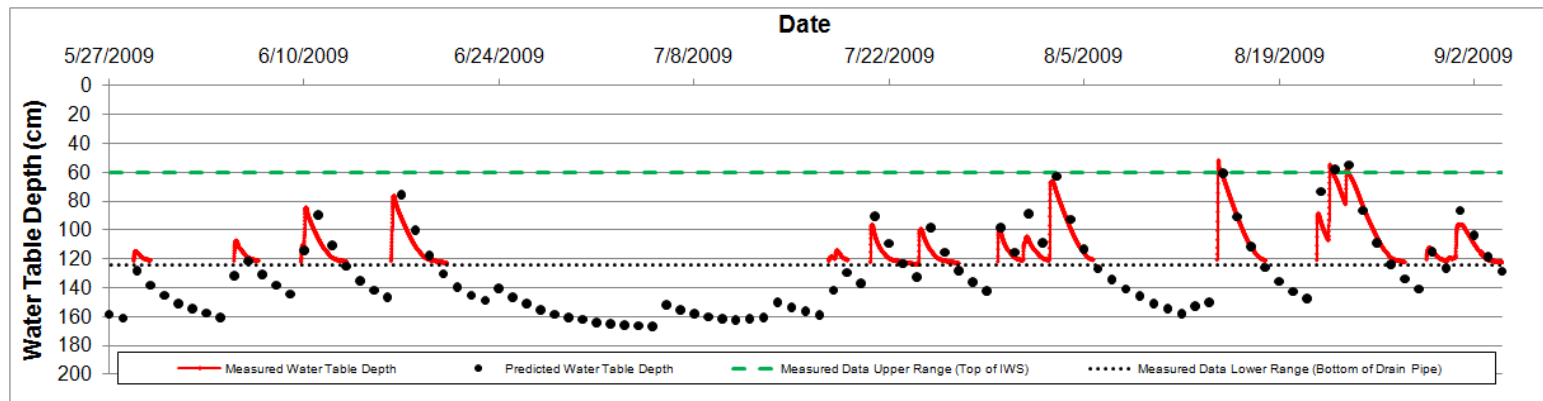


Figure 7.11: Comparison of predicted versus measured water table depths for SCL cell [May to September 2009].

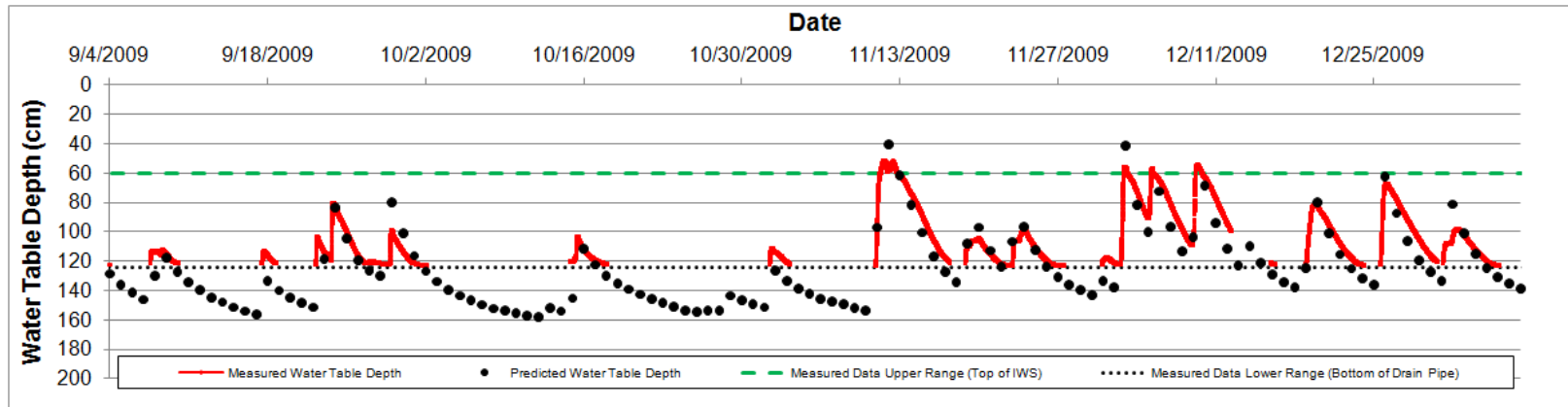


Figure 7.12: Comparison of predicted versus measured water table depths for SCL cell [September 2009 to January 2010].

7.5.3.2 Sand Cell

The Sand cell represented a type of system that had extremely high infiltration rates into the cell and into the surrounding soil. The shallow IWS period was used as the calibration period because exfiltration was measured during this period and the deep IWS period was used as the validation period. The infiltration rate was so fast that surface ponding was never recorded during the shallow IWS period. The range of measured exfiltration/seepage rates was 60-90 mm/hr (2.4-3.6 in/hr), so 75 mm/hr (3.0 in/hr) was used in DRAINMOD. The media and underlying soil at this site were both classified as a sand texture. For both monitoring periods, there was essentially no outflow and all the runoff left as exfiltration. After setting the deep seepage parameters to the measured exfiltration rate and the internal water storage zone depth to its appropriate levels in the calibration period, DRAINMOD successfully predicted the exfiltration/ET volume to within one percent of the measured volume. Likewise, in the validation period, the predicted exfiltration/ET volume was within one percent of the measured volume. The model slightly over-predicted the drainage portion from this cell during the calibration period, but the net difference in predicted and measured volumes was only two percent of the cumulative runoff volume (29 cm/bioretenction surface area out of 1440 cm/bioretenction surface area of runoff).

Table 7.8: Comparison of measured/estimated and predicted (modeled) results for the Sand cell at Rocky Mount.

Monitoring Period	Method of Comparison	Fate of Runoff: (cm per bioretention surface area per monitoring period [percent of annual runoff])			
		<i>Runoff</i>	<i>Drainage</i>	<i>Overflow</i>	<i>Exfiltration/ET</i>
Calibration Period [Shallow IWS Zone Period] (13Jan09 – 11Jan10)	Measured/estimated volume [percent of annual runoff]	1416	4 [0.3%]	0 [0.0%]	1412 [99.7%]
	Predicted volume [percent of annual runoff]	1440	33 [2.5%]	0 [0.0%]	1407 [97.4%]
	Difference between measured and predicted volumes	24	29	0	-5
	Percent difference between measured and predicted volumes	2%	651%	0%	<1%
Validation Period [Deep IWS Zone Period] (14Sept07 – 13Jan09)	Measured/estimated volume [percent of annual runoff]	1762	5 [0.3%]	30 [1.7%]	1727 [98.0%]
	Predicted volume [percent of annual runoff]	1765	6 [0.3%]	8 [0.5%]	1751 [99.2%]
	Difference between measured and predicted volumes	3	1	-22	24
	Percent difference between measured and predicted volumes	0%	18%	-73%	1%

7.6 ANALYSIS OF INPUT PARAMETERS

Existing bioretention specifications at Rocky Mount and Nashville were altered to analyze the overall impact of different design specifications on the model and the implications for design recommendations. Long-term simulations were also conducted based on 60 years of historical hourly rainfall and daily temperature records. Weather files from the Raleigh-Durham International Airport were used in most of the long-term simulations. For these cases, long-term simulations were conducted for a bioretention cell designed per

NC standards to capture a 25-mm (1.0 in) design event (NCDENR 2009). Wilmington weather files were only used in one set of long-term simulations, which is clearly noted. When the Wilmington weather files were used, the design event was increased to 38 mm (1.5 in) (NCDENR 2009). For the long-term simulations, the NC design standard specifications were altered to determine the implications of variant designs. The average annual rainfall depths at the Raleigh-Durham and Wilmington airports during this period (1950-2009) were 106.9 cm (42.07 in) and 139.3 cm (54.85 in), respectively (NOAA 2011).

7.6.1 Drainage Configuration

Underdrain configuration has a major impact on hydrologic performance. The Rocky Mount site had nearly all of the runoff leave via exfiltration because of the combination of the IWS zone and the high hydraulic conductivity of the underlying soil. To simulate how the Nashville site would have performed had an IWS zone been included during the post-repair period, the outlet under controlled drainage (DRAINMOD input) was set at 30 cm from the surface for both cells. These results, as shown in Table 7.9, illustrate how the IWS drainage configuration substantially reduced the drainage volume released by these cells. An additional 24 and 39 percent of annual runoff now left as exfiltration from the 0.6-m and 0.9-m media depth cells, respectively. For both sets of cells, the amount of exfiltration nearly doubled by adding an elevated underdrain outlet. This change is relatively easy and inexpensive, so this would be a viable option to improve hydrologic performance of bioretention cells, especially for retrofits. In some cases, one potential drawback would be increased overflow volume.

Table 7.9: Summary of Nashville site fate of runoff if an IWS zone was included that had an outlet 30 cm from the surface of the media.

Cell Description (Drainage Configuration)	Annual Fate of Runoff: (cm per bioretention surface area per year [percent of annual runoff])				
	Runoff	Drainage	Overflow	Exfiltration	ET
0.6-m Media (conventional)	2302	1190 [52%]	265 [12%]	733 [32%]	114 [5%]
0.9-m Media (conventional)	2235	1010 [45%]	204 [9%]	904 [40%]	117 [5%]
0.6-m Media (IWS outlet 30 cm from surface)	2302	616 [27%]	283 [12%]	1290 [56%]	114 [5%]
0.9-m Media (IWS outlet 30 cm from surface)	2235	144 [6%]	200 [9%]	1775 [79%]	117 [5%]

The reason for the good hydrologic performance of the Nashville site in Table 7.9 was attributable to its moderately permeable underlying soils. To model the performance for cells with more restrictive underlying soils, the standard NC design guidance methods were used to size a typical bioretention cell (NCDENR 2009). Model simulations were run for a conventional drainage configuration and for an IWS zone with the outlet set at 30 cm from the surface. A range of underlying soil types was considered. The profile consisted of a 30-cm average surface storage depth, 5-cm mulch layer, 90-cm media layer, 10-cm sand layer, and 20-cm gravel layer. The saturated hydraulic conductivity of the fill media was 2.5 cm/hr. The 15-cm diameter drains were spaced 4.5 m apart, and the drainage coefficient for all simulations was set at 60 cm/day to avoid having the hydraulic capacity of the underdrains limit the maximum drainage rate. By setting the drainage coefficient to 60 cm/day, the hydraulic capacity of the underdrains would not be reached under fully saturated and ponded conditions. The deep seepage parameters had a restricting layer thickness of 60 cm and piezometric head of 60 cm of an aquifer directly below the restrictive layer. The vertical conductivity of the restricting layer varied between 0.01, 0.1, and 0.5 cm/hr, to represent a range of underlying soils. Simulations were conducted for a 60-year period using weather records from the Raleigh-Durham International Airport. Results are presented in Table 7.10. As mentioned earlier, the Rocky Mount SCL cell, with a sandy clay loam underlying soil,

had an exfiltration/seepage rate of 0.30 cm/hr. Based on measured exfiltration/seepage rates of other Piedmont bioretention field sites described in Appendix A, the 0.01 and 0.1 cm/hr rates would be representative of clay influenced underlying soils. The results show that the IWS zone increased the total volume of water leaving as exfiltration. Predicted annual exfiltration volumes were 8, 38, and 65 percent of the annual runoff volume for the conductivity values of the restricting layer of 0.01, 0.1, and 0.5 cm/hr, respectively. Without the IWS zone, predicted annual exfiltration volumes were only 1, 5, and 16 percent of annual runoff volume, respectively. The IWS zone increased predicted annual exfiltration volume by approximately 10, 8, and 4 times for conductivities of the restricting layer of 0.01, 0.1, and 0.5 cm/hr, respectively. However, predicted overflow volumes were also increased. As the hydraulic conductivity of the underlying soils decreases, the time necessary to drain the IWS zone increases. Therefore, when successive extreme events occur at sites with restrictive underlying soils, the IWS zone will not be fully drained, so less storage will be available in the media. The IWS zone configuration would produce more overflow from the second event than predicted for conventional drainage. However, since successive extreme events are not common, the increase of annual exfiltration likely offsets the minor volume increase associated with overflow for most cases.

Table 7.10: Analysis of the impact of an IWS zone with restrictive underlying soils.

Drainage Configuration	Conductivity of Restricting Layer (cm/hr)	Annual Fate of Runoff: (cm per bioretention surface area per year [percent of annual runoff])				
		Runoff	Drainage	Overflow	Exfiltration	ET
Conventional	0.01	1420	1214	96	10	101
			[85%]	[7%]	[1%]	[7%]
IWS	0.01	1420	1093	118	108	101
			[77%]	[8%]	[8%]	[7%]
Conventional	0.1	1420	1148	96	76	101
			[81%]	[7%]	[5%]	[7%]
IWS	0.1	1420	672	106	542	101
			[47%]	[7%]	[38%]	[7%]
Conventional	0.5	1420	1003	95	221	101
			[71%]	[7%]	[16%]	[7%]
IWS	0.5	1420	303	95	923	100
			[21%]	[7%]	[65%]	[7%]

The setup in Table 7.10 was used for the following set of long-term simulations, except the vertical conductivity of underlying soils remained constant at 0.1 cm/hr to represent moderately restrictive underlying soils. This rate is characteristic of a soil type that ranges between clay and sandy clay loam. Also, the drainage configuration for these simulations did *not* include an IWS zone; they were all conventionally drained. Results for the set of simulations given in Table 7.11 show the effect of reducing the drainage coefficient (the hydraulic capacity of the underdrain system) by restricting the underdrain outlet. The intention of metering outflow would be to keep the drainage water in the profile for longer periods to increase the hydraulic residence time and potential for denitrification and water quality treatment (Brown et al. 2011b). One way of metering outflow would be to restrict the pipe outlet. The results from Table 7.11 show that restricting outflow would increase exfiltration volume; however, it also increases overflow. Drainage rates are decreased, so the cell is more frequently saturated and the surface storage zone becomes overwhelmed more often, resulting in increased annual overflow. When the drainage coefficient was reduced to 2.5 cm/day, the amount of exfiltration was nearly equal to the amount of exfiltration for the design with an IWS zone that was set 30 cm from the surface (Table 7.10). The difference

between these two designs was that annual overflow was approximately 2.5 times higher for the cell with the low drainage coefficient (an additional 151 cm/bioretention surface area per 1420 cm/bioretention area of annual runoff). Using DRAINMOD's facility to analyze the hydrology of wetlands, simulation results were analyzed to find the number of times in each calendar year that the water table was within 30 cm of the base of the surface storage zone for 14 consecutive days. When the hydraulic capacity of the underdrains was not a limiting factor (drainage coefficient = 60 cm/day), this never occurred. When the drainage coefficient was reduced to 10, 5, and 2.5 cm/day, the total number of years in which this condition occurred for the 60 year simulation period were 0, 1, and 19 years, respectively. The average longest consecutive period for each calendar year in which the water table was within the top 30 cm of the profile for drainage coefficients of 10, 5, and 2.5 were 4.0, 7.3, and 12.8 days, respectively.

Table 7.11: Analysis of reducing drainage coefficient for a conventionally drained bioretention cell with restrictive underlying soils (vertical conductivity of underlying soils = 0.1 cm/hr).

Drainage Coefficient (cm/day)	Annual Fate of Runoff: (cm per bioretention surface area per year [percent of annual runoff])				
	<i>Runoff</i>	<i>Drainage</i>	<i>Overflow</i>	<i>Exfiltration</i>	<i>ET</i>
60	1420	1148 [81%]	96 [7%]	76 [5%]	101 [7%]
45	1420	1133 [80%]	99 [7%]	88 [6%]	101 [7%]
30	1420	1098 [77%]	107 [8%]	115 [8%]	101 [7%]
15	1420	1001 [70%]	136 [10%]	183 [13%]	101 [7%]
10	1420	925 [65%]	161 [11%]	234 [16%]	101 [7%]
5	1420	747 [53%]	205 [14%]	367 [26%]	101 [7%]
2.5	1420	535 [38%]	257 [18%]	528 [37%]	101 [7%]

When the underlying soil became very restrictive (hydraulic conductivity of 0.01 cm/hr), the frequency of the water table present in the top 30 cm of the profile occurred for longer periods and more frequently. When the drainage coefficient was 10, 5, and 2.5 cm/day, the total number of years in which the water table was present in the top 30 cm for

14 consecutive days increased to 1, 37, and 60 years, respectively. The average longest consecutive period for each calendar year in which the water table was within the top 30 cm of the profile for drainage coefficients of 10, 5, and 2.5 were 6.2, 16.7, and 50.1 days, respectively. When the drainage coefficient was reduced to 2.5 cm/day, the water table was within the top 30 cm of the profile for at least 14 consecutive days for 5.3 times a year, with the longest consecutive period in one calendar year lasting 125 days. Therefore, restricting the outlet from a conventionally drained bioretention cell could cause it to satisfy the hydrologic condition for a wetland. It could also harm the vegetation, lead to the possible dissolution and release of pollutants trapped near the surface of the media, and cause the bioretention media to become hydric. Therefore, for sites with restrictive underlying soils (i.e., hydraulic conductivity < 0.01 cm/hr), it would be more beneficial to include an IWS zone than to restrict outflow in a conventionally drained system.

7.6.2 Drainage Area to Bioretention Surface Area Ratio

Another important design parameter is the drainage area to bioretention surface area ratio. For a fixed design event (25 mm), increasing the average surface storage depth will decrease the surface area (footprint) required for the bioretention cell. This not only reduces the spatial opportunity cost, but decreases the amount of specialized media needed to be hauled in, to further decrease the construction costs. Long-term simulations were run for a 25-mm design event that had moderately restrictive underlying soils (vertical conductivity of underlying soils = 0.1 cm/hr). The surface storage volume of the bioretention cell was held constant, while the drainage area to bioretention area ratio varied based off of changing the average surface storage depth. The media had a saturated hydraulic conductivity of 2.5 cm/hr, and the drainage coefficient was set high enough (60 cm/day) to avoid limiting the drainage rate. The drainage configuration for these simulations did not include an IWS zone; they were conventionally drained. Decreasing the area required for the bioretention cell had a substantial impact on overflow and ET, as shown in Table 7.12. As drainage area to bioretention area ratio increased, runoff, drainage, exfiltration, and overflow increased. ET

in terms of depth per bioretention surface area remained constant, but as the relative bioretention surface area decreased, ET decreased as a percentage of runoff.

Table 7.12: Analysis of drainage area to bioretention area ratio for bioretention cells designed to capture the 25-mm event (media saturated hydraulic conductivity = 2.5 cm/hr).

Drainage Area: Bioretention Area	Ave. Surface Storage Depth (cm)	Annual Fate of Runoff: (cm per bioretention surface area per year [percent of annual runoff])				
		<i>Runoff</i>	<i>Drainage</i>	<i>Overflow</i>	<i>Exfiltration</i>	<i>ET</i>
6.5:1	15	717	537 [75%]	21 [3%]	58 [8%]	101 [14%]
10.2:1	23	1064	844 [79%]	51 [5%]	68 [6%]	101 [9%]
14.0:1	30	1420	1148 [81%]	96 [7%]	76 [5%]	101 [7%]
21.6:1	45	2133	1733 [81%]	210 [10%]	90 [4%]	101 [5%]
29.1:1	60	2837	2287 [81%]	346 [12%]	103 [4%]	101 [4%]

The same analysis was done (Table 7.13) for a saturated hydraulic conductivity of the fill media of 5.0 cm/hr. This conductivity value is similar to that of the Nashville site (post-repair). The drainage coefficient was also doubled (DC = 120 cm/day) to avoid limitation of drainage rate by the hydraulic capacity of the underdrains. Increasing hydraulic conductivity increased drainage and reduced overflow. It also reduced water table elevations in the cell quicker which reduced exfiltration. Overall, doubling the hydraulic conductivity resulted in approximately half as much overflow.

Table 7.13: Analysis of drainage area to bioretention area ratio for bioretention cells designed to capture the 25-mm event (media saturated hydraulic conductivity = 5.0 cm/hr).

Drainage Area: Bioretention Area	Ave. Surface Storage Depth (cm)	Annual Fate of Runoff: (cm per bioretention surface area per year [percent of annual runoff])				
		<i>Runoff</i>	<i>Drainage</i>	<i>Overflow</i>	<i>Exfiltration</i>	<i>ET</i>
6.5:1	15	717	566 [79%]	9 [1%]	43 [6%]	99 [14%]
10.2:1	23	1064	888 [83%]	24 [2%]	53 [5%]	100 [9%]
14.0:1	30	1420	1212 [85%]	48 [3%]	60 [4%]	100 [7%]
21.6:1	45	2133	1841 [86%]	118 [6%]	74 [3%]	100 [5%]
29.1:1	60	2837	2442 [83%]	209 [7%]	86 [3%]	100 [4%]

As presented in Chapter 4, the surface storage volumes of the bioretention cells were undersized with respect to the 25-mm design event (approximately one-half to two-thirds of the design capacity); however, they were able to treat nearly 90 percent of the runoff for one year. The results from these 60-year simulations showed that bioretention cells following the NC recommendation of an average surface storage depth of 23 cm will be able to treat 95 percent of annual runoff (Table 7.12). If treating 90 percent of annual runoff is a common target water quality capture percentage for LID practices, this implies that current design standards are over-sizing the surface storage zone. These conservative methods provide a factor of safety in the design methodology for cases in which bioretention cells are undersized due to construction errors or if the surface becomes clogged due to lack of maintenance. However, if regulators require as-built surveys and are guaranteed maintenance will occur regularly, the current NC bioretention design standards should allow for the surface storage volume to be reduced.

Current NC design standards only provide guidance and grant credit to systems that are designed to handle the design event. This “one size fits all” approach hinders retrofits and other site designs where land constraints are present. By understanding performance

from undersized and oversized systems, better design guidance can be provided. In exploring the impact of over-sizing and under-sizing bioretention cells, the surface storage depth was cut in half and doubled for two different combinations of surface storage depth and drainage area to bioretention area ratios that could capture the 25-mm event. The surface storage depths for the design event were simulated for 23 and 30 cm, which are common depths in current NC designs. The same hydraulic conductivity of the media, drainage coefficient, drainage configuration, and deep seepage parameters were used as in the simulations from Table 7.12. The biggest impact of changing the surface storage depth was on overflow. Reducing the depth by half doubled the overflow volume, and doubling the depth reduced the overflow volume by approximately two-thirds. When the 23-cm average surface storage depth was reduced by half, the bioretention cell was able to treat 90 percent of annual runoff. Finally, since the surface area remained constant, ET and exfiltration were nearly identical for all three variations (Table 7.14).

Table 7.14: Over-sizing and under-sizing bioretention cells based on surface storage depth.

Drainage Area: Bioretention Area	Ave. Surface Storage Depth (cm)	Annual Fate of Runoff: (cm per bioretention surface area per year [percent of annual runoff])				
		<i>Runoff</i>	<i>Drainage</i>	<i>Overflow</i>	<i>Exfiltration</i>	<i>ET</i>
10.2:1	11.5 ^a	1064	788 [74%]	108 [10%]	67 [6%]	101 [9%]
10.2:1	23 ^b	1064	844 [79%]	51 [5%]	68 [6%]	101 [9%]
10.2:1	46 ^c	1064	877 [82%]	17 [2%]	69 [6%]	101 [9%]
14.0:1	15 ^a	1420	1045 [74%]	201 [14%]	74 [5%]	101 [7%]
14.0:1	30 ^b	1420	1148 [81%]	96 [7%]	76 [5%]	101 [7%]
14.0:1	60 ^c	1420	1211 [85%]	31 [2%]	78 [5%]	101 [7%]

^a Under-sized surface storage volume (one-half of design surface storage volume)

^b Sized per NCDENR (2009) standard

^c Over-sized surface storage volume (double of design surface storage volume)

If land area is a constraint or concern, the more common way to oversize and undersize a system would be to alter the surface area of the bioretention cell. Altering the surface area will impact the volume of media required in the design, which will also increase or decrease the cost to construct the bioretention cell. To compare the impact of altering bioretention surface area, the surface storage depth was held constant and the surface area was either halved or doubled (Table 7.15). The same combinations of surface storage depth for the design event (25 mm) and other design specifications were used. By changing the surface area, the footprint of the bioretention cell and volume of the media consequently changed. Therefore, exfiltration and ET for both combinations varied. By doubling the area, exfiltration and ET increased and overflow decreased. The opposite occurred when the area was reduced by half. However, it is important to note that despite the reduction of surface area (by one-half), the bioretention cell was still able to treat approximately 82 and 77 percent of the annual runoff volume for a surface storage depth of 23 and 30 cm, respectively. Because the volume of the media was changed by a factor of two in Table 7.15, the impact on overflow in comparison to the design event area was more extreme. Reducing the area by one-half increased the overflow volume by more than three times, while doubling the area reduced the overflow volume by approximately 80 percent.

Table 7.15: Over-sizing and under-sizing bioretention cells based on surface area.

Drainage Area: Bioretention Area	Ave. Surface Storage Depth (cm)	Annual Fate of Runoff: (cm per bioretention surface area per year [percent of annual runoff])				
		<i>Runoff</i>	<i>Drainage</i>	<i>Overflow</i>	<i>Exfiltration</i>	<i>ET</i>
5.1:1 (double area) ^a	23	585	427 [73%]	5 [1%]	53 [9%]	100 [17%]
10.2:1 (25-mm event) ^b	23	1064	844 [79%]	51 [5%]	68 [6%]	101 [9%]
20.4:1 (half area) ^c	23	2021	1467 [73%]	368 [18%]	85 [4%]	101 [5%]
7.0:1 (double area) ^a	30	764	594 [78%]	10 [1%]	60 [8%]	101 [13%]
14.0:1 (25-mm event) ^b	30	1420	1148 [81%]	96 [7%]	76 [5%]	101 [7%]
28.0:1 (half area) ^c	30	2734	1901 [70%]	637 [23%]	95 [3%]	101 [4%]

^a Over-sized surface storage volume (double of design surface storage volume)

^b Sized per NCDENR (2009) standard

^c Under-sized surface storage volume (one-half of design surface storage volume)

Chapter 4 highlighted the importance of including intra-event infiltration in the calculations of the percentage of annual runoff treated by the media. It also presented results for two bioretention cells with surface storage capacities between one-half and two-thirds of that required by design standards. These cells treated nearly 90 percent of annual runoff, which is a common target water quality capture percentage for LID practices. Using DRAINMOD, a variety of combinations of media types, surface storage depths, and area ratios could be simulated to determine what the actual size of the surface storage zone needs to be to treat 90 percent of annual runoff on a long-term basis. In Table 7.16, the bioretention area required to treat 90 percent of annual runoff is given for a variety of media hydraulic conductivities, DCs, and average surface storage depths. These results are based on analysis of the predicted performance of the cells for a 60-year period of weather record. The percentage of the current design standard design event is given for comparison. Unless otherwise specified in the table, DRAINMOD inputs were identical to those in Table 7.12. The media consistency at the Nashville site was between the 2.5 and 5.0 cm/hr saturated

hydraulic conductivity and the average surface storage depth was approximately 23 cm, so that is why one-half to two-thirds of design capacity was almost able to treat the 90 percent event. For these configurations, 90 percent of annual runoff could be treated by providing only 51 to 70 percent of the standard 25-mm design event capacity.

Table 7.16: Varying design parameters for several bioretention cells that would treat 90 percent of annual runoff in Piedmont, NC (Raleigh-Durham weather [1950-2009]).

Media Saturated Hydraulic Conductivity (cm/hr)	Drainage Coefficient (cm/day)	Ave. Surface Storage Depth (cm)	Drainage Area: Bioretention Area	Percentage of Design Event Capacity^a
2.5	60 ^b	23	14.5:1	70%
2.5	60 ^b	30	16.9:1	83%
5.0	90	23	19.1:1	53%
5.0	120 ^b	23	20.0:1	51%
5.0	90	30	21.7:1	65%
5.0	120 ^b	30	22.8:1	61%

^a The design event capacity is based on sizing the surface storage volume using methods in NCDENR (2009); the design event for Raleigh, NC is 25 mm (1 inch). The drainage area to bioretention area ratio for a 100 percent impervious drainage area is 10.2:1 and 14.0:1 when the average surface storage depth is 23 and 30 cm, respectively.

^b Drainage coefficient exceeds maximum rate allowable by Kirkham equation under saturated conditions, so drainage rate is not limited by hydraulic conductivity of underdrains.

A similar exercise was performed for the coastal counties where the design event is 38 mm (1.5 in). Requiring capture of the larger design event reduces the drainage area to bioretention area ratio. For these simulations, long-term data from Wilmington International Airport were used. The same combinations of media saturated hydraulic conductivity, drainage coefficient, and surface storage depth were explored. Results in Table 7.17 show that bioretention cells are being oversized in the coastal counties as well. Interestingly, the percentages of the respective design event capacities required to treat 90 percent of annual runoff were similar for Raleigh-Durham and Wilmington.

Table 7.17: Varying design parameters for several bioretention cells that would treat 90 percent of annual runoff in coastal counties of NC (Wilmington weather [1950-2009]).

Media Saturated Hydraulic Conductivity (cm/hr)	Drainage Coefficient (cm/day)	Ave. Surface Storage Depth (cm)	Drainage Area: Bioretention Area	Percentage of Design Event Capacity^a
2.5	60 ^b	23	8.6:1	70%
2.5	60 ^b	30	10.2:1	81%
5.0	90	23	11.4:1	53%
5.0	120 ^b	23	11.9:1	50%
5.0	90	30	13.0:1	64%
5.0	120 ^b	30	13.7:1	61%

^a The design event capacity is based on sizing the surface storage volume using methods in NCDENR (2009); the design event for Wilmington, NC is 38 mm (1.5 inch). The drainage area to bioretention area ratio for a 100 percent impervious drainage area is 6.0:1 and 8.3:1 when the average surface storage depth is 23 and 30 cm, respectively.

^b Drainage coefficient exceeds maximum rate allowable by Kirkham equation under saturated conditions, so drainage rate is not limited by hydraulic capacity of underdrains.

7.6.3 Media Type

Media type is a very important parameter because it controls the water storage availability in the media. For example, the media used at the Rocky Mount site had substantially more water storage potential for an IWS layer than that used for Nashville because it had a higher drainable porosity. When the water table was at bottom of cell, there was greater storage available in the Rocky Mount media because soil water contents were lower at low suctions (close to the water table). An example of how the Rocky Mount site would have been affected if the media from Nashville had been used there is described in Table 7.18. In these simulations, the infiltration parameters remained constant when the Nashville media was substituted. The main impact was that an approximately 9 to 12 percent of annual runoff that was leaving via exfiltration would have left the cell as outflow (drainage and overflow) when the media with more fine particles was used (Nashville media).

Table 7.18: Comparison of SCL performance at Rocky Mount had a different media (from Nashville site) been used. (Infiltration parameters remained constant)

Cell Description (Media Type)	Annual Fate of Runoff: (cm per bioretention surface area per year [percent of annual runoff])				
	Runoff	Drainage	Overflow	Exfiltration	ET
SCL Cell Deep IWS (actual media)	1559	155 [9.9%]	111 [7.1%]	1161 [74.4%]	133 [8.5%]
SCL Cell Deep IWS (Nashville media)	1559	338 [21.7%]	111 [7.1%]	979 [62.8%]	133 [8.5%]
SCL Cell Shallow IWS (actual media)	1272	269 [21.2%]	88 [7.0%]	802 [63.0%]	112 [8.8%]
SCL Cell Shallow IWS (Nashville media)	1272	388 [30.5%]	88 [7.0%]	684 [53.8%]	112 [8.8%]

7.7 CONCLUSIONS

Bioretention cells are becoming one of the most popular low impact development stormwater practices; their level of performance is very site specific because of the impact of underlying soils, design specifications, and climate conditions. DRAINMOD was used to simulate performance of four bioretention cells that had varying media depths, media types, drainage configurations, surface storage volumes, and underlying soils. Each of the four cells was monitored for two, year-long monitoring periods, in which one of the design parameters was altered. Results showed that DRAINMOD can be used to predict the hydrologic response to runoff entering bioretention cells on a continuous, long-term basis. The annual water balance calculated in DRAINMOD is most useful to: (1) determine whether predevelopment hydrology has been restored and (2) to estimate effluent pollutant loads.

The results of the validation of DRAINMOD after calibration showed that it can be used reliably to simulate the hydrologic response of runoff entering a bioretention cell. DRAINMOD accurately predicted runoff volumes from drainage areas with a varying degree of impervious percentage and consistency of the impervious area (depressions versus smoothly graded asphalt). The Nash-Sutcliffe coefficients for runoff from each site's

drainage area exceeded 0.99 for both the calibration and validation periods. At Nashville, during the post-repair period, the Nash-Sutcliffe coefficients for drainage and exfiltration/ET both exceeded 0.8 during the calibration and validation periods. In the calibration and validation periods for the pre-repair period, the Nash-Sutcliffe coefficients for drainage, overflow, and exfiltration/ET were all in the range of 0.6-0.9. Good model agreement between predicted and measured water table depth occurred at the Rocky Mount site because exfiltration rates were measured from actual events. At the SCL cell, the average absolute error for water table depths was 7.8 cm, and the linear trend of the predicted and measured data had a coefficient of determination of approximately 0.82 and a slope of approximately 1.04. For both the calibration and validation periods, the predicted (modeled) volume of exfiltration/ET was within five percent of the estimated volume at the SCL cell, and it was within one percent for the Sand cell. Nash-Sutcliffe coefficients for the SCL cell during both the calibration and validation periods were 0.92.

A continuous, long-term model could allow designers and regulators to move away from the current “one size fits all” design approach and work towards a "flexible" bioretention design methodology that allows for over-sizing and under-sizing bioretention cells based on site characteristics. By modeling a variety of different combinations of under-sized and over-sized systems, DRAINMOD can be used to evaluate the effect of cell size and design parameters on amount of runoff treated and effluent pollutant loads. For example, analysis of systems considered herein showed that reducing the bioretention cell surface area by one-half would still allow for approximately 80 percent of the annual runoff volume to be infiltrated into the media and treated.

Modeled results showed that current bioretention design guidance is somewhat over-sizing the surface storage volume necessary to treat 90 percent of runoff. The degree to which the cells are being over-sized is dependent on the saturated hydraulic conductivity of the media, drainage coefficient, and drainage area to bioretention area ratio. For a site with moderately restrictive underlying soil (hydraulic conductivity = 0.1 cm/hr), the surface storage volume required to treat 90 percent of annual runoff only needed to be 70 percent of

the design capacity as given by the N.C. recommended guidelines for both Raleigh-Durham (Piedmont) and Wilmington (coastal counties).

Media volume is very important for treatment of runoff through ET and exfiltration and to decrease overflow volume. The model simulations showed that as media area increased, ET and exfiltration volumes increased and overflow volume decreased. This was because the relative size of the bioretention cell in comparison to the drainage area increased, which increased the opportunity for plants to promote ET.

Finally, including an IWS zone substantially reduced total outflow (overflow and drainage). The impact was the greatest when the underlying soils had higher hydraulic conductivities, but an improvement also occurred for restrictive underlying soils. On an annual basis, even the most restrictive underlying soils (such as clay) had less outflow volume when an IWS zone was included, provided that the hydraulic capacity of the drainage network (drainage coefficient) was not a limiting factor.

A technique of metering outflow by restricting the drain pipes for conventionally drained bioretention cells was also compared to using an IWS zone in areas with restrictive underlying soils. Restricting drainage rates resulted in more exfiltration when compared to using conventional drainage; however, it did not exceed the volume of exfiltration when compared to an IWS zone configuration that had the outlet set 0.3 m from the surface and a media depth of 0.9 m. Restricting the drainage rate increased overflow volume and resulted in water tables closer to the surface for extended periods of time.

7.8 ACKNOWLEDGEMENTS

The authors would like to acknowledge the Water Resources Research Institute of the University of North Carolina (WRRI-UNC) for funding the calibration of this model and NC Department of Environment and Natural Resources (NCDENR) and the Cooperative Institute for Coastal and Estuarine Environmental Technology (CICEET) for funding data collection. Thanks to Wilson Huntley and Shawn Kennedy for assistance with soil sampling and installation of monitoring equipment and Brian Phillips for creating long-term rainfall files.

7.9 REFERENCES

- Braga, A., Horst, M., and Traver, R. G. (2007). "Temperature effects on the infiltration rate through an infiltration basin BMP." *Journal of Irrigation and Drainage Engineering*, 133(6), 593-601.
- Brander, K. E., Owen, K. E., and Potter, K. W. (2004). "Modeled impacts of development type on runoff volume and infiltration performance." *Journal of the American Water Resources Association*, 40(4), 961-969.
- Brown, R. A., and Hunt, W. F. (2011a). "Impacts of media depth on effluent water quality and hydrologic performance of under-sized bioretention cells." *Journal of Irrigation and Drainage Engineering*, 137(3), 132-143.
- Brown, R. A., and Hunt, W. F. (2011b). "Underdrain configuration to enhance bioretention infiltration to reduce pollutant loads." *Journal of Environmental Engineering*, (under review).
- Davis, A. P., Hunt, W. F., Traver, R. G., and Clar, M. (2009). "Bioretention technology: Overview of current practice and future needs." *Journal of Environmental Engineering*, 135(3), 109-117.
- Dussailant, A. R., Wu, C. H., and Potter, K. W. (2004). "Richards equation model of a rain garden." *Journal of Hydrologic Engineering*, 9(3), 219-225.
- Dussailant, A. R., Cuevas, A., and Potter, K. W. (2005). "Raingardens for stormwater infiltration and focused groundwater recharge: Simulations for different world climates." *Water Science and Technology: Water Supply*, 5(3-4), 173-179.
- Emerson, C. H., and Traver, R. G. (2008). "Multiyear and seasonal variation of infiltration from storm-water best management practices." *Journal of Irrigation and Drainage Engineering*, 134(5), 598-605.
- Gee, G. W., and Bauder, J. W. (1986). "Particle-size analysis." *Methods of soil analysis. Part 1: Physical and mineralogical methods*, A. Klute, ed., Soil Science Society of America, Madison, Wis., 383-411.
- Hatt, B. E., Fletcher, T. D., and Deletic, A. (2009). "Hydrologic and pollutant removal performance of stormwater biofiltration systems at the field scale." *Journal of Hydrology*, 365(3-4), 310-321.
- He, Z., and Davis, A. P. (2011). "Process modeling of stormwater flow in a bioretention cell." *Journal of Irrigation and Drainage Engineering*, 137(3), 121-131.

- Heasom, W., Traver, R. G., and Welker, A. (2006). "Hydrologic modeling of a bioinfiltration best management practice." *Journal of the American Water Resources Association*, 42(5), 1329-1347.
- Hunt, W. F., Smith J. T., Jadlocki S. J., Hathaway, J. M., and Eubanks, P. R. (2008). "Pollutant removal and peak flow mitigation by a bioretention cell in urban Charlotte, NC." *Journal of Environmental Engineering*, 134(5), 403-408.
- Jones, M. P., and Hunt, W. F. (2009). "Bioretention impact on runoff temperature in trout sensitive waters." *Journal of Environmental Engineering*, 135(8), 577-585.
- Kirkham, D. (1957). "Theory of land drainage." *Drainage of agricultural lands: Agronomy monograph No. 7*, J. N. Luthin, ed., American Society of Agronomy, Madison, Wisc., 139-181.
- Klute, A. (1986). "Water retention: Laboratory methods." *Methods of soil analysis. Part 1: Physical and mineralogical methods*, A. Klute, ed., Soil Science Society of America, Madison, Wis., 635-662.
- Li, H., Sharkey, L. J., Hunt, W. F., and Davis, A. P. (2009). "Mitigation of impervious surface hydrology using bioretention in North Carolina and Maryland." *Journal of Hydrologic Engineering*, 14(4), 407-415.
- Lucas, W. C. (2010). "Design of integrated biofiltration-detention urban retrofits with design storm and continuous simulation methods." *Journal of Hydrologic Engineering*, 15(6), 486-498.
- Moody, W. T. (1967). "Nonlinear differential equation of drain spacing." *Journal of Irrigation and Drainage Division*, ASCE, 92(IR2), 1-9
- Nash, J. E., and Sutcliffe, J. V. (1970). "River flow forecasting through conceptual models part 1 – A discussion of principles." *Journal of Hydrology*, 10(3), 282-290.
- N.C. Department of Environment and Natural Resources (NCDENR). (2009). "Chapter 12: Bioretention." *Stormwater best management practices manual*, North Carolina Department of Environment and Natural Resources, Division of Water Quality, Raleigh, N.C., 12.1-12.30.
- National Oceanic and Atmospheric Administration (NOAA). (2011). "World's largest archive of climate data: National climatic data center." National Oceanic and Atmospheric Administration, National Climatic Data Center, Asheville, N.C. <<http://www.ncdc.noaa.gov/oa/ncdc.html>>.

- Palhegyi, G. E. (2010). "Modeling and sizing bioretention using flow duration control." *Journal of Hydrologic Engineering*, 15(6), 417-425.
- Pandit, A., and Heck, H. H. (2009). "Estimations of soil conservation service curve numbers for concrete and asphalt." *Journal of Hydrologic Engineering*, 14(4), 335-345.
- Passeport, E., Hunt, W. F., Line, D. E., Smith, R. A., and Brown, R. A. (2009). "Field study of the ability of two grassed bioretention cells to reduce storm-water runoff pollution." *Journal of Irrigation and Drainage Engineering*, 135(4), 505-510.
- Skaggs, R. W. (1978). "A water management model for shallow water table soils." *Technical Report No. 134*, Water Resources Research Institute of the University of North Carolina, N.C. State University, Raleigh, N.C., 1-128.
- Skaggs, R. W. (1980). "DRAINMOD: Reference report - Methods for design and evaluation of drainage-water management systems for soils with high water tables." U.S. Department of Agriculture – Soil Conservation Service, Fort Worth, TX.
- Skaggs, R. W. (1982). "Field evaluation of a water management simulation model." *Transactions of the ASAE*, 25(3), 666-674.
- Skaggs, R. W., and Khaleel, R. (1982). "Chapter 4: Infiltration." *Hydrologic modeling of small watersheds: Monograph No. 5*, American Society of Agricultural Engineers, St. Joseph, Mich., 121-166.
- Skaggs, R. W. (1999). "Drainage simulation models." *Agricultural drainage: Monograph No. 38*, R. W. Skaggs and J. van Schilfgaarde, eds., American Society of Agronomy, Madison, Wisc., 469-500.
- State Climate Office (SCO). (2011). "North Carolina climate retrieval and observations network of the southeast database (N.C. CRONOS)." State Climate Office of North Carolina, Raleigh, N.C. < <http://www.nc-climate.ncsu.edu/cronos>>.
- Thornthwaite, C. W. (1948). "An approach toward a rational classification of climate." *The Geographical Review*, 38(1), 55-94.
- U.S. Army Corps of Engineers (USACE). (2000). "Hydrologic modeling system HEC-HMS technical reference manual." USACE, Hydrologic Engineering Center, Davis, Calif.
- U.S. Environmental Protection Agency (USEPA). (2007). "National water quality inventory: Report to Congress—2002 reporting cycle." *Rep. No. EPA 841-R-07-001*, USEPA, Washington, D.C.

Youssef, M. A., Skaggs, R.W., Chescheir, G. M., and Gilliam, J. W. (2005). "The nitrogen simulation model, DRAINMOD-N II." *Transactions of the ASAE*, 48(2), 611-626.

8 IMPACTS OF CONSTRUCTION ACTIVITY ON BIORETENTION PERFORMANCE

(This chapter was printed in a revised format)

Authors: R. A. Brown, W. F. Hunt III

Published: Journal of Hydrologic Engineering

Volume 15, Number 6, Pages 386-394

8.1 ABSTRACT

Bioretention cells are incorporated as part of low impact development (LID) because of their ability to release runoff as exfiltration to the surrounding soil or evapotranspiration to the atmosphere. However, little care is taken as to the techniques used to excavate bioretention cells, and there is little concern as to the soil-moisture condition during excavation. Certain excavation techniques and soil-moisture conditions create higher levels of compaction which consequently reduce infiltration capacity. Two excavation techniques, the conventional “scoop” method which purposefully smears the underlying soil surface and the “rake” method which uses the teeth of an excavator’s bucket to scarify the underlying soil surface, were tested. Field tests were conducted on three soil types (sand, loamy sand, and clay) under a variety of antecedent soil-moisture conditions. Multiple hydraulic conductivity, surface infiltration, and soil compaction measurements were taken for each excavated condition. In all cases, the rake method of excavation tended to yield more permeable, less compacted soils than the scoop method. The difference of infiltration and hydraulic conductivity between the two excavation techniques was statistically significant ($p < 0.05$) when tests were conducted in wet soil conditions. Also, the infiltration rate at the clay site was significantly lower ($p < 0.05$), and the hydraulic conductivity at the sandy site was significantly lower ($p < 0.05$) when the scoop methodology was used. Based on results of the

experiment and because essentially no extra cost is associated with the rake method of excavation, it is recommended over the conventional scoop method. Another recommendation is to excavate under relatively dry soil conditions. The use of the rake method under dry soil conditions is expected to increase long-term exfiltration from bioretention cells.

8.2 INTRODUCTION

Approximately one third of the estuaries and lakes/reservoirs in the United States have been assessed as part of the National Water Quality Inventory, and 32 percent of these estuaries and 47 percent of these lakes/reservoirs were identified as impaired. The main cause of impairment was nutrients and one of the top three sources of nutrients was urban storm water runoff (USEPA 2007). Regionally, two of the most productive estuaries in the United States are the Pamlico and Albemarle Sounds in North Carolina (NCDENR 1994) and the Chesapeake Bay (Chesapeake Bay Program 2008). Stringent storm water regulations have been put in place for cities and counties in the Neuse and Tar-Pamlico River basins and 20 coastal counties in North Carolina (NCDENR 2007) and in the Chesapeake Bay watershed (Chesapeake Bay Program 2008).

To reduce the negative effects caused by urbanization and to meet the new storm water rules, strategies, such as low impact development (LID), that employ infiltration are increasingly adopted. The goal of LID is to plan and construct a site so that the hydrology and water quality mimic that of the initial undeveloped site (Davis 2008). Bioretention is a very common LID practice which meets several design goals: hydrologic, water quality, and aesthetic.

Bioretention combines a natural and engineered system to manage storm water from developed areas. They are designed to at least treat the water quality volume of runoff. Bioretention removes runoff pollutants through adsorption, biological decomposition, filtration, and sedimentation (Davis et al. 2001). Bioretention cells also function to remove

pollutant loads through outflow reductions due to exfiltration and evapotranspiration (Hunt et al. 2006; Jones and Hunt 2009; Li et al. 2009).

While a recent flurry of research has been conducted on bioretention cells, limited data on how construction activity impacts their performance are available. Some data are available on innovative construction techniques to improve exfiltration in stormwater best management practices (BMPs). One study by Tyner et al. (2009) examined ways to improve exfiltration in permeable pavement systems in regions with clay soil. They found that exfiltration could be significantly improved when the subgrade was treated with boreholes, subsoil ripping, or trenching. Disturbing the compacted bottom layer created a significant increase in exfiltration compared to the undisturbed control plot (Tyner et al. 2009). If construction processes are optimized to promote higher exfiltration rates from the bottom layer and sides of bioretention cells, outflow volume will decrease which will consequently decrease pollutant loads released to the storm drain network. More exfiltration also contributes to meeting another LID goal of maintaining predevelopment groundwater recharge to help restore stream base flow and groundwater components of the hydrologic cycle (Davis et al. 2009). However, with more exfiltration, the potential for transporting additional pollutant loads to the surrounding soil or the groundwater increases.

The potential for groundwater contamination from over infiltration has been a well noted concern (Clark and Pitt 2007; Pitt et al. 1999, 2002; Shuster et al. 2007). However, Clark and Pitt (2007) and Pitt et al. (1999) both found that for stormwater, when pretreated by sedimentation, which occurs in bioretention, the potential for groundwater contamination is low for metals, pesticides, and most organics. Because many states, such as North Carolina (NCDENR 2007) require 0.6 m (2 ft) of separation between the bottom of the infiltrating practice and the seasonally high water table, the likelihood groundwater contamination is further reduced. The pollutants studied have been shown not to migrate beyond this 0.6 m (2 ft) soil depth (Dierkes and Geiger 1999; Kwiatkowski et al. 2007). Provided infiltration BMPs are sited properly, they are not expected to negatively impact groundwater (Kwiatkowski et al. 2007).

A goal of LID is to promote infiltration, thereby reducing runoff. During development, soil compaction occurs that consequently decreases infiltration rates. Compaction has an important influence on soil hydraulic properties, including soil-water retention, soil water diffusivity, and saturated and unsaturated hydraulic conductivities, which govern infiltration rates (Horton et al. 1994). Pitt et al. (2002) found that soils in urban areas usually undergo major modifications that result in increased runoff, such as compaction during construction. Additional changes that affect natural infiltration are the removal of surface soils and exposure of subsurface soils during earth moving practices. Earth moving equipment compacts the soil which decreases subsoil permeability (Gregory et al. 2006). Rainfall on exposed subsoil has also been shown to cause surface sealing in clay and sandy soils, which will decrease infiltration rates (Gimenez et al. 1992; Radcliffe et al. 1991). In order to avoid surface sealing, construction should be sequenced to avoid rainfall on the exposed cut.

Gregory et al. (2006) examined the effects of compaction on infiltration rates at urban construction sites in North Central Florida by using a double-ring infiltrometer. Infiltration was measured in noncompacted and compacted soils from three land types—natural forest, planted forest, and pasture. The infiltration rates had wide variability, but overall, construction activity reduced infiltration rates 70 to 99 percent at all sites. A cone penetrometer was used to measure soil compaction, and it showed the maximum compaction levels occurred between 20 and 30 cm (8 to 12 in.) below the soil surface. For the sandy soils in North Central Florida, this study showed that even the lowest levels of compaction resulted in significantly lower infiltration rates. In addition to significantly decreasing infiltration rates, soil compaction resulting from vehicular traffic in urban development construction significantly increased soil bulk density.

Pitt et al. (2008) showed similar results to Gregory et al. (2006): typical soil compaction considerably reduced infiltration rates. Tests on both clay and sandy soils showed that infiltration rates were significantly reduced in compacted soils, and clay soils were less able to withstand low levels of compaction compared to sandy soils. Both Gregory

et al. (2006) and Pitt et al. (2008) related specific levels of compaction to infiltration rates, and they showed that using a soil cone penetrometer is a relatively reliable way to determine areas affected by compaction and therefore be expected to have decreased infiltration rates.

In Pitt et al. (2008), 153 double-ring infiltration tests were run to examine the effects of infiltration in sandy versus clay, wet versus dry, and compacted versus noncompacted soils. The set point for separating wet and dry soils was a soil-moisture content of 20 percent. A soil was considered compacted if the cone index exceeded 2,070 kPa (300 psi) in the top 7.6 cm (3 in.). Compaction had the greatest effect on sandy soil infiltration rates but there was little effect on infiltration rate resulting from an increase in soil-water content. In clay soils, compaction and soil-moisture content both negatively affected infiltration rates. Pitt et al. (2008) found that saturated and compacted clay soils resulted in little effective infiltration, while dry, noncompact, clay soils had relatively high infiltration rates. For dry, noncompact, clay soils, the mean field infiltration rate was 24.5 cm/h ($n=18$), where the mean infiltration rate for the other three conditions of clay soils was 0.5 cm/h ($n=60$) (Pitt et al. 2008). Akram and Kemper (1979) tested the impact of compaction on varying water contents in soils. Their research showed that as water content in the soil approached field capacity, the effect of compaction resulted in maximum bulk densities and minimum infiltration rates; therefore, construction activity should be avoided in saturated soils.

The objective of this project was to examine how the construction of bioretention cells impacted the in-situ soil's ability to exfiltrate stormwater, thus impacting groundwater recharge. This was accomplished by testing two different excavation techniques in two major soil types (sandy and clayey) and in two soil-moisture conditions (wet and dry). The infiltration rate, saturated hydraulic conductivity, bulk density, and level of compaction for each of the eight conditions were measured. The results from these data will be used to make recommendations for excavation techniques and conditions to promote the highest levels of exfiltration from bioretention cells.

8.3 CONSTRUCTION DESCRIPTION

An expert excavator who understood the importance of using consistency in the excavation techniques for the purposes of research was contracted for this project to construct the bioretention cells. The excavation techniques were a “rake” versus a “scoop” approach. Examples of the two methods can be seen in Fig. 8.1. The “rake” approach used the teeth of the backhoe bucket to scarify and till the surface, where the “scoop” technique had more smearing and compaction associated with it. The “scoop” technique is consistent with sewer and utility line placement where the surface is smoothed and compacted to minimize shifting and settling. Due to the maximum compaction levels from construction activity occurring between 20 to 30 cm (8 to 12 in.) below the surface of the impacted soil layer (Gregory et al. 2006), emphasis was placed on using consistency in technique for excavating the final 30 cm (12 in.) of soil to the desired bottom depth of the bioretention cell.



Figure 8.1: Photos demonstrating rake method (left) versus scoop method (right) for excavation.

The second phase studied was excavating in different soil-moisture conditions—wet soil versus dry soil. In order to test the difference of these conditions, excavation in dry soil took place after at least a week of dry, warm weather. To test for excavation in wet soil, the

top layer of soil was excavated, leaving approximately 30 cm (12 in.) of soil between the surface and the proposed bottom layer of the bioretention cell. An earthen berm was built around the testing area, and it was manually irrigated overnight to saturate the soil. By removing the top layer of soil, the soil at the proposed bottom layer of the bioretention cell became saturated quicker so final excavation could proceed on the following day. This replicated finishing excavation the day after rainfall. One cell was designated as the “wet” cell and the other was designated as the “dry” cell, and each of these was divided into two roughly equal sized sections to test the different excavation techniques. The soil cores and infiltration tests were each taken at three locations in each subplot, as noted in Fig. 8.2. Fig. 8.3 displays the layout of sampling equipment in the field.

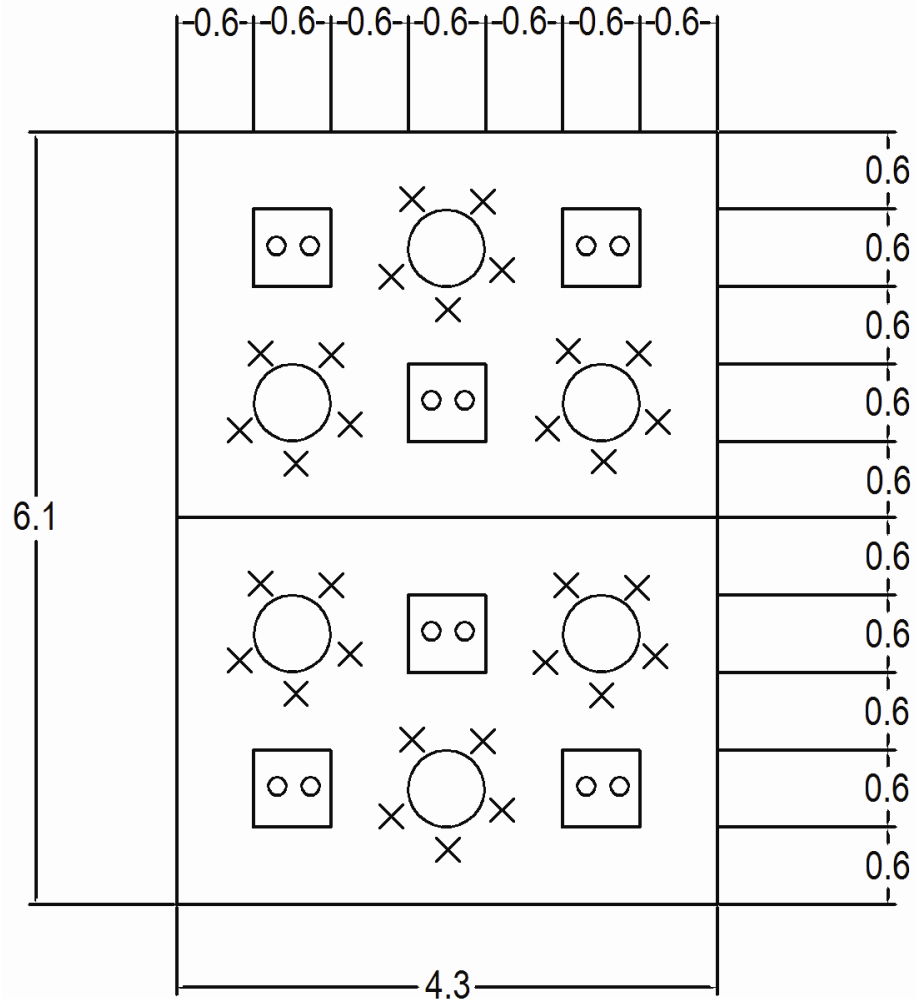


Figure 8.2: Overhead schematic of the soil testing layout. Its dimensions are 4.3 m by 6.1 m (14 ft by 20 ft) with 0.6 m (2 ft) spacing between each soil test site. The plot was split in half to test for the two excavation techniques. The large circles represent infiltration test sites and the X's represent soil compaction test sites. The small circles in the rectangular boxes indicate sites where soil cores were taken. All units are in meters.



Figure 8.3: Layout of soil cores (circles) and double-ring infiltrimeters (rectangles) in the field for the site that employed the scoop method. The soil texture from the rake method can be seen in the top of the photo.

Bioretention cells were constructed in an area of clay soil, representative of the Piedmont region of North Carolina (NCSU Lake Wheeler Field Research Facility in Raleigh), and in an area of sandy soil, representative of the Upper Coastal Plain of North Carolina (Nash County Agricultural Center in Nashville). The two cells constructed in Raleigh each received rooftop runoff from 255 m² (2,740 ft²). The watershed at the Nashville site was rather large [0.7 ha (1.8 acre)] but more permeable, so only one cell was constructed. The cell was separated into two parts by an internal berm to test the effects by excavating in wet versus dry soil. North Carolina design standards recommend a fill media depth of 0.6–1.2 m (2–4 ft) and 0.76 m (30 in) is recommended for nitrogen treatment (NCDENR 2007). Using this as guidance, a typical fill media depth of 0.6–0.9 m (2–3 ft) was used for this study to ensure the excavation depth was consistent with typical bioretention cell construction.

8.4 MONITORING METHODS

Prior to construction, three soil permeability tests were run at the site of each proposed bioretention cell and at the proposed final excavation depth, 0.9 m (3 ft). Soil permeability was tested using a compact constant head permeameter, commonly referred to as an Amoozemeter. This device is used to determine permeability in an unsaturated soil. The procedure for determining soil permeability followed Amoozegar (2006). Soil cores were also taken with a soil auger to determine soil texture at the site.

After excavation was complete, field testing took place. The order of testing was as follows: (1) soil samples were collected and weighed on-site to test for gravimetric moisture content of the soil at the time of construction; (2) double-ring infiltrometers and soil cores were placed at test sites to avoid foot traffic; (3) soil was tested for compaction; and (4) infiltration tests were run and soil cores were taken. Once these tests were completed, the cells were backfilled with gravel and bioretention fill media and there was no further testing at the site. For each combination of excavation technique, soil type, and soil moisture condition, there were two soil samples collected for measuring gravimetric soil-moisture content; six soil cores to test for hydraulic conductivity and bulk density; three infiltration tests; and 15 soil compaction measurements.

All of the soil tests were conducted prior to backfilling the bioretention cell with gravel and sandy fill media, so the reported infiltration rates are not the final infiltration rates. The final infiltration rates are lower than the reported values because of the impact of backfilling. Despite the reduced infiltration rates, the impact is not expected to be severe enough to negate the effects of excavation technique or soil moisture condition found in this study. Amerson et al. (1991) examined how compaction, fines, and contact area of gravel affected infiltration. Their main conclusion was that the fines associated with gravel were a greater problem than compaction by falling gravel or the contact area effect. Since North Carolina bioretention guidelines require washed gravel, the negative impact on infiltration from backfilling should be minimized. Small and large gravel, with median particle sizes of 1 cm (0.4 in.) and 3 cm (1.2 in.), respectively, were dropped from 1.2 m (4 ft). The results

showed that there was no statistical difference between measured infiltration rates from the “controlled” undisturbed soil and sites where small and large gravel were dropped (Amerson et al. 1991).

Infiltration rates were measured using double-ring infiltrometers. These rings had diameters of 30 and 61 cm (12 and 24 in.), and they were inserted 10 to 20 cm (4 to 8 in.) into the ground with care not to disturb the surface integrity. The procedure used followed a falling head test, similar to that performed by Bean et al. (2007). The double ring prevents divergent flow of water in layered soil from the middle ring by forcing water to travel in the vertical direction only (ASTM 2003). Tests were run for at least 90 min or until all of the water infiltrated, but steady state typically occurred within the first ten minutes or less. For cases when the initial infiltration was more rapid than the steady state rate, the initial couple data points were removed before calculating the least-squares line. The infiltration rates were determined by fitting the least-squares line to a plot of inner ring water depth versus time. An example of typical infiltration data are displayed in Fig. 8.4, as well as the linear regression line with corresponding equation and coefficient of determination (r^2). Of 24 infiltration tests, 14 had r^2 values greater than 0.98. For the four tests that had r^2 values less than 0.95, the water level drawdown was 5 mm or less in 90 to 120 min. Accuracy in reading a scale to the nearest millimeter on 10-min intervals accounts for the lower r^2 values. The drawback of the infiltrometer is that it only tests the infiltration at the surface layer, so soil cores were also taken to test for hydraulic conductivity in the laboratory. Similar to the study of Gregory et al. (2006), five cone index measurements were taken near each infiltration test site. A Spectrum Field Scout SC-900 hand cone penetrometer was used to measure compaction. This instrument did not work as well in clay soils because the range of the device was usually exceeded [greater than 6,200 kPa (900 psi)] at shallow depths.

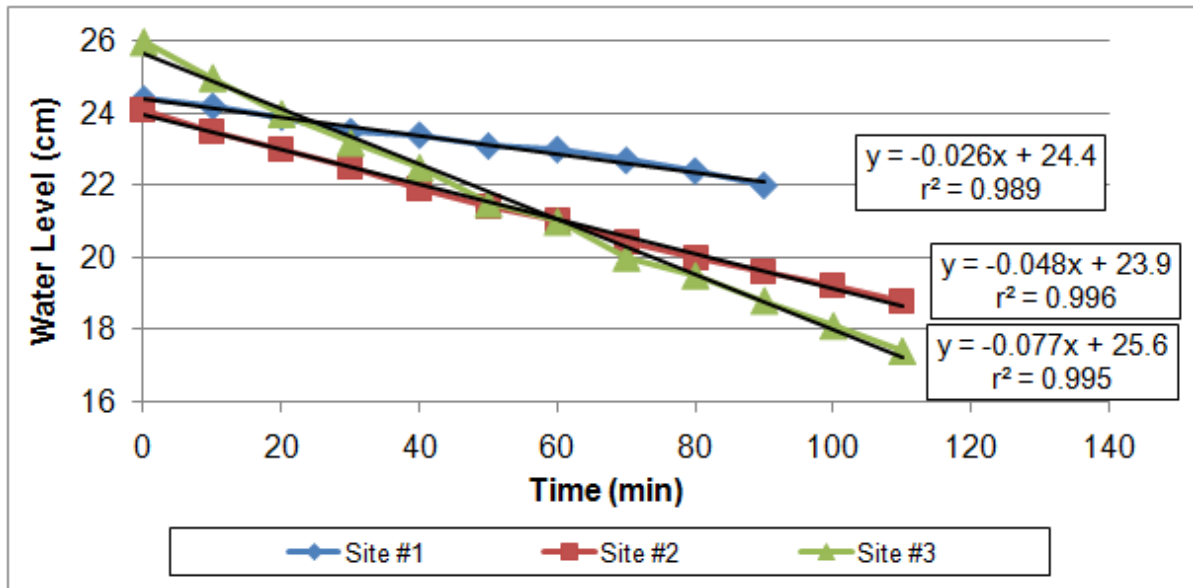


Figure 8.4: Typical graph of double-ring infiltrometer inner ring depths versus time. Linear regression lines were applied to the data to determine the surface infiltration rate. Data presented are specific to the dry, scoop test plot at the Nashville site.

The procedure to determine soil-moisture conditions followed ASTM D2216 (ASTM 2005), and the procedure from Klute (1986) was followed to determine saturated hydraulic conductivity. A constant head permeability test was performed on the 7.6 cm (3 in.) diameter soil cores to determine the saturated hydraulic conductivity. Afterwards, the cores were oven-dried at 110°C and weighed to determine the mass of the dry solids. Bulk density was calculated by dividing the mass of the dry solids by the known volume of the soil core. Following the tests, the soil from each set of two soil cores was mixed and particle size analysis tests were run on the mixed soil using the hydrometer method (Gee and Bauder 1986).

The pooled datasets for infiltration and saturated hydraulic conductivity were not normally distributed. A Box-Cox transformation was applied to the infiltration and saturated hydraulic conductivity data, with shift parameters of 0.22 and 0.44, respectively (Box and Cox 1964). Box-Cox transformation was used because it provided the most consistent variances, and Levene's test (homogeneity of variance test) showed Box-Cox to be the best

method of transformation. Once the transformed dataset was normally distributed, three-factor ANOVA was run using the statistical analysis package SAS, version 9.1.3. The pooled data were then separately analyzed in two categories, using two-factor ANOVA. In the first category, the data were separated by soil moisture condition (dry versus wet), and in the other category the data were separated by major soil type (sandy versus clayey). The impacts of the remaining two factors (excavation technique and soil type/soil moisture condition) were examined on infiltration and saturated hydraulic conductivity. Also, the first order interactions of the remaining two factors were analyzed to determine whether there was an effect or a constant difference across the factors.

8.5 RESULTS

8.5.1 Nashville (Sandy Soil Site)

Bioretention cell construction at the Nash County Agricultural Center, in Nashville, took place from August 2–3, 2008. The weather conditions for the two days during construction were mostly sunny with high temperatures above 36°C (97°F). In Nashville, N.C., the antecedent weather conditions for the two weeks prior to construction were hot and dry. The high temperature for the previous week ranged from 34–37°C (93–98°F). The weather data were collected at a rain gauge and ambient air temperature logger, located 1 km (0.6 mi) from the construction site, which was part of another ongoing monitoring project by NCSU. In the 9 days prior to excavation, the rain gauge only recorded 0.18 cm (0.07 in.) of rainfall on July 31. No overland runoff was observed, nor expected, from this one event. Due to the lack of rainfall, it was assumed that initial construction did indeed take place under dry soil conditions.

Initial soil cores were taken at depths of 1.2 m (4 ft), and they showed soils with high sand content. The results from six initial soil permeability tests, 90 cm (3 ft) below the surface in the proposed area for the bioretention cell was a mean permeability of 16.6 cm/h, with a standard deviation of 12.9. The reason for the high standard deviation was due to two of the sites having low permeability values (1.0 and 2.1 cm/h) because they had higher clay

content. During excavation, it was discovered that the region with higher clay content was more prevalent than anticipated. The soil texture, as classified by the USDA was loamy sand for the dry test plot and sand for the wet test plot. These two plots were separated by 1.5 m (5 ft). The average soil particle distribution from the test soil cores for the dry and wet test plots were 84.0% sand, 1.8% silt, and 14.2% clay; 91.5% sand, 4.0% silt, and 4.6% clay, respectively.

Gravimetric soil-moisture content was measured in the loamy sand layer and sandy layer immediately above it in the dry test plot. The average gravimetric soil-moisture content was 3.2% for the sand layer and 11.4% for the loamy sand layer, with standard deviations of 0.7 and 1.5%, respectively. The average gravimetric soil-moisture content of the samples in the wet cell was 9.4% with standard deviation of 0.7%. According to Pitt et al. (2008), both of these sites would have been classified as dry.

The results from the field and laboratory soil tests are displayed in Table 8.1. For both soil types tested, infiltration and saturated hydraulic conductivity were greater when the rake method was used. This is assumed to be due to higher levels of soil compaction associated with more scoop method bucket contact which consequently had higher soil bulk density. With higher levels of compaction and larger bulk densities, water movement through the soil slows down (Horton et al. 1994).

Table 8.1: Results from soil tests for hydraulic conductivity (K_{Sat}), surface infiltration, and dry bulk density for Nashville site.

Site	Type	K_{Sat} (cm/hr)			Infiltration (cm/hr) (n=3)		Bulk Density (kg/cm ³)		
		Ave.	Std. Dev.	<i>n</i> ^a	Ave.	Std. Dev.	Ave.	Std. Dev.	<i>n</i>
"Dry" / (loamy sand)	Scoop	3.98	3.58	4	3.0	1.5	1.74	0.068	4
	Rake	7.31	6.08	6	6.7	5.0	1.70	0.018	6
"Wet" / (sand)	Scoop	7.93	6.77	5	43.6	16.8	1.67	0.035	5
	Rake	21.6	7.45	6	61.9	26.5	1.61	0.035	6

^a It was later discovered that results from two of the soil cores from the "dry-scoop" test site and one of the cores from the "wet-scoop" test site were invalid due to cracks in the cores created during collection.

The rake versus the scoop construction methodologies were able to be tested in two situations: (1) a dry loamy sand soil and (2) a wet sandy soil. Hydraulic conductivity was greater by 84 and 172 percent for the dry and wet situations, respectively, when a rake methodology was used. Similarly, when using the rake method, the average surface infiltration rate was greater by 123 and 42 percent in the dry and wet situation, respectively. The cause for this improvement is partially explained by lower bulk densities associated with the rake methodology (Table 8.2).

Table 8.2: Changes in performance by using rake method over scoop method.

Site	Method for Improvement	Average Difference		
		K_{Sat}	Infiltration	Bulk Density
"Dry" / (loamy sand)	Excavation Technique - Rake	84%	123%	-2.4%
"Wet" / (sand)	Excavation Technique - Rake	172%	42%	-3.8%

The negative relationship of hydraulic conductivity versus dry bulk density is shown in Fig. 8.5. Larger bulk densities associated with the soil samples from the scoop method have lower hydraulic conductivities. Plotting the residuals of hydraulic conductivity versus the residuals of bulk density and taking into account the effects of excavation technique and soil-moisture condition, there was a statistically significant negative association of hydraulic conductivity to bulk density (p -value=0.017).

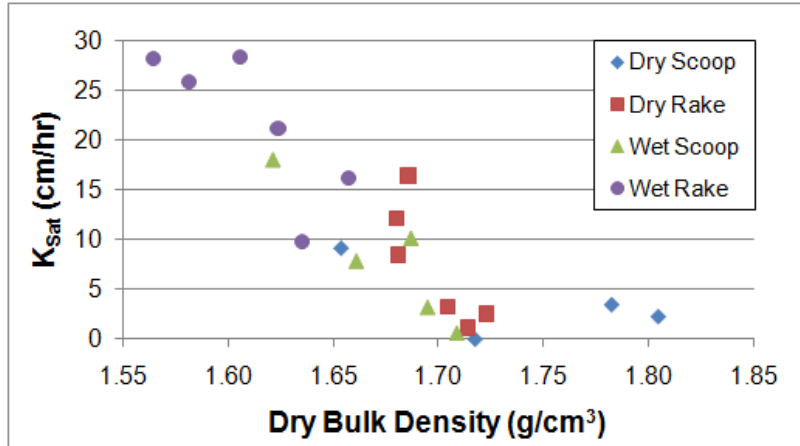


Figure 8.5: Saturated hydraulic conductivity versus dry bulk density for the Nashville site.

Scarifying the soil by using the teeth of the bucket improved exfiltration by helping to prevent a restrictive layer from forming. A graph of the average compaction levels found in the wet cell is displayed in Fig. 8.6, and it is apparent from this plot that the scoop method has higher levels of compaction. The average of the five compaction levels associated with each infiltration test is displayed in Table 8.3. Of the 12 infiltration tests, the four test sites that would be considered compacted by Pitt et al. (2008) were among the four lowest infiltration rates.

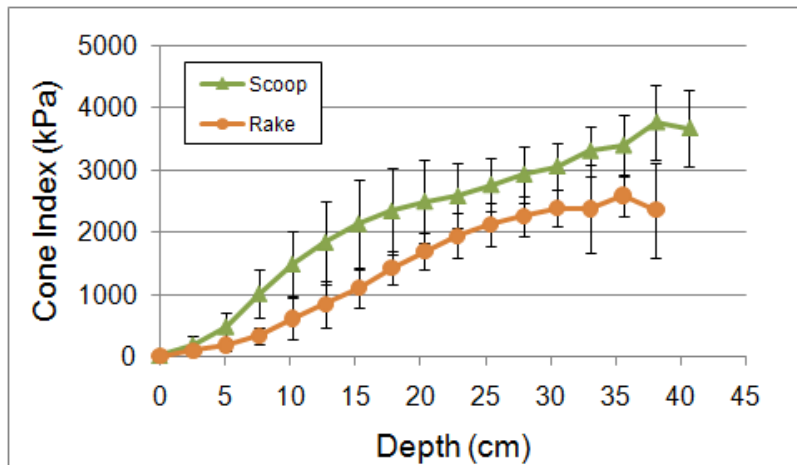


Figure 8.6: Average compaction levels in the “wet” cell test plot for the scoop versus rake excavation methods at the Nashville site with error bars that represent standard deviation.

Table 8.3: Average soil cone index for individual infiltration test sites with corresponding infiltration rates.

Test Plot	Depth (cm)	2.5	7.6	15.2	22.9	30.5	40.6	Infiltration (cm/hr)	High Comp ^a
	Test #	Average Soil Cone Index (kPa)							
Wet Rake	1	130	320	1100	2150	2530		83.5	
	2	90	320	850	1690	2300		32.4	
	3	100	420	1400	2010	2390	2600	69.9	
Wet Scoop	1	150	830	1540	2110	3150	4350	38.6	
	2	200	870	2280	2610	2980	3720	62.3	
	3	270	1380	2610	3040	3050	2910	29.8	
Dry Rake	1	560	2660	4650	4260	4360		3.4	X
	2	10	230	1250	2990	3280		12.5	
	3	550	3740	5840	6600			4.2	X
Dry Scoop	1	1030	3470	5000	4130	4130	5080	1.5	X
	2	340	2080	3280	3690	2870	2720	2.9	X
	3	360	1940	3410	3350	3370	2820	4.6	

^a High compaction if soil cone index > 2070 kPa in top 7.6 cm (Pitt et al. 2008).

8.5.2 Raleigh (Clay Soil Site)

Bioretention cell construction at Lake Wheeler Field Labs, in Raleigh, took place from October 10–12, 2008. The weather conditions for the three days during construction were cloudy with high temperatures exceeding 21°C (70°F). In Raleigh, the antecedent weather conditions for nine days prior to construction were warm and dry. The high temperature for the previous week ranged from 20–27°C (68–81°F). The first day of construction, there were light afternoon showers, with total rainfall amounts of 0.8 mm (0.03 in.), as reported from a nearby rain gauge monitored by the State Climate Office of NC— 0.8 km (0.5 mi) from the construction site. The only rain event that occurred during the 2 weeks prior to construction was 1.12 cm (0.44 in.) event during the morning of October 1st—9 days prior to construction. To avoid having light rain affect the soil moisture condition of the dry cell, a plastic sheet was placed over the site of construction and the surrounding area. No

overland runoff was observed nor expected from this one event. Due to the lack of rainfall, it was assumed that initial construction did indeed take place under dry soil conditions.

Soils with high clay content were found when taking initial soil cores at this site. The results from six initial soil permeability tests showed soils with very low permeability. Three tests were run at each of the future bioretention cells location and at an approximate depth of the bottom of the cell. The dry cell had an average predisturbance permeability of 0.88 cm/day with a standard deviation of 0.11 cm/day, while the wet cell had an average predisturbance permeability of 0.69 cm/day with a standard deviation of 0.72 cm/day. The magnitude of the predisturbed permeability was much less than the saturated conductivity values found after excavation. A possible explanation for the variation could be due to smearing that may have occurred while augering boreholes to test for predisturbed permeability. The variation could also be as a result of continuous macropores present in the soil cores that were taken after excavation (Bouma 1982).

The average gravimetric soil-moisture content for the dry cell was 21.8% with standard deviations of 7.6%. The average gravimetric soil-moisture content for the wet cell was 28.7% with standard deviation of 1.8%. According to Pitt et al. (2008), both of these sites would have been classified as wet. Despite the extended dry period, the clay subsoil did not drain as fast as the sandy soil so the soil maintained higher water content.

The results from the field and laboratory soil tests are displayed in Table 8.4. Similar to the results from the Nashville site, infiltration and saturated hydraulic conductivity were greater when the rake method was used. This is also assumed to be due to higher levels of soil compaction associated with more scoop method bucket contact. In Table 8.4, the average saturated hydraulic conductivities are three to four times greater than the average infiltration rates. The discrepancy between these two measurements could be explained by the presence of macropores. When measuring saturated hydraulic conductivity in soil horizons that have continuous macropores, the impact on the range of hydraulic conductivity was up to a factor of 200 for the one soil type tested (Bouma, 1982). Infiltration tests are performed in the field, so if macropores exist, they will draw the water down fast initially, but would slow down and

approach steady state once the macropores are full of water. Bouma (1982) observed a steady infiltration rate occurred after 5 min which was consistent with the measured infiltration data. Based on these results, the field measured infiltration rate would be more representative of the conditions that will control exfiltration through the bottom of the bioretention cell.

Table 8.4: Results from soil tests for hydraulic conductivity (K_{Sat}), infiltration, and dry bulk density for Raleigh site.

Site	Type	K_{Sat} (cm/hr)			Infiltration (cm/hr) (n=3)		Bulk Density (kg/cm ³)		
		Ave.	Std. Dev.	<i>n</i> ^a	Ave.	Std. Dev.	Ave.	Std. Dev.	<i>n</i>
"Dry" / (clay)	Scoop	1.81	2.13	4	0.4	0.5	1.48	0.090	6
	Rake	2.29	2.88	6	0.8	0.5	1.63	0.075	6
"Wet" / (clay)	Scoop	0.62	0.77	5	0.2	0.1	1.37	0.103	6
	Rake	4.37	5.65	6	1.2	0.3	1.17	0.054	6

^a It was later discovered that results from two of the soil cores from the "dry-scoop" test site and one of the cores from the "wet-scoop" test site were invalid due to cracks in the cores created during collection.

The four combinations of soil type/soil condition for the excavation technique methodologies at this site were: (1) rake method for a dry sandy loam soil with clay subsoil; (2) scoop method for a dry clay soil; and (3) and (4) rake and scoop methods for a wet clay soil. When the rake methodology was used under wet soil conditions, hydraulic conductivity and infiltration rate were 605 and 400 percent greater, respectively, compared to when the scoop methodology was used. When excavation took place using the scoop methodology, hydraulic conductivity and infiltration rate were 192 and 79 percent greater, respectively, when excavation took place under dry conditions compared to wet conditions (Table 8.5).

Table 8.5: Changes in performance by varying excavation technique and soil moisture condition.

Site	Method for Improvement	Average Difference		
		K_{Sat}	Infiltration	Bulk Density
"Scoop" / (clay)	Soil Moisture Condition - Dry	192%	79%	8.0%
"Wet" / (clay)	Excavation Technique - Rake	605%	400%	-14.5%

When using the rake method in the dry cell, despite higher infiltration and hydraulic conductivity, the bulk density was larger. It is assumed that this was due to lower clay content in the soil at the test site. The average soil composition for the rake and scoop method for the dry cell were 75.5% sand, 16.4% silt, and 8.0% clay; and 35.8% sand, 12.4% silt, and 51.9% clay, respectively. As classified by the USDA, the texture of the soil of the rake method was sandy loam, and the texture of the soil of the scoop method was clay. Also, the soil texture of the wet cell was clay for both excavation techniques with an average soil composition of 24.7% sand, 9.6% silt, and 65.8% clay. The average of the five compaction levels associated with each infiltration test is displayed in Table 8.6. All the test sites would be considered compacted by Pitt et al. (2008).

Table 8.6: Average soil cone index for individual infiltration test sites with corresponding infiltration rates.

Test Plot	Depth (cm)	2.5	7.6	12.7	Infiltration (cm/hr)	High Comp. ^a
	Test #	Average Soil Cone Index (kPa)				
Wet Rake	1	491	4191	5090	1.0	X
	2	469	3417	4148	1.1	X
	3	323	2645	4930	1.5	X
Wet Scoop	1	927	3074	4302	0.3	X
	2	1579	4211	4886	0.2	X
	3	1227	4602	5619	0.2	X
Dry Rake	1	298	3150	4891	1.2	X
	2	1931	4827	6206	0.2	X
	3	429	3010	5684	0.9	X
Dry Scoop	1	201	2758	3587	1.0	X
	2	333	3916	4316	0.3	X
	3	1345	4392	4897	0.0	X

^a High compaction if soil cone index > 2070 kPa in top 7.6 cm (Pitt et al. 2008).

8.5.3 Combined Results

The datasets were pooled to test the impacts that excavation technique, soil moisture condition, soil type, and interactions among the three had on infiltration and saturated hydraulic conductivity. The p -values for the combinations based on soil condition are presented in Table 8.7. Analyzing the data based on soil moisture condition showed there is a significant impact of excavation technique on infiltration and saturated hydraulic conductivity for the wet condition (p -values=0.034 and 0.005, respectively), but there is no significant impact for the dry condition. The interaction of excavation technique and soil type is greater than 0.05 for all cases so there is a constant difference across these factors, meaning that the same type of impact is observed in both clay and sandy soils for the rake method and for the scoop method of excavation.

Table 8.7: Effects of soil condition on infiltration and saturated hydraulic conductivity (p-values).

Factor (Soil Condition – dry vs. wet)	Excavation Technique (rake vs. scoop)	Excavation Technique & Soil Type
Infiltration (dry)	0.156	0.925
K _{Sat} (dry)	0.508	0.573
Infiltration (wet)	0.034	0.476
K _{Sat} (wet)	0.005	0.623

The *p*-values for the combinations based on soil type are presented in Table 8.8. Analyzing the data based on soil type showed there is a significant impact of excavation technique on saturated hydraulic conductivity in sandy soil (*p*-value=0.024) and infiltration rate in clay soil (*p*-value=0.046), but there is no significant impact on infiltration rate in sandy soil or saturated hydraulic conductivity in clay soil. There was no effect on soil condition in the clay site but there was a significant impact on infiltration and saturated hydraulic conductivity at the sandy site. This is due to the dry cell having higher clay content. According to the USDA classification system, the soil texture of the wet and dry cells were sand and loamy sand, respectively. Finally, the interaction of excavation technique and soil condition is greater than 0.05 for all cases. This means that the same type of impact is observed in both wet and dry soil for the rake method and for the scoop method of excavation.

Table 8.8: Effects of soil type on infiltration and saturated hydraulic conductivity (p-values).

Factor (Soil Type – clay vs. sand)	Excavation Technique (rake vs. scoop)	Soil Condition (dry vs. wet)	Excavation Technique & Soil Condition
Infiltration (clay)	0.046	0.521	0.600
K _{Sat} (clay)	0.173	0.952	0.202
Infiltration (sand)	0.150	<0.0001	0.844
K _{Sat} (sand)	0.024	0.030	0.222

The hydrological significance of excavating bioretention cells under ideal conditions is the water in the media will be able to drawdown and fully empty in a shorter time period. The impact on performance will have the greatest effect for bioretention cells that include an internal water storage zone or for those constructed without underdrains because faster drawdown will allow for more available storage volume in the media to fully capture more events or larger portions of events. Prior to backfilling the cell with gravel and sand, the impact of using the rake method for excavation in dry loamy sand (Table 8.2) and in wet clay (Table 8.5) can allow for the infiltration rate to be two and four times greater, respectively, than when the scoop method is used. This could potentially lead to complete drawdown occurring up to two to four times faster if ideal excavation techniques and conditions are used. Li et al. (2009) and Passeport et al. (2009) showed that an internal water storage zone is capable of completely capturing events without generating outflow. For consecutive events over a short period of time, performance is reduced because the water storage zone is not completely drained (Li et al. 2009). Through use of innovative construction techniques, the water storage zone could drain faster and fully capture or capture more of the following event. Another case is for bioretention constructed without underdrains like that in Emerson and Traver (2008). The bioinfiltration traffic island was constructed by mixing the in-situ soil with sand. If innovative construction techniques are used, runoff can drain from the sandy media faster and allow for availability of more storage volume in the media and create a larger driving pressure head.

8.6 CONCLUSIONS

Based on the data collected, it was determined that excavating the final 30 cm (12 in.) using the teeth on the bucket to rake the surface, instead of using the bucket to scoop and make the surface smooth, improved the soil properties that govern infiltration. The rake method scarified the bottom layer in the bioretention cell and prevented compaction and reduction of pore spaces, which is evidenced by smaller average bulk densities. This helped promote the underlying soil's ability to exfiltrate water from bioretention cells to the underlying soils. The potential for exfiltration was reduced when using the scoop method

because it compacted the soils to a greater extent, as evidenced by higher bulk densities. With higher exfiltration rates, the volume of water entering the storm drain network is expected to decrease, thus reducing pollutant load.

In particular, when excavating in wet conditions, the hydraulic conductivity and infiltration rate associated with the scoop method were significantly less than that of the rake method (p -values=0.005 and 0.034, respectively). Under dry conditions, there was no statistical significance associated with excavation technique, but the trend showed improved infiltration and hydraulic conductivity when using the rake method. The hydraulic conductivity associated with the scoop method of excavation were significantly less at the sandy soil sites (p -value=0.024), and the infiltration rate associated with the scoop method of excavation was significantly less at the clay soil sites (p -value=0.046). Based on the results of this study and because there is no extra cost associated with the rake method, it is recommended to use the rake excavation technique in preference to the “conventional” scoop method for future bioretention or other infiltration BMP projects to decrease outflow volume and pollutant loads. The same recommendation of scarifying the soil surface with the teeth of the bucket can also be applied to the side walls of the excavated pit to promote exfiltration from the sides of bioretention cells.

For pure sand environments, because of extremely high infiltration rates and hydraulic conductivities, excavation may take place under wet or dry soil conditions. For clay to loamy sand, however, excavation during a dry soil condition is recommended. The infiltration rates were less impacted in dry soil compared to wet soil. In general, excavation should be avoided during or immediately following a rainfall event, or if a rainfall event will occur before the cell’s media can be replaced. The authors encourage readers to verify that the “rake” method complies with local code.

8.7 ACKNOWLEDGEMENTS

The writers acknowledge the Cooperative Institute for Coastal and Estuarine Environmental Technology (CICEET) for funding this project. Thanks to the NCSU faculty,

Dr. Aziz Amoozegar, Dr. Greg Jennings, Dr. Wayne Skaggs, and Dr. Jason Osborne. The writers sincerely appreciate Joe Wright for his help in excavating the bioretention cells exactly how they needed to be. Thanks to everyone involved with this project at the Lake Wheeler Research Facility and Nash County Agricultural Center for their cooperation, in particular Mike Wilder, Bill Lord, Joni Tanner, Ken Snyder, and Todd Marcom. Also thanks to the NCSU staff and students, Jess Roberts, Ryan Winston, Jon Hathaway, Brian Phillips, Wilson Huntley, Chris Niewoehner, Shawn Kennedy, Jackie McNett, Natalie Gurkin, and “little” Bill Hunt for their assistance.

8.8 REFERENCES

- Akram, M., and Kemper, W. D. (1979). “Infiltration of soils as affected by the pressure and water content at the time of compaction.” *Soil Science Society of America Journal*, 43(1), 1080–1086.
- Amerson, R. S., Tyler, E. J., and Converse, J. C. (1991). “Infiltration as affected by compaction, fines, and contact area of gravel.” *Proceedings, 6th National Symposium on Individual and Small Community Sewage Systems: On-site Wastewater Treatment*, American Society of Agricultural Engineers, St. Joseph, Mich., 214–222.
- Amoozegar, A. (2006). “Amoozometer.” *Encyclopedia of soil science*, R. Lal, ed., Taylor and Francis, London, 86–92.
- ASTM. (2003). “Standard test method for infiltration rate of soils in field using double-ring infiltrometer.” *ASTM D3385-03*, West Conshohocken, Pa.
- ASTM. (2005). “Standard test methods for laboratory determination of water (moisture) content of soil and rock by mass.” *ASTM D2216-05*, West Conshohocken, Pa.
- Bean, E. Z., Hunt, W. F., and Bidelspach, D. A. (2007). “Field survey of permeable pavement surface infiltration rates.” *Journal of Irrigation and Drainage Engineering*, 133(3), 249–255.
- Bouma, J. (1982). “Measuring the hydraulic conductivity of soil horizons with continuous macropores.” *Soil Science Society of America Journal*, 46(1), 438–441.
- Box, G. E., and Cox, D. R. (1964). “An analysis of transformations.” *Journal of the Royal Statistical Society*, 26(B), 211–246.

- Chesapeake Bay Program. (2008). "Air and water pollution." *Bay pressures*, <<http://www.chesapeakebay.net>> (Oct. 23, 2008).
- Clark, S. E., and Pitt, R. (2007). "Influencing factors and a proposed evaluation methodology for predicting groundwater contamination potential from stormwater infiltration activities." *Water Environment Research*, 79(1), 29–36.
- Davis, A. P., Shokouhian, M., Sharma, H., and Minami, C. (2001). "Laboratory study of biological retention for urban stormwater management." *Water Environment Research*, 73(1), 5–14.
- Davis, A. P. (2008). "Field performance of bioretention: Hydrology impacts." *Journal of Hydrologic Engineering*, 13(2), 90–95.
- Davis, A. P., Hunt, W. F., Traver, R. G., and Clar, M. E. (2009). "Bioretention technology: Overview of current practice and future needs." *Journal of Environmental Engineering*, 135(3), 109–117.
- Dierkes, C., and Geiger, W. F. (1999). "Pollution retention capabilities of roadside soils." *Water Science and Technology*, 39(2), 201–208.
- Emerson, C. H., and Traver, R. G. (2008). "Multiyear and seasonal variation of infiltration from storm-water best management practices." *Journal of Irrigation and Drainage Engineering*, 134(5), 598–605.
- Gee, G. W., and Bauder, J. W. (1986). "Particle-size analysis." *Methods of soil analysis. Part 1: Physical and mineralogical methods*, A. Klute, ed., Soil Science Society of America, Madison, Wis., 383–411.
- Gimenez, D. C., Dirksen, R., Miedema, L. A., Eppink, A. J., and Schoonderbeck, D. (1992). "Surface sealing and hydraulic conductances under varying-intensity rains." *Soil Science Society of America Journal*, 56(1), 234–242.
- Gregory, J. H., Dukes, M. D., Jones, P. H., and Miller, G. L. (2006). "Effect of urban soil compaction on infiltration rate." *Journal of Soil and Water Conservation*, 61(3), 117–124.
- Horton, R., Ankeny, M. D., and Allmaras, R. R. (1994). "Effects of compaction on soil hydraulic properties." *Soil compaction in crop production*, B. D. Soane and C. van Ouwerkerk, eds., Elsevier Science, London, 141–165.
- Hunt, W. F., Jarrett, A. R., Smith, J. T., and Sharkey, L. J. (2006). "Evaluating bioretention hydrology and nutrient removal at three field sites in North Carolina." *Journal of Irrigation and Drainage Engineering*, 132(6), 600–608.

- Jones, M. P., and Hunt, W. F. (2009). "Bioretention impact on runoff temperature in trout sensitive waters." *Journal of Environmental Engineering*, 135(8), 577– 585.
- Klute, A. (1986). "Water retention: Laboratory methods." *Methods of soil analysis. Part 1: Physical and mineralogical methods*, A. Klute, ed., Soil Science Society of America, Madison, Wis., 635–662.
- Kwiatkowski, M., Welker, A. L., Traver, R. G., Vanacore, M., and Ladd, T. (2007). "Evaluation of an infiltration best management practice utilizing pervious concrete." *Journal of the American Water Resources Association*, 43(5), 1208–1222.
- Li, H., Sharkey, L. J., Hunt, W. F., and Davis, A. P. (2009). "Mitigation of impervious surface hydrology using bioretention in North Carolina and Maryland." *Journal of Hydrologic Engineering*, 14(4), 407–415.
- N.C. Department of Environment and Natural Resources (NCDENR). (1994). *Tar-Pamlico basinwide water quality management plan: December 1994*, North Carolina Department of Environmental and Natural Resources, Division of Water Quality, Raleigh, N.C.
- N.C. Department of Environment and Natural Resources (NCDENR). (2007). "Chapter 12: Bioretention." *Stormwater best management practices manual*, North Carolina Department of Environment and Natural Resources, Division of Water Quality, Raleigh, N.C., 12.1–12.31.
- Passeport, E., Hunt, W. F., Line, D. E., Smith, R. A., and Brown, R. A. (2009). "Field study of the ability of two grassed bioretention cells to reduce storm-water runoff pollution." *Journal of Irrigation and Drainage Engineering*, 135(4), 505–510.
- Pitt, R., Chen, S., and Clark, S. (2002). "Compacted urban soils effects on infiltration and bioretention stormwater control designs." *Proceedings, 9th International Conference on Urban Drainage*, ASCE, Reston, Va..
- Pitt, R., Chen, S., Clark, S., Swenson, J., and Ong, C. (2008). "Compaction's impacts on urban storm-water infiltration." *Journal of Irrigation and Drainage Engineering*, 134(5), 652–658.
- Pitt, R., Clark, S., and Field, R. (1999). "Groundwater contamination potential from stormwater infiltration practices." *Urban Water*, 1, 217–236.
- Radcliffe, D. E., West, L. T., Hubbard, R. K., and Asmussen, L. E. (1991). "Surface sealing in coastal plains loamy sands." *Soil Science Society of America Journal*, 55(1), 223–227.

- Shuster, W. D., Gehring, R., and Gerken, J. (2007). "Prospects for enhanced groundwater recharge via infiltration of urban storm water runoff: a case study." *Journal of Soil and Water Conservation*, 62(3), 129–137.
- Tyner, J. S., Wright, W. C., and Dobbs, P. A. (2009). "Increasing exfiltration from pervious concrete and temperature monitoring." *Journal of Environmental Management*, 90(8), 2636–2641.
- U.S. Environmental Protection Agency (USEPA). (2007). "National water quality inventory: Report to Congress—2002 reporting cycle." *Rep. No. EPA 841-R-07-001*, USEPA, Washington, D.C.

9 RECOMMENDATIONS FOR FUTURE WORK

This research has described the benefits and drawbacks in performance for various bioretention design specifications. One key parameter that increased performance was constructing cells in sandier underlying soils because the soils promoted higher exfiltration rates. This led to greater outflow reduction and pollutant load reduction. However, no research has focused on the fate of runoff and treatment potential after runoff exfiltrates into surrounding soils. Is there any potential for further treatment after the water enters the underlying soil, or would the water be contaminating otherwise clean groundwater? Bioretention cells are typically installed to treat parking lot or rooftop runoff, and some of the pollutants of concern from these areas are heavy metals and oil/grease. With previous research showing that these are mostly trapped within the top 0.2 m of the bioretention media, exfiltrated water is expected to be “clean.” However, dissolved nutrients [such as orthophosphate (Ortho-P) and nitrate plus nitrite ($\text{NO}_{2,3}\text{-N}$)] would most likely be washed through the filter media. Perhaps groundwater will pass through a riparian buffer before entering the surface water; however, the specific fate of dissolved nutrients is unknown.

This research demonstrated that a longer hydraulic residence time of runoff in the filter media increased nitrogen treatment. The data showed that the cell with an internal water storage (IWS) zone and sandy clay loam underlying soil had better concentration reductions than (1) the cell with an IWS zone and sand underlying soil and (2) both sets of cells that had conventional drainage. Therefore, an IWS zone would be preferred over conventional drainage for nitrogen treatment. A potential drawback of using IWS is when the IWS zone is unable to completely drain between events. If the underlying soils have a low hydraulic conductivity, the bottom portion of the media may remain saturated most of the time, leading to increased outflow volume. The reason for increased outflow volume is due to the IWS zone configuration reducing the hydraulic gradient from the underdrains. This could limit the infiltration rate and result in increased overflow volume. A method for designers to weigh options of increased outflow volume vis-a-vis potential water quality

treatment for various IWS design configurations and IWS zone depths is to use DRAINMOD. During the design process, a balance must be struck between water quality treatment and hydrologic performance. The Rocky Mount data showed that bioretention cells with underlying soils that ranged from sandy clay loam to sand should have the IWS zone maximized (while still including a small aerobic zone (outlet to be set no closer than 0.3 m (1 ft) from the surface of the media)). For all of the other soils types, DRAINMOD could be used to determine the ideal IWS depth.

Since hydraulic residence time is very important for water quality treatment, a design modification of metering the outflow from the underdrains would keep runoff in the media for longer durations of time. However, water must be released at a rate fast enough to allow enough storage for subsequent events. This type of design was modeled in DRAINMOD using a decreased drainage coefficient.

Similar to balancing water quality and hydrologic performance for individual cells, physical and chemical performance should also be balanced for bioretention cells in series with other stormwater control measures. The additional benefits of flow rate and outflow reduction and water quality treatment also need to be balanced with cost. Future questions about installing bioretention in series with other practices include: (1) the type of practice bioretention should be paired with and (2) whether the other practice should utilize different treatment mechanisms. Different practices in series with bioretention could be field monitored; however, a hydrologic model that incorporates cost is needed to better understand the cost to benefit ratio.

Since the difference in performance for the two cells at Rocky Mount was more related to the varying underlying soils, research is still needed to explore how vegetation type impacts treatment. This would ideally be completed as a laboratory study because of the increased uncertainty of other factors in field studies (as experienced at Rocky Mount). It could be possible that if sod is used and it includes a layer of underlying soil from the sod nursery, it could be primed with microbes and have different levels of treatment as compared to mulch. Also, it is important for future field studies to measure the initial and final

chemical characteristics of the media and of the mulch or soil associated with sod. This will increase understanding of the fate and sources of different pollutants and to more accurately compute mass balances. Also, to better understand the processes taking place in the media during and between events, it is recommended to collect storm samples from consecutive events, as described in Chapter 5. Additionally, samples could be collected at different periods during the same storm. Although it could not be verified that the Nashville site was fertilized, some additional source was introduced that resulted in net export of Ortho-P and $\text{NO}_{2,3}\text{-N}$. Therefore, it is important for designers and regulators to make certain that those maintaining these cells do not add unnecessary sources of nutrients, such as fertilizers.

As this dissertation was the first attempt to model bioretention cells using DRAINMOD, there is a lot of potential to continue to evolve this application and to test it for other sites. For future calibration efforts, a longer continuous dataset where the site characteristics are not altered halfway through would be preferred. This will allow for longer calibration and validation periods. For future projects, it is recommended to measure water table depths within the bioretention cell at the midpoint between the drains, instead of in the standpipe from the IWS zone outlet. This worked for the Rocky Mount site because the hydraulic conductivity was higher than typical bioretention media. Drawbacks of the water table monitoring at Rocky Mount were that measurements were invalid when the water table was above the top of the IWS zone and below the gravel layer. To avoid these issues, it is recommended to install deeper wells beneath the bottom of the bioretention cell. This will allow for better understanding of seepage properties.

APPENDICES

A. APPENDIX: USER'S MANUAL FOR MODELING BIORETENTION WITH DRAINMOD

Background

The steps described in this section can be followed to model the hydrologic response of runoff entering a bioretention cell using DRAINMOD. Suggestions for model inputs for typical conditions of bioretention cells in North Carolina are provided. However, stronger model agreement to the actual response of a bioretention cell can be achieved through collection of site specific information. One method to measure the hydrologic response is to measure the water table depth at the midpoint between the drains. From the author's experience, measuring water table recession within the media for a conventionally drained bioretention cell is a difficult task because of the short hydraulic residence time, and currently, the shortest time period output in DRAINMOD is daily. For a conventional drainage design, it would be more appropriate to monitor the volume of runoff, drainage, and overflow from several events that are of varying size and use these volumes to compare to the modeled results.

As mentioned in Chapter 7, drainage rates are computed using Kirkham's equation (when there is surface ponding and the media is saturated) and Hooghoudt's equation (when the water table is below the surface). Water table fluctuations are computed using two water balance equations, where one is for a section of soil of unit surface area which extends from the impermeable layer to the surface at the midway point between the drains and the other is for the amount of runoff and storage on the surface. Even though the shortest output time period for water table depth is daily, DRAINMOD normally computes water table fluctuations and drainage rates on an hourly basis. However, it also computes at time increments of 0.05 hours or less when the rainfall rate exceeds the infiltration capacity. When there is rapid drainage and no rainfall, the time increment is increased to 2 hours. Finally, with slow drainage and ET rates and no rainfall, the time increment is increased to daily. More detailed information about DRAINMOD's governing equations, model

components, how various model utilities (weather, soil, and contributing area runoff) function, and ways to measure model input parameters are provided in the DRAINMOD Reference Report (Skaggs 1980), Skaggs (1991), and the DRAINMOD Help File that is associated with the program.

Step 1: Opening a File

Open DRAINMOD, and in the “*Project*” heading, select “*Open Project.*” Open any existing project file (.prj); an example is *DHP.pri*.

Step 2: Creating a Contributing Area Runoff File

In the “*Project*” heading, select “*Save As.*” In the dropdown menu, select the .prj file, and select “*Save File(s).*” Give the file a unique name, such as, ‘BRContArea,’ and select “*Save.*” In the pop-up, “*Would you like to save both the .prj and .gen files?,*” select “*Yes.*” In the next pop-up, “*Would you like to open the saved .prj file as a new project?,*” select “*Yes.*” Then the user interface will appear (Fig. A.1). This new project will be used to simulate runoff from an impervious contributing surface area (bioretention cell drainage area). The user can enter a unique project description, and must select the following boxes highlighted in Fig. A.1: (1) “*Project Type: Hydrology,*” (2) “*PET: Thornthwaite,*” (3) “*Subsurface Water Mgmt.: Conventional Drainage,*” (4) “*Output Options: Hydrology: Daily, Monthly, Yearly and Rankings,*” and (5) “*Output Options: Hydrology: Hourly Surface Runoff / Water Loss (Surface Runoff).*” Additionally, the user will need to select appropriate start and end periods based on the period of interest and the length of time of available weather information.

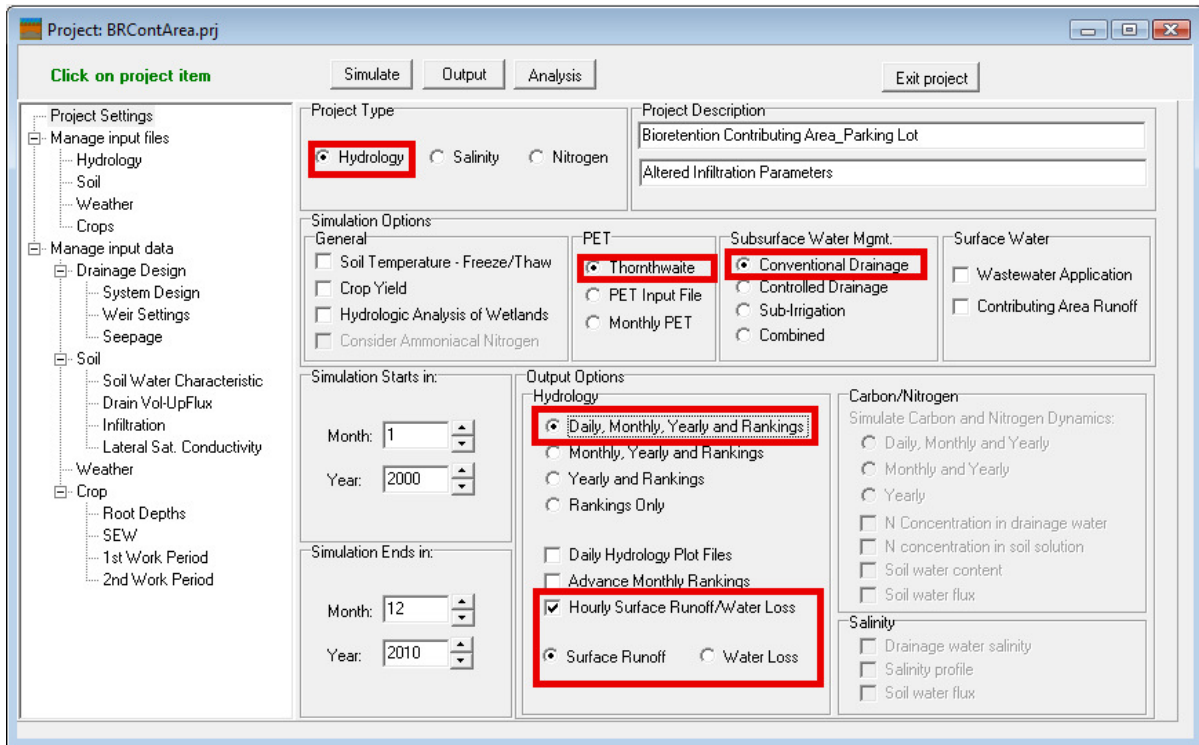


Figure A.1: User interface for contributing area runoff file.

Step 3: Creating Weather Files

The user either needs to select existing weather files or create new files using the DRAINMOD utility function for creating a weather file. In this utility, the user can create temperature, rainfall, or potential evapotranspiration (PET) files. As highlighted in Fig. A.2, the DRAINMOD utilities (weather, soil, and contributing area runoff) are used to create the necessary input files (weather, soil, and hydrology) to run the model.

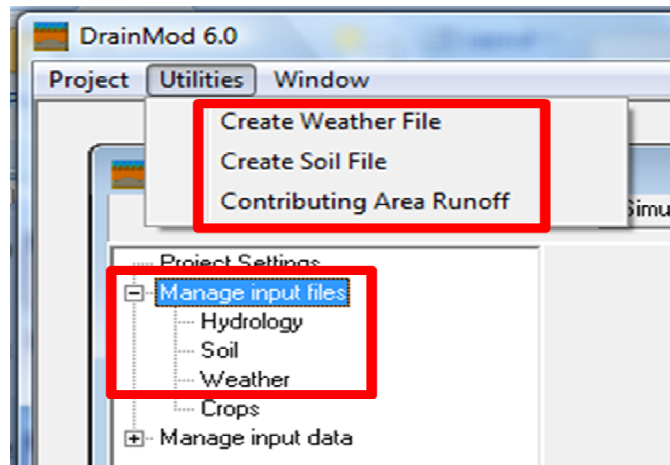


Figure A.2: Location of DRAINMOD utilities and input files.

If creating new weather files, the required data include: (1) daily maximum air temperature, (2) daily minimum air temperature, and (3) either hourly or daily rainfall depth. Using hourly rainfall measurements will provide more precision to properly model runoff to and infiltration into the bioretention cell; however, with some long-term climate monitoring stations, hourly measurements are not always available. Hourly rainfall measurements are typically available for long durations (i.e. 60 years) at airport weather stations. The following website, <http://www.ncdc.noaa.gov/oa/climate/stationlocator.html/>, through the National Climatic Data Center, a part of the National Oceanic and Atmospheric Administration, provides hourly rainfall records at some sites that date back prior to 1950.

If daily rainfall depths are used, the model evenly distributes rainfall for a specified duration and period of the day. The median rainfall duration for the Rocky Mount, NC site was 6.7 and 6.4 hours for the first and second monitoring periods, respectively, so it would be recommended to distribute the rainfall over 6 hours for sites with a similar climate. This number should be based on what the typical rainfall duration is expected to be for the location of the site. In the subroutine for PET, the daily PET is distributed for the 12 hours between 6:00 a.m. and 6:00 p.m., and if rainfall is occurring, PET equals 0. So, as a way to avoid overestimating or underestimating the amount of ET that actually occurs over the period of the simulation, assume that the rainfall hours should be distributed to evenly split

Once the appropriate *.wea* files are created, the weather utility can be used to create the temperature (*.tem*) and rainfall (*.rai*) files needed to run in DRAINMOD. The interface for the weather utility is shown in Fig. A.4. The first step is to browse for the appropriate *.wea* file. Once chosen, select the appropriate weather variable and units. As discussed earlier, for daily rainfall, there is the option for the duration to distribute daily rainfall, and its starting hour. After these tasks are complete, select “*Create*,” and the utility will create either a *.rai* file for rainfall or a *.tem* file for temperature. These files can then be selected in the tab “*Manage Input Files: Weather*.”

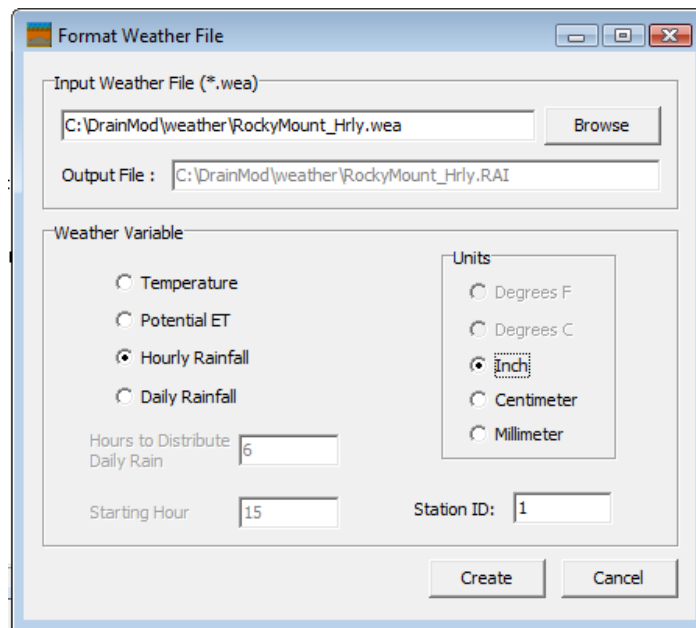


Figure A.4: Interface of DRAINMOD weather utility.

There are a few options to include PET calculations in DRAINMOD. If the region of interest has detailed meteorological data, PET can be calculated with whichever method is desired and enough data exists for. The simplest method to calculate PET is using the Thornthwaite method; however, it is not as precise as other methods because it has the fewest number of inputs. This method only requires mean monthly air temperature. The mean monthly air temperature is used to calculate the heat index from the site. The calculation of

heat index (I) is described in Equation A.1, where T_i is the mean monthly temperature in degrees Celsius. Daily PET values were estimated using the daily maximum and minimum temperatures and the calculated heat index.

$$I = \sum_{i=1}^{12} \left(\frac{T_i}{5} \right)^{1.514} \quad (\text{A.1})$$

In DRAINMOD, there is an option to include monthly correction factors for the Thornthwaite method to improve accuracy of the daily PET estimates. Amatya et al. (1995) calculated correction factors for three sites in eastern North Carolina (Tarboro, Carteret, and Plymouth). Tarboro is the closest site and is within 35 km of both field sites presented in this dissertation (Rocky Mount and Nashville). Table A.1 presents the Thornthwaite PET correction factors for Tarboro and for the average of three stations in eastern NC (Amatya et al. 1995). If the Thornthwaite method is used to calculate PET, enter the following information in the “*Manage Input Data: Weather*” tab: (1) latitude of the site in degrees and minutes, (2) monthly factors based on Table A.1, and (3) the calculated heat index of the site (Equation 1). An example of the input PET data at the Nashville site is presented in Fig. A.5.

Table A.1: Thornthwaite correction factors for Tarboro and three eastern NC stations (Amatya et al. 1995).

Month	Tarboro Site	Average for 3 Eastern NC Stations
January	1.65	1.94
February	2.13	2.32
March	2.27	2.09
April	1.84	1.73
May	1.44	1.23
June	1.11	1.02
July	0.92	0.89
August	0.99	0.84
September	1.05	0.95
October	1.05	1.07
November	1.47	1.23
December	1.29	1.38

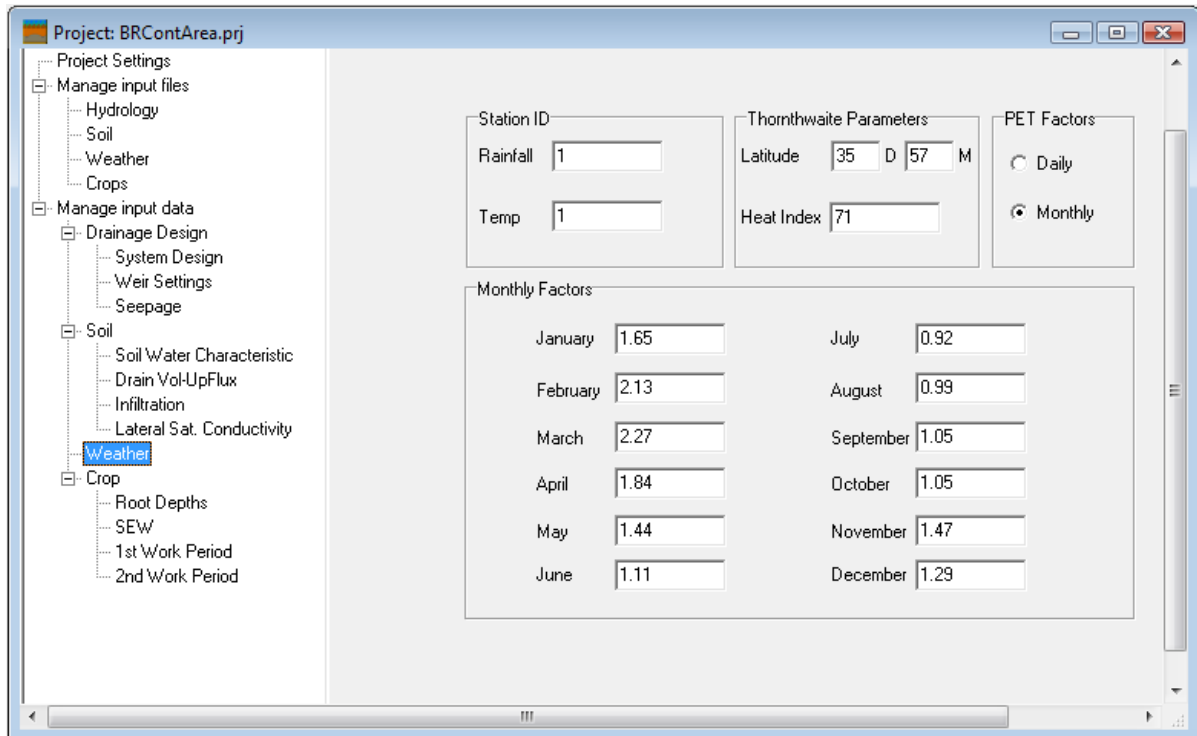


Figure A.5: Input PET data for Nashville site for using the monthly Thornthwaite method with correction factors.

Step 4: Create Soil File for Asphalt (Parking Lot)

To create a soil file for asphalt, open an existing soil file (.sin); an example is “Portse.sin.” Then, under the “Manage Input Data: Soil: Infiltration” tab, change the Green Ampt parameters to those shown in Fig. A.6. These changes will make the surface behave more similarly to an impervious surface, where infiltration is almost non-existent.

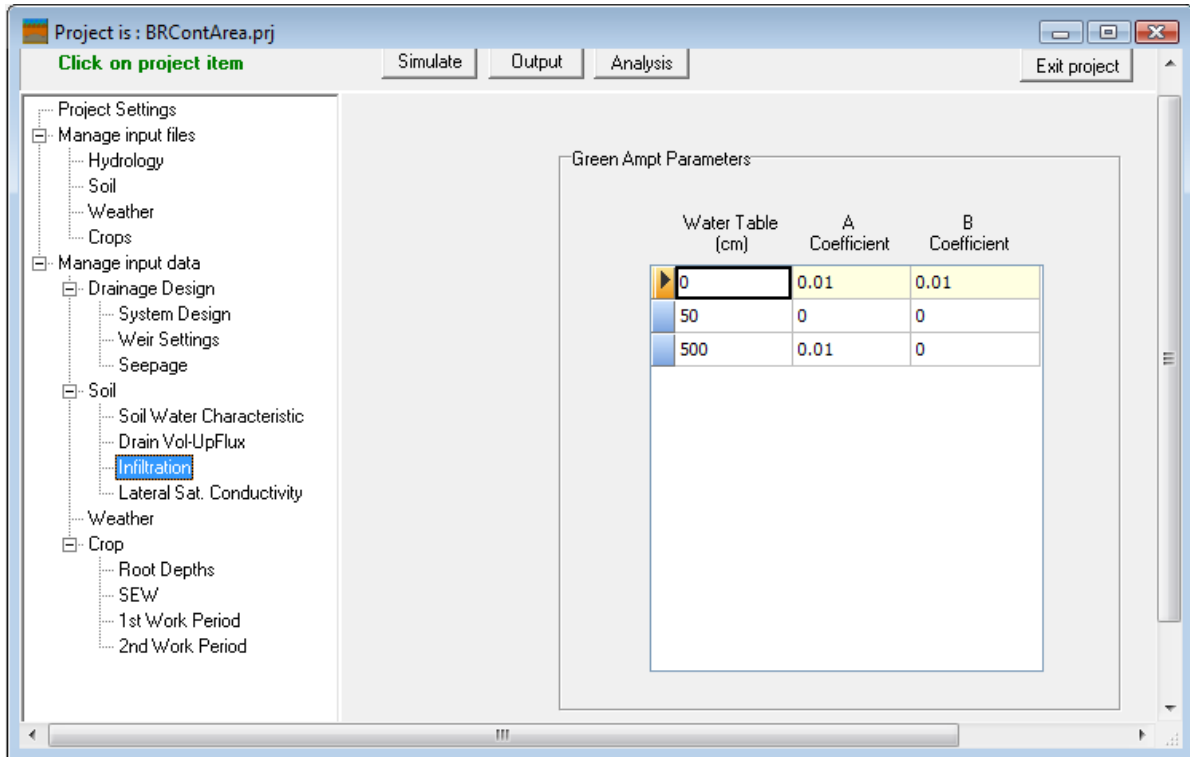


Figure A.6: Adjusted Green Ampt infiltration parameters for parking lot soil file.

Step 5: Change Drainage Design for Parking Lot

As the final step to model parking lot runoff, the system design in DRAINMOD needs to be changed as well. This can be accomplished with wide drain spacing and shallow drain depth and surface storage. If the contributing area is nearly 100 percent impervious and has smoothly graded pavement, the parameters under the “*Manage Input Data: Drainage Design: System Design*” tab should be changed to those shown in Fig. A.7. If there is a substantial percentage of pervious surfaces or if the paved surface has larger depressions, the maximum surface storage depth (S_m) should be increased to more accurately model all sizes of events. A detailed description on the calibration of this term is presented in Chapter 7. The inputs for the system design are a shallow and very wide drain spacing and a shallow surface storage depth. These characteristics provide for very limited drainage and surface storage, which will result in a large proportion of rainfall to run off the surface.

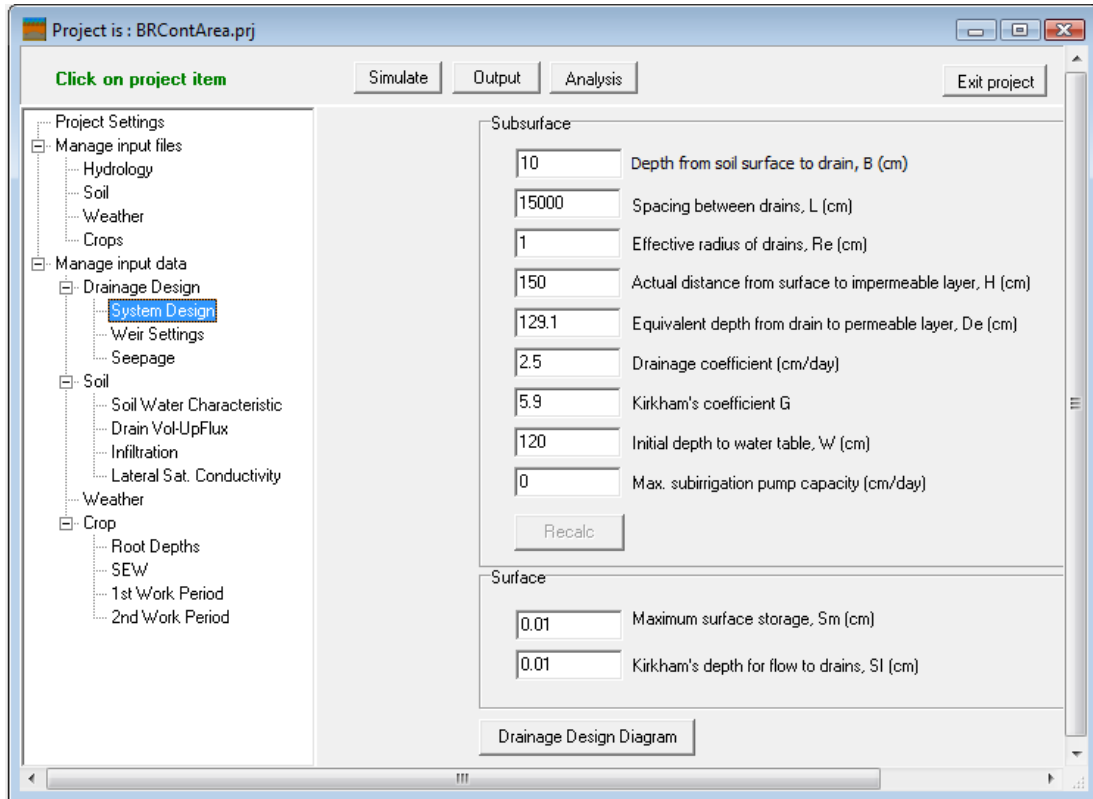


Figure A.7: Adjusted drainage system design for an impervious surface (parking lot).

Step 6: Run DRAINMOD for Parking Lot Runoff

The parking lot contributing area file has been completed, so select “*Simulate: Run Current*” and “*OK.*” Now, the user can view the daily, monthly, and yearly output files for runoff by selecting “*Output: View*” and then selecting either the *.day*, *.mon*, or *.yr* files, respectively. The hydrology output abbreviations and how they relate to bioretention cells are described in Table A.2. By running the simulation, it also creates a *.sro* file (surface runoff), which will be used to create the contributing runoff file. This is visible by selecting “*All files*” under the file type.

Table A.2: Description of DRAINMOD hydrology outputs in terms of bioretention meaning.

DRAINMOD Output	Bioretention Meaning
RAIN ^a	Volume of runoff into the bioretention cell plus direct rainfall
INFIL ^a	Volume of runoff and rainfall that infiltrated into the media
ET ^a	Evapotranspiration volume
DRAIN ^a	Drainage volume
DTWT	Depth to water table from surface of the media
TVOL ^a	Available water storage volume in the bioretention media
STOR	Depth of water in the surface storage zone
RUNOFF ^a	Overflow volume
VERTSP ^a	Vertical seepage/exfiltration volume

^a All volumes are expressed in depth of water (cm) across the bioretention surface area. To transform these units into a volume, multiply the depth (cm) by the bioretention surface area.

In examining the daily output, the modeled daily abstraction typically ranged from 0.8 to 1.6 mm (0.03 to 0.06 in), which as presented in Chapters 2-6, is consistent with the initial abstraction depths calculated for a curve number of 98 – 0.5 to 1.5 mm (0.02 to 0.06 in). The range of abstraction depths in the model was a result of rainfall duration; longer durations had larger abstraction depths. For the yearly output, the average runoff was approximately 90 percent of the rainfall depth, which is a close estimate for a standard asphalt parking lot. Due to shallow depressions in pavement, a small fraction of each event is abstracted. In Line et al. (2011), the average runoff to rainfall ratio was calculated to be 0.89 for a 97 percent impervious, 3.0-ha commercial shopping center that was comprised of primarily an asphalt parking lot. If the modeled abstraction depths are not within the user’s range of expected abstraction, the maximum surface storage depth can be adjusted.

Step 7: Create Contributing Runoff File

Once the abstraction depths are satisfactory, the *.sro* file needs to be converted into an *.ovr* file (overland runoff) using the “*Contributing Area Runoff*” utility. First, the user needs to create an input file (*.inp*). In Fig. A.8, an example of an *.inp* file, line 1 lists the number of *.sro* files, and line 2 lists the time of concentration (hr), instantaneous unit hydrograph (IUH) adjustment factor, contributing area (ha), and source of the *.sro* file. The easiest way to do

this is to open the “*Inputs*” folder where DRAINMOD is stored on the user’s computer, copy an existing *.inp* file, and rename it. Then open the file in the “*Contributing Area Runoff*” utility. Select the listed *.sro* file and select “*Clear,*” then select “*Add,*” and select the *.sro* file that was just created. In this utility, the user must enter the time of concentration, contributing area, and IUH adjustment factor (Fig. A.9). Typical values for time of concentration and IUH adjustment factor for a standard parking lot draining less than 1 ha would be 0.1 hours and 1.67, respectively. Then select “*Create*” and “*OK*” to create the contributing runoff file.

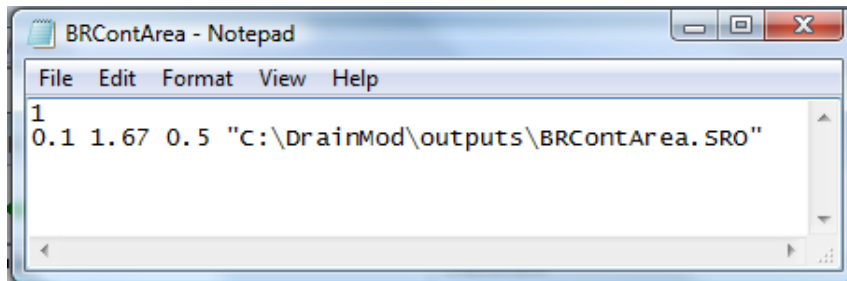


Figure A.8: Example of an *.inp* file.

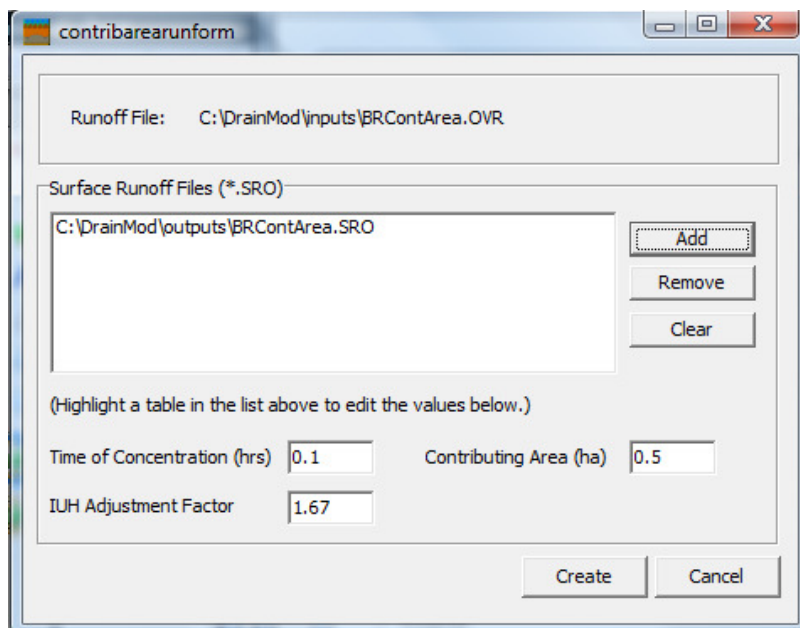


Figure A.9: User interface for contributing area runoff utility.

Step 8: Setup DRAINMOD for Bioretention Cell Design

Select “Project: Save As,” select the .prj file from the drop down list, and select “Save File(s).” Rename this file because it will now be the new file for the bioretention cell design; an example is “BRCell.” Select “Save,” then “Yes” to save both the .prj and .gen files, and then “Yes” to open this new file to begin the input for the bioretention design. In this new project, the user needs to check “Surface Water: Contributing Area Runoff” and then depending on the drainage configuration of the bioretention design, “Surface Water Mgmt.: Conventional Drainage” for conventional drainage or “Surface Water Mgmt.: Controlled Drainage” for an internal water storage (IWS) design. These parameters are highlighted in Fig. A.10. If the surface storage zone of a bioretention cell releases overflow into another cell, the user can keep the following boxed checked: “Output Options: Hydrology: Hourly Surface Runoff/Water Loss.” This will create a .sro file for overflow from the bioretention cell. If only one bioretention cell is modeled, it is not necessary to check this box. The user should verify that the simulation period is still appropriate for the available weather files.

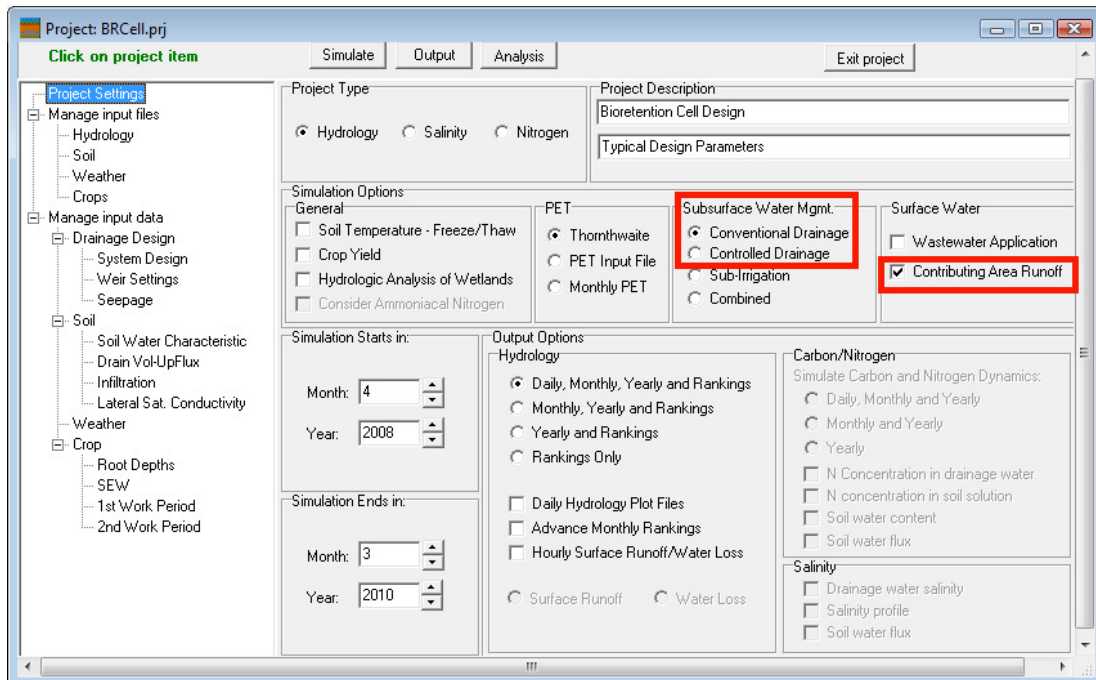


Figure A.10: User interface for bioretention design file.

Step 9: Adding Contributing Runoff File

In the “Manage Input Files: Hydrology” tab, add the .*ovr* file that was just created by selecting “Browse.” Then enter the drainage area to bioretention cell area ratio in the box for “Field Ratio,” this is highlighted in Fig. A.11.

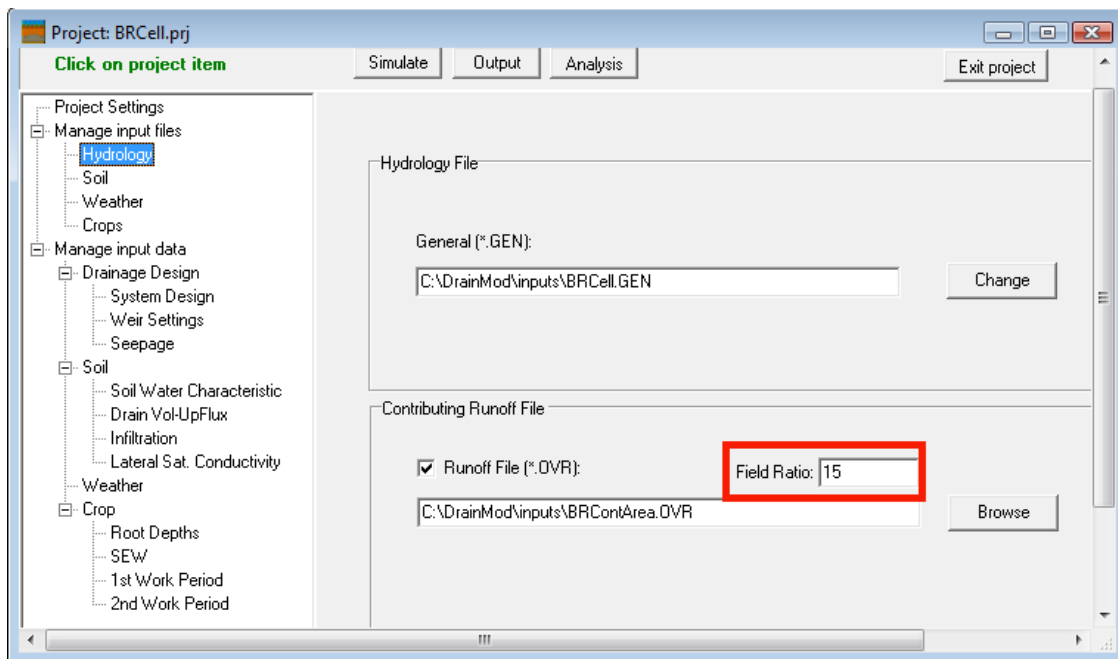


Figure A.11: User interface for adding contributing runoff file and drainage area to bioretention area ratio.

Step 10: Add/Create Soil File for Bioretention Media.

The specific soil-water characteristic for bioretention media must then be accounted for in the model. Either an existing soil-water characteristic curve from previously measured bioretention media can be used or a new soil-water characteristic curve should be measured. As part of this project, soil-water characteristic curves were measured using a pressure plate apparatus (tension table) (Fig. A.12) for several different types of bioretention media, including more recent designs that followed the N.C. design guidance for media composition. This test measures water released from a saturated soil core at various pressures, and these

relationships are presented in Table A.3. If the relationships from Table A.3 are used to model a current design, it would be recommended to use the Nashville or Knightdale characteristic for the bioretention media, the Rocky Mount characteristic for underlying sand (if sand choking layer is present), and the Rocky Mount characteristic for guidance for underlying gravel. If creating a new soil file in DRAINMOD, saturated hydraulic conductivity is required in addition to the soil-water characteristic curve. This can be measured by running a constant head permeability test, as described in Klute (1986).

Table A.3: Soil-water characteristic relationships for a variety of bioretention media.

Pressure (cm)	Volumetric Water Content (cm ³ /cm ³)							
	<i>Rocky Mount</i>	<i>Nashville</i> ^a	<i>Knightdale</i> ^a	<i>Louisburg</i>		<i>Graham</i>	<i>Greensboro</i>	
0	0.350	0.344	0.356	0.319	0.345	0.373	0.441	0.399
-4	0.291	0.342	0.355	0.319	0.344	0.296	0.428	0.392
-6			0.355	0.319	0.344	0.283	0.423	0.388
-10	0.175	0.337	0.350	0.281	0.339	0.237	0.383	0.378
-20			0.280	0.200	0.222	0.191	0.285	0.317
-30	0.05	0.221	0.245	0.176	0.189	0.173	0.236	0.262
-50			0.209	0.157	0.166	0.155	0.192	0.208
-60	0.045	0.189						
-75			0.189	0.145	0.151	0.145	0.173	0.190
-100	0.044	0.172	0.176	0.137	0.142	0.137	0.164	0.182
-200	0.044	0.151	0.148	0.121	0.122	0.124	0.147	0.168
-300	0.044	0.139	0.133	0.112	0.112	0.115	0.138	0.158
-400	0.044	0.131	0.124	0.109	0.106	0.109	0.132	0.152
-600		0.117						
Notes	Too sandy (96% sand)	Typical N.C. Media	Typical N.C. Media	Looser fill (L2)	More compact (L1)	Mostly Stalite (Expanded Slate)	IWS Cell	Conv. Cell
Field Study Refs.	Chapter 2	Chapters 3-5	Unpublished	Sharkey 2006 (close to typical design)		Passeport et al. 2009	Hunt et al. 2006 (old design, more topsoil)	

^a Bioretention media that meets current N.C. standards (NCDENR 2009). Ideal soil-water characteristic curves for typical N.C. bioretention media.



Figure A.12: Pressure plate apparatus (tension table) used to measure soil-water characteristic curves.

If creating a new soil file (.*soi*), the “*Create Soil File*” utility is used. A .*soi* file is needed to run the utility, so the easiest way to make one is by opening the “*Soils*” folder where DRAINMOD is stored on your computer, copy an existing .*soi* file, and rename it. Then open this file in the “*Create Soil File*” utility. The interface of the utility is shown in Fig. A.13. In this utility, existing layers from this file can be deleted and new layers can be added with specific soil-water characteristic relationships. For each layer, soil-water content at a 15000 cm tension must be included. For each layer, the bottom depth and saturated hydraulic conductivity are also required. Additionally, root depth, maximum root depth for

Green Ampt calculations, and layer of the soil-water characteristic to use for DRAINMOD's maximum root depths are needed. Root depth is dependent on the type of vegetation. Once completed, select "Create." This will create several relationships for volume drained and upward flux at various water table depths and Green and Ampt infiltration parameters, and it creates a .sin file, which will be selected in the "Manage Input Files: Soil" tab. An example of a .soi file is presented in Fig. A.14. The various line inputs are as follows:

Line 1: Title

Line 2: Number of layers

Line 3: Layer 1: Number of inputs for the layer, saturated conductivity (cm/hr), depth at the bottom of the layer (cm)

Lines 4-14: Volumetric water content (cm^3/cm^3), tension (pressure) (cm) [must include a 15000 cm tension for each layer]

Line 15: Layer 2: Number of inputs for the layer, saturated conductivity (cm/hr), depth at the bottom of the layer (cm)

Lines 16-26: Volumetric water content (cm^3/cm^3), tension (pressure) (cm) [must include a 15000 cm tension for each layer]

Layer X...

...

Last Line: Maximum root depth for Green-Ampt calculations (cm), root depth (cm), layer of the soil-water characteristic to use for DRAINMOD's maximum root depths

Create Soil File

Title:

Layer 1 of 4

THETA (cm ³ /cm ³)	Head (cm)
<input type="text" value=".344"/>	<input type="text" value="0.0"/>
<input type="text" value=".342"/>	<input type="text" value="4.0"/>
<input type="text" value=".337"/>	<input type="text" value="10.0"/>
<input type="text" value=".221"/>	<input type="text" value="30.0"/>
<input type="text" value=".189"/>	<input type="text" value="60.0"/>
<input type="text" value=".172"/>	<input type="text" value="100.0"/>
<input type="text" value=".151"/>	<input type="text" value="200.0"/>
<input type="text" value=".139"/>	<input type="text" value="300.0"/>

Bottom depth of layer (cm)

Saturated Conductivity (cm/hr)

Root Depth Soil Layer

Max Root Depth

Figure A.13: Interface for “*Create Soil File*” utility.

```

Nash_BRC-3 - Notepad
File Edit Format View Help
Nashville3-ft
04 0
11      4      6
.344    0.0
.342    4.0
.337    10.0
.221    30.0
.189    60.0
.172   100.0
.151   200.0
.139   300.0
.131   400.0
.117   600.0
.020 15000.0
11      3.5     90
.344    .0
.342    4.0
.337    10.0
.221    30.0
.189    60.0
.172   100.0
.151   200.0
.139   300.0
.131   400.0
.117   600.0
.02    15000.0
11      15     100
.350    0.0
.291    4.0
.175    10.0
.100    30.0
.065    60.0
.044   100.0
.044   200.0
.044   300.0
.044   400.0
.044   600.0
.010 15000.0
11      200    120
.300    0.0
.100    4.0
.050    10.0
.050    30.0
.045    60.0
.044   100.0
.044   200.0
.044   300.0
.044   400.0
.044   600.0
.010 15000.0
90, 45, 2

```

Figure A.14: Example of .soi file.

Step 11: *Verify/Enter Weather Information for Bioretention Site*

If the weather information is different from the contributing runoff file, the new information should be entered. Verify PET information in the “*Manage Input Data: Weather*” tab is correct and that the proper temperature (.tem) and rainfall (.rai) files are

selected in the “*Manage Input Files: Weather*” tab. If these are new or different, follow the instructions in Step 3.

Step 12: Enter Design Parameters.

In the “*Manage input data: Drainage Design: System Design*” tab, as shown in Fig. A.15, the top box contains information based on how the drain pipes are installed: depth from soil surface to drain, drain spacing, effective drain radius, and depth to impermeable layer. The depth to impermeable layer is the depth to the bottom of the gravel layer. For drain spacing, if the drains are evenly spaced, this would be the distance between them; otherwise, an effective drain spacing can be calculated by dividing the bioretention surface area by the overall drain pipe length. The effective drain radius was selected as the actual drain radius because the drains were surrounded by a gravel envelope. If a gravel envelope is not installed, the effective drain radius would be smaller than the actual drain radius. For corrugated drain pipes with total openings being 1.5 to 2 percent of the wall area, effective radii would be 0.5 and 1.5 cm for corrugated drain pipes with diameters of 10 and 15 cm, respectively (Skaggs, 1980). The next box is for the drainage coefficient, which is used by the model to limit the maximum drainage from the system if the drainage rates are limited by pipe size, valves, or other structural features. If the drainage rates are limited by these and enough monitoring data from the site are available, the drainage coefficient can be measured as the maximum drainage rate when the entire profile is saturated and the surface storage zone is fully ponded. It is probable that the drainage rate will be limited by the drain spacing, drain depth, or conductivity of the soil. In this case, the maximum drainage rate allowed by DRAINMOD will be what it calculates using the Kirkham equation under the fully saturated and ponded condition. The final box is for surface storage design parameters. The maximum surface storage in the model input is actually the *average* ponding depth in a bioretention cell. This parameter will control when overflow occurs. Kirkham’s depth is a function of the roughness of the surface. With most of the flow entering in the region nearest to the drain, the Kirkham’s depth is the depth in which water no longer freely moves on the surface (Kirkham 1957). If the surface of a bioretention cell is relatively smooth with few

shallow depressions, this could be set to 0.5 to 1 cm. Diagrams of agricultural fields with drainage pipes and a bioretention cell with an IWS drainage configuration are displayed in Figs. A.16 and A.17, respectively. Model inputs are highlighted in these diagrams.

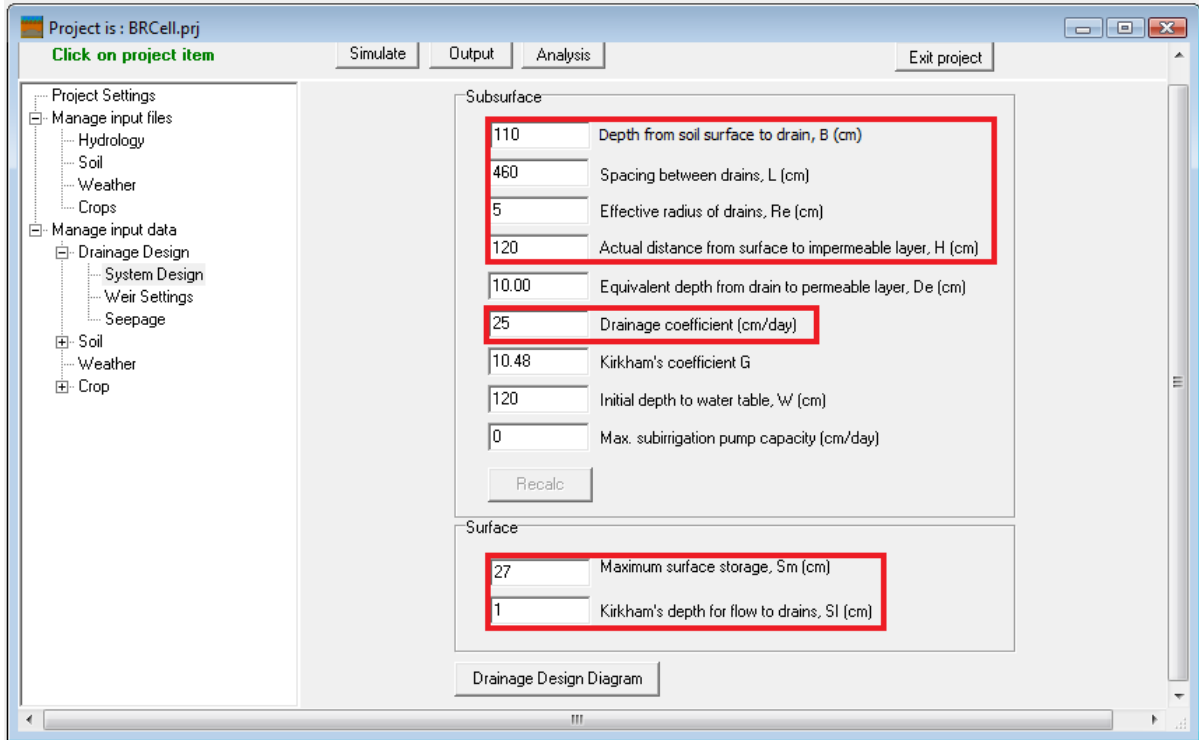


Figure A.15: System design interface in DRAINMOD.

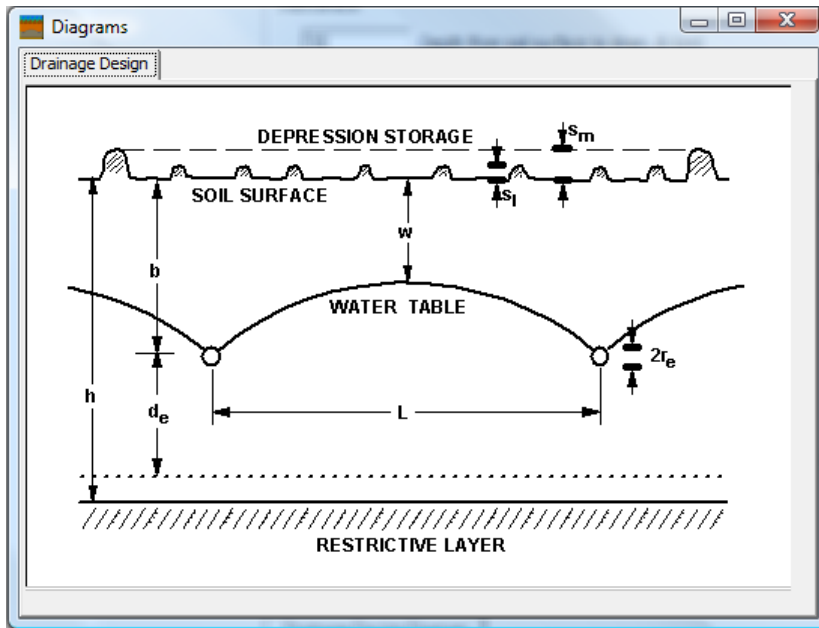


Figure A.16: Drainage design diagram for agricultural field with drainage pipes.

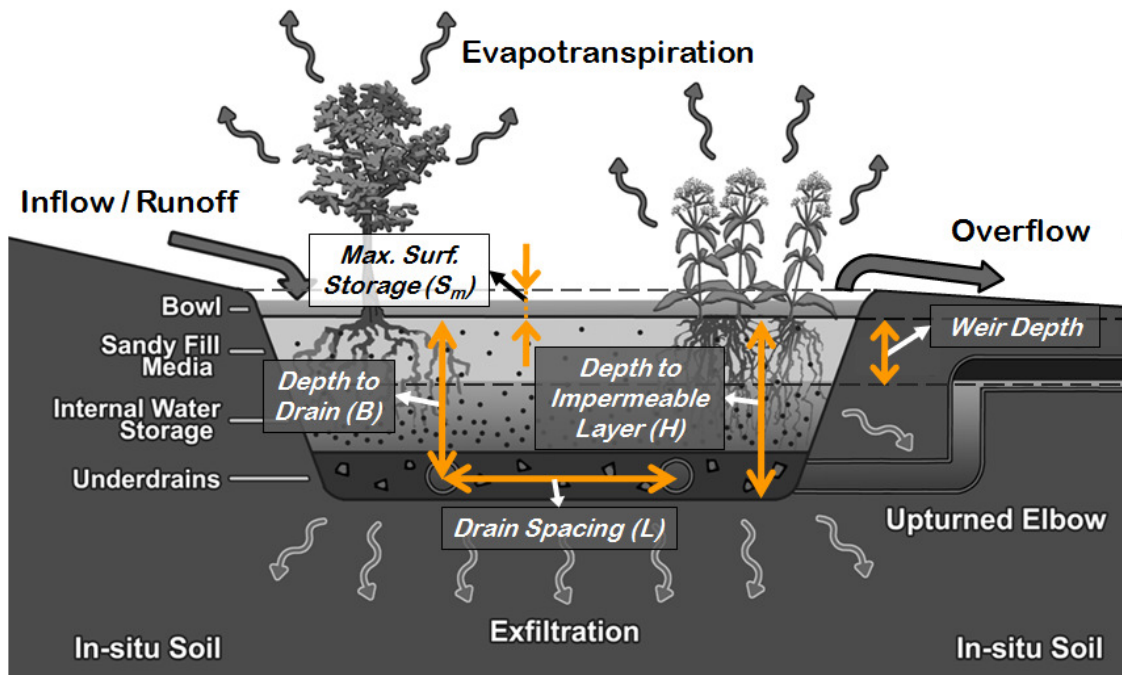


Figure A.17: Drainage design diagram for bioretention cell with an IWS drainage configuration.

The next set of model inputs are for the saturated hydraulic conductivities of the various layers. These are entered into the “*Manage input data: Soil: Lateral Sat. Conductivity*” tab, as shown in Fig. A.18. Then, the effective root depths are entered in the “*Manage input data: Crop: Root Depths*” tab, as shown in Fig. A.19. The root depths were allowed to vary throughout the year to account for planting and harvesting in agricultural fields; however, it is most likely that the bioretention cells will be only planted once, so these values can be constant throughout the year. The root depth will depend on the type of vegetation that is planted.

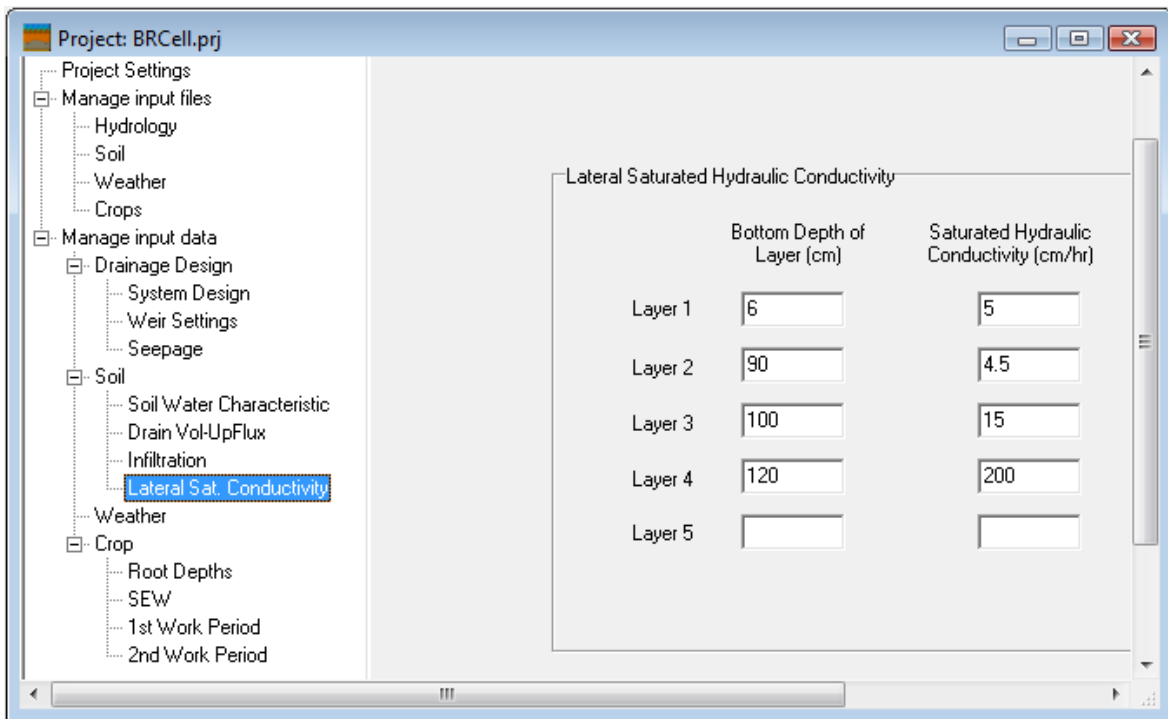


Figure A.18: Interface for lateral saturated hydraulic conductivity for multiple layers.

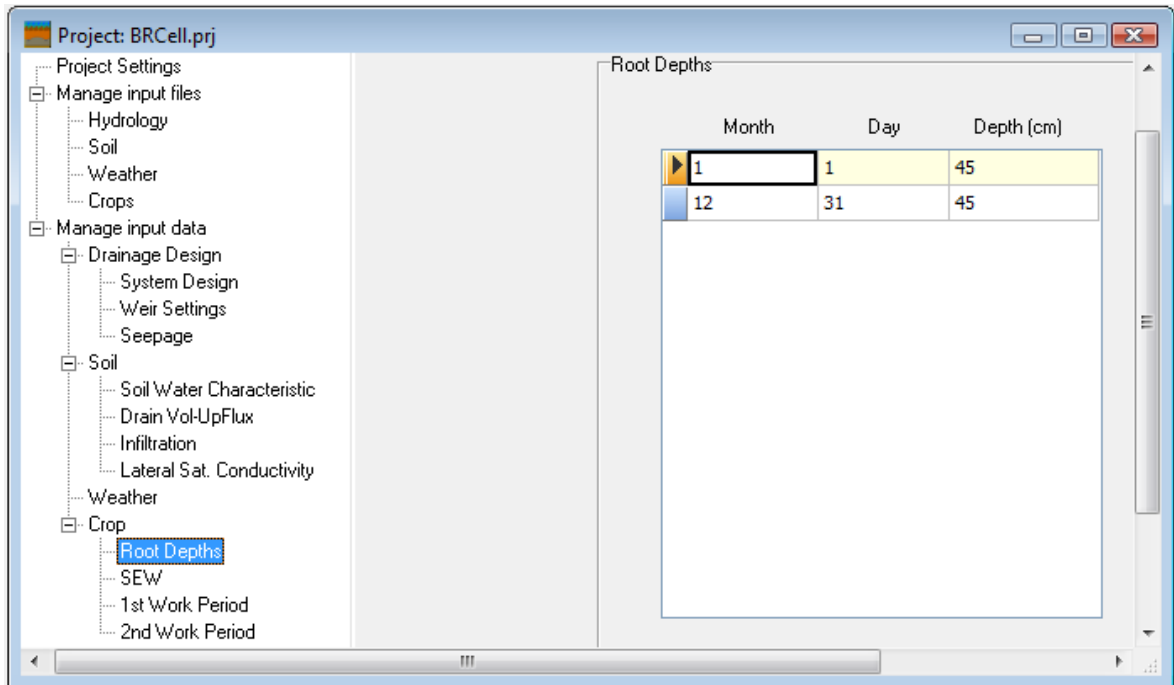


Figure A.19: Interface for crop root depths.

One of the final and most important factors for modeling the hydrologic performance of bioretention cells is accounting for seepage or exfiltration. An example of the seepage parameters and a diagram for vertical seepage are displayed in Fig. A.20. As part of this project, water table recession was measured with water level loggers, manufactured by Infinities USA, at the midpoint between drain pipes or from the upturned pipe for the IWS outlet (Rocky Mount site only). They were only measured for cells with an IWS zone because it was easier to distinguish when recession was due to drainage and seepage or seepage only. Once drainage stopped, seepage was the primary way that water table dropped. Examples of measured seepage rates and underlying soil types for several bioretention cells monitored in North Carolina are displayed in Table A.4.

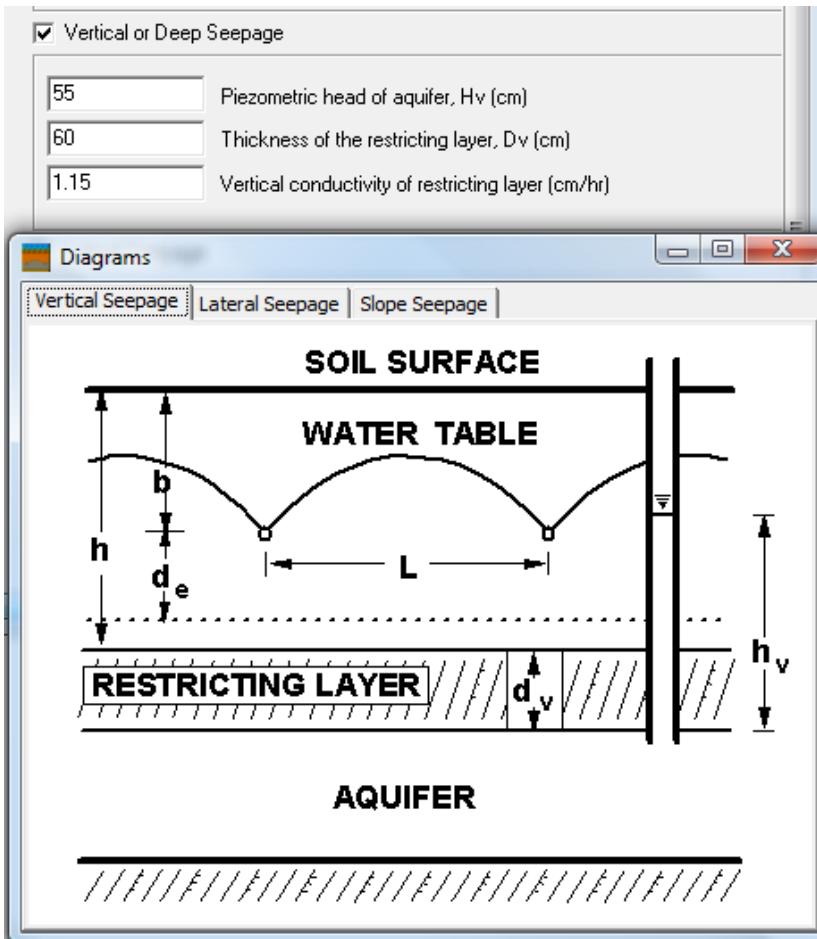


Figure A.20: Interface and diagram for vertical seepage parameters.

Table A.4: Measured seepage rates from various bioretention cells in North Carolina.

Bioretention Cell Location	Measured Seepage Rate	Underlying Soil Type	Field Study Reference
Greensboro 1 (Greensboro, NC)	0.3-0.5 mm/hr (0.01-0.02 in/hr)	Clay Loam ^a	Hunt et al. 2006; Sharkey 2006
Graham-North (Graham, NC)	0.2 mm/hr (0.01 in/hr)	Clay	Passeport et al. 2009
Graham-South (Graham, NC)	3.7 mm/hr (0.15 in/hr)	Sandy Loam	Passeport et al. 2009
RM Sand (Rocky Mount, NC)	60-90 mm/hr (2.4-3.6 in/hr)	Sand	Chapter 2
RM SCL (Rocky Mount, NC)	2.1-3.3 mm/hr (0.08-0.13 in/hr)	Sandy Clay Loam	Chapter 2
K-Small (Knightdale, NC)	0.5-0.8 mm/hr (0.02 to 0.03 in/hr)	Sandy Clay Loam / Clay ^a	Unpublished
K-Large (Knightdale, NC)	0.3-0.4 mm/hr (0.01 to 0.02 in/hr)	Sandy Clay Loam / Clay ^a	Unpublished

^a Soil type determined from soil series characteristics described in the local soil survey.

If the bioretention cell is designed with an IWS zone, this can be modeled by using “*Controlled Drainage*” under the “*Subsurface Water Mgmt.*” tab, as shown in Fig A.10. Once this is selected, the raised outlet depth can be adjusted in the “*Manage input data: Drainage Design: Weir Settings*” tab. Since the raised outlet should not be restricted with backwater from the stormwater pipe or ditch that it is draining into, the ditch characteristics should be set to the smallest values possible to prevent water from backing up into the ditch and forcing itself back into the media. The “*Bottom width of the ditch*” and “*Ditch side slope,*” can both be entered as 0.01, as shown in Fig. A.21, and the “*Weir Settings: Depth*” should be the depth from the bottom of the surface storage zone to the top out the outlet pipe, as shown in Fig. A.17.

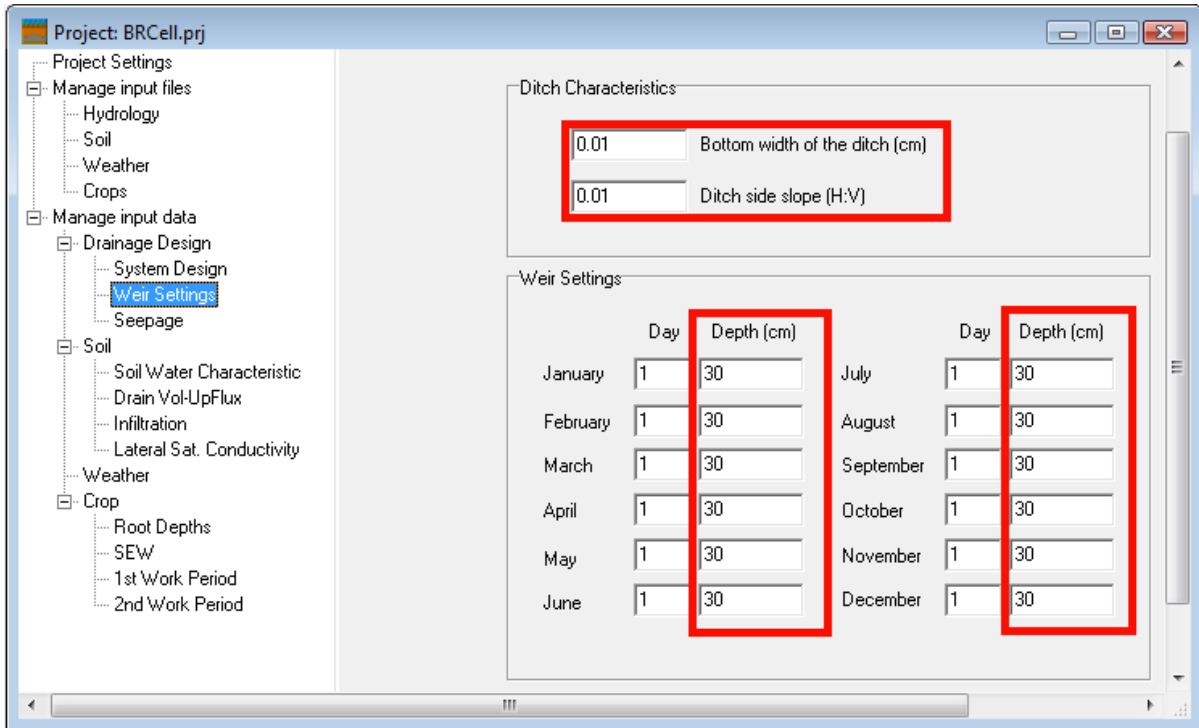


Figure A.21: Interface for controlled drainage weir settings (IWS zone configuration).

Step 13: *Run simulation.*

The bioretention design is now complete, so select “*Simulate: Run Current*” and “*OK.*” Now, the user can view the daily, monthly, and yearly output files for runoff by selecting “*Output: View*” and then selecting either the *.day*, *.mon*, or *.yr* files, respectively. The hydrology output abbreviations are described in Table A.2. If modeling a monitored bioretention cell, the fate of runoff for individual events can be used to compare modeled and measured data. If a monitoring well was installed at the midpoint between drains, it could be used to compare the modeled output of depth to water table (“*DTWT*”).

References:

Hunt, W. F., Jarrett, A. R., Smith, J. T., and Sharkey, L. J. (2006). “Evaluating bioretention hydrology and nutrient removal at three field sites in North Carolina.” *Journal of Irrigation and Drainage Engineering*, 132(6), 600-608.

- Kirkham, D. (1957). "Theory of land drainage." *Drainage of agricultural lands: Agronomy monograph No. 7*, J. N. Luthin, ed., American Society of Agronomy, Madison, Wisc., 139-181.
- Klute, A. (1986). "Water retention: Laboratory methods." *Methods of soil analysis. Part 1: Physical and mineralogical methods*, A. Klute, ed., Soil Science Society of America, Madison, Wis., 635-662.
- Line, D. E. Brown, R. A., and Hunt, W. F. (2011). "Effectiveness of "LID" for commercial development." *Journal of Environmental Engineering*, (under review).
- Passeport, E., Hunt, W. F., Line, D. E., Smith, R. A., and Brown, R. A. (2009). "Field study of the ability of two grassed bioretention cells to reduce storm-water runoff pollution." *Journal of Irrigation and Drainage Engineering*, 135(4), 505-510.
- Sharkey, L. J. (2006). "The performance of bioretention areas in North Carolina: A study of water quality, water quantity, and soil media." M.S. Thesis, North Carolina State University, Raleigh, N.C.
- Skaggs, R. W. (1980). "DRAINMOD: Reference report - Methods for design and evaluation of drainage-water management systems for soils with high water tables." U.S. Department of Agriculture – Soil Conservation Service, Fort Worth, TX.
- Skaggs, R. W. (1991). "Drainage." *Modeling plant and soil systems: Agronomy monograph No. 31*, J. Hanks and J. Ritchie, eds., American Society of Agronomy, Madison, Wisc., 205-243.

B. APPENDIX: EXAMPLE SAS CODE

Comparison of TN and TP concentrations to “fair” and “good” WQABI standards that are presented in McNett et al. (2010) using paired t-test, Wilcoxon signed-rank test, and sign test. This specific code was written for runoff into the Rocky Mount bioretention cells, but by changing the TN and TP concentrations, it could be applied to drainage or grab samples from either bioretention cell.

```
data Runoff;
input TN TP;
logTN=log10(TN);
logTP=log10(TP);
cards;
1.661 0.104
.
.
0.830 0.073
;
data b; set Runoff;
ods select BasicMeasures TestsForLocation GoodnessOfFit;
SC=TN-0.99;
SC2=logTN+0.00436;
SC3=TN-2.16;
SC4=logTN-0.3346;
SC5=TP-0.11;
SC6=logTP+0.9586;
SC7=TP-0.22;
SC8=logTP+0.6576;
proc univariate data=b;
var SC SC2 SC3 SC4 SC5 SC6 SC7 SC8;
histogram/ normal;
run;
```

Comparison of runoff and outflow concentrations from paired events (paired t-test, Wilcoxon signed-rank test, and sign test). This specific code was written for TN analysis from the Nashville bioretention cells, but by changing either the concentrations or locations, it could be applied to other pollutants or the Rocky Mount bioretention cells, respectively.

```
data TN;
input inflow outflow2ft outflow3ft;
linflow=log10(inflow);
loutflow2ft=log10(outflow2ft);
loutflow3ft=log10(outflow3ft);
cards;
1.006 0.425 0.443
. . .
. . .
0.577 0.590 0.806
;
data b; set TN;
ods select BasicMeasures TestsForLocation GoodnessOfFit;
SC=Inflow-outflow2ft;
SC2=linflow-loutflow2ft;
SC3=Inflow-outflow3ft;
SC4=linflow-loutflow3ft;
SC5=outflow2ft-outflow3ft;
SC6=loutflow2ft-loutflow3ft;
proc univariate data=b;
var SC SC2 SC3 SC4 SC5 SC6;
histogram/ normal;
run;
```

Analysis of correlations (Spearman and Pearson) between pollutant concentrations and environmental factors (antecedent dry period [ADP], precipitation depth [precip], percent of runoff infiltrated [infil], and media temperature [temp]). This specific code was written for analysis of outflow from the 0.6-m media depth Nashville bioretention cells, but by changing the concentrations, it could be applied to the 0.9-m media depth cells or runoff monitoring location.

```

data 2ftOutflow;
input TKN TAN OrgN NOx TN TP PartP OrthoP TSS ADP precip infil temp;
cards;
0.852 0.061 0.791 0.296 1.148 0.189 0.101 0.088 16 275 1.09 1.00 44.3
. . . . . . . . . . . . . . . .
. . . . . . . . . . . . . . . .
0.360 0.025 0.335 0.230 0.590 0.076 0.035 0.041 5 137 0.80 1.00 34.5
;
data b; set 2ftOutflow;
ods select GoodnessOfFit;
proc univariate normal plot data=b;
var TKN TAN OrgN NOx TN TP PartP OrthoP TSS ADP precip infil temp;
histogram/ normal;
proc corr;
var TKN TAN OrgN NOx TN TP PartP OrthoP TSS ADP precip infil temp;
run;
proc corr spearman;
var TKN TAN OrgN NOx TN TP PartP OrthoP TSS ADP precip infil temp;
run;

```

The following code was specifically used to analyze how excavation technique (rake and scoop), soil moisture condition (wet and dry), and soil type (clay and sand) affected saturated hydraulic conductivity. The data were transformed with a Box Cox transformation, and the code to determine the transformation factor is also included.

```

options formdlm="-";
/*Code to read in Ksat values from the various combinations of excavation technique, soil
type, and soil condition. To run for infiltration, change Box Cox transformation factor to the
most appropriate value, and change the Ksat rates to the infiltration rates.*/
data sandyksat;
  soiltype="sandy";
  array ctype{2} $ ("wet","dry");
  array ttype{2} $ ("scoop","rake");
  do i = 1 to 2;
  do j = 1 to 2;
    input ksat @;
    soilcond=ctype{i};
    technique=ttype{j};
    output;
  end;
end;
/*Sand Site: WS_Ksat WR_Ksat DS_Ksat DR_Ksat */
cards;
1.86  27.05  2.28  4.79
14.06 19.08  2.26  7.33
7.81  18.66  9.14  9.82
;

data clayksat;
  soiltype="clay";
  array ctype{2} $ ("wet","dry");
  array ttype{2} $ ("scoop","rake");
  do i = 1 to 2;
  do j = 1 to 2;
    input ksat @;
    soilcond=ctype{i};
    technique=ttype{j};
    output;
  end;
end;

```

```

end;
/*Clay Site: WS_Ksat WR_Ksat DS_Ksat DR_Ksat */
cards;
0.39  1.46  3.07  0.22
1.12  6.08  4.16  5.10
0.08  5.58  0.001 1.55
;

data both;
  set clayksat sandyksat;
  ksat=max(.01,ksat);
  bci=ksat**.44;
  /*0.44 will change based on factor that is best suited for a Box-Cox transformation (see
code below)*/
run;

/*Code for determining Box-Cox transformation factor*/
data next; set both;
do lamb= .15 to 0.55 by .01 ;
  Gmean = exp(0.864); ** Geometric mean **;
  denom = lamb*Gmean**(lamb-1);
  Y = (ksat**lamb-1)/denom;
  ** ref: Pg. 239, Box, Hunter & Hunter **;
output; end;
lamb=0;
Y = Gmean*log(ksat);
output;
proc sort; by lamb;
proc glm data=next noprint;
  by lamb;
  class technique soilcond soiltype;
  model y=technique|soilcond|soiltype;
output out=out1 residual=r;

proc summary nway css data=out1; var r;
class lamb;
  output out=out1 css=css;
proc print;
data graph; set out1; dfe=16;
  t = tinv(.975,dfe); crit = 2.85623*(1+t*t/dfe);
proc gplot; plot css*lamb;
run;

```

```
/*Code for comparing Ksat values between soil type (clay versus sand) or soil condition (wet versus dry)*/
```

```
proc sort;
```

```
  by soiltype;
```

```
  /*by soilcond; (replace with previous line for comparing wet to dry)*/
```

```
run;
```

```
proc glm data=both;
```

```
  by soiltype;
```

```
  /*by soilcond; (replace with previous line for comparing wet to dry)*/
```

```
  class technique soilcond soiltype;
```

```
  model bci=technique|soilcond|soiltype;
```

```
  means technique|soilcond|soiltype;
```

```
  output out=two r=r p=p;
```

```
run;
```

```
proc gplot data=two;
```

```
  plot r*soiltype=soilcond;run;
```

```
proc glm data=both;
```

```
  by soiltype;
```

```
  /*by soilcond; (replace with previous line for comparing wet to dry)*/
```

```
  class technique soilcond soiltype;
```

```
  model bci=technique*soilcond*soiltype;
```

```
  means technique*soilcond*soiltype/hovtest;
```

```
run;
```

```
proc gplot;
```

```
  plot r*p=technique;
```

```
run;
```

```
proc gchart data=plotme;
```

```
  vbar r;
```

```
run;
```